Study on the effect of plasma parameters and catalyst on growth and field emission properties of carbon nanotubes (CNTs)

By

AARTI TEWARI

(2K13/Ph. D. AP/07)

Department of Applied Physics (DTU)

Submitted

in fulfillment of the requirement of the degree of Doctor of Philosophy to the

DELHI TECHNOLOGICAL UNIVERSITY (DTU)

BAWANA ROAD, DELHI-110 042, INDIA.

APRIL-2016

CERTIFICATE

This is to certify that the thesis entitled "**Study on the effect of plasma parameters and catalyst on growth and field emission properties of carbon nanotubes (CNTs)"** submitted by Aarti Tewari with registration number (2K13/Ph.D. AP/07) to Delhi Technological University, Delhi for the award of the degree of Doctor of Philosophy is a bonafide record of the research work carried out by her under my supervision and guidance. The content of the thesis, in full or parts have not been submitted to any other Institute or University for the award of any other degree or diploma.

Prof. (Dr.) Suresh C. Sharma
Supervisor
HOD, Applied Physics
Delhi Technological University (DTU)
Shahbad Daulatpur, Bawana Road
Delhi-110042

TABLE OF CONTENTS

Page No.

ACKNOWLEDGMENT

At the outset, I would like to thank my supervisor Prof. Suresh C. Sharma, Head of Department of Applied Physics, DTU for his continuous support, patient guidance, and motivation throughout my time as his student. He has always been very supportive and responded promptly to all my queries. It has been a long journey with him and I have enjoyed all days that I have spent with him even when the time was little difficult.

I am also thankful to Prof. M.S. Sodha[Former Dy. Director IIT Delhi; Former Vice-Chancellor of Lucknow, Indore and Bhopal Universities] for valuable discussions and useful suggestions from time to time.

I would also like to thank my parents, brother and N.V. for all their support, love and care. They have always stood by me in my failures and success. I know I am not a very easy person with all my tantrums and short temper. So my heartfelt thanks to them for bearing me.

I would also thank Mrs. Pratibha Malik. It was only in DTU that I met her for the first time during our admission interview and since then she has been a great friend and colleague. She has made by journey easy by her jokes, leg pulling and not to forget her famous dialogue “aur kitna padhogi”.

Also, my thanks goes to all those people who tried making time difficult for me. Thanks to them that I have emerged as a strong, confident and fearless person.

ABSTRACT

Carbon nanotubes are allotropes of carbon with cylindrical nano structure. The structure of a nanotube is similar to graphite, with a difference that the sheets are rolled to form a tube and capped at least one end. CNTs have found applications in field emission displays, nanoscale electronic devices, biosensors and hydrogen storage medium. There are various techniques through which CNTs can be synthesized but CNT synthesized in a plasma medium are known to be vertically aligned at low growth temperatures. The present thesis is a rigorous and detailed study of parameters affecting CNT growth in plasma and the consequent field emissions from them.

In the research work, we have developed a theoretical model describing the growth of CNT in plasma with and without catalyst, separately. The model detailing CNT growth in plasma without catalyst is extended to study the effect of plasma parameters, plasma compositions, different plasma mediums, and negative ions on the growth of CNT and the results obtained have been extended to present an estimate of the behavior of field enhancement factor of CNT. The broad outcomes of the research are that the plasma parameters (electron density and temperature , ion density and temperature), relative density of negative ions, fractional concentration of light positive ion, decreases the radius of CNT and since the field enhancement factor is inversely proportional to radius , it can be estimated that field enhancement factor would increase with all the above parameters. The CNT growth on a catalyst-substrate surface in a plasma environment is a complex process and therefore a model is developed underlining the numerous complex growth processes in a plasma

environment. The impact of plasma parameters, plasma power, substrate bias, substrate temperatures, different carrier gases and their flow rates on the height and radius of CNT is thoroughly studied. The outcomes of present research can be extended to improve field emission from the CNTs at low temperatures.

LIST OF FIGURES

Chapter 6

Chapter 7

Chapter 8

LIST OF TABLES

CHAPTER 1

INTRODUCTION

1.1: Motivation

Carbon Nanotube (CNT) was seen as early as 1978, by Abrahamson *et al.* [1] while working with standard carbon arc. In 1978, they published an article describing, "a thick mat of fine fibers has been found on the surface of the graphite and carbon anode of the low current arc operated in nitrogen" [2]. But, due to research environment during those times their work went unnoticed until in 1985, when a new form of carbon named buckminister fullerene (C60) or the "buckyball", was reported by Kroto *et al.* [3]. But, it was Iijima [4] in 1991 who was the first to present CNT with diameter up to 3-10 nm and the length up to 1μm.

1.1.1: Structure of CNT

CNTs consist of graphene sheet rolled up in tube of a few nanometers diameter and length of many microns. The structure of a nanotube is similar to graphite, with a difference that the sheets are rolled to form a tube and capped at least one end. Each layer of graphene constitutes carbon atoms arranged in hexagons to form a honeycomb structure. The carbon bonding in graphite is sp^2. Carbon has atomic number 6 with electronic configuration of $1s^2\ 2s^2\ 2p^2$. The $1s^2$ orbital contains strongly bound electrons and the four valence electrons occupy the 2s and 2p orbitals. The covalent bonds in carbon materials arises due to 2s, $2p_x$, $2p_y$,and $2p_z$ orbitals. The three possible hybridizations that can occur in C are sp, sp^2 and sp^3. In CNT, the hybridization of carbon is sp^2 and the sp^2

bonding state gives rise to chain structure. In sp^2 hybridization, the 2s orbital mixes with the three 2p orbitals i.e., $2p_x$,$2p_y$,and $2p_z$ forming three sp^2 orbitals with one p orbital remaining.

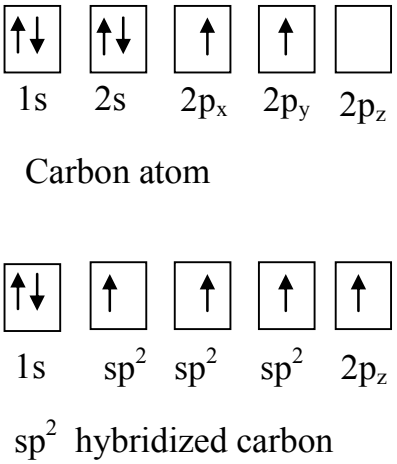

Fig. 1: Illustrates the orbitals of the carbon atom and sp^2 hybridized carbon

These sp^2 orbitals form the strong sigma (σ) bonds between the carbon atoms in graphite planes while the p_z provide the weak Vander-wall bonds in between the planes. The graphite layers when viewed perpendicularly gives a honeycomb pattern of graphite. If these patterns are wrapped back on top of themselves such that their edges are joined and one of their end is open and the other is closed, then tubes of graphite are formed. Fig. 2 illustrates the formation of CNTs.

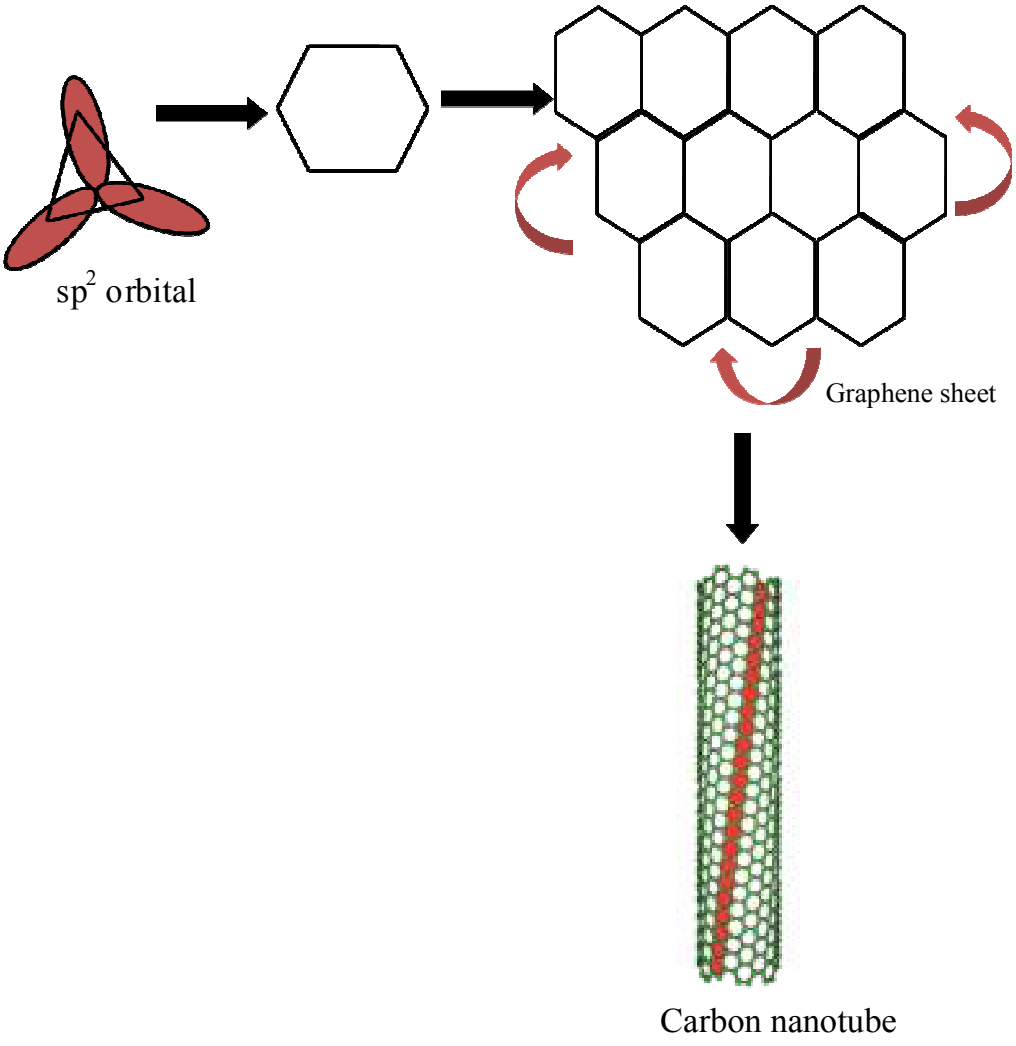

Fig. 2. Depicts the formation of CNT

1.2 : Classification of CNTs on the number of sheets rolled up and the direction of rolling of sheets

1.2.1: Depending on the number of sheets rolled up:

a. Single-Walled Carbon Nanotubes (SWCNTs):

Bethune *et al.* [5] at IBM and Iijima [6] at NEC, Japan were the first to prepare SWCNTs by metal catalyzed direct current arc using graphite

electrodes under a helium atmosphere. Most SWCNTs have a diameter close to 1 nanometer (1nm =10^{-9} m), with a tube length that can be many millions of times longer. SWCNT is shown in Fig.3.

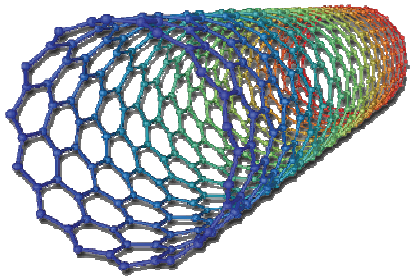

Fig. 3. Depicts an image of SWCNT [7]

b. Multi-Walled Carbon Nanotubes (MWCNTs):

Multi-walled carbon nanotubes (MWCNTs) as shown in Fig.4 consist of a number of layers of graphene rolled as concentric cylinders. The interlayer distance between two graphene layers in MWCNTs is 0.34 nm. The diameter of MWCNTs can range upto hundreds of nanometers.

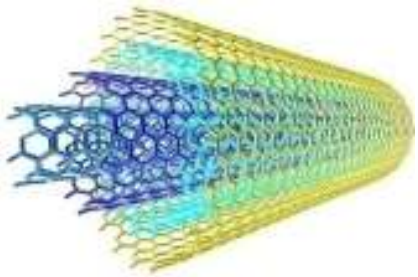

Fig. 4. Displays an image of MWCNT [8]

1.2.2: Depending on the way of folding

We define a hexagon by two integers (n, m) with n=0,1,2,3….. and m=0,1,2,3…., and $\hat{x}\ and\ \hat{y}$ are the unit vectors then the position of each hexagon is given by vector $\vec{R}$ as

$$\vec{R} = n\hat{x} + m\hat{y},$$

The vector $\vec{R}$ that denotes the position of a hexagon is called as a 'chiral vector'. A tube which is obtained by rolling the sheet along the chiral vector R (n,m) is called a chiral tube. The chiral angle 'θ' is the angle between the *x-axis* and chiral vector $\vec{R}$ and is used to denote the folding. In order to uniquely define different types of tubes, chiral angle between $0< \theta< \pi/6$ is sufficient. A chiral tube is identical to its mirror images and achiral tube is not identical to its mirror images.

a. Zigzag CNT:

These are formed for θ=0 and chirality (n,0) i.e., by folding graphene sheets parallel to the x-axis. The name zig-zag owes to the zigzag arrangement of carbon atoms. They are 'achiral' tubes i.e., they are not similar to their mirror images.

b. Armchair CNT:

These are formed for $\theta = \pi/6$ and chirality (n, n). They are also 'achiral'.

c. Helical CNT:

Their chiral angle ranges between 0 and $\pi/6$ and chirality is (n, m). They are 'chiral'.

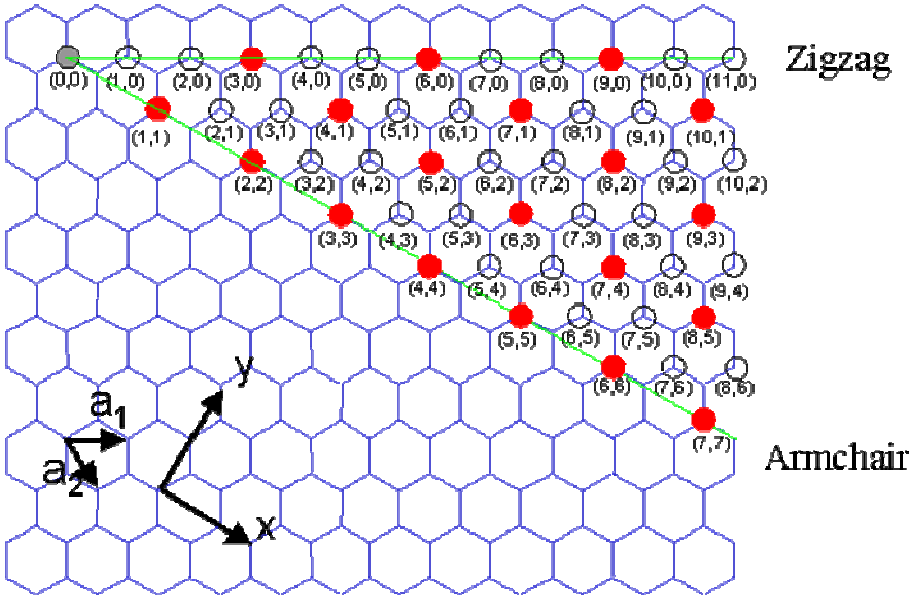

Fig.5. Illustrates the arrangement of atoms in Zigzag and Armchair CNT in a graphene sheet [9]

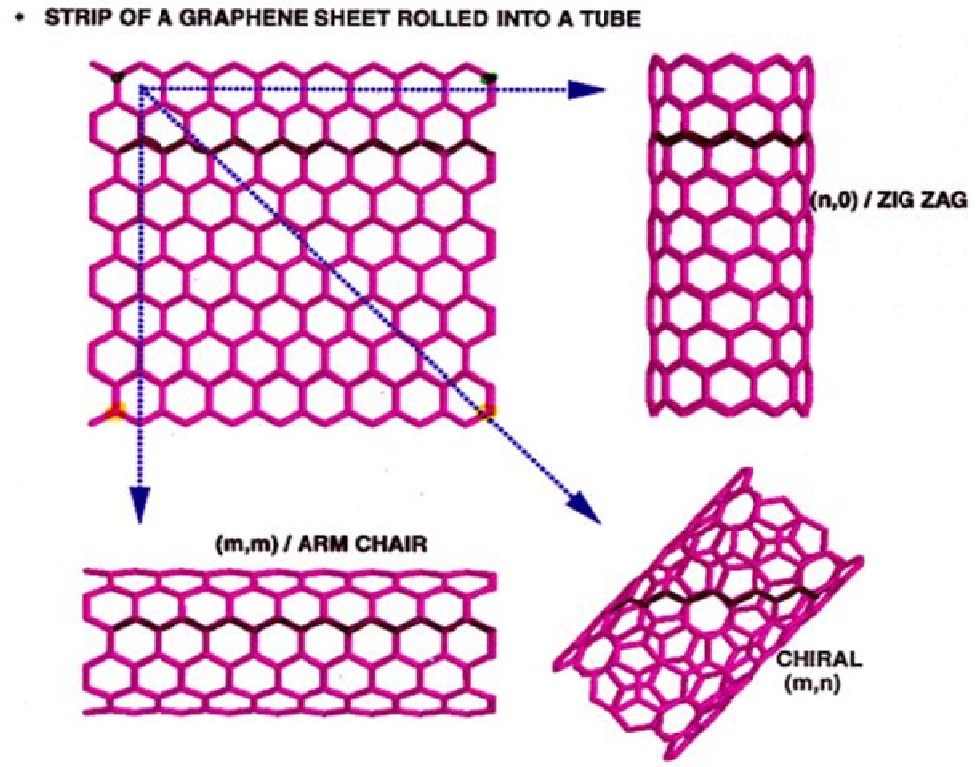

Fig. 6. Illustrates the Zigzag, Chiral and Arm chair CNT [10]

1.3: Properties of Carbon Nanotubes

1.3.1: Mechanical Properties of CNT

Carbon nanotubes are the strongest and stiffest materials known. The immense strength is the result of covalent sp^2 bonds formed between the individual carbon atoms. The stiffness of a material is measured in terms of its Young's modulus which is defined as the ratio of the stress (force per unit area) along an axis to the strain (ratio of deformation over initial length) along that axis in the range of stress in which Hooke's law holds[11]. CNTs are known to have the largest Young's modulus of nearly 1.8 TPa. Moreover, the maximum stress that a material can withstand is given by its tensile strength, which is a measurement of the force required to pull something such as rope, wire, or a structural beam to the point where it breaks. A comparison of Young's modulus, tensile strength, and density of diamond, graphite, different types of CNTs, and stainless steel is tabulated in Table 1.

S. No.	Material	Young's Modulus (in T Pa)	Tensile Strength (in G Pa)	Density (g/cm^3)
1.	Diamond	1.05 [12] and 0 .7-1.2[13]	0.8-1.4 [13]	3.52
2.	Graphite	1.6 in Plane [14]	0.01-0.08 [13]	2.26
3.	SWCNT	1[13] and 1.8[15]	50-200 [13]	1.55 for SWCNT bundle [19]
4.	MWCNT	0.7-1.8 [14]	11-63[16]	2.5 for 10 walls with outer diameter of 20nm[20]
5.	Stainless Steel	0.186 [17]-0.214[18]	0.38[17] – 1.55[18]	7.85

Table 1. Comparison of physical properties of different materials

1.3.2: Electrical Properties:

A mean free path of ~ 2 μm, with a resistivity of 10^{-6} Ω cm for electrons in metallic tubes has been measured [21] which is better than the conductivity of copper (Cu) at room temperature. The highest current density measured in metallic SWCNT is ~ 10^9 A/cm^2 [22]. The semiconducting SWNTs exhibit high hole mobility (p-type) of ~ 2×10^4 cm^2/ Vs, which is comparable to the in-plane mobility of graphene (3×10^4 cm^2/ Vs) and better than silicon (Si) (1.5×10^3 cm^2/ Vs for electron mobility and 4.5×10^2 cm^2/Vs for hole mobility). The resistivity for 350 nm long cross- section MWCNTs with 20nm diameter prepared through arc discharge method was calculated to be 9×10^{-4} Ω cm and resistance was 10kΩ[23]. The resistivity of SWCNTs grown through arc-discharge method is 10^{-4} Ω cm [24].

1.3.3: Electronic Properties:

The electronic properties of CNTs are highly dependent on their diameters and the direction in which the graphene sheet is rolled up to form nanotubes [25]. The armchair nanotubes are reported to be metallic whereas zig-zag nanotubes are semiconducting [26].

1.3.4: Thermal Properties:

The thermal properties of nanotubes are associated with its specific heat and thermal conductivity. The CNTs are known to be exceedingly good conductors of heat better than diamond. Hone *et al.* [27] have reported the specific heat of SWNT bundles with average diameter of 1.25 nm from 300 to 4K. Above 4K, the experimental curve was in accordance with theoretical curve for single walled CNTs but deviated remarkably from graphene and graphite curves upto 100K. Lasjaunias *et al*. [28] measured specific heat to 0.1K for SWNT bundles. They further

elucidated that for CNTs the bundling of graphene sheet into tubes reduced the low-energy phonon density of states. Mizel *et al.* [29] reported that for SWNT, the specific heat changed its dependence on temperature (T) from $T^{1/2}$ to linear T. Moreover, as the size of SWNT bundles was increased, the linear variation of specific heat with temperature decreases whereas at high temperatures, specific heat showed a mixed 2D-3D behavior due to weak intertube interaction. Yi *et al*. [30] revealed the linear dependence of specific heat of MWNTs for a temperature range of 10K to 300K. The thermal conductivity (κ) of carbon based material is through atomic vibrations. The sp^3 bond makes diamond good thermal conductors but the presence of sp^2 bonds in CNTs bestows them with high thermal conductivity. Berber *et al.* [31] reported the thermal conductivity of CNTs to be 6600W/mK at room temperature. The thermal conductivity of bulk samples of CNTs aligned by high magnetic fields was greater than 200W/mK whereas for unaligned samples it was one order smaller than diamond. Llaguno *et al*. [32], showed a linear dependence of (κ) with temperature for CNTs with average diameter of 1.2nm and 1.4 nm at low temperatures. For 1.4 nm diameter samples, at 35K κ/T increases whereas for 1.2 nm the increase of κ/T is at 40K. Kim *et al.* [33] measured the thermal conductivity of MWNTs as 3000W/mK at room temperature.

1.3.5: Magnetic Properties:

CNTs exibhit weak magnetism but the exact reasons behind weak magnetism are not fully known. Cespedes *et al.* [34] calculated the average room temperature magnetization to be 0.1 Bohr magnetons per carbon atom and found that CNTs were magnetized when placed in

contact with the magnetic material by the transfer of spin from the magnetic substrate to the nanotube.

1.4: Applications of CNT:

1.4.1: Electron Field Emission Property:

Field emission is the extraction of electron from a solid surface by tunneling through a potential barrier, which is approximately equal to the work function of the material, ϕ .

According to Fowler and Nordheim [35], the emitted current (I) depend exponentially on the applied field (E) and work function (ϕ) as:

$$I = \frac{q^3 E^2 \alpha}{8\pi h \phi t^2(y)} \exp\left[\frac{-8\pi (2m_e)^{\frac{1}{2}} \phi^{\frac{3}{2}} \nu(y)}{3 h q E}\right],$$

where α is the emission site area (in cm^2) ,h is the Planck's constant, m_e is the electron mass, q is the electronic charge, $y = \frac{\Delta\phi}{\phi}$, and ν(y) and t(y) are the Nordheim elliptic functions. A straight line obtained between ln (J/E^2) and (1/E) is called Fowler -Nordheim plot.

The local electric field strongly depends on the shape of a surface and can be significantly enhanced at the apex of sharp features. An important parameter known as the geometric field-enhancement factor (β) expresses this influence

$$\beta = \frac{E_a}{E_m}$$

where

E_a is the actual electric field at the tip of CNT and E_m is the macroscopic electric field.

Kokkorakis *et al.* [36, 37] calculated the field enhancement factor of the open and closed CNTs through simulation, and showed that β depends on h/ρ, where h is the height of the carbon nanotube and ρ the radius of its cap. Miller [38] solved analytically the field enhancement factor of the floated sphere case using the image method, as $\beta = \beta_0$(1-h/d) , where h is the height of the sphere center and d is the anode-cathode distance. Wang *et al.* [39] calculated the field enhancement factor when the anode-cathode distance d is much larger than the height h of CNT using a floating sphere method as $\beta = \frac{h}{\rho} + 3.5$, h being the height and ρ the radius of CNT. Wang *et al.* [40] also calculated β for the CNT array as $\beta = \frac{h}{\rho} + 3.5 - W$, where $W \equiv \left(\frac{h}{R}K\right)$ is the function of intertube distance R and represents the coulomb field interaction between the CNTs. Filip *et al.* [41] obtained the enhancement factor including the screening effect among CNTs as, $\beta = 1 + s\left(\frac{(d-h)}{\rho} - 1\right)$, where s is the screening effect parameter.

1.4.1.1: Flat Panel Display:

The fabrication of flat panel display from CNTs is an important application of CNT as it consumes low power with high brightness, fast response rate, and a wider temperature range of operation. Choi *et al*. [42] fabricated one such flat panel display from SWCNT as illustrated in Fig.7. It consists of nanotube-epoxy stripes on the cathode glass plate and phosphor coated Indium-Tin-Oxide (ITO) stripes on anode plate. A 230V is required to generate a display of 76 μmA/mm^2 at 30 μm anode-cathode

distance. A pulse of ±150V is switched among anode and cathode stripes in order to obtain image.

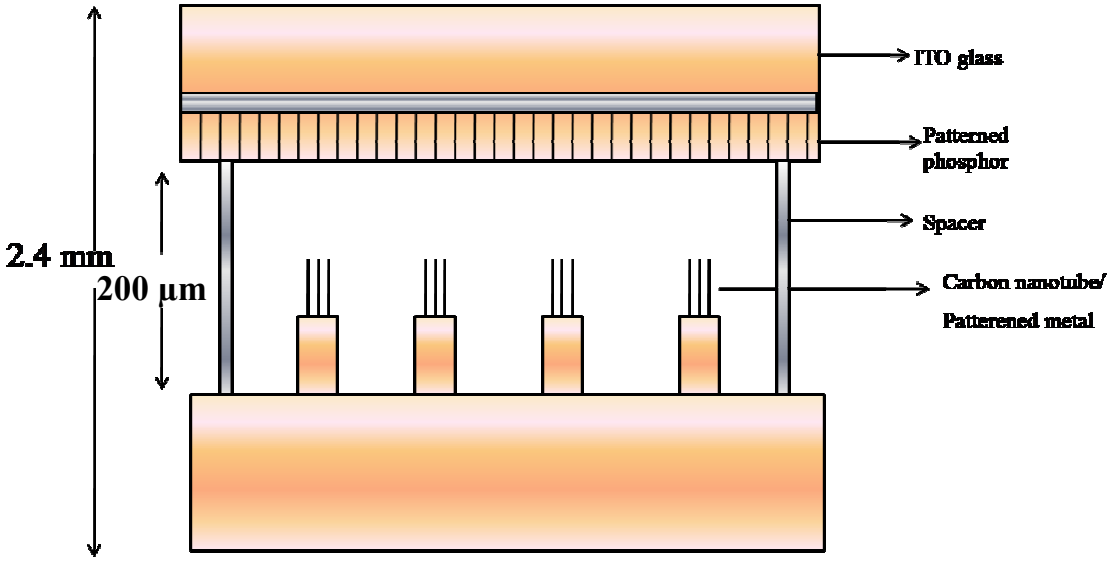

Fig. 7. SWNT flat panel display

1.4.1.2: Transistors:

CNTFET (Carbon Nanotube Field Effect Transistors) consists of channel made by a single-semiconducting CNT and the "gate" is separated from the channel by a thin insulator film placed on a nanotube. Fig.8 illustrates one such CNT transistors. It consist of semiconducting CNT of 1nm diameter separating two metal electrodes at the top and a silicon (Si) surface coated with silicon dioxide(SiO_2)[43,44].When an electric field is applied to the silicon through the gate , electrodes turn on and off the flow of currents across the CNT by controlling the movement of charge carriers onto it.

The CNTFET are reported to have high transconductance, high carrier velocity and the p-CNTFET produces ~1500 A/m of the on current per unit width at a gate overdrive of 0.6 V while p-MOSFET produces ~500 A/m at the same gate voltage.

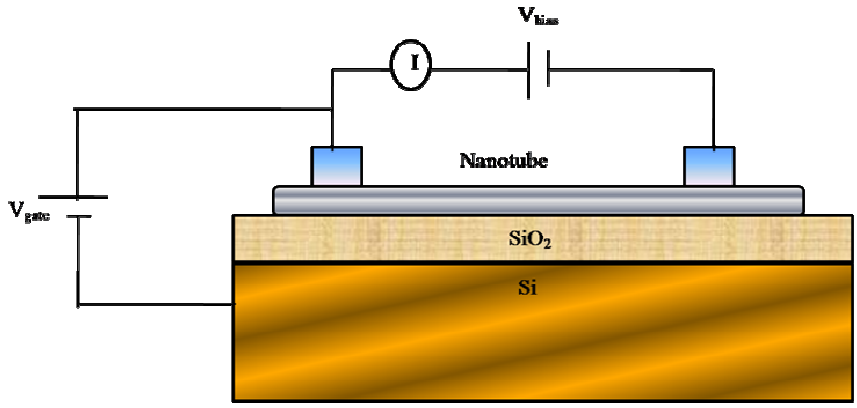

Fig. 8. Schematic of carbon nanotube transistor

1.4.2: Hydrogen Storage:

The faster growing demand of alternative sources of energy in comparison to rapid depleting fossils fuels can be met with hydrogen. Hydrogen is a versatile energy source that is easy to produce with high utilization efficiency and more importantly it is environment compatible. However, one of the problems with hydrogen is its storage as liquid hydrogen is expensive and compressed hydrogen is dangerous.

CNT have an ability to absorb high-density hydrogen at room temperature and atmospheric pressure. Dillon *et al.* [45] found that hydrogen is absorbed by SWCNT via the interaction of chemical bonds of hydrogen with the Vander-wall forces of SWCNT. They showed that

hydrogen condensed to density of 5-10 wt% inside narrow SWCNT of 12 A. Chen *et al.* [46] have reported thatCNT doped with lithium (Li) and potassium (K) had a high uptake of 20 wt% and 14 wt% ,respectively under ambient conditions.

1.5 : Synthesis Methods of CNT

CNTs can be synthesized through various techniques. Some of those techniques are detailed below.

1.5.1 : Arc Discharge Method:

In an electric arc-discharge method [47], the arc is produced in helium atmosphere between two electrodes in a reactor. Both the cathode and anode rods are made of graphite. The anode is filled with mixture of metallic catalyst and graphite powder. When a high current is passed through an anode and cathode, the plasma of helium gas created by high currents, evaporates the carbon atoms. This method produces large quantity of SWCNTs along with MWCNTs and fullerenes. Due to high growth temperature, the technique produces crystalline CNTs with high yield but it is difficult to produce aligned CNTs. Bethune *et al.*[48] have generated SWCNT in the form of soot when a graphite rod used as an anode was doped with metal catalyst as such as iron (Fe) or cobalt (Co) .

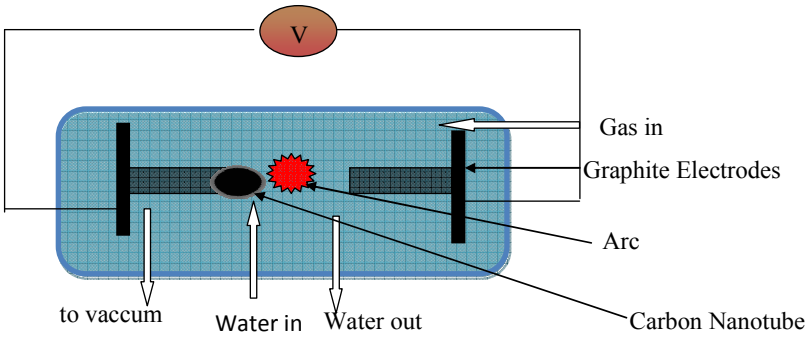

Fig. 9. A schematic of arc–discharge method to grow CNT

1.5.2: Laser Ablation Method:

In this technique, a laser beam is focused onto a metal-graphite-composite target of diameter 6-7mm[49].The target is made of a graphite metal composite with 0.5 atomic percent of nickel (Ni) and cobalt (Co). During the laser ablation method, the furnace is heated to a temperature of 1200 ^{0}C and the laser beam ablates the graphite target. A flow of inert gas is introduced in the furnace to carry the grown nanotubes to the cold finger. This technique produces high quality single walled carbon nanotube (SWCNT).

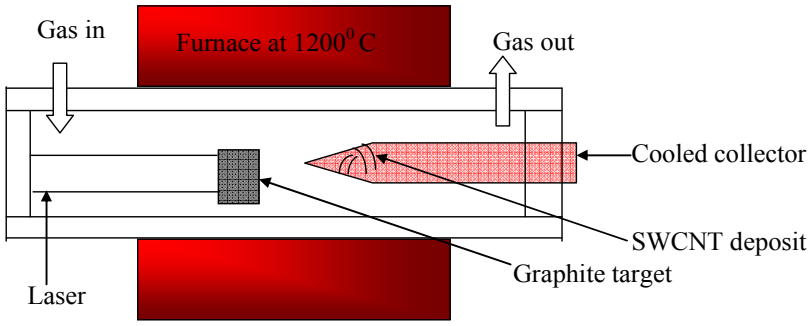

Fig. 10. Schematic of laser ablation method to grow CNT

1.5.3: Chemical Vapor Deposition (CVD) Method:

In CVD, since heat is the main source for process reactions to occur, it is often referred to as thermal CVD (T-CVD) [50]. The temperature ranges from 400 ^{0}C to 1000 ^{0}C for production of nanostructures in T-CVD. In catalytic CVD (C-CVD), the catalyst helps in the decomposition of vapor species at the catalyst particle surface. C-TCVD has recently been used to synthesize MWCNT [51] and SWCNT [52]. In this, the catalyst-particle

is heated to higher temperatures in a furnace where hydrocarbon gas decomposes, diffuses, and finally incorporates into catalyst particle to form nanostructures [53].

The following steps were proposed by Baker *et al*.[54] to occur during growth of nanostructures through CVD:

1)The hydrocarbon gas (acetylene or methane) first decomposes and then adsorps on the metal catalyst surface.

2)The carbon species diffuses through catalyst particle and precipitates on the rear face to form the body of the filament. In this case, diffusion is the rate determining step.

3)An excess accumulation of carbon occurs on the front surface since the supply of carbon onto the front face is faster in order to prevent physical blocking of the active surface. In this case, carbon forms the skin around the main filament body.

4) This process continues until the tip of the metal catalyst particle is deactivated. The deactivation or "poisoning" of catalyst particle occurs due to the carbon formed around the catalyst particle and prevents the hydrocarbon gas from further reaching the catalyst particle and thereby finally terminating the growth.

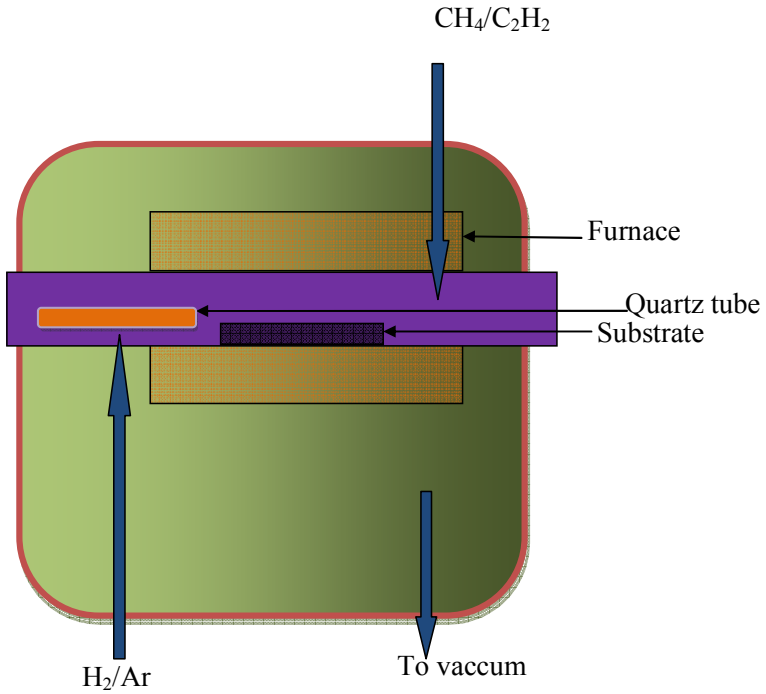

Fig. 11. Schematic of chemical vapor deposition (CVD) technique to grow CNT

There are two different types of CNT growth seen in catalyst-aided CVD mainly:

a) Tip-type growth modes: In this mode, the catalyst is detached from the substrate and goes at the tip of the growing nanostructure.

b) Base-type growth modes: In this, catalyst-particle remains at the base of the substrate.

The reason for two different types of growth modes has been proposed by Baker *et al.* [55]. According to Baker *et al.* [55], two growth mechanism occurs due to the interaction of catalyst with the substrate. The interaction is characterized by the contact angle of the catalyst with the support surface at a given growth temperature. A large contact angle corresponds to a weak interaction, while a small angle is indicative of strong interaction. It has been reported that nickel (Ni) on silicon-dioxide (SiO_2) has a large contact angle at 700 °C i.e., a weak interaction between the

substrate and catalyst such that CNT precipitation across the catalyst surface pulls the catalyst particle up and the tip-type growth of CNT is observed [56]. Whereas when cobalt(Co) or iron (Fe) were deposited on silicon(Si) [57-59] ,a small contact angle between the substrate and catalyst indicates strong interaction such that CNT precipitation across the catalyst surface cannot overcome the strong interaction between the catalyst and substrate and catalyst particle remains at the base and base-type growth was observed.

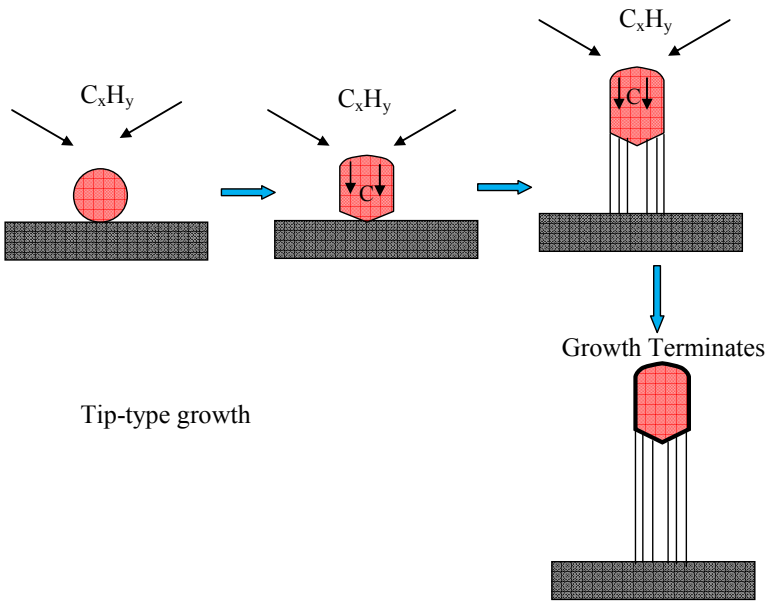

Fig. 12. Representation for tip-type growth of CNT

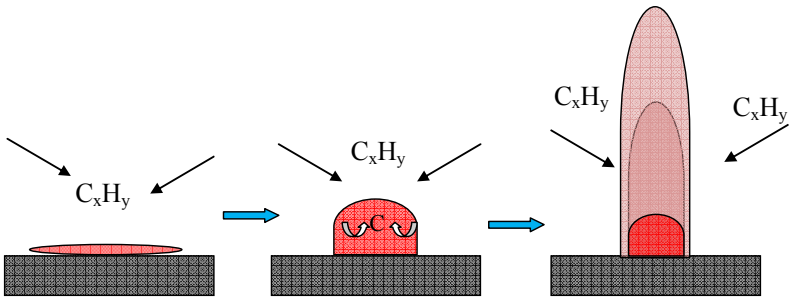

Fig. 13. Representation for base-type growth of CNT

1.5.4: Plasma Enhanced Chemical Vapor Deposition (PECVD) Method:

PECVD uses gaseous sources as in CVD but in CVD, thermal energy is used to activate the gas [53]. In PECVD, electron impact processes are the main source for activation of gas. In PECVD, since electron undergoes collisions, at lower pressures the electron temperature is higher than the gas temperature hence the entire system is not heated to higher temperatures as in conventional CVD.

In PECVD, there is a discharge chamber in which hydrocarbon gas (C_2H_2/CH_4), carrier gas (Ar, NH_3), etching gas (H_2) is introduced by mass flow controllers. A catalyst is placed over substrate. The different input power sources such as direct-current (dc PECVD), hot-filament dc (HF-dc PECVD), magnetron type radio frequency (rf PECVD), inductively coupled plasma(ICP- PECVD), microwave (M-PECVD), electron

cyclotron resonance (ECR- PECVD), hollow cathode glow discharge (HCGD), and corona discharge plasma etc. are used to initiate dissociation of gases[53].

1.5.4.1: Direct-current plasma-enhanced chemical-vapor deposition (dc- PECVD):

In dc-PECVD, a conductive substrate is placed over a heater, which acts as a cathode, and the gas showerhead for introducing gas into the chamber, serves as anode [53, 60-66]. Merkulov *et al.* [50] have successfully prepared vertically aligned carbon nanofibres(VACNF) using dc-PECVD. Different techniques like evaporation, sputtering, electrode plating are used for preparing catalyst. In this technique, the vacuum chamber is evacuated to desired pressures before introducing ammonia (NH_3) gas. The catalyst nanoparticle is formed as a result of pretreatment by ammonia plasma, which acts as necessary seeds for growth of VACNFs. One major drawback of this technique is the requirement of conductive substrate [53].

1.5.4.2:Radio-frequency plasma-enhanced chemical-vapor deposition (rf-PECVD):

In order to overcome the limitations of dc PECVD, the reactors with substrate placed over one of the electrode with an rf-source coupled to the plasma is used. Hirata *et al.* [67] have grown nanostructures by using magnetron-type rf plasma by using a magnetic field up to 340 G. The nanostructures grown were similar to VACNF grown by dc PECVD. Two different types of rf -PECVD used are capacitively coupled rf - PECVD and inductively coupled rf -PECVD. Using IC-PECVD, carbon nanofibres and nanotubes by Delzeit *et al.* [68], free standing VACNFs

by Caughman *et al.* [69] , Honda *et al.* [70] and Lee *et al*. [71] , have been synthesized.

1.5.4.3: Microwave plasma-enhanced chemical-vapor deposition (MPECVD):

High frequency fields up to 2.45GHz are used in this technique. The highly energetic electrons with larger number density, created in MPECVD increases the dissociation of gases in the chamber. The technique produces atomic hydrogen, which etches away the amorphous carbon and helps in the formation of nanostructures [53]. Using this technique, dense forest of VACNF have been synthesized by Bower *et al.* [58, 72]. The parameters used are frequency =2.45GHz, pressure=0.3 Torr, substrate bias=1000V, temperature= 825^0C, the ratio of gas flow rate of acetylene to ammonia is 10% to 30%.

Srivastava *et al*. [73] have used a 700 W, 2.45 GHz power source to synthesize high density and uniformly distributed carbon nano-petals on nickel (Ni) coated Si substrates by MPECVD technique at relatively low temperature over an area of 20x20 mm^2 using argon (Ar) and methane (CH_4) mixture as precursor gases. The schematic of the MPECVD technique as used by Srivastava *et al*. [73] is given below:

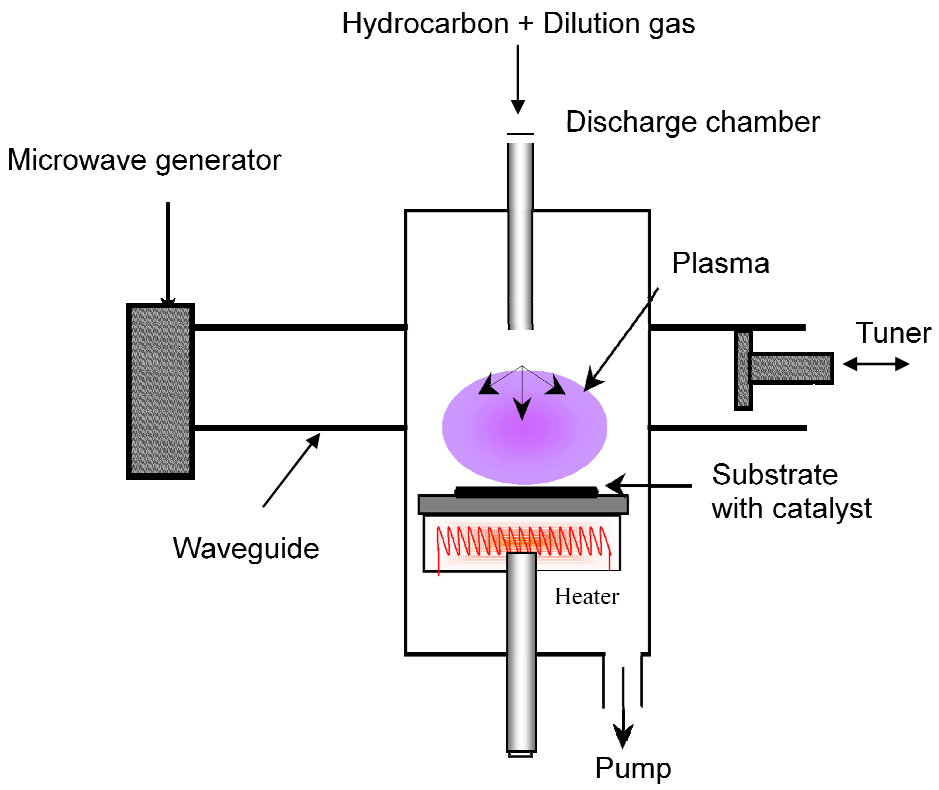

Fig. 14. Schematic of the MPECVD technique as used by Srivastava *et al*. [73]

I. Processes in a plasma environment during carbon nanostructure growth

During the growth of nanostructures by PECVD process, an important process is the formation of plasma sheath. The plasma sheath is defined as a layer in plasma with greater density of positive ions compared to its bulk counterpart, to balance the negative charge on the surface of material with which it is in contact with.

After the plasma sheath is formed some of the processes that occur are dissociation of gases within the chamber due to applied power, dissociation of catalyst particle into nanoparticles due to applied plasma power , advent of excited species to the catalyst nanoparticle surface ,

sputtering of ions on the catalyst surface, removal of undissociated molecule from catalyst surface, incorporation of carbon particles into the growing graphene layer on the surface as a result of diffusion and dissolution of carbon particles into catalyst nanoparticle and finally the chemical etching to shape the tips of nanostructures[53].

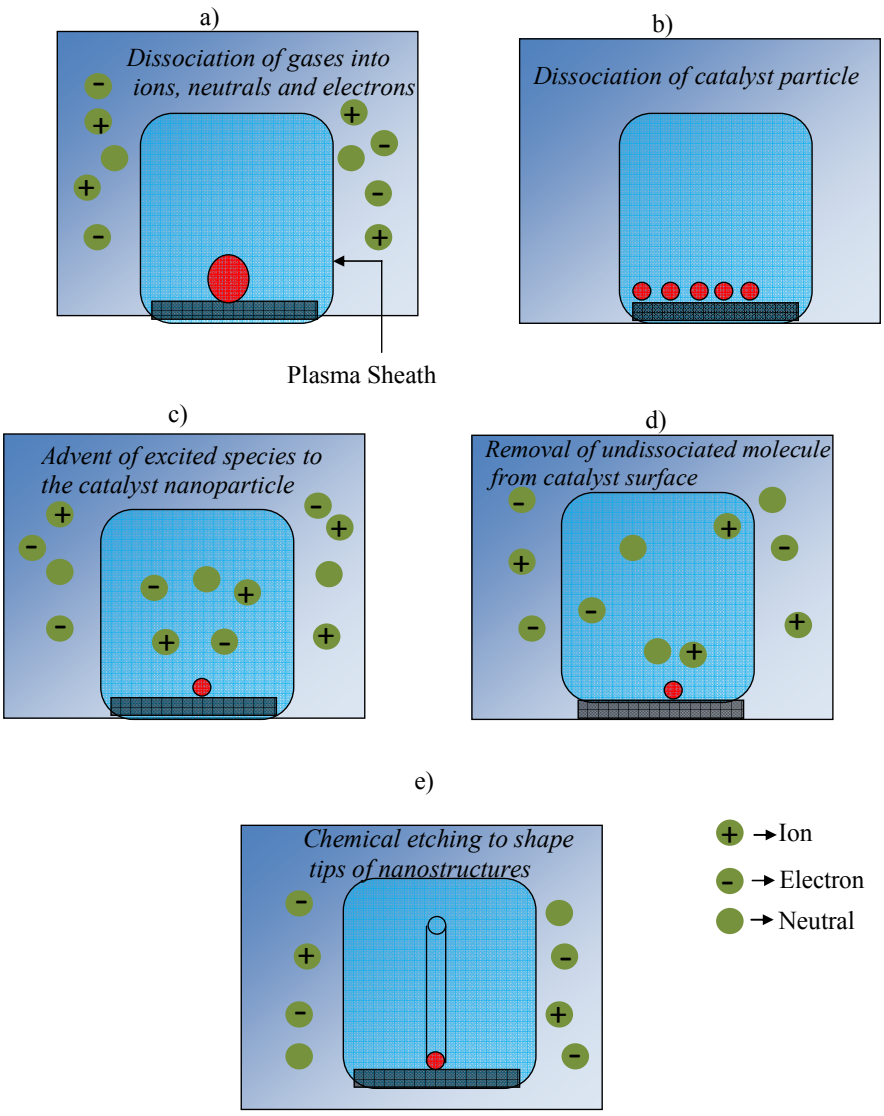

Fig.15. Illustration of the processes during CNT growth during PECVD

II. The formation of plasma sheath:

If there is a surface in contact (like substrate) with the plasma then the following processes occur: [74]

i) Electrons being more mobile than ions reach the surface faster and after some time, a negative electric potential with respect to plasma bulk is created which further repels the electrons advent towards the surface but attracts the positive ions to the surface.

ii) As more and more electrons deposit on the surface, potential further decreases thereby resulting in a stronger ion flux to the surface and much reduced electron flux.

iii) The net current flowing through the substrate becomes zero at the floating wall potential.

iv) As a result of this, an electric field that is directed from plasma bulk to the surface arises, which now accelerates the positive ions towards the substrate and repels the electrons from the surface.

v) Finally, a charge-separating region in the plasma, called as "plasma sheath" is created in a very narrow region of the substrate.

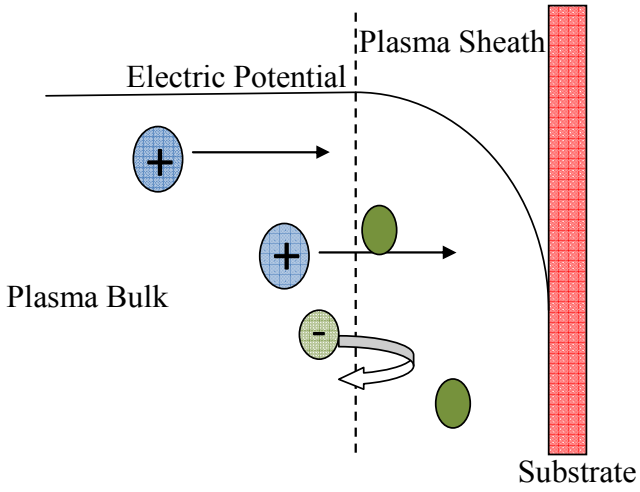

Fig. 16. Representation of plasma sheath

A simple analysis as given by Ostrikov and Xu [74], and Lieberman and Lichtenberg [75] , F.F. Chen [76] gives the plasma sheath width λ_s as,

m_i = Ion mass ,
u_0 = Initial velocity of ion ,
u = Final velocity of ion ,
$\phi(x)$= Electrostatic potential ,
n_0 = Initial number density of ions
$n_i(x)$ = Number density of ions at a position x,
ε_0 = Permitivity,
e= Electronic Charge,
λ_D = Debye length,
λ_s = Plasma sheath width,

A. From Conservation of Energy:

$$\frac{1}{2}m_i u^2 = \frac{1}{2}m_i u_0^2 - e\phi(x) \qquad (1)$$

Rearranging Eq.(1)

$$u^2 = u_0^2 - \frac{2e\phi(x)}{m_i}$$

$$\frac{u^2}{u_0^2} = 1 - \frac{2e\phi(x)}{m_i u_0^2}$$

$$\frac{u(x)}{u_0} = \left(1 - \frac{2e\phi(x)}{m_i u_0^2}\right)^{\frac{1}{2}} . \qquad (2)$$

B. The Ion Continuity Equation:

$$n_0 u_0 = n_i(x)\, u(x)$$

$$n_i(x)\frac{u(x)}{u_0} = n_0.$$

Substituting the value of $\frac{u(x)}{u_0}$ from Eq.(2)

$$n_i(x)\left(1 - \frac{2e\phi(x)}{m_i u_0^2}\right)^{\frac{1}{2}} = n_0$$

$$n_i(x) = n_0\left(1 - \frac{2e\phi(x)}{m_i u_0^2}\right)^{-\frac{1}{2}} . \qquad (3)$$

C. Poisson's Equation:

$$\varepsilon_0 \frac{\partial^2\phi(x)}{\partial x^2} = e(n_e - n_i) \qquad (4)$$

Assume that the number density of electrons is very small as compared to the ions i.e., $n_e << n_i$

$$\frac{\partial^2\phi(x)}{\partial x^2} = \frac{e\left(n_e(x) - n_i(x)\right)}{\varepsilon_0}$$

Substituing $n_i(x)$ from Eq.(3) and $n_e(x) = \exp\left(\frac{e\phi}{k_B T_e}\right)$

$$\frac{d^2\phi(x)}{dx^2} = \frac{en_0}{\varepsilon_0}\left\{\exp\left(\frac{e\phi}{k_B T_e}\right) - \left(1 - \frac{2e\phi(x)}{m_i u_0^2}\right)^{-\frac{1}{2}}\right\}. \quad (5)$$

For sheath to perform its function, $n_i(x) > n_e(x)$ for all x in the sheath

$$\exp\left(\frac{e\phi}{k_B T_e}\right) < \left(1 - \frac{2e\phi(x)}{m_i u_0^2}\right)^{-\frac{1}{2}}$$

For small $|\phi|$, expanding exponential part to its first powers and binomially expanding

$$\left(1 - \frac{2e\phi(x)}{m_i u_0^2}\right)^{-\frac{1}{2}},$$

$$1 + \frac{e\phi}{k_B T_e} < \left(1 + \frac{e\phi(x)}{m_i u_0^2}\right)$$

Since $\phi < 0$,

$$\frac{1}{k_B T_e} > \frac{1}{m_i u_0^2}$$

$$u_0 > \sqrt{\frac{k_B T_e}{m_i}}$$

$$u_B = \text{Bohm Velocity} = \sqrt{\frac{k_B T_e}{m_i}}$$

This u_B is known as Bohm velocity.

For longer time scales and when applied potential is large, the ion conservation energy and flux conservation reduces to

$$\frac{1}{2} m_i u^2(x) = -e\phi(x) \quad (6)$$

$$J_0 = en_i(x)u(x) \quad (7)$$

Solving for J_0 which is the ion current in the sheath

$$n_i(x) = \frac{J_0}{e}\left(\frac{-2e\phi}{m_i}\right)^{-\frac{1}{2}} \tag{8}$$

Now, Poisson's equation is

$$\frac{\partial^2\phi(x)}{\partial x^2} = -\frac{en_i(x)}{\varepsilon_0}$$

Substituting $n_i(x)$from Eq.(8) Poisson's eq. becomes

$$\frac{\partial^2\phi(x)}{\partial x^2} = \frac{J_0}{\varepsilon_0}\left(\frac{-2e\phi}{m_i}\right)^{-\frac{1}{2}} \tag{9}$$

Multiply Eq.(9) by $\frac{d\phi(x)}{dx}$ and integrate from 0 to x,we get

$$\frac{1}{2}\left(\frac{d\phi(x)}{dx}\right)^2 = 2\frac{J_0}{\varepsilon_0}\left(\frac{2e}{m_i}\right)^{-\frac{1}{2}}(-\phi)^{\frac{1}{2}}.$$

Since $\frac{d\phi(x)}{dx} \approx E \approx 0$ and $\phi(x) \approx 0$ at x=0

Taking negative square root, since $\frac{d\phi(x)}{dx}$ is negative and again integrating from 0 to x , we get

$$-\phi^{\frac{3}{4}} = \frac{3}{2}\left(\frac{J_0}{\varepsilon_0}\right)^{\frac{1}{2}}\left(\frac{2e}{m_i}\right)^{-\frac{1}{4}}x$$

Let $\phi = -V_0$ and $x = \lambda_s$ (plasma sheath width), we get J_0 as

$$J_0 = \frac{4}{9}\varepsilon_0 \left(\frac{2e}{m_i}\right)^{\frac{1}{2}} \frac{V_0^{\frac{3}{2}}}{\lambda_s^2}$$

Now, substituting for $J_0 = en_s u_B$ and u_B = Bohm Velocity = $\sqrt{\frac{k_B T_e}{m_i}}$ in J_0

$$\lambda_s = \frac{\sqrt{2}}{3}\lambda_D \left(\frac{2eV_0}{k_B T_e}\right)$$

III. Substrates and Catalysts:

Substrates play a very important role in the growth of carbon-based nanostructures by PECVD technique. It acts as a medium between the nanostructure and catalyst. The temperature of the substrate is a crucial parameter during PECVD growth of nanostructures. Mainly silicon (Si) and silicon dioxide (SiO_2) are used as substrates. The catalyst helps in breaking bonds and in adsorbing carbon at its surface. The carbon diffuses into catalyst nanoparticle to form carbon nanostructures [77]. Nickel (Ni), iron (Fe), cobalt (Co) etc., are used as catalyst. A brief description of the combination of catalyst and substrate, technique and resulting nanostructure is tabulated in Table 2.

S. No.	Substrate	Catalyst	Technique	Resulting Nanostructures
1.	Si	Co	MPECVD	CNF[58]
2.	Si	Co ,Fe, Ni	MPECVD	VACNF[78]
3.	Si	Co, Ni	MPECVD	VACNF[79]
4.	SiO_2 on Si	Fe	PECVD	VACNF[56]
5.	Si	Fe, Ni	MPECVD	CNF[80]
6.	Si	Fe-Ni-Cr, Ni	MPECVD	CNF[81]
7.	Si	Co	MPECVD	CNF[82]

Table 2. Shows various combinations of substrate-catalyst to produce nanostructures using PECVD

IV. Process parameters during PECVD growth of carbon nanostructures:

a) Type of hydrocarbon gas:

Acetylene (C_2H_2) and methane (CH_4) are commonly used hydrocarbon gas during the growth of carbon nanotubes by PECVD process. The hydrocarbon gas is the source of carbon, necessary for the growth of CNTs. CNT fabrication using acetylene as a feed gas has been done by Loffler *et al.* [83] , Dubosc *et al.* [84] , Han *et al.* [85] , Kim *et al.* [86] whereas CNT fabrication using methane as feed gas has been achieved by Honda *et al.* [87] , Choi *et al.* [88] .

The advantages of acetylene as a feed gas over methane are:

1) The time required for growth of CNTs is reduced.
2) Vertical alignment and uniformity of CNTs grown from acetylene is better.
3) CNTs at comparatively low temperature are obtained when acetylene is used as a hydrocarbon source gas.

The disadvantages of methane over acetylene as a feed gas are:

1) The methane gas adsorbs on the catalyst particle at higher temperatures compared to acetylene.
2) Since only high purity methane is acceptable for this synthesis and methane of high purity is relatively expensive.

b) Etching gas:

Hydrogen (H_2) and ammonia (NH_3) are the commonly used etching gases in the growth of carbon nanotubes. The etching process of ammonia and hydrogen can be either to fragment the catalyst film into nanoparticles and in removing the amorphous carbon from the CNTs to shape CNT tips. The role of hydrogen in the etching of CNT has been described by

Choi *et al.* [88] , Chen *et al.* [89] , Zhang *et al.* [90] , Lin *et al.* [91] , Wang *et al.* [92] among others. Lin *et al.* [91] have reported that the etching of amorphous carbon by atomic hydrogen is promoted by high energy ions. Srivastava *et al.* [93] have reported that the oxide films without the H_2 plasma pretreatment or treated for lesser time resulted in CNT films with high percentage of carbonaceous particles and with embedded particles/ nanorods distributed discontinuously in the cavity of the nanotubes.

Ammonia (NH_3) is also used in etching either the catalyst particle or the CNTs. Chhowalla *et al.* [56] have reported that NH_3 was required to fragment the thick catalyst layer. Teo *et al.* [94] have reported that by suitably adjusting the acetylene (C_2H_2) to ammonia (NH_3) gas ratios, the undesirable surface carbon on the non-patterned areas of the substrate was eliminated. Kim *et al.* [95] have established the balance between the thickness of catalysts and the NH_3 etching time as one of the most important parameters in growing CNTs by PECVD.

c) Plasma Power:

Plasma power plays a crucial role during the growth of CNTs. The electric field within the plasma sheath increases as plasma power is increased. This enhanced sheath electric field can be used in the alignment of CNTs. Because with increase in plasma power the gas ionizes more that creates more energetic plasma species. These highly energetic plasma species bombards the catalyst particle such that initially nano catalyst particles and later CNTs of smaller diameter are created. The role of plasma power has been well described by many studies. There can be many power sources like, inductively coupled power supply[68],radio frequency power supply [96], high frequency dc power

supply[97], microwave power supply [72,98] , electron-cyclotron power supply[99] etc.

The plasma power has been widely used to obtain sharp tips of CNTs. To cite a few of them, Srivastava *et al.* [73] have grown petal like nanostructured thin films and pointed that at higher microwave power , carbon petals of relatively smaller sizes were obtained. Loffler *et al.* [83] have increased the plasma power during PECVD process to sharpen the tips of CNTs. Abdi *et al.* [100] established that as plasma power was increased, size of Ni particle decreased which then resulted in CNTs of smaller diameters. Choi *et al.* [101] have established that the growth rate and the density of CNTs increase with the reduction of the rf power density.

d) Substrate temperature:

Substrate temperature is identified as an important parameter in controlling the growth of CNTs by PECVD process. There have been works where an external heating source is used for attaining desired substrate temperatures for nanostructure growth. PECVD has an advantage of removing the use of external heating source because the ions bombarding the surface are sufficient for raising the substrate temperatures to desired values required for nano structure growth. The increase in substrate temperature increases the growth rate of CNTs and that has been reported by Loffler *et al.* [83] , Han *et al*. [102] , Baratunde *et al.* [103] , Lee *et al.* [104] , and others. Mehdipour *et al.* [105] have reported that the growth rate as a function of substrate temperature increases as ion and electron temperatures are increased.

e) Carrier gas:

A varied number of carrier gases like argon (Ar), ammonia (NH_3), nitrogen (N_2), and hydrogen (H_2) are used in the growth of CNTs. Different gases behave differently during the growth of CNTs and have varied effects on the growth profiles of CNTs. The growth rate of CNT increases in Ar gas environment has been observed by Toussi *et al.* [106] , Kayastha *et al.* [107] , whereas H_2 decreases the growth of CNT has been reported by Kayastha *et al.* [107] , Yap *et al.* [108] , Reynolds *et al.* [109]. Ammonia provides a better growth environment for CNTs than N_2 is suggested by Mi *et al.* [110] and Mi and Jia [111].

The flow rate of the gas also affects the growth of CNT. It is reported [109,112] that as the flow rate of carrier gas increases, the growth rate of CNT also increases corresponding to the particular carrier gas.

The flow rate of gas as given by Denysenko *et al.* [112]

$I_j\left(\frac{cm^{-3}}{s}\right) = \frac{4.4\times10^{17} J_j[sccm]}{V}$ is the inflow for species j. J_j is the gas inlet flow rate[112] (in standard cubic centimeter per minute) and V is the volume of the chamber(in cm^3) [112] .

$O_j\left(\frac{cm^{-3}}{s}\right) = \frac{n_j\, \nu_{pump}}{V}$ is the outflow for species j [112] . ν_{pump} is the pumping rate in cm^3/s . n_j is the number density of species j in cm^{-3}.

f) Plasma parameters

The electron density (n_e) and temperature (T_e), ion density (n_i) and temperature (T_i) are regarded as the plasma parameters. The plasma parameters immensely affects the nanostructure growth.

Srivastava *et al.* [73] have synthesized carbon films via MPECVD and they found that the increase in the microwave power causes more ionization of the gas, which increases the density of plasma species of

relatively higher energy and at this higher density, increased nucleation of graphitic clusters occurs that leads to the formation of carbon petals of relatively smaller size. Lee *et al.* [113] have revealed that the plasma treatment can modify the surface morphology and enhance the field emission characteristics of the CNTs.

Denysenko *et al.* [114] have shown that at low substrate temperatures (>1000 K), the atomic hydrogen and ion fluxes from the plasma can strongly affect the nanotubes growth. Levchenko *et al.* [115] have suggested that the plasma-aided process is a very efficient tool to control the nanotube aspect ratio, in comparison to the neutral flux deposition primarily because of the controllable deposition of ionic building blocks (BBs) and increased influx directly onto the nanotube lateral surfaces.

1.6: Effect of plasma on the field emission properties from CNT

Since from the above discussions it is amply clear that plasma has huge influence on the growth of CNT therefore plasma and the associated parameters can be modeled to obtain desired shapes and structures of CNT. Now, there are a large number of areas where CNT finds applications like in flat panel displays, field effect transistors, solar cells, hydrogen storage, drug delivery etc. but the present thesis aims to study the field emission characteristics of CNT. Although, the field emission occurs in vacuum but since plasma affects the CNT growth it is safe to say that plasma does play a role in field emission from CNT. There are studies that highlight the effect of plasma treatment on the field emissions from CNT. Different plasma treatments have different effects on the field emissions from CNT like carbon tetra fluoride (CF_4) plasma treatment hamper the field emission from CNT films [116], an external rf plasma irradiation of argon (Ar) gas to well- aligned MWCNTs enhances the

field emission current[117], plasma treated CNT films were reported with superior field emission FE behavior[118], among CNTs treated with the H_2, Ar and CF_4 ,the field emission was highest for CNTs treated with H_2 plasma [113].

The work in the present thesis is evaluation of the dependence of growth profile (namely the radius and height) of CNT on the plasma parameters for CNT grown with and without catalyst and then through the results obtained finding a rough estimate of the variation of field enhancement factor with plasma parameters.

1.7: Objectives and organization of thesis

Since from the above discussion it is evident that the growth of CNT in plasma is a complex process and the catalyst plays a vital role during the growth of CNT.

The inclusion of catalyst into the discussion provides a better insight into the processes that occur during the growth of CNT in a plasma medium. The formation of plasma sheath, adsorption , desorption of plasma species on catalyst-substrate surfaces, thermal dissociation ,dehydrogenation ,bulk and surface diffusion of the growth species on catalyst-substrate surfaces and various other processes needs to be studied for the growth of CNT in a plasma medium. The objectives of the present thesis therefore are to study the effect of plasma parameters and catalyst on the growth and subsequent estimation of field emission properties of carbon nanotubes. The thesis is organized to provide a comprehensive and rigorous study on the growth of CNT in a plasma medium and effects of plasma parameters and catalyst on the CNT growth and consequently the field emission properties of CNT.

Chapter 1 reviews as to what is CNT, its types, properties of CNT and the various techniques through which it can be synthesized. The processes and various parameters in the PECVD technique are discussed in detail. The objectives and organization of the thesis is also included.

Chapter 2 discuses the growth of CNT by condensation in plasma. The chapter discusses various processes in plasma during the growth of CNT by condensation. A theoretical model is developed in this regard comprising equations for kinetics and energy balance of the plasma species, and the growth rate equation of CNT.

Chapter 3 describes the growth of spherical CNT tip and cylindrical CNT surfaces, separately using the model developed in Chapter 2. The number density and energy balance equations for plasma species are solved to study the dependence of radius of CNT on plasma parameters (electron density and temperature, ion density and temperature). By obtaining the dependence of radius of spherical CNT tip and cylindrical CNT surfaces on plasma parameters, the consequent variation in the field enhancement factor of the CNT is also estimated.

Chapter 4 describes the effect of negative ions on the growth of CNT in a plasma medium through condensation process. In this respect, the number density balance of plasma species and negative ions and their energy balance are solved to find the dependence of radius of CNT on the relative density of negative ions. The dependence of field emission factor of the CNT on the negative ion parameter is also approximated.

Chapter 5 discusses the growth of CNT by condensation in different plasma mediums. The parameters corresponding to different plasma mediums are fed into plasma kinetics and growth equations to study the

evolution of radius of spherical CNT tip placed over cylindrical surfaces in different plasmas. The field enhancement factor for CNTs obtained in different plasma medium is also analyzed.

Chapter 6 describes the effect of plasma compositions on the growth and field emission properties of carbon nanotubes. Two types of positive ions with heavy to light ion ratio of 11.5 are considered in the plasma. The number density balance and growth rate equation in the presence of both light and heavy positive ions are solved and the fractional light ion concentration is varied to study its effects on radius of spherical CNT tip and field emission behavior of CNTs is estimated.

Chapter 7 includes the modeling of CNT growth on a catalyst –substrate surface in reactive plasma medium. A theoretical model for the growth of CNT assisted by catalyst in the plasma is developed. The model developed includes the possible processes that occur during the CNT growth. The plasma sheath kinetics, adsorption, desorption, dehydrogenation, thermal dissociation, diffusion, accretion and other processes are incorporated to develop the model. The model possibly underlines the mechanism behind the CNT growth in an environment where hydrocarbon, etching ,and carrier gases produces numerous species in plasma via varied complex processes that traverse through plasma sheath to deposit on the catalyst-substrate surfaces to grow carbon nanotubes. A detailed study on the effect of plasma density and temperature, plasma power, and substrate bias on the growth profiles of the CNT is presented.

Chapter 8 discusses the effect of substrate temperature on the growth of CNT with conical tip in a plasma medium. In the present chapter, the role

of substrate temperature on the growth of CNT is reviewed and the substrate temperature is varied to understand its repercussions on the growth of CNT through the model developed in Chapter 7. The potential for the conical CNT tip is calculated and used in the growth model. The variation of height of cylindrical CNT surface and radius of conical CNT tip with substrate temperature is plotted for different plasma density and temperature and the possible reasons behind the observed effects is particularized.

Chapter 9 details the effect of different carrier gases and their flow rates on the growth attributes of CNT. The three different types of carrier gases are considered and their inflow and outflow rates into and from the chamber, respectively are included in the model along with the processes that transpires during the growth of CNT on a catalyst-substrate surface in a plasma environment. The flow rates of all the three carrier gases are varied individually to investigate their ramifications on the number density of hydrocarbon and hydrogen ions to eventually outline the consequences of flow rates on the growth profiles of CNT in different carrier gas environments.

Chapter 10 concludes and presents the future scope of the research work carried out in the present thesis.

References

[1] J. Abrahamson, P. G. Wiles, Brian L. Rhoades, Carbon **37**, 1873(1999).

[2] J. Abrahamson and P. G. Wiles, Carbon **16**, 341(1978).

[3] H. W. Kroto, J. R. Heath, S.C. O'Brien, R. F. Curl and R.E. Smalley, Nature **318**,162(1985).

[4] S. Iijima, Nature **354,** 56(1991).

[5] D.S. Bethune, C. H. Kiang, M. S. De Vries, G. Gorman, R. Savoy, J. Vazquez and R. Beyers, Nature **363**, 605(1993).

[6] S. Iijima, Nature **363**, 603 (1993).

[7]https://www.dsiac.org/resources/dsiac_journal/fall-2014/carbon-nanotubes- small-structures-big-promis.

[8] https://mardisantoso88.wordpress.com/2012/05/02/22/.

[9] https://notendur.hi.is//~egillsk/stuff/annad/Egill.Slides2.pdf .

[10] http://www.trynano.org/nanomaterials/carbon-nanotubes.

[11] https://en.wikipedia.org/wiki/Young%27s_modulus.

[12] *The Properties of Natural and Synthetic Diamond*, (edited by J. E. Fields Academic, London, 1992).

[13]W. D. J. Callister, *Materials Science and Engineering an Introduction*, (6th ed. Wiley, New York, 2003).

[14] E. W. Wong, P. E. Sheehan, and C. M. Lieber, Science **277**, 1971(1997).

[15] M. M. J. Treacy, T. W. Ebbesen, and J. M. Gibson, Nature (London) **381**,678 (1996).

[16] M. F. Yu, O. Lourie, M. J. Dyer, K. Moloni, T. F. Kelly, and R. S. Ruoff, Science **287**, 637 (2000).

[17]"Properties of Stainless Steel". Australian Stainless Steel

Development Association.

[18]"Stainless Steel – 17-7PH (Fe/Cr17/Ni 7) Material Information".

[19] S. Datta, *Electronic Transport in Mesoscopic Systems*, Cambridge University Press, London (1995).

[20]Christophe Laurent, Emmanuel Flahaut, and Alain Peigney, Carbon **48,** 2994(2010).

[21] C.J. Lee, S.C. Lyu, H-W. Kim, J.H. Lee, and K.I. Cho, Chem. Phys. Lett. **359**, 115(2002).

[22] P. L. McEuen and J-Y. Park, MRS Bulletin **29**, 272 (2004).

[23]C. Schonenberger, A. Bachtold, C. Strunk, J. P. Salvetat, and L. Forro, Appl. Phys. A: Mater. Sci. Process. **A69**, 283 (1999).

[24] A. Thess,R. Lee, P. Nikolaev, H. Dai, P. Petit, J. Robert,C. Xu, Y. Hee Lee, S. Gon Kim, A. G. Rinzler, D. T. Colbert, G. E. Scuseria, D. Tomanek, J. E. Fischer ,and R.E. Smalley, Science **273**, 483 (1996).

[25] N. Hamada, S. Sawada ,and A. Oshiyama, Phys. Rev. Lett. **68**, 1579 (1992).

[26] J. Bernholc, D. Brenner, M. Buongiorno Nardelli, V. Meunier, and C. Roland, Annu. Rev. Mater. Res. **32**, 347(2002).

[27]J. Hone, B. Batlogg, Z. Benes,A. T. Johnson, J. E. Fischer, Science **289**,1730 (2000).

[28]J. C. Lasjaunias, K. Biljaković, Z. Benes, J. E. Fischer, and P. Monceau , Phys. Rev. B. **65**, 113409(2002).

[29]Ari Mizel, Lorin X. Benedict, Marvin L. Cohen, Steven G. Louie, A. Zettl,Nasser K. Budraa, and W. P. Beyermann**,** Phys. Rev. B. **60**,3264(1999).

[30]W. Yi, L. Lu, Zhang Dian-lin, Z. W. Pan, and S. S. Xie , Phys. Rev.

B **59**,R9015(1999).

[31]S. Berber , Y. K. Kwon , D. Tomanek , Phys. Rev. Lett. **84**, 4613(2000).

[32] M.C. Llaguno, J. Hone , A.T. Johnson, J.E. Fischer, arXiv preprint cond- mat/0108142 (2001).

[33]P. Kim, L. Shi, A. Majumdar, and P. L. McEuen Phys. Rev. Lett. **87**, 215502(2001).

[34]O. Cespedes, M. S. Ferreira, S. Sanvito, M. Kociak and J. M. D. Coey , J. Phys. Cond. Matt. **16**, L155(2004).

[35]R. H. Fowler and L. Nordheim, Proc. R. Soc. London Ser. A **119**, 173 (1928).

[36]G. C. Kokkorakis, A. Modinos, and J. P. Xanthakis, J. Appl. Phys. **91**, 4580 (2002).

[37]G. C. Kokkorakis, J. A. Roumeliotis, and J. P. Xanthakis, J. Appl. Phys. **95**, 1468 (2004).

[38]H. C. Miller, J. Appl. Phys. **38**, 4501 (1967).

[39]X Q. Wang, M. Wang, P. M. He ,and Y. B. Xu, J. Appl. Phys. **96**,6752 (2004).

[40]X.Q. Wang, M. Wang, Z.H. Li, Y.B. Xu, and P.M. He, Ultramicroscopy **102**,181(2005).

[41]V. Filip, D. Nicolacscu, M. Tanemura, and F. Okuyama, Ultramicroscopy **89**,39 (2001) .

[42] W. B. Choi, D. S. Chung, J. H. Kang, H. Y. Kim, Y. W. Jin, I. T. Han, Y. H.Lee, J. E. Jung, N. S. Lee, G. S. Park and J. M. Kim, Appl. Phys. Lett. **75**, 3129(1999).

[43]A.P. Graham, G.S. Duesberg, W. Hoenlein, F. Kreupl, M. Liebau, R. Martin ,B. Rajasekharan, W. Pamler, R. Seidel, W. Steinhoegl, E.

Unger, Appl. Phys. A **80**,1141(2005).

[44]Ali Javey , Jing Guo , Damon B. Farmer , Qian Wang , Erhan Yenilmez , Roy G. Gordon , Mark Lundstrom , and Hongjie Dai, Nano Lett. **4**,1319(2004).

[45]A. C. Dillon, K. M. Jones, T. A. Bekkedahl, C. H. Kiang, D. S. Bethune and M. J. Heben, Nature **386**, 377(1997).

[46] P. Chen , X. Wu ,J. Lin , K. L. Tan ,Science **285**,91(1999).

[47] E.G. Gamaly, and T. W. Ebbesen, Phys. Rev. B **52** ,2083 (1995).

[48] D. S. Bethune, C. H. Kiang, M. S. De vries, G. Gorman, R. Savoy, J. Vazquez , and R. Beyers, Nature **363**, 605 (1993).

[49] T. Guo, P. Nikolaev, A. Thess, D.T. Colbert, R.E. Smalley ,Chem. Phys. Lett. **243**,49(1995).

[50]V. I. Merkulov, D. K. Hensley, A. V. Melechko, M. A. Guillorn, D. H.Lowndes, and M. L. Simpson, J. Phys. Chem. B **106**, 10570 (2002).

[51]W. Z. Li, S. S. Xie, L. X. Qian, B. H. Chang, B. S. Zou, W. Y. Zhou, R. A. Zhao, and G. Wang, Science **274**, 1701 (1996).

[52]A. M. Cassell, J. A. Raymakers, J. Kong, and H. J. Dai, J. Phys. Chem. B **103**, 6484 (1999).

[53]A. V. Melechko, V. I. Merkulov, T. E. McKnight, M. A. Guillorn, K. L.Klein, D. H. Lowndes, and M. L. Simpson, J. Appl. Phys. **97**, 041301(2005).

[54] R. T. K. Baker, M. A. Barber, R. J. Waite, P. S. Harris, and F. S. Feates, J. Catal. **26**, 51 (1972).

[55]R. T. K. Baker, Carbon **27**, 315 (1989).

[56]M. Chhowalla K. B. K. Teo, C. Ducati, N. L. Rupesinghe, G. A. J.

Amaratunga, A. C. Ferrari, D. Roy, J. Robertson ,and W. I. Milne, J. Appl. Phys. **90**, 5308 (2001).

[57]S. S. Fan, M. G. Chapline, N. R. Franklin, T. W. Tombler, A. M. Cassell, and H. J. Dai, Science **283**, 512 (1999).

[58]C. Bower, O. Zhou, W. Zhu, D. J. Werder, and S. H. Jin, Appl. Phys. Lett. **77**, 2767 (2000).

[59]J. I. Sohn, S. Lee, Y. H. Song, S. Y. Choi, K. I. Cho, and K. S. Nam, Appl. Phys. Lett. **78**, 901 (2001).

[60]V. I. Merkulov, D. H. Lowndes, Y. Y. Wei, G. Eres, and E. Voelkl, Appl. Phys. Lett. **76**, 3555 (2000).

[61]V. I. Merkulov, A. V. Melechko, M. A. Guillorn, D. H. Lowndes, and M. L. Simpson, Appl. Phys. Lett. **79**, 2970 (2001).

[62]Y. Y. Wei, G. Eres, V. I. Merkulov, and D. H. Lowndes, Appl. Phys. Lett. **78**, 1394 (2001).

[63]V. I. Merkulov, M. A. Guillorn, D. H. Lowndes, M. L. Simpson, and E. Voelkl, Appl. Phys. Lett. **79**, 1178 (2001).

[64] K. B. K. Teo, M. Chhowalla, G. A. J. Amaratunga, W. I. Milne, G. Pirio, P.Legagneux, F. Wyczisk, J. Olivier and D. Pribat, J. Vac. Sci. Technol. B **20**,116 (2002).

[65] K. B. K. Teo, S-B Lee, M. Chhowalla, V. Semet, Vu Thien Binh, O. Groening, M. Castignolles, A. Loiseau, G. Pirio, P. Legagneux, D. Pribat, D. G. Hasko, H. Ahmed, G. A. J. Amaratunga and W. I. Milne, Nanotechnology **14**, 204 (2003).

[66]M. Tanemura, K. Iwata, K. Takahashi, Y. Fujimoto, F. Okuyama, H. Sugie, and V. Filip, J. Appl. Phys. **90**, 1529 (2001).

[67]T. Hirata, N. Satake, G. H. Jeong, T. Kato, R. Hatakeyama, K. Motomiya, and K. Tohji, Appl. Phys. Lett. **83**, 1119 (2003).

[68]L. Delzeit, I. McAninch, B. A. Cruden, D. Hash, B. Chen, J. Han, and M. Meyyappan, J. Appl. Phys. **91**, 6027 (2002).

[69]J. B. O. Caughman, L. R. Baylor, M. A. Guillorn, V. I. Merkulov, D. H. Lowndes, and L. F. Allard, Appl. Phys. Lett. **83**, 1207 (2003).

[70]S. Honda, M. Katayama, K. Y. Lee, T. Ikuno, S. Ohkura, K. Oura, H. Furuta, and T. Hirao, Jpn. J. Appl. Phys. Part 2 **42**, L441 (2003).

[71]Kuei-Yi Lee, Mitsuhiro Katayama, Shin-ichi Honda, Takashi Kuzuoka,Takashi Miyake, Yasuhiro Terao, Jung-Goo Lee, Hirotaro Mori, Takashi Hirao and Kenjiro Oura, Jpn. J. Appl. Phys. Part 2 **42**, L804 (2003).

[72]C. Bower, W. Zhu, S. H. Jin, and O. Zhou, Appl. Phys. Lett. **77**, 830 (2000).

[73]S. K. Srivastava, A. K. Shukla, V. D. Vankar, and V. Kumar, Thin Solid Films **492**, 124 (2005).

[74]K. Ostrikov and S. Xu, *Plasma Aided Nanofabrication: From Plasma Sources to Nanoassembly* (Wiley-VCH, Weinheim, Germany, 2007).

[75]M. A. Lieberman and A. J. Lichtenberg, *Principles of Plasma Discharges and Materials Processing* (Wiley Interscience Publication, USA, 1994).

[76] F.F. Chen, *Introduction to Plasma Physics and Controlled Fusion*(Plenum,New York,1984).

[77] M. S. Kim, N. M. Rodriguez, and R. T. K. Baker, J. Catal. **131**, 60 (1991).

[78]W. Hofmeister, W. P. Kang, Y. M. Wong, and J. L. Davidson, J. Vac. Sci. Technol. B **22**, 1286 (2004).

[79]H. Sato, H. Tagegawa, and Y. Saito, J. Vac. Sci. Technol. B **21**, 2564 (2003).

[80]Q. Zhang, S. F. Yoon, J. Ahn, B. Gan, Rusli, and M. B. Yu, J. Phys. Chem. Solids **61**, 1179 (2000).

[81]O. M. Kuttel, O. Groening, C. Emmenegger, and L. Schlapbach, Appl. Phys. Lett. **73**, 2113 (1998).

[82]M. Okai, T. Muneyoshi, T. Yaguchi, and S. Sasaki, Appl. Phys. Lett. **77**, 3468 (2000).

[83]R. Loffler, M. Haffner, G. Visanescu, H. Weigand, X. Wang, D. Zhang, M. Fleischer, A. J. Meixner, J. Fortagh, and D. P. Kern, Carbon **49**, 4197 (2011).

[84]M. Dubosc , S. Casimirius, M.-P. Besland, C. Cardinaud, A. Granier, J.-L. Duvail, A.Gohier, T.Minea, V.Arnal, and J.Torres, Materials for Advanced Metallization **84**, 2501(2007).

[85]Jae-Hee Han, Chong Hyun Lee,Duk-Young Jung, Chul-Woong Yang, Ji-BeomYoo, Chong-Yun Park, Ha Jin Kim, SeGi Yu, Whikun Yi, Gyeong Su Park , I.T. Han, N.S. Lee, and J.M. Kim, Thin Solid Films Proc. of the 2nd Asian Conf. on Chemical Vapour Depostion **409**,120(2002).

[86] D. Kim , S.H. Lim , A.J. Guilley , C.S. Cojocaru , J.E. Bouree , L. Vila, J.H. Ryu, K.C. Park, and J. Jang, Thin Solid Films **516**, 706(2008).

[87]Shin-ichi Honda, Mitsuhiro Katayama, Kuei-Yi Lee, Takashi Ikuno, Shigeharu Ohkura, Kenjiro Oura, Hiroshi Furuta ,and Takashi, Jpn. J. Appl. Phys. **42 Part 2, Number 4B ,** L441 (2003).

[88]Young Chul Choi, Dong Jae Bae, Young Hee Lee, and Byung Soo Lee,Gyeong-Su Park, Won Bong Choi, Nae Sung Lee, and Jong Min Kim, J. Vac. Sci. Technol. A **18**, 1864(2000).

[89] S. Y. Chen, L. W. Chang, C. W. Peng, H. Y. Miao, and Juh-Tzeng

Lue, J. Nanosci. and Nanotech. **5,** 1(2005).

[90]Guangyu Zhang, David Mann, Li Zhang, Ali Javey, Yiming Li, ErhanYenilmez, Qian Wang, James P. McVittie,Yoshio Nishi, James Gibbons, and Hongjie Dai, PNAS **102**, 16141(2005).

[91] Y. Y. Lin, H. W. Wei, K.C .Leou, H. Lin, C. H. Tung, M. T. Wei, C. Lin ,and C. H. Tsai , J. Vac. Sci. Technol B **24** ,97 (2006).

[92]Y. Y. Wang, S. Gupta, M. Liang, and R. J. Nemanich , J. Appl. Phys. **97**, 104309(2005).

[93] S. K.Srivastava, V. D.Vankar, and V.Kumar, Nano-Micro Lett. **2**, 46 (2010).

[94] K. Teo, M. Chhowalla, G. A. J. Amaratunga, W. I. Milne, D. G. Hasko, G.Pirio, P. Legagneux, F. Wyczisk, and D. Pribat, Appl. Phys. Lett. **79**, 1534 (2001).

[95]Sang-Gook Kim, Sooh-Yung Kim, and Hyung-Woo Lee, Trans. Nonferrous Met. Soc. China **21**,130(2011).

[96]Z. F. Ren, Z. P. Huang, J. W. Xu, J. H. Wang, P. Bush, M. P. Siegal, and P. N. Provencio, Science **282**, 1105 (1998).

[97]B. O. Boskovic, V. Stolojan, R. U. A. Khan, S. Haq, and S. R. P. Silva, Nat. Mater. **1**, 165 (2002).

[98]O. M. Kuttel, O. Groening, C. Emmenegger, and L. Schlapbach, Appl. Phys. Lett. **73**, 2113 (1998).

[99] C. H. Lin, H. L. Chang, C. M. Hsu, A. Y. Lo, and C. T. Kuo, Diamond Relat. Mater. **12**, 1851 (2003).

[100]Y. Abdi, E. Arzi ,and S. Mohajerzadeh, NanoMat. Nanotech. **44**, 149 (2008).

[101]Young Chul Choi, Young Min Shin, Young Hee Lee, and Byung Soo Lee Gyeong-Su Park Won Bong Choi, Nae Sung Lee and Jong

Min Kim, Appl. Phys. Lett. **76**, 2367(2000).

[102]Jae-Hee Han , Sun Hong Choi , Tae Young Lee, Ji-Beom Yoo, Chong-Yun Park , Ha Jin Kim ,In-Taek Han , Se Gi Yu , Whikun Yi , Gyeong Soo Park , MinhoYang , Nae Sung Lee, and J.M. Kim, Thin Solid Films **409**,126 (2002) .

[103]A. Cola Baratunde, B. Amama Placidus , Xu Xianfan, and S. Fisher Timothy, J. Heat Transfer **130**, 114503(2008).

[104]Yun Tack Lee ,Jeunghee Park, Young Sang Choi, Hyun Ryu ,and Hwack Joo Lee, J. Phys. Chem. B **106***,* 7614 (2002) .

[105]H. Mehdipour, K. Ostrikov, and A. E. Rider, Nanotechnology **21**, 455605 (2010).

[106]Setareh Monshi Toussi, Fakhru'l-razi, A. L. Chuah ,and A.R. Suraya, Sains Malaysiana **40**,197(2011).

[107]Vijaya Kayastha and Yoke Khin Yap, Svetana Dimovski ,and Yury Gogotsi, Appl. Phys. Lett. **85**, 3265(2004).

[108]Yoke Khin Yap , Vijaya Kayastha , Steve Hackney , Svetlana Dimovski ,and Yury Gogotsi, Mat. Res. Soc. Symp. Proc. **818,** M11.31.1 (2004).

[109]Carolyn Reynolds, Binh Duong, and Supapan Seraphin, J. Undergraduate Res. in Phys. August **23**, 27 (2010).

[110] Wanliang Mi, Jerry Yuesheng Lin, Qian Mao, Yongdan Li, and Baoquan Zhang, J. Natural Gas Chem. **14**,151(2005).

[111]Wanliang Mi and Dongmei Jia, J. Chil. Chem. Soc **55**, 153 (2010).

[112]I. B. Denysenko , S. Xu, J. D. Long, P.P. Rutkevych, N.A. Azarenkov ,and K. Ostrikov , J. Appl. Phys. **95,** 2713(2004).

[113]S. F. Lee, Y. P. Chang, and L. Y. Lee, J. Mater. Sci. Mater. Electron. **20**, 851 (2009).

[114] I. Denysenko, K. Ostrikov, M. Y. Yu, and N. A. Azarenkov, J. Appl. Phys. **102**, 074308 (2007).

[115] I. Levchenko, K. Ostrikov, J. Khachan, and S. V. Valdimirov, Phys. Plasmas **15**, 103501 (2008).

[116] Y.W. Zhu, F.C. Cheong, T. Yu, X.J. Xu, C.T. Lim, J.T.L. Thong, Z.X. Shen,C.K. Ong, Y.J. Liu, A.T.S. Wee, C.H. Sow, Carbon **43**, 395(2005).

[117] K. S Ahn, J. S Kim, C. O. Kim, J. P. Hong, Carbon **41,** 2481(2003).

[118] T. Feng, J. Zhang , Q. Li, Physica E. **36**, 28(2007).

CHAPTER 2

MODELING CARBON NANOTUBE GROWTH WITHOUT CATALYST

2.1: Brief outline of the work in the chapter

The present chapter focuses on developing a theoretical model for the growth of carbon nanotube (CNT) without catalyst. A theoretical model comprising charge neutrality, kinetics of electrons, positively charged ions, and neutral atoms and their energy balance, for the CNT growth without catalyst is developed.

2.2: Introduction

The growth mechanism of CNT in plasma environment has been an important field of research in recent years. CNT of different shapes and sizes have been synthesized in a plasma environment. Different parameters such as the growth temperature, density of participating species, plasma compositions, electric fields, etc., are reported to impact CNT growth.

Earlier studies on CNT have attributed different reasons to CNT growth. Pulse current electrochemical deposition is reported by Tu *et al.*[1] to be an effective technique for preparing nickel (Ni) nanoparticles with different nucleation site densities. Harris [2] reasoned that the precursor for multi-walled and single- walled tubes was a fullerene type soot material that contains the seed for nanotube growth.

The radius of the embryonic dust grains decreases with the number density of dust particles was investigated by Sodha *et al.* [3] in their theoretical model. Moreover, Sodha *et al*. [4] also reported that the

generation and accretion of electrons in a complex plasmas with cylindrical particles and found that for a given value of surface potential $\left(\frac{eV_S}{k_B T}\right)$, the value of the thermionic emission $\left(\frac{n_{th}}{n_0}\right)$ is higher in the case of spherical particles than cylindrical ones.

The effect of electric field on the anode sheath for the growth of aligned CNTs in glow discharge plasma is investigated and it has been reported that the nanotubes grow in those regions where electric field is enhanced due to depletion of positive ions in anode sheath [5]. Shoji *et al.* [6] have shown that the size of spherical carbon particle in methane (CH_4) plasma is determined by the balance of electric field and gravitational force acting on growing carbon particles in plasma boundary.

Nagai *et al*. [7] have reported that the particle radius initially increases with time and then approaches a saturation value in methane/argon (CH_4/ Ar) columnar plasma. The effect of plasma composition during plasma-enhanced chemical vapor deposition (PECVD) growth of CNTs has been studied by Bell *et al*. [8] and they observed that ammonia (NH_3) gas in plasma suppresses acetylene (C_2H_2) decomposition and encourages CNT formation and C_2H_2 is the dominant precursor in the growth of CNT. Moreover, Kim *et al*. [9] have shown enhanced growth of CNT in nitrogen(N_2) and ammonia (NH_3) environment and reasoned that nitrogen incorporation into the CNT wall and its cap, decreases the activation energies required for nucleation and growth of the tubular graphitic layer.

The field emission properties of carbon nanotubes are another important area of research. The current density of 10 mA/cm^2 from single walled carbon nanotubes (SWNTs) have been obtained with operating voltages

that are much lesser than other field emitters [10]. The field emission properties of CNT are affected by various factors such as plasma parameters, substitutional atoms, dimensional effects, and anode-cathode distance, etc., [11-13].

Srivastava *et al*.[11] have synthesized carbon films via microwave plasma enhanced chemical vapor deposition (MPECVD) using a mixture of methane and argon(Ar) gases on nickel (Ni) coated and silicon (Si) substrates and found that the increase in microwave power causes more ionization of the gas, which increases the density of plasma species of relatively higher energy. Moreover, increased nucleation of graphitic clusters is expected to occur, and this leads to formation of carbon petals of relatively smaller size and higher density at increased microwave power.

Zhang *et al.* [12] have studied the effect of substitutional atoms in the tip on the field emission properties of capped carbon nanotubes and found that carbon nanotube substituted with nitrogen could have improved field emission properties, as the substituted tube has lower work function and unsaturated dangling bonds at the tip.

Nilsson *et al.* [13] have studied the field emission from patterned CNT films and revealed a strong dependence of the field emission on the density and the morphology of the carbon nanotube. The low and high density films yield low current because of low emitter density and screening effects, respectively.

Xu. *et a1*. [14] have investigated the geometrical field enhancement factor β of individual nanotubes by in-situ transmission electron microscopy and a linear dependence of β on the distance d between the carbon nanotube tip and its counter anode is predicted. In this case, the

field enhancement factor β from multi-walled carbon nanotubes (MWCNTs) decreases with CNT radius as $\beta \propto r^{-\frac{1}{2}}$.

More importantly, Botti *et al.* [15] have prepared self-assembled CNTs without a catalyst via the low-velocity spraying of carbon particles on a heated silicon substrate. In this case, they have revealed that with the proper choice of deposition temperature, well aligned CNT are self-assembled from the nanosized carbon particles without a catalyst.

2.3: Theoretical Model

We consider the plasma containing electrons, positively charged ions of type A and B, and neutral atoms of type A and B. The type A refers to carbon whereas type B can be hydrogen, argon, ammonia, nitrogen, neon etc., depending on the type of plasma considered. The positively charged ions are assumed to be singly ionized. There are four ways for the growth of the CNTs in a complex plasma environment without the catalyst, e.g., cluster formation, nucleation, coagulation, and growth of embryonic nanotubes by condensation. All the four steps are important, but the present work is limited to growth of embryonic nanotubes by condensation in complex plasma. In the present section, we develop a theoretical model incorporating the charge neutrality equation, charging of CNT and the number balance of the plasma species i.e., electrons, ions and neutrals. Since the temperature of the plasma species is also an important factor for the growth of the CNT, the present model includes the energy balance of the plasma species.

The kinetics involved in the formation of embryonic CNT is not included in the present work and the work is limited to investigating the effect of plasma parameter (i.e., electron density and temperature, ion density and temperature), plasma mediums, plasma composition, parameters

associated with different types of plasma species such as negative ions on the growth of CNT through accretion of ionic and neutral particle. Moreover, it is assumed that all the ions that are incident on the CNT surface transfer their charge and are neutralized.

The processes that are assumed in the present model are:

1.The neutral species within the plasma ionizes to form ions and electrons.

2. The ions and electrons recombine to form neutral species.

3. Both these processes occur such that the charge neutrality condition within the plasma is always maintained.

4. The initial charge on carbon nanotube is considered to be negative such that positive ions would accrete on its surface.

5. The positive ions from the plasma sticks and accretes on the surface of CNT. The ions that accretes on the surface of CNT get neutralized and are converted to neutrals.

6. The initial radius of the embryonic CNT is calculated either by equating the total ion and electron collection current on its surface or through the surface potential on the CNT surface.

7. The collision of electrons with neutrals and ions and with the CNT within the plasma is also considered but it is assumed that the ionized state of the participating species after the collision remains unchanged. Only the energy transfer among the species is assumed to occur during the collision.

8. The energy dissociated to the surrounding by the plasma species is also considered.

A. Charge neutrality equation

According to charge neutrality condition, within the plasma the positive charge is equal to the net negative charge such that the plasma as a whole is considered electrically neutral. Eq. (1) therefore equates the net negative and positive charge in the plasma.

$$Zn_{ct} + n_{iA} + n_{iB} = n_e, \quad (1)$$

where

Z= the amount of charge on CNT(dimensionless),

n_{ct} = the number density of the CNT (in cm^{-3}),

n_{iA}= number density of ion A(in cm^{-3}),

n_{iB}= number density of ion B(in cm^{-3}),

n_e= number density of electron(in cm^{-3}).

B. Charging of the CNTs

Initially the CNT is assumed to be negatively charged such that over a period, the accretion of ions to the CNT decreases the initial negative charge and CNT gets positively charged during growth. Therefore, both the ion and electron currents at the surface of the CNT contribute to the charge developing on the CNT surface. Now, the positive ions collected on the CNT surface are neutralized on the CNT surface by transferring their charge. Therefore, the positive ion collection currents would increase the positive charge on CNT surface whereas electron current would depreciate positive charge on CNT surface.

Let Z is the amount of charge over the entire CNT surface, then the time evolution of charge on the entire CNT surface can be expressed through Eq. (2) which describes the charge developed on the CNT due to

accretion of electrons and positively charged ions on the surface of the CNT.

$$\frac{dZ}{d\tau} = n_{iAct} + n_{iBct} - \gamma_e n_{ect} \ , \qquad (2)$$

n_{ect}, n_{iAct} and n_{iBct} are the electron and ion collection currents on the CNT. The expression for electrons and collection currents are dependent on the surface on which electrons and ions are collected. They are described in detail for spherical and cylindrical surface in Chapter 3. The units of the collection currents is sec^{-1} . γ_e is the sticking coefficient of constituent electrons at the surface of CNT and is dimensionless. τ is the time (in sec).

C. Growth rate equation of electron density

It is assumed that the dissociative ionization of neutrals produces ions and electrons hence it increases the number density of electrons in the plasma , whereas recombination of electrons and ions to produce neutrals would decrease the electron number density in plasma. Thus, Eq. (3) describes the growth rate of electron density in the plasma.

$$\frac{dn_e}{d\tau} = \left(\beta_A n_A + \beta_B n_B\right) - \left(\alpha_A n_e n_{iA} + \alpha_B n_e n_{iB}\right) - \gamma_e n_{ct} n_{ect}, \qquad (3)$$

where

β_j is the coefficient of ionization of the constituent neutral atoms due to external agency (in sec), and $\alpha_j(T_e) = \alpha_{j0}\left(\frac{300}{T_e}\right)^k cm^3/\text{sec}$ is the

coefficient of recombination of electrons and positively charged ions [16],

κ =-1.2 is a constant , $\alpha_{A0} = \alpha_{B0} = n_{e0} \times 10^{-7} \left(\frac{1}{T_{e0}} \right)^{-1.2}$ and j refers to

either type A species (i.e., carbon) or type B species (i.e., hydrogen, argon, ammonia , nitrogen, neon) as the case may be.

The first term in Eq.(3) is the rate of gain in electron density per unit time due to ionization of neutral atoms and second term is the decrease in the electron density due to electron–ion recombination and the third term is the loss in electron density because of the electron collection current at the surface of CNT.

D. Growth rate equation of positively charged ion density

For the positive ions within the plasma , the process considered are that the dissociative ionization of neutrals produces ions and electrons ,thereby the ion's number density increases, the recombination of ions and electrons to produce neutrals decreases ion number density in plasma. Moreover, the ions collected on the surface of the CNT would decrease their number density in plasma.

$$\frac{dn_{iA}}{d\tau} = \beta_A n_A - \alpha_A n_e n_{iA} - n_{ct} n_{iAct}, \tag{4}$$

$$\frac{dn_{iB}}{d\tau} = \beta_B n_B - \alpha_B n_e n_{iB} - n_{ct} n_{iBct} \ . \tag{5}$$

The first term in Eqs.(4) and (5) is the gain in ion density per unit time on account of ionization of neutral atoms, the second term is the decrease in ion density due to electron-ion recombination, and the third term denotes the loss in ion density due to ion collection current at the surface of CNT.

E. Growth rate equation of neutral atoms

The Eqs. (6) and (7) describes the number density balance of neutral atoms in plasma assuming that recombination of ions and electron produces neutrals and the neutral number density thus increases whereas dissociative ionization of neutrals to produce ions and electrons decreases their number density in the plasma bulk. Also, the ions that are collected on the CNT surface gets neutralized and hence increases the neutral atoms density in plasma .The neutral collection current would decrease their number density in plasma is also assumed in Eqs.(6) and (7).

$$\frac{dn_A}{d\tau} = \alpha_A n_e n_{iA} - \beta_A n_A + n_{ct}\left(1-\gamma_{iA}\right) n_{iAct} - n_{ct}\gamma_A n_{Act} \ , \qquad (6)$$

$$\frac{dn_B}{d\tau} = \alpha_B n_e n_{iB} - \beta_B n_B + n_{ct} n_{iBct} \ , \qquad (7)$$

γ_A is the sticking coefficient of neutrals on CNT surface and γ_{iA} is the sticking coefficient of ions on CNT surface, both γ_A and γ_{iA} are dimensionless.

The first term in Eqs. (6) and (7) is the gain in neutral atom density per unit time due to electron–ion recombination, the second term is the decrease in neutral density due to their ionization, the third term is the gain in neutral density due to neutralization of the ions collected at the surface of CNT . The last term in Eq. (6) is the accretion of neutral atoms of species A on the surface of the CNT.

F. Growth rate equation of the mass of CNT

The accretion of neutral and ionic species of type A (i.e., carbon) is assumed to be responsible for the growth of CNT. The Eq. (8) describes the growth rate of mass of CNT (with constant density) over a period of time.

$$\frac{dm_{ct}}{d\tau} = \left(m_A \gamma_A n_{Act} + m_{iA} \gamma_{iA} n_{iAct} \right) \quad , \qquad (8)$$

where

The first and second term in Eq.(8) are the gain in the mass of the CNT due to collection of atomic and ionic species A (i.e., carbon), respectively. The m_{ct} is the mass of CNT and is equal to product of the volume of the CNT surface and its density for e.g., for spherical surface

$m_{ct} = \frac{4}{3}\pi a^3 \rho_{ct}$ is the mass of the CNT for a spherical CNT tip , a is the radius of spherical CNT tip , and ρ_{ct} is the density of spherical CNT tip, $m_{ctcy} = \pi r^2 l \rho_{ctcy}$ is the mass of the CNT for a cylindrical CNT surface , r is the radius of cylindrical CNT surface , l is the length of cylindrical CNT surface and ρ_{ctcy} is the density of cylindrical CNT surface.

m_A is the mass of neutral carbon atom, m_{iA} is the mass of ionic species of carbon (type A). The unit of m_{ct} , m_A ,and m_{iA} is gm (gram) and τ is the time in second (sec). γ_{iA} and γ_A are the sticking coefficients of neutral and ionic species of carbon (type A),respectively and are dimensionless.

G. Energy balance equation of electrons

The ionization of neutrals to produce electrons and ions increases the energy of electrons whereas the recombination of electrons and ions to produce neutrals decreases the energy of electrons. The accretion of electrons on the CNT surface and the collision of electrons with CNT surface depreciates the energy of electrons. Since the temperature of electrons is more than the temperature of neutral and ions , the collision

of electrons with either neutrals or with ions would decrease the electron energy.

$$\frac{d}{d\tau}\left(\frac{3}{2}n_e k_B T_e\right)$$

$$=\left(\beta_A n_A \varepsilon_A+\beta_B n_B \varepsilon_B\right)-\left(\frac{3}{2}k_B\right)\left(\alpha_A n_e n_{iA}+\alpha_B n_e n_{iB}\right)T_e-n_{ct}n_{ect}\left\{\gamma_e \varepsilon_{ec}^{lh}+\right.$$

$$\left.\delta_{ect}(1-\gamma_e)\times\left[\varepsilon_{ec}^{s}-\left(\frac{3}{2}k_B\right)T_{ct}\right]\right\}-\left(\frac{3}{2}k_B\right)\left[\nu_{eA}\delta_{eA}+\nu_{eB}\delta_{eB}\right](T_e-T_n)n_e$$

$$-\left(\frac{3}{2}k_B\right)\times\left(\nu_{eAi}\delta_{eAi}+\nu_{eBi}\delta_{eBi}\right)\left(T_e-T_i\right)n_e\ ,$$

(9)

where

$\frac{3}{2}n_e k_B T_e$ is the thermal energy of electrons ,

T_n is the temperature of neutral atoms (in K) , T_{ct} is the temperature of CNT (in K), ε_j is the mean energy of electrons due to ionization of neutral atoms and (in eV) and for neutral atom of type A ε_A is expressed as ,

$$\varepsilon_A=\frac{3}{2}k_B T_e+\frac{3k_B}{2\left(\alpha_A(T_e)\times n_{iA}\right)}\left[\left\{\nu_{eA}\times\delta_{eA}\times\left(T_e-T_n\right)\right\}+\left\{\nu_{eAi}\times\delta_{eAi}\times\left(T_e-T_i\right)\right\}\right]$$

and for neutral atom of type B ε_B is expressed as

$$\varepsilon_B=\frac{3}{2}k_B T_e+\frac{3k_B}{2\left(\alpha_B(T_e)\times n_{iB}\right)}\left[\left\{\nu_{eB}\times\delta_{eB}\times\left(T_e-T_n\right)\right\}+\left\{\nu_{eBi}\times\delta_{eBi}\times\left(T_e-T_i\right)\right\}\right]$$

$\varepsilon_{ec}^{lh}(Z)$ is the mean energy of electrons (in eV) at a large distance from the surface of CNT [16] and for spherical CNT tip $\varepsilon_{ec}^{lh}(Z)=\varepsilon_{ec}^{s}(Z)-\left(\frac{Ze^2}{a}\right)$

and for cylindrical surface $\varepsilon_{ec}^{lh}(Z) = k_B T_e \left[2 - \left(\frac{eV_s}{k_B T_e} \right) \right]$

$\varepsilon_{ec}^{S}(Z) = 2k_B T_e$ is the mean energy of electrons collected by CNT(in eV)[16],

$\nu_{ej} = \nu_{ej0} \left(\frac{n_j}{n_{j0}} \right) \left(\frac{T_e}{T_{e0}} \right)^{\frac{1}{2}}$ is the electron collision frequency(in sec^{-1}) due to elastic collisions with neutral atoms [17] and $\nu_{ej0} = (8.3 \times 10^5) \pi r_j^2 n_{j0} T_{e0}^{\frac{1}{2}}$

$\nu_{eji} = \nu_{eji0} \left(\frac{n_{ji}}{n_{ji0}} \right) \left(\frac{T_e}{T_{e0}} \right)^{-\frac{3}{2}}$ is the electron collision frequency(in sec^{-1}) due to elastic collisions with positively charged ions[17],

$\nu_{eji0} = \left(5.5 \frac{n_{e0}}{T_{e0}^{\frac{3}{2}}} \right) \ln \left(\frac{220 T_{e0}}{n_{ij0}^{\frac{1}{3}}} \right)$,

$\delta_{ej} \approx 2 \left(\frac{m_e}{m_j} \right)$ is the fraction of excess energy of an electron lost in a collision with the neutral atom [3] and is dimensionless,

$\delta_{eji} \approx 2 \left(\frac{m_e}{m_{ji}} \right)$ is the fraction of excess energy of an electron lost in a collision with a positively charged ion [3] and is dimensionless,

$\delta_{ect} \approx 2 \left(\frac{m_e}{m_{ct}} \right)$ is the fraction of excess energy of an electron lost in a collision with a CNT [3] and is dimensionless,

m_j is the mass of a neutral atom (in gm),

m_{ji} is the mass of an ion(in gm),

m_e is the mass of electron (in gm),

r_j is the mean radii of the atomic and the ionic species,

n_j is the number density of neutral atoms (in cm^{-3}),

T_{e0} is the temperature of electrons in the absence of CNT (in eV),

$\frac{\nu_{ej0}}{\nu_{eji0}}$ is the electron collision frequency due to collisions with atoms/ ions in the absence of CNT and is dimensionless,

n_{e0} is the initial number density of electrons (in cm^{-3}),

n_{j0} is the initial number density of neutral atoms (in cm^{-3}).

The first term in Eq.(9) is the power gained per unit volume by electrons due to ionization of neutral atoms, the second term is the energy loss per unit volume per unit time due to recombination with positively charged ions in plasma, and the third term is the energy loss per unit volume per unit time due to the sticking accretion and elastic collisions of electron at the surface of the CNT. The fourth term is the energy loss per unit volume per unit time due to elastic electron – neutral collisions and the fifth term is the energy loss per unit volume per unit time due to elastic electron- ion collision.

The LHS of Eq.(9) can be written as

$$\left(\frac{3}{2}k_B\right)n_e\left(\frac{dT_e}{d\tau}\right)+\left(\frac{3}{2}k_B\right)T_e\left(\frac{dn_e}{d\tau}\right)$$

Substituting the value of $\frac{dn_e}{d\tau}$ from Eq. (3) in the above Eq., we get

$$\left(\frac{3}{2}k_B\right)n_e\left(\frac{dT_e}{d\tau}\right)=$$

$$-\left(\frac{3}{2}k_B\right)T_e\left(\beta_A n_A+\beta_B n_B\right)+\left(\frac{3}{2}k_B\right)T_e\left(\alpha_A n_e n_{iA}+\alpha_B n_e n_{iB}\right)+\left(\frac{3}{2}k_B\right)T_e\gamma_e n_{ct} n_{ect}$$

$$+\left(\beta_A n_A\varepsilon_A+\beta_B n_B\varepsilon_B\right)-\left(\frac{3}{2}k_B\right)\left(\alpha_A n_e n_{iA}+\alpha_B n_e n_{iB}\right)T_e-n_{ct}n_{ect}\left\{\gamma_e\varepsilon_{ec}^{lh}+\delta_{ect}\left(1-\gamma_e\right)\right.$$

$$\left.\times\left[\varepsilon_{ec}^{s}-\left(\frac{3}{2}k_B\right)T_{ct}\right]\right\}-\left(\frac{3}{2}k_B\right)\left[\nu_{eA}\delta_{eA}+\nu_{eB}\delta_{eB}\right]\left(T_e-T_n\right)n_e-\left(\frac{3}{2}k_B\right)$$

$$\left(\nu_{eAi}\delta_{eAi}+\nu_{eBi}\delta_{eBi}\right)\left(T_e-T_i\right)n_e,$$

On rearranging the above equation, we get

$$\left(\frac{3}{2}k_B\right)n_e\left(\frac{dT_e}{d\tau}\right)=\left[\left(\beta_A n_A\varepsilon_A+\beta_B n_B\varepsilon_B\right)-\left(\frac{3}{2}k_B\right)\left(\beta_A n_A+\beta_B n_B\right)T_e\right]-$$

$$n_{ct}n_{ect}\left\{\gamma_e\left[\varepsilon_{ec}^{lh}-\left(\frac{3}{2}k_B\right)T_e\right]+\delta_{ect}\left(1-\gamma_e\right)\left[\varepsilon_{ec}^{s}-\left(\frac{3}{2}k_B\right)T_{ct}\right]\right\}-\left(\frac{3}{2}k_B\right)$$

$$\left\{\left[\nu_{eA}\delta_{eA}+\nu_{eB}\delta_{eB}\right]\left(T_e-T_n\right)+\left(\nu_{eAi}\delta_{eAi}+\nu_{eBi}\delta_{eBi}\right)\left(T_e-T_i\right)n_e\right\}.$$

(10)

H. Energy balance equation for positively charged ions

The ionization of neutrals to produce electrons and ions increases the ion energy whereas the recombination of electrons and ions to produce neutrals decreases the energy of ions. The accretion of ions on the CNT surface depreciates the energy of ions. Since the temperature of ion is less than the temperature of electron, the collision of electrons with ions would increase the ion energy whereas since the ion temperature is more than the neutral temperature, the collision of ions with neutrals decreases the ion energy. Because both species of ions are assumed to be at the same temperature, the ion–ion collisions do not contribute to the energy balance.

$$\frac{d}{d\tau}\left[\frac{3}{2}\left(n_{iA}+n_{iB}\right)k_B T_i\right]$$

$$=\left(\beta_A n_A \varepsilon_{iA}+\beta_B n_B \varepsilon_{iB}\right)+\left(\frac{3}{2}k_B\right)n_e\left(\nu_{eAi}\delta_{eAi}+\nu_{eBi}\delta_{eBi}\right)\times\left(T_e-T_i\right)$$

$$-\left(\frac{3}{2}k_B\right)\left(\alpha_A n_e n_{iA}+\alpha_B n_e n_{iB}\right)T_i-n_{ct}\left(n_{iAct}\varepsilon^l_{iAc}+n_{iBct}\varepsilon^l_{iBc}\right)-$$

$$\left(\frac{3}{2}k_B\right)\left[\left(\nu_{iAA}\delta_{iAA}+\nu_{iAB}\delta_{iAB}\right)n_{iA}+\left(\nu_{iBA}\delta_{iBA}+\nu_{iBB}\delta_{iBB}\right)n_{iB}\right]\left(T_i-T_n\right)$$

,(11)

where

$\frac{3}{2}\left(n_{iA}+n_{iB}\right)k_B T_i$ is the thermal energy of ions ,

$\varepsilon^l_{ijc}(Z)$ is the mean energy of positively charged ions (at large distance from the surface of the CNT) collected by the CNT [16] (in eV), for spherical CNT tip $\varepsilon^l_{ijcs}(Z)=\left[\frac{2-Z\alpha_{ji}}{1-Z\alpha_{ji}}\right]k_B T_i$

whereas for cylindrical CNT surface

$$\varepsilon^l_{ijc}(Z)=k_B T_i n_{ij} rl\left(\frac{2\pi k_B T_i}{m_{ij}}\right)^{\frac{1}{2}}\left[\left(\frac{4}{\sqrt{\pi}}\right)\left(\frac{eV_S}{k_B T_i}\right)^{\frac{1}{2}}+\left(2-\left(\frac{eV_S}{k_B T_i}\right)^{\frac{1}{2}}\right)\exp\left[\frac{eV_S}{k_B T_i}\right]erfc\left[\left(\frac{eV_S}{k_B T_i}\right)^{\frac{1}{2}}\right]\right]$$

,V_s is the surface potential of cylindrical CNT.

ε_{ij} is the mean energy of positively charged ions(in eV) produced by the ionization of neutral atoms[16] and for ion A and B are expressed as

$$\varepsilon_{iA}=\frac{3}{2}k_B T_{iA}+\frac{3k_B}{2\left(\alpha_A(T_e)\times n_{iA}\right)}\left[\left\{\nu_{iAA}\times\delta_{iAA}\times\left(T_i-T_n\right)\right\}-\left\{\nu_{eAi}\times\delta_{eAi}\times\left(T_e-T_i\right)\right\}\right]$$

$$\varepsilon_{iB}=\frac{3}{2}k_B T_{iB}+\frac{3k_B}{2\left(\alpha_B(T_e)\times n_{iB}\right)}\left[\left\{\nu_{iBB}\times\delta_{iBB}\times\left(T_i-T_n\right)\right\}-\left\{\nu_{eBi}\times\delta_{eBi}\times\left(T_e-T_i\right)\right\}\right]$$

$\nu_{ijj'}=\nu_{ijj'0}\left(\frac{n_{j'}}{n_{j'0}}\right)\left(\frac{m_{j'}T_i+m_{ij}T_n}{\left(m_{j'}T_{i0}+m_{ij}T_{n0}\right)}\right)^{\frac{1}{2}}$ is the collision frequency (in sec^{-1} of a j type of ion with j' ion of neutral atom[17],

$$\nu_{ijj'0}=\left(\frac{8}{3}\right)\left(2\pi k_B\right)^{\frac{1}{2}}(r_{ij}+r_{j'})^2\left(\frac{n_{j'0}m_{j'}}{\left(m_{ij}+m_{j'}\right)}\right)\left[\left(\frac{T_{i0}}{m_{ij}}\right)+\left(\frac{T_{n0}}{m_{j'}}\right)\right]^{\frac{1}{2}},$$

$\delta_{ijj'}=\left[\frac{2m_{ij}}{(m_{j'}+m_{ij})}\right]$ is the fraction of the excess energy of a j type positively charged ion, lost in a collision with neutral j' kind of neutral atom and is dimensionless,

T_{i0} and T_{n0} are the initial temperatures of positively charged ion and neutral, respectively [17] (in K).

The first term in Eq.(11) is the energy gained per unit volume per unit time by the positively charged ions due to the ionization of neutral atoms, the second term is the energy gained per unit volume per unit time due to the elastic collision of ions with electrons, the third term is the energy loss per unit volume per unit time due to electron –ion recombination , the fourth term is the energy loss per unit volume per unit time due to the sticking accretion of ions at the surface of the CNT, and

the last term is the energy lost per unit volume per unit time due to elastic collision with neutral species.

The LHS of Eq.(11) can be written as

$$\left(\frac{3}{2}k_B\right)\left(n_{iA}+n_{iB}\right)\left(\frac{dT_i}{d\tau}\right)+\left(\frac{3}{2}k_B\right)T_i\left(\frac{d\left(n_{iA}+n_{iB}\right)}{d\tau}\right)$$

Substituting the value of $\frac{d\left(n_{iA}+n_{iB}\right)}{d\tau}$ from Eqs.(4) and (5) after multiplying by $\left(\frac{3}{2}k_B\right)T_i$ in above Eq. , we get

$$\left(\frac{3}{2}k_B\right)\left(n_{iA}+n_{iB}\right)\left(\frac{dT_i}{d\tau}\right)$$

$$\begin{aligned}
&= -\frac{3}{2}k_BT_i\left(\beta_An_A+\beta_Bn_B\right)+\frac{3}{2}k_BT_i\left(\alpha_An_en_{iA}+\alpha_Bn_en_{iB}\right)+\frac{3}{2}k_BT_in_{ct}\left(n_{iAct}+n_{iBct}\right)+\\
&\left(\beta_An_A\varepsilon_{iA}+\beta_Bn_B\varepsilon_{iB}\right)+\left(\frac{3}{2}k_B\right)n_e\left(\nu_{eAi}\delta_{eAi}+\nu_{eBi}\delta_{eBi}\right)\times\left(T_e-T_i\right)\\
&-\left(\frac{3}{2}k_B\right)\left(\alpha_An_en_{iA}+\alpha_Bn_en_{iB}\right)T_i-n_{ct}\left(n_{iAct}\varepsilon^l_{iAc}+n_{iBct}\varepsilon^l_{iBc}\right)-\\
&\left(\frac{3}{2}k_B\right)\left[\left(\nu_{iAA}\delta_{iAA}+\nu_{iAB}\delta_{iAB}\right)n_{iA}+\left(\nu_{iBA}\delta_{iBA}+\nu_{iBB}\delta_{iBB}\right)n_{iB}\right]\left(T_i-T_n\right)
\end{aligned}$$

On rearranging, we get

$$\left(\frac{3}{2}k_B\right)\left(n_{iA}+n_{iB}\right)\left(\frac{dT_i}{d\tau}\right)=$$

$$\begin{aligned}
&\left[\left(\beta_An_A\varepsilon_{iA}+\beta_Bn_B\varepsilon_{iB}\right)-\left(\frac{3}{2}k_B\right)\left(\beta_An_A+\beta_Bn_B\right)T_i\right]+\left(\frac{3}{2}k_B\right)n_e\left(\nu_{eAi}\delta_{eAi}+\nu_{eBi}\delta_{eBi}\right)\\
&\times\left(T_e-T_i\right)-n_{ct}\left\{\left[n_{iAct}\left[\varepsilon^l_{iAc}-\left(\frac{3}{2}k_B\right)T_i\right]+n_{iBct}\left[\varepsilon^l_{iBc}-\left(\frac{3}{2}k_B\right)T_i\right]\right]\right\}-\left(\frac{3}{2}k_B\right)\times\\
&\left[\left(\nu_{iAA}\delta_{iAA}+\nu_{iAB}\delta_{iAB}\right)n_{iA}+\left(\nu_{iBA}\delta_{iBA}+\nu_{iBB}\delta_{iBB}\right)n_{iB}\right]\left(T_i-T_n\right).
\end{aligned}$$

(12)

I. Energy balance equation for neutral atoms

The ionization of neutrals to produce electrons and ions decreases the neutral atoms energy whereas the recombination of electrons and ions to produce neutrals increases the energy of neutral. The accretion of neutral on the CNT surface depreciates the energy of neutral. Since the temperature of neutral is less than the temperature of electron and ion, the collision of neutral with ions and electrons would increase the neutral energy. The neutralization of ions incident on the CNT surface would increase the energy of neutrals. The neutral dissipates some part of the energy to the surrounding.

$$
\begin{aligned}
&\frac{d}{d\tau}\left[\frac{3}{2}\left(n_A+n_B\right)k_B T_n\right] \\
&=\left[\left(\frac{3}{2}k_B\right)\left(\alpha_A n_e n_{iA}+\alpha_B n_e n_{iB}\right)\left(T_e+T_i\right)+\left(\alpha_A n_e n_{iA} I_{pA}+\alpha_B n_e n_{iB} I_{pB}\right)\right]+ \\
&\left\{\left(\frac{3}{2}k_B\right)\left[n_e\left(\nu_{eA}\delta_{eA}+\nu_{eB}\delta_{eB}\right)\left(T_e-T_n\right)+\left[\left(\nu_{iAA}\delta_{iAA}+\nu_{iAB}\delta_{iAB}\right)n_{iA}+\right.\right.\right. \\
&\left.\left.\left.\left(\nu_{iBA}\delta_{iBA}+\nu_{iBB}\delta_{iBB}\right)n_{iB}\right]\times\left(T_i-T_n\right)\right]\right\}+\left(\frac{3}{2}k_B\right)n_{ct}\left[\left(1-\gamma_{iA}\right)n_{iAct}+n_{iBct}\right]T_{ct} \\
&-\left\{\left(\frac{3}{2}k_B\right)n_{ct}\left[n_{Act}\left[\gamma_A T_n+\delta_{Act}\left(1-\gamma_A\right)\left(T_n-T_{ct}\right)\right]+n_{Bct}\delta_{Bct}\left(T_n-T_{ct}\right)\right]\right\} \\
&-\left(\frac{3}{2}k_B\right)\left(\beta_A n_A+\beta_B n_B\right)T_n-E_{diss},
\end{aligned}
\tag{13}
$$

where

I_{pj} is the ionization energy of the constituent atomic species (in eV),

$E_{diss}=\left(E_{A,diss}+E_{B,diss}\right)$, $E_{j,diss}$ is the energy dissipated per unit volume per unit time by neutral atoms into the surrounding atmosphere

and is assumed to be equal to the difference between the temperature of the neutral atomic species and the ambient temperature.

$E_{j,diss} = E_{j,diss0}\left[\frac{\left(T_j - T_a\right)}{\left(T_{j0} - T_a\right)}\right]$, The constant $E_{j,diss0}$ is obtained by imposing the ambient condition of the complex plasma system in Eq.(13) for both constituent neutral species[17] (in eV).

$\delta_{jct} = \left[\frac{2m_j}{\left(m_j + m_{ct}\right)}\right]$ is the fraction of excess energy of an atom lost in a collision with the CNT and is dimensionless, and T_a is the ambient temperature (in K).

The first term in Eq. (13) is the power gained per unit volume by the neutral species due to recombination of electrons and positively charged ions, the second term is the rate of power gained per unit volume by neutral atoms in elastic collision with electrons and positively charged ions. The third term is the energy gained per unit volume per second due to formation of neutrals at the surface of the CNT due to ion and electron accretion. The fourth term refers to the thermal energy lost per unit volume per unit time by neutral atoms accretion on and collision with CNT tip. The fifth term is the energy lost per unit volume per unit time due to ionization of neutral atoms. The last term is the energy dissipation rate per unit volume by neutral atoms to the surrounding atmosphere.

The LHS of Eq.(13) can be written as

$$\frac{3}{2}\left(n_A + n_B\right)k_B\left(\frac{dT_n}{d\tau}\right) + \frac{3}{2}k_B T_n\left(\frac{d\left(n_A + n_B\right)}{d\tau}\right)$$

Substituting the value of $\frac{d\left(n_A+n_B\right)}{d\tau}$ from Eqs.(6) and (7) and multiplying by $\frac{3}{2}k_BT_n$ in Eq.(13) ,we get

$$\frac{3}{2}\left(n_A+n_B\right)k_B\left(\frac{dT_n}{d\tau}\right)=$$

$$-\frac{3}{2}k_BT_n\left(\alpha_An_en_{iA}+\alpha_Bn_en_{iB}\right)+\frac{3}{2}k_BT_n\left(\beta_An_A+\beta_Bn_B\right)-\frac{3}{2}k_BT_nn_{ct}\left(\left(1-\gamma_{iA}\right)n_{iAct}+n_{iBct}\right)$$
$$+\frac{3}{2}k_BT_nn_{ct}\gamma_An_{Act}+\left[\left(\frac{3}{2}k_B\right)\left(\alpha_An_en_{iA}+\alpha_Bn_en_{iB}\right)\left(T_e+T_i\right)+\right.$$
$$\left.+\left(\alpha_An_en_{iA}I_{pA}+\alpha_Bn_en_{iB}I_{pB}\right)\right]+\left\{\left(\frac{3}{2}k_B\right)\left[n_e\left(\nu_{eA}\delta_{eA}+\nu_{eB}\delta_{eB}\right)\left(T_e-T_n\right)+\right.\right.$$
$$\left.\left.\left[\left(\nu_{iAA}\delta_{iAA}+\nu_{iAB}\delta_{iAB}\right)n_{iA}+\left(\nu_{iBA}\delta_{iBA}+\nu_{iBB}\delta_{iBB}\right)n_{iB}\right]\times\left(T_i-T_n\right)\right]\right\}+\left(\frac{3}{2}k_B\right)$$
$$n_{ct}\left[\left(1-\gamma_{iA}\right)n_{iAct}+n_{iBct}\right]T_{ct}-\left(\frac{3}{2}k_B\right)n_{ct}\left[n_{Act}\left[\gamma_AT_n+\delta_{Act}\left(1-\gamma_A\right)\left(T_n-T_{ct}\right)\right]\right.$$
$$\left.+n_{Bct}\delta_{Bct}\left(T_n-T_{ct}\right)\right]-\left(\frac{3}{2}k_B\right)\left(\beta_An_A+\beta_Bn_B\right)T_n-E_{diss},$$

On rearranging above equation, we obtain

$$\frac{3}{2}\left(n_A+n_B\right)k_B\left(\frac{dT_n}{d\tau}\right)=$$
$$\left[\left(\frac{3}{2}k_B\right)\left(\alpha_An_en_{iA}+\alpha_Bn_en_{iB}\right)\left(T_e+T_i-T_n\right)+\left(\alpha_An_en_{iA}I_{pA}+\alpha_Bn_en_{iB}I_{pB}\right)\right]$$
$$+\left(\frac{3}{2}k_B\right)\left[n_e\left(\nu_{eA}\delta_{eA}+\nu_{eB}\delta_{eB}\right)\left(T_e-T_n\right)+\left[\left(\nu_{iAA}\delta_{iAA}+\nu_{iAB}\delta_{iAB}\right)n_{iA}+\right.\right.$$
$$\left.\left.\left(\nu_{iBA}\delta_{iBA}+\nu_{iBB}\delta_{iBB}\right)n_{iB}\right]\times\left(T_i-T_n\right)\right]+\left(\frac{3}{2}k_B\right)n_{ct}\left[\left(1-\gamma_{iA}\right)n_{iAct}+n_{iBct}\right]\left(T_{ct}-T_n\right)$$
$$-\left(\frac{3}{2}k_B\right)n_{ct}\left[n_{Act}\delta_{Act}\left(1-\gamma_A\right)\times\left(T_n-T_{ct}\right)\ +n_{Bct}\delta_{Bct}\left(T_n-T_{ct}\right)\right]-E_{diss}.$$

(14)

J. Energy balance for CNT

The processes such as electron, ion, and neutral accretion on the CNT surface affect the energy of CNT and some part of CNT energy is lost to the surrounding through conduction and radiation processes.

$$\frac{d}{d\tau}\left(m_{ct}C_pT_{ct}\right)=\left\{n_{ect}\left[\gamma_e\ \varepsilon^s{}_{ec}+(1-\gamma_e)\delta_{ect}\left[\varepsilon^s{}_{ec}-\left(\frac{3}{2}k_B\right)T_{ct}\right]\right]\right\}$$
$$-\left\{\left(\frac{3}{2}k_B\right)\left\{\left(n_{Act}\left[\gamma_A T_n+\delta_{Act}\left(1-\gamma_A\right)\left(T_n-T_{ct}\right)\right]\right)+\left(n_{Bct}\delta_{Bct}\left(T_n-T_{ct}\right)\right)\right\}\right\}+$$
$$\left\{\left[n_{iAct}\left(\varepsilon^s{}_{iAc}+I_{pA}\right)+n_{iBct}\left(\varepsilon^s{}_{iBc}+I_{pB}\right)\right]\right\}-\left\{\left(\frac{3}{2}k_B\right)\left[\left(1-\gamma_{iA}\right)n_{iAct}+n_{iBct}\right]T_{ct}\right\}$$
$$-\left\{Area\left[\varepsilon\sigma\left(T_{ct}^4-T_a^4\right)+n_A\left(\frac{8k_BT_n}{\pi m_A}\right)^{\frac{1}{2}}+n_B\left(\frac{8k_BT_n}{\pi m_B}\right)^{\frac{1}{2}}\right]k_B\left(T_{ct}-T_n\right)\right\}. \qquad (15)$$

where

$\varepsilon^s_{ijc}(Z)$ is the mean energy collected by ions at the surface of CNT[16](in eV) ,

C_p is the specific heat of the material of the CNT at constant pressure (in ergs/gm K),

$\in$ is the emissivity of the material of the CNT and is dimensionless,

σ is the Stefan –Boltzmann constant (in erg sec^{-1} cm^{-2} K^{-4}),

Area refers to the total surface area of CNT and for spherical CNT tip of CNT Area= $4\pi a^2$ and for cylindrical surface area = $2\pi r(r+l)$, where a is the radius of spherical CNT tip and r is the radius and l is the length of cylindrical CNT surface.

The first three terms in Eq.(15) are the rate of energy transferred to the CNT due to sticking accretion and elastic collision by constituent species of complex plasma. The fourth term is the energy carried away by the

neutral species (generated by the recombination of the accreted ions and electrons) from the CNT per unit volume per unit time. The last term is the rate of energy dissipation of the CNT through radiation and conduction to the host gas[18].

2.4: APPLICABILITY OF THE PRESENT MODEL

The theoretical model so developed can be employed to study the growth of carbon nanotube in a plasma environment. The effect of plasma environment i.e., the density and temperature of the plasma species (i.e., electrons and ions), the different plasma mediums, various plasma compositions i.e., light and heavy ions , effect of negative ions, on the growth of carbon nanotube can be studied through the present model. The results obtained from the present model can be extended to realize the practical applications of the CNT.

References

[1] Y. Tu, Z. P. Huang, D. Z. Wang, J. G. Wen, Z. F. Ren, Appl. Phys. Lett. **80**, 21(2002).

[2] Peter J. F. Harris ,Carbon **45**,229(2007).

[3] M. S. Sodha , Shikha Misra, S. K. Mishra, Sweta Srivastava, J. Appl. Phys.**107**,103307(2010).

[4] M. S. Sodha, S. K. Mishra and S. Misra, Phys. Plasmas **17**,113705 (2010).

[5] A. F. Pal ,T. V. Rakhimova, N. V. Suetin, M. A. Timofeev, A. P. Filippov, Plasma Phys. Reports **33**,43 (2007).

[6] Fumiya Shoji , Zonbao Feng, Akihiko Kono, Tatsuzo Nagai, Appl. Phys. Lett. **89**, 171504(2006).

[7] Tatsuzo Nagai, Zongbao Feng, Akihio Kono, Fumiya Shoji, Phys. Plasmas **15,** 050702(2008).

[8] M. S. Bell, R.G. Lacerda, K. B. K. Teo, N. L. Rupesinghe, M. Chhowalla, Appl. Phys. Lett. **85**, 7(2004).

[9]Tae –Young Kim, Kwang-Ryeol Lee, Kwang Yong Eun, Kyu-Hwan Oh, Chem. Phys. Lett. **372**, 603(2003).

[10]J.M. Bonard, J.P. Salvetat, Thomas Stockli, W.A. de Heer, Appl. Phys. Lett. **73**, 918 (1998).

[11]S. K. Srivastava, A.K. Shukla, V. D. Vankar, and V. Kumar, Thin Solid Films **492**, 124(2005).

[12] Ghang Zhang, W. Duan and B. Gu, Appl. Phys. Lett. **80**, 2589 (2002).

[13] L. Nilsson, O. Groening, C. Emmenegger, O. Kuettel, E. Schaller, L. Schapbach, H. Kind, J.M. Bonard and K. Kern, Appl. Phys. Lett.**76**, 2071(2000).

[14] Zhi Xu, X. D. Bai and E. G. Wang, Appl. Phys. Lett. **88**, 133107(2006).

[15] S. Botti, R. Ciardi and M. L. Terranova, S. Piccirillo, V. Sessa, M. Rossi, and M. Vittori-Antisari ,Appl. Phys. Lett. **80**, 1441(2002).

[16] M. S. Sodha and S. Guha, Adv. Plasma Phys. **4**, 219 (1971).

[17] A. V. Gurevich, *Nonlinear Phenomena in the Ionosphere* (Springer, New York, 1978).

[18] M. Rosenberg, D. A. Mendis, and D. P. Sheehan, IEEE Trans. Plasma Sci. **27**, 239(1999).

CHAPTER 3

ROLE OF PLASMA PARAMETERS ON GROWTH OF SPHERICAL CNT TIP AND CYLINDRICAL CNT SURFACES (WITHOUT CATALYST) AND THEIR FIELD EMISSION PROPERTIES.

3.1: Brief outline of the work in the chapter

The present chapter focuses on the effect of plasma parameters (i.e., electron density and temperature, ion density and temperature) on the growth of spherical carbon nanotube (CNT) tip and cylindrical CNT surfaces, separately and estimation of field enhancement factor of CNT from the results obtained.

3.2: Introduction

Carbon nanotubes (CNTs) are being extensively studied because of their excellent properties e.g., mechanical properties, high chemical stability, thermal conductivity, large aspect ratio (i.e., ratio of height of CNT to radius of CNT), etc. The growth of CNT in plasma is an active field of research and plasma parameters impacts CNT growth.

In the plasma assisted growth of CNTs, parameters specific to the glow discharge must be considered. The voltage, current, power, and resultant field distributions within the discharge, plays a vital role in shaping the outcome of the growth process. The plasma is used for both the deposition of thin conformal films and for etching, depending on the choice of conditions. [1]

Low temperature plasmas are an extensive and multifaceted tool for material processing such as thin film deposition, etching, surface

activation and functionalization, and plasma polymerization[2,3]. This low temperature operation is possible owing to the activation of the gas by the energetic electrons, while the gas itself remains at temperatures at or slightly above room temperature [4]. Indeed, in low temperature plasma, the electrons cause ionization, excitation, and dissociation. The dissociation reactions lead to the formation of highly reactive radicals. The ionization process creates ions and electrons that are accelerated by the applied electric field. These ions and electrons can subsequently participate in various reactions, including dissociation reactions, leading to the formation of more radicals. Finally, also the excited atoms and molecules, which are generally more reactive than the ground-state species, contribute to the enhanced reactivity of the processing gas, thereby omitting the need for high temperatures to achieve chemical reactions [5].

Srivastava *et al*. [6] have synthesized carbon films via microwave plasma enhanced chemical vapor deposition (MPECVD) using a mixture of methane(CH_4) and argon (Ar) gases on nickel (Ni) coated silicon(Si) substrates and found that increase in microwave power causes more ionization of the gas, which increases the density of plasma species of relatively higher energy. Moreover, increased nucleation of graphitic clusters is expected to occur, and this leads to formation of carbon petals of relatively smaller size and higher density at increased microwave power.

Pal *et al*. [7] have grown arrays of aligned CNT on silicon substrate in the anode sheath of glow discharge and found that nanotubes grow in those regions where electric field is enhanced due to depletion of positive ions in anode sheath.

Levchenko *et al*. [8] have found that the distribution of the ion current along the nanotip lateral surface is strongly nonuniform and can be controlled by the plasma density. Their results suggest that the plasma parameters are important factors that enables to efficiently manipulate the microscopic ion fluxes onto the substrate and nanotip surfaces, eventually leading to the possibility of the efficient carbon nanotip growth control.

Levchenko *et al*. [9] have suggested that the plasma-aided process, in contrast to the neutral flux deposition, is an efficient tool to control the nanotip aspect ratio. The nanotip aspect ratio can be controlled by adjusting the plasma parameters such as the degree of ionization, plasma density, and electron temperature, etc.

Levchenko *et al*. [10] have pointed out that by using the plasma extracted ion fluxes, the CNTs can be uniformly coated and treated along the entire length. Manipulating the plasma parameters makes it possible to direct the ion flux to preselected areas on the nanotube surfaces. This effect can also be used for deterministic synthesis of dense CNT arrays in low-temperature plasmas.

The field emission properties of carbon nanotubes are also another important area of research, because they give very high values of the current density as compared to the already existing field emission devices. The field emission properties of CNT and the effect of various factors such as plasma parameters [11], substitutional atoms[12], dimensional effects[13], anode-cathode distance[14] etc., on field emission from CNT have also been extensively studied. Lee *et al.* [11] have investigated the effect of plasma treatment on the surface morphology and field emission characteristics of CNT and revealed that

the plasma treatment can modify the surface morphology and enhance the field emission characteristics of the CNTs.

Jang *et al.* [15] have fabricated the CNT through direct current plasma-enhanced chemical vapor deposition (dc-PECVD) using different ammonia (NH_3) pre-treatment plasma currents and have analyzed the field emission behavior of well-aligned carbon nanotubes. The field emission properties of the multi-walled carbon nanotubes (MWCNTs) exhibit a strong dependence on the morphology parameters such as the length, radius, and density of nanotubes.

Kyung *et al*. [16] have studied the growth and field emission properties of MWCNTs by using atmospheric pressure PECVD and investigated the structural and electrical characteristics for its possible applications as field emitters in field emission display devices (FED). The results show the turn-on field to be 2.92V/μm, and the emission field at 1mA/cm^2 to be 5.325 V/μm, which is appropriate for FED emitters.

Wang *et al.* [17] have grown vertically aligned CNT films with diameters smaller than 5 nm and have investigated the electron field emission properties of the films by variable distance field emission and temperature-dependent field electron emission microscopy (T-FEEM). The films showed an emission site density of ~104/cm^2 and a threshold field of 2.8 V/ μm. The results showed the strong dependence of size of CNT on its field emission properties.

In the present chapter, we investigate the effect of plasma parameters on the growth of spherical CNT tip and cylindrical CNT surfaces, separately using the model developed in Chapter 2. An estimate of the field enhancement factor from spherical CNT tip and cylindrical carbon nanotube surfaces is also done from the results obtained.

3.3: Model for growth of spherical CNT tip and cylindrical CNT surfaces in plasma

Following the consideration in the previous chapter of a plasma containing electrons, positively charged ions of type A(carbon) and B(neon), neutral atoms of type A(carbon) and B(neon), the growth of CNT (spherical CNT tip and cylindrical CNT surface, separately) by condensation of embryonic nanotubes in plasma is investigated. The equations for growth of spherical tip of CNT and cylindrical CNT surfaces are presented separately.

The initial radius of spherical CNT tip (a_0) can be estimated by equating the accretion of electrons and positively charged ions on the CNT, i.e., electron collection current on the CNT(n_{ects}) is equal to total ion collection at CNT ($n_{iActs}+n_{iBcts}$)

$$n_{ects} = n_{iActs} + n_{iBcts} \tag{1}$$

where

$n_{ects} = \pi a^2 \left(\frac{8k_B T_e}{\pi m_e}\right)^{\frac{1}{2}} n_e \exp\left[Z\alpha_e\right]$ is the electron collection current at the surface of spherical CNT tip [18] (in sec^{-1}) and $\alpha_e = \left(\frac{e^2}{ak_B T_e}\right)$,

$n_{ijcts} = \pi a^2 \left(\frac{8k_B T_i}{\pi m_{ij}}\right)^{\frac{1}{2}} n_{ij}\left[1 - Z\alpha_i\right]$ is the ion collection current of a spherical CNT [18] (in sec^{-1}) where j refers to either A (carbon) ion or B (neon) ion and $\alpha_i = \left(\frac{e^2}{ak_B T_i}\right)$, Z is the amount of charge on the CNT(dimensionless).

Substituting the values of n_{ects} and n_{ijcts} (for both A (carbon) and (neon)) in Eq.(1) we get,

$$\pi a^2\left(\frac{8k_BT_e}{\pi m_e}\right)^{\frac{1}{2}} n_e \exp\left[\frac{Ze^2}{ak_BT_e}\right] = \pi a^2\left(\frac{8k_BT_i}{\pi m_{iA}}\right)^{\frac{1}{2}} n_{iA}\left[1-\frac{Ze^2}{ak_BT_i}\right] + \pi a^2\left(\frac{8k_BT_i}{\pi m_{iB}}\right)^{\frac{1}{2}} n_{iB}\left[1-\frac{Ze^2}{ak_BT_i}\right], \tag{2}$$

or

$$\left(\frac{8k_BT_e}{\pi m_e}\right)^{\frac{1}{2}} n_e \exp\left[\frac{Ze^2}{ak_BT_e}\right] = \left(\frac{8k_BT_i}{\pi m_{iA}}\right)^{\frac{1}{2}} n_{iA}\left[1-\frac{Ze^2}{ak_BT_i}\right] + \left(\frac{8k_BT_i}{\pi m_{iB}}\right)^{\frac{1}{2}} n_{iB}\left[1-\frac{Ze^2}{ak_BT_i}\right], \tag{3}$$

or

For Z = -1, i.e., we assume that initially at $\tau=0$ the CNT is negatively charged, and initial radius of CNT is a_0,

$$\left(\frac{T_e}{m_e}\right)^{\frac{1}{2}} n_e \exp\left[-\frac{e^2}{a_0k_BT_e}\right] = \left(\frac{T_i}{m_{iA}}\right)^{\frac{1}{2}} n_{iA}\left[1+\frac{e^2}{a_0k_BT_i}\right] + \left(\frac{T_i}{m_{iB}}\right)^{\frac{1}{2}} n_{iB}\left[1+\frac{e^2}{a_0k_BT_i}\right], \tag{4}$$

$$n_e\left(\frac{T_e}{m_e}\right)^{\frac{1}{2}} \exp\left(-\frac{e^2}{a_0k_BT_e}\right) = \left(1+\frac{e^2}{a_0k_BT_i}\right)\left[n_{iA}\left(\frac{T_i}{m_{iA}}\right)^{\frac{1}{2}} + n_{iB}\left(\frac{T_i}{m_{iB}}\right)^{\frac{1}{2}}\right], \tag{5}$$

Now, the initial radius [19] of cylindrical CNT surface (r_0) can be estimated through the surface potential on cylindrical CNT

$$V_S = -\frac{2e}{l}\log\frac{\lambda_d}{r_0} \quad , \tag{6}$$

where

V_s = surface potential on CNT (in Stat V),

l = length of the cylindrical CNT (in μm),

$\lambda_d^{-2} = \lambda_e^{-2} + \lambda_i^{-2}$,

λ_d is the Debye length of the plasma,

$\lambda_e \left(= \sqrt{\frac{T_{e0}}{4\pi n_{e0} e^2}} \right)$ is the electron Debye length for the electrons present in the plasma, $\lambda_i \left(= \sqrt{\frac{T_{i0}}{4\pi n_{i0} e^2}} \right)$ is the ion Debye length for ions present in the plasma,

n_{i0} is the ion number density (in cm^{-3}),

n_{e0} = the number density of electron (in cm^{-3}),

T_{e0} = the electron temperature (in eV),

a_0 = the initial radius of spherical CNT tip (in nm),

r_0 = the initial radius of cylindrical CNT surface (in nm),

k_B = Boltzmann's constant(in ergs/K),

T_{i0} = the ion temperature (in K),

n_{iA} = the number density of ion A (in cm^{-3}),

m_{iA} = the mass of ion A(in gms),

n_{iB} = the number density of ion B (in cm^{-3}),

m_{iB} = the mass of ion B (in gms), and

e = the electronic charge(in StatC).

The processes assumed for the growth of CNT in plasma are same as discussed in Chapter 2 .

A. Charge on CNT

Following the charge neutrality condition i.e., treating the plasma as electrically neutral. Eqs. (7) and (8) equates the net negative and positive charge in the plasma for spherical tip and cylindrical surfaces, respectively.

$$Z_S n_{ct} + n_{iA} + n_{iB} = n_e, \tag{7}$$

$$Z_{cy} n_{ct} + n_{iA} + n_{iB} = n_e \tag{8}$$

Z_s= amount of charge on spherical CNT tip (dimensionless) ,

Z_{cy}= amount of charge on cylindrical CNT surface (dimensionless),

n_{ct} = the number density of the CNT(in cm^{-3}).

B. Charging of CNT

Let Z_s is the amount of charge over the spherical CNT tip, Z_{cy} is the amount of charge on cylindrical CNT surface, then the time evolution of charge on the entire CNT surface can be expressed through Eqs. (9) and (10) for spherical CNT tip and cylindrical CNT surface , respectively. The Eqs. (9) and (10) describes the charge developed on the CNT due to accretion of electrons and positively charged ions on the surface of the CNT.

$$\frac{dZ_S}{d\tau} = n_{iActs} + n_{iBcts} - \gamma_{es}\, n_{ects}\ , \tag{9}$$

$$\frac{dZ_{cy}}{d\tau} = n_{iActcy} + n_{iBctcy} - \gamma_{ecy}\, n_{ectcy}\ , \tag{10}$$

where

a) $n_{ects} = \pi a^2 \left(\frac{8k_B T_e}{\pi m_e} \right)^{\frac{1}{2}} n_e \exp\left[Z\alpha_e \right]$ is the electron collection current at the surface of spherical CNT tip [18] (in $\sec^{-1}$) and $\alpha_e = \left(\frac{e^2}{ak_B T_e} \right)$.

b) $n_{ijcts} = \pi a^2 \left(\frac{8k_B T_i}{\pi m_{ij}} \right)^{\frac{1}{2}} n_{ij} \left[1 - Z\alpha_i \right]$ is the ion collection current on a spherical CNT tip [18] (in $\sec^{-1}$) and $\alpha_i = \left(\frac{e^2}{ak_B T_i} \right)$

c) $n_{ectcy} = n_e rl \left(\frac{2\pi k_B T_e}{m_e} \right)^{\frac{1}{2}} \exp\left[\frac{eV_s}{k_B T_e} \right]$ is the electron collection current at the surface of cylindrical CNT [19] (in $\sec^{-1}$) .

d) $n_{ijctcy} = n_{ij} rl \left(\frac{2\pi k_B T_i}{m_{ij}} \right)^{\frac{1}{2}} \left\{ \frac{2}{\sqrt{\pi}} \left(\frac{eV_s}{k_B T_i} \right)^{\frac{1}{2}} + \exp\left[\frac{eV_s}{k_B T_i} \right] erfc\left[\left(\frac{eV_s}{k_B T_i} \right)^{\frac{1}{2}} \right] \right\}$

is the ion collection current of a cylindrical CNT [19] (in $\sec^{-1}$) , j refers to either A(carbon) or B(neon) positively charged ion, γ_{es} and γ_{ecy} are the sticking coefficient of constituent electron at the surface of the spherical CNT tip and cylindrical CNT surface, respectively and are dimensionless.

The first and second term in Eqs.(9) and (10) denotes charge developed the CNT due to ion collection currents of type A(carbon) and B(neon) on spherical CNT tip and cylindrical CNT surface, respectively and third

term denotes the denotes charge developed on spherical CNT tip and cylindrical CNT surface, because of electron collection current.

C. Balance equation for electron, ion and neutral number densities for spherical CNT tip

a) Number density balance for electrons

As discussed earlier in Chapter 2, the number density balance equation of electrons is developed considering that within the plasma the neutrals ionizes to produce ions ,electrons and the electron and ion recombines to form neutrals. The electron collection current to CNT also affects the electron number density.

$$\frac{dn_e}{d\tau} = \left(\beta_A n_A + \beta_B n_B\right) - \left(\alpha_A n_e n_{iA} + \alpha_B n_e n_{iB}\right) - \gamma_{es} n_{ct} n_{ects}, \qquad (11)$$

where

β_A and β_B are the coefficients of ionization of the constituent neutral atoms of A(carbon) and B(neon) due to external agency (in sec), and $\alpha_A(T_e) = \alpha_{A0}\left(\frac{300}{T_e}\right)^k cm^3/\sec$ and $\alpha_B(T_e) = \alpha_{B0}\left(\frac{300}{T_e}\right)^k cm^3/\sec$ are the coefficients of recombination of electrons and positively charged ions [18] of A(carbon) and B(neon),respectively where k=-1.2 is a constant

, $\alpha_{A0} = \alpha_{B0} = n_{e0} \times 10^{-7}\left(\frac{1}{T_{e0}}\right)^{-1.2}$ and $n_{ects} = \pi a^2 \left(\frac{8k_B T_e}{\pi m_e}\right)^{\frac{1}{2}} n_e \exp\left[\frac{Ze^2}{ak_B T_e}\right]$

is the electron collection current at the surface of spherical CNT tip [18] (in sec^{-1}) and n_{ct} is the CNT number density (in cm^{-3}).

The first term in Eq.(11) is the rate of gain in electron density per unit time due to ionization of neutral atoms and second term is the decrease in the electron density due to electron–ion recombination and the third term is the loss in electron density because of the electron collection current on the spherical CNT tip.

b) Number density balance for ions

The number density balance equation of ions is established assuming that within the plasma, the ionization of neutrals produces ions, electrons, and the electron and ion recombines to form neutrals. Some of the ions accrete on CNT tip.

$$\frac{dn_{iA}}{d\tau} = \beta_A n_A - \alpha_A n_e n_{iA} - n_{ct} n_{iActs}, \tag{12}$$

$$\frac{dn_{iB}}{d\tau} = \beta_B n_B - \alpha_B n_e n_{iB} - n_{ct} n_{iBcts}\ , \tag{13}$$

where

$$n_{iActs} = \pi a^2 \left(\frac{8k_B T_i}{\pi m_{iA}}\right)^{\frac{1}{2}} n_{iA}\left[1 - \frac{Ze^2}{ak_B T_i}\right], n_{iBcts} = \pi a^2 \left(\frac{8k_B T_i}{\pi m_{iB}}\right)^{\frac{1}{2}} n_{iB}\left[1 - \frac{Ze^2}{ak_B T_i}\right]$$

are the ion collection currents at the surface of spherical CNT tip [18](in sec^{-1}), n_A and n_B are the neutral atom number density (in cm^{-3}).

The first term in Eqs. (12) and (13) is the gain in ion density per unit time on account of ionization of neutral atoms, the second term is the decrease in ion density due to electron-ion recombination, and the third term denotes the loss in ion density due to ion collection current on spherical CNT tip.

c) Number density balance for neutrals

The processes such as recombination of electrons and ions, ionization of neutrals , accretion of neutrals and ions on the CNT surface are accounted in the balance equation of neutral atom density.

$$\frac{dn_A}{d\tau} = \alpha_A n_e n_{iA} - \beta_A n_A + n_{ct}\left(1-\gamma_{iA}\right) n_{iActs} - n_{ct}\gamma_A n_{Acts} \ , \qquad (14)$$

$$\frac{dn_B}{d\tau} = \alpha_B n_e n_{iB} - \beta_B n_B + n_{ct} n_{iBcts} \ , \qquad (15)$$

where

$$n_{Acts} = \pi a^2 \left(\frac{8k_B T_n}{\pi m_A}\right)^{\frac{1}{2}} n_A, \ n_{Bcts} = \pi a^2 \left(\frac{8k_B T_n}{\pi m_B}\right)^{\frac{1}{2}} n_B$$

are the neutral collection currents at the surface of spherical CNT tip [18] (in sec^{-1}).

γ_A is the sticking coefficient of carbon neutrals on spherical CNT tip and γ_{iA} is the sticking coefficient of carbon ions on spherical CNT tip, both γ_A and γ_{iA} are dimensionless.

The first term in Eqs. (14) and (15) is the gain in neutral atom density per unit time due to electron–ion recombination, the second term is the decrease in neutral density due to their ionization, the third term is the gain in neutral density due to neutralization of the ions collected on spherical CNT tip. The last term in Eq. (14) is the accretion of neutral atoms of species A(carbon) on spherical CNT tip.

D. Balance equation for electron, ion and neutral number densities for cylindrical CNT surface

a) Number density balance for electrons

Assuming the processes as discussed earlier for electron number balance , Eq.(16) describes number density balance equation for electrons for the growth of cylindrical CNT surface.

$$\frac{dn_e}{d\tau} = \left(\beta_A n_A + \beta_B n_B\right) - \left(\alpha_A n_e n_{iA} + \alpha_B n_e n_{iB}\right) - \gamma_{ecy} n_{ct} n_{ectcy}, \quad (16)$$

where

$n_{ectcy} = n_e rl \left(\frac{2\pi k_B T_e}{m_e}\right)^{\frac{1}{2}} \exp\left[\frac{eV_s}{k_B T_e}\right]$ is the electron collection current on the cylindrical CNT surface [19] (in sec^{-1}).

The first term in Eq.(16) is the rate of gain in electron density per unit time due to ionization of neutral atoms and second term is the decrease in the electron density due to electron–ion recombination and the third term is the loss in electron density because of the electron collection current on the cylindrical CNT surface.

b) Number density balance for ions

Assuming the processes as discussed earlier for ion number balance, Eqs. (17) and (18) describes number density balance equation for ions for the growth of cylindrical CNT surface.

$$\frac{dn_{iA}}{d\tau} = \beta_A n_A - \alpha_A n_e n_{iA} - n_{ct} n_{iActcy}, \quad (17)$$

$$\frac{dn_{iB}}{d\tau} = \beta_B n_B - \alpha_B n_e n_{iB} - n_{ct} n_{iBctcy}, \quad (18)$$

where

$$n_{iActcy} = n_{iA} rl \left(\frac{2\pi k_B T_i}{m_{iA}}\right)^{\frac{1}{2}} \left\{\frac{2}{\sqrt{\pi}}\left(\frac{eV_s}{k_B T_i}\right)^{\frac{1}{2}} + \exp\left[\frac{eV_s}{k_B T_i}\right] erfc\left[\left(\frac{eV_s}{k_B T_i}\right)^{\frac{1}{2}}\right]\right\}$$

$$n_{iBctcy} = n_{iB}{}^{rl}\left(\frac{2\pi k_B T_i}{m_{iB}}\right)^{\frac{1}{2}}\left\{\frac{2}{\sqrt{\pi}}\left(\frac{eV_s}{k_B T_i}\right)^{\frac{1}{2}} + \exp\left[\frac{eV_s}{k_B T_i}\right] erfc\left[\left(\frac{eV_s}{k_B T_i}\right)^{\frac{1}{2}}\right]\right\}$$

are the ion collection currents at the cylindrical CNT surface [19](in sec^{-1}) for A(carbon) and B (neon),respectively.

The first term in Eqs. (17) and (18) is the gain in ion density per unit time on account of ionization of neutral atoms, the second term is the decrease in ion density due to electron-ion recombination, and the third term denotes the loss in ion density due to ion collection current on cylindrical CNT surface.

c) Number density balance for neutrals

Assuming the processes as discussed earlier for number balance of neutrals, Eqs.(19) and (20) describes number density balance equation of neutrals for the growth of cylindrical CNT surface.

$$\frac{dn_A}{d\tau} = \alpha_A n_e n_{iA} - \beta_A n_A + n_{ct}\left(1-\gamma_{iA}\right) n_{iActcy} - n_{ct}\gamma_A n_{Actcy}, \qquad (19)$$

$$\frac{dn_B}{d\tau} = \alpha_B n_e n_{iB} - \beta_B n_B + n_{ct} n_{iBctcy}, \qquad (20)$$

where

$$n_{Actcy} = \pi rl\left(\frac{2k_B T_n}{m_A}\right)^{\frac{1}{2}} n_A \;,\quad n_{Bctcy} = \pi rl\left(\frac{2k_B T_n}{m_B}\right)^{\frac{1}{2}} n_B$$

are the neutral collection currents at the cylindrical CNT surface [19](in sec^{-1}),n_A and n_B are the neutral atom number density (in cm^{-3}).

The first term in Eqs. (19) and (20) is the gain in neutral atom density per unit time due to electron–ion recombination, the second term is the decrease in neutral density due to their ionization, the third term is the

gain in neutral density due to neutralization of the ions collected at the surface of CNT. The last term in Eq. (19) is the accretion of neutral atoms of species A (carbon) on the cylindrical CNT surface.

E. Growth rates for the mass of spherical CNT tip and cylindrical CNT surface

The accretion of ions and neutrals of carbon are considered as the main growth process for both spherical CNT tip and cylindrical CNT surface.

$$\frac{dm_{cts}}{d\tau} = \left(m_A \gamma_A n_{Acts} + m_{iA} \gamma_{iA} n_{iActs} \right), \quad (21)$$

$$\frac{dm_{ctcy}}{d\tau} = \left(m_A \gamma_A n_{Actcy} + m_{iA} \gamma_{iA} n_{iActcy} \right), \quad (22)$$

where

$m_{cts} = \frac{4}{3}\pi a^3 \rho_{cts}$ is the mass of the CNT for a spherical CNT tip , a is the radius of spherical CNT tip , and ρ_{cts} is the density of spherical CNT tip,

$m_{ctcy} = \pi r^2 l \rho_{ctcy}$ is the mass of the CNT for a cylindrical CNT surface , r is the radius of cylindrical CNT surface , l is the length of cylindrical CNT surface and ρ_{ctcy} is the density of cylindrical CNT surface.

The first and second term in Eqs.(21) and (22) are the gain in the mass of the spherical CNT tip and cylindrical CNT surface, respectively due to collection of atomic and ionic species A (i.e., carbon), respectively.

F. Energy balance equation of electrons, ions and electrons and

spherical CNT tip for spherical CNT tip case

Following the same approach as in chapter 2, the energy balance equation of electrons, ions and electrons for spherical CNT tip case can be written as

a) Energy balance for electrons

The energy balance of electrons is accounted based on the dissociative ionization process of neutrals, the electron collection current on the CNT and their collisions with CNT and the collision of electrons with neutrals and ions.

$$\left(\frac{3}{2}k_B\right)n_e\left(\frac{dT_e}{d\tau}\right)=\left[\left(\beta_A n_A\varepsilon_A+\beta_B n_B\varepsilon_B\right)-\left(\frac{3}{2}k_B\right)\left(\beta_A n_A+\beta_B n_B\right)T_e\right]-n_{ct}n_{ects}$$
$$\left\{\left[\gamma_{es}\varepsilon_{ecs}^{lh}-\left(\frac{3}{2}k_B\right)T_e\right]+\delta_{ects}\left(1-\gamma_{es}\right)\left[\varepsilon_{ecs}^{s}-\left(\frac{3}{2}k_B\right)T_{ct}\right]\right\}$$
$$-\left(\frac{3}{2}k_B\right)\left[\nu_{eA}\delta_{eA}+\nu_{eB}\delta_{eB}\right]\left(T_e-T_n\right)n_e-\left(\frac{3}{2}k_B\right)\left\{\left(\nu_{eAi}\delta_{eAi}+\nu_{eBi}\delta_{eBi}\right)\right.$$
$$\left.\left(T_e-T_i\right)\right\}n_e. \qquad (23)$$

where

$\frac{3}{2}n_e k_B T_e$ is the thermal energy of electrons ,

n_e is the number density of electrons(in cm^{-3}), T_e is the electron temperature (in eV), T_{ct} is the CNT temperature (in K), and T_n is the neutral temperature (in K).

$\varepsilon_{ecs}^{lh}(Z)=\varepsilon_{ecs}^{s}(Z)-\left(\frac{Ze^2}{a}\right)$ is the mean energy of electrons(in eV) at a large distance from the surface of spherical CNT tip [18],

$\varepsilon_{ecs}^{s}(Z)=2k_B T_e$ is the mean energy of electrons (in eV) collected by spherical CNT tip [18],

$\nu_{eA} = \nu_{eA0}\left(\frac{n_A}{n_{A0}}\right)\left(\frac{T_e}{T_{e0}}\right)^{\frac{1}{2}}$ and $\nu_{eB} = \nu_{eB0}\left(\frac{n_B}{n_{B0}}\right)\left(\frac{T_e}{T_{e0}}\right)^{\frac{1}{2}}$ are the electron collision frequency (in sec^{-1}) due to elastic collisions with neutral atoms A(carbon) and B(neon), respectively [20] , and

$\nu_{eA0} = (8.3\times10^5)\pi {r_A}^2 n_{A0} {T_{e0}}^{\frac{1}{2}}$ and $\nu_{eB0} = (8.3\times10^5)\pi {r_B}^2 n_{B0} {T_{e0}}^{\frac{1}{2}}$,

$\nu_{eAi} = \nu_{eAi0}\left(\frac{n_{iA}}{n_{iA0}}\right)\left(\frac{T_e}{T_{e0}}\right)^{-\frac{3}{2}}$ and $\nu_{eBi} = \nu_{eBi0}\left(\frac{n_{iB}}{n_{iB0}}\right)\left(\frac{T_e}{T_{e0}}\right)^{-\frac{3}{2}}$ are the electron collision frequency (in sec^{-1}) due to elastic collisions with positively charged ion of type A(carbon) and type B(neon)[18], respectively.

$\nu_{eAi0} = \left(5.5\frac{n_{e0}}{{T_{e0}}^{\frac{3}{2}}}\right)\ln\left(\frac{220T_{e0}}{{n_{iA0}}^{\frac{1}{3}}}\right)$ and $\nu_{eBi0} = \left(5.5\frac{n_{e0}}{{T_{e0}}^{\frac{3}{2}}}\right)\ln\left(\frac{220T_{e0}}{{n_{iB0}}^{\frac{1}{3}}}\right)$,

$\delta_{eA} \approx 2\left(\frac{m_e}{m_A}\right)$ and $\delta_{eB} \approx 2\left(\frac{m_e}{m_B}\right)$ are the fraction of excess energy of an electron lost in a collision with the neutral atom A(carbon) and B(neon), respectively[18] and are dimensionless,

$\delta_{eAi} \approx 2\left(\frac{m_e}{m_{iA}}\right)$ and $\delta_{eBi} \approx 2\left(\frac{m_e}{m_{iB}}\right)$ are the fraction of excess energy of an electron lost in a collision with a positively charged ion A(carbon) and B(neon), respectively [18] and are dimensionless,

$\delta_{ects} \approx 2\left(\frac{m_e}{m_{cts}}\right)$ is the fraction of excess energy of an electron lost in a collision with a CNT [18] and is dimensionless where,

$m_{cts} = \frac{4}{3}\pi a^3 \rho_{cts}$ is the mass of the CNT for a spherical CNT tip , a is the radius of spherical CNT tip , and ρ_{cts} is the density of spherical CNT tip.

The first term in Eq.(23) is the power gained per unit volume by electrons due to ionization of neutral atoms, the second term is the energy loss per unit volume per unit time due to the sticking accretion and elastic collisions of electron at the spherical CNT tip, the third term is the energy loss per unit volume per unit time due to elastic electron - atom collisions. The fourth term is the energy loss per unit volume per unit time due to elastic electron- ion collision.

b) Energy balance for ions

The energy balance equation for ions is formed based on the dissociative ionization of neutrals, collisions with neutrals and electrons and their collection on the CNT surface.

$$\left(\frac{3}{2}k_B\right)\left(n_{iA}+n_{iB}\right)\left(\frac{dT_i}{d\tau}\right)=$$
$$\left[\left(\beta_A n_A \varepsilon_{iA}+\beta_B n_B \varepsilon_{iB}\right)-\left(\frac{3}{2}k_B\right)\left(\beta_A n_A+\beta_B n_B\right)T_i\right]+\left(\frac{3}{2}k_B\right)n_e\left(\nu_{eAi}\delta_{eAi}+\nu_{eBi}\delta_{eBi}\right)$$
$$\times\left(T_e-T_i\right)-n_{ct}\left\{\left(n_{iActs}\left[\varepsilon^l_{iAcs}-\left(\frac{3}{2}k_B\right)T_i\right]\right)+\left(n_{iBcts}\left[\varepsilon^l_{iBcs}-\left(\frac{3}{2}k_B\right)T_i\right]\right)\right\}-\left\{\left(\frac{3}{2}k_B\right)\times\right.$$
$$\left.\left[\left(\nu_{iAA}\delta_{iAA}+\nu_{iAB}\delta_{iAB}\right)n_{iA}+\left(\nu_{iBA}\delta_{iBA}+\nu_{iBB}\delta_{iBB}\right)n_{iB}\right]\left(T_i-T_n\right)\right\}. \quad (24)$$

where

$\frac{3}{2}\left(n_{iA}+n_{iB}\right)k_B T_i$ is the thermal energy of ions ,

n_{iA} and n_{iB} are the number density of positively charged ions of type A(carbon) and type B(neon), respectively(in cm^{-3}),T_i is the ion temperature (in K), T_n is the temperature of neutral (in K).

$\varepsilon^{l}_{iAcs}(Z)=\left[\frac{2-Z\alpha_{Ai}}{1-Z\alpha_{Ai}}\right]k_B T_i$ and $\varepsilon^{l}_{iBcs}(Z)=\left[\frac{2-Z\alpha_{Bi}}{1-Z\alpha_{Bi}}\right]k_B T_i$ are the mean energy (in eV) of positively charged ions, A(carbon) and B(neon),respectively (at large distance from the surface of the CNT) collected by the spherical CNT tip [18] .

ε_{ij} is the mean energy(in eV) of positively charged ions produced by the ionization of neutral atoms [18] and for ion A(carbon) and B(neon) are expressed as

$$\varepsilon_{iA}=\frac{3}{2}k_B T_{iA}+\frac{3k_B}{2\left(\alpha_A(T_e)\times n_{iA}\right)}\left[\left\{\nu_{iAA}\times\delta_{iAA}\times\left(T_i-T_n\right)\right\}-\left\{\nu_{eAi}\times\delta_{eAi}\times\left(T_e-T_i\right)\right\}\right]$$

$$\varepsilon_{iB}=\frac{3}{2}k_B T_{iB}+\frac{3k_B}{2\left(\alpha_B(T_e)\times n_{iB}\right)}\left[\left\{\nu_{iBB}\times\delta_{iBB}\times\left(T_i-T_n\right)\right\}-\left\{\nu_{eBi}\times\delta_{eBi}\times\left(T_e-T_i\right)\right\}\right]$$

$$\nu_{iAA}=\nu_{iAA0}\left(\frac{n_A}{n_{A0}}\right)\left(\frac{m_A T_i+m_{iA}T_n}{\left(m_A T_{i0}+m_{iA}T_{n0}\right)}\right)^{\frac{1}{2}},\nu_{iAB}=\nu_{iAB0}\left(\frac{n_B}{n_{B0}}\right)\left(\frac{m_B T_i+m_{iA}T_n}{\left(m_B T_{i0}+m_{iA}T_{n0}\right)}\right)^{\frac{1}{2}}$$

$$\nu_{iBA}=\nu_{iBA0}\left(\frac{n_A}{n_{A0}}\right)\left(\frac{m_A T_i+m_{iB}T_n}{\left(m_A T_{i0}+m_{iB}T_{n0}\right)}\right)^{\frac{1}{2}},\nu_{iBB}=\nu_{iBB0}\left(\frac{n_B}{n_{B0}}\right)\left(\frac{m_B T_i+m_{iB}T_n}{\left(m_B T_{i0}+m_{iB}T_{n0}\right)}\right)^{\frac{1}{2}}$$

are the collision frequencies(in sec^{-1}) of a j type of ion with j' ion of neutral atom[18],and

$$\nu_{iAA0} = \left(\frac{8}{3}\right)\left(2\pi k_B\right)^{\frac{1}{2}}(r_{iA}+r_A)^2\left(\frac{n_{A0}m_A}{\left(m_{iA}+m_A\right)}\right)\left[\left(\frac{T_{i0}}{m_{iA}}\right)+\left(\frac{T_{n0}}{m_A}\right)\right]^{\frac{1}{2}},$$

$$\nu_{iAB0} = \left(\frac{8}{3}\right)\left(2\pi k_B\right)^{\frac{1}{2}}(r_{iA}+r_B)^2\left(\frac{n_{B0}m_B}{\left(m_{iA}+m_B\right)}\right)\left[\left(\frac{T_{i0}}{m_{iA}}\right)+\left(\frac{T_{n0}}{m_B}\right)\right]^{\frac{1}{2}},$$

$$\nu_{iBA0} = \left(\frac{8}{3}\right)\left(2\pi k_B\right)^{\frac{1}{2}}(r_{iB}+r_A)^2\left(\frac{n_{A0}m_A}{\left(m_{iB}+m_A\right)}\right)\left[\left(\frac{T_{i0}}{m_{iB}}\right)+\left(\frac{T_{n0}}{m_A}\right)\right]^{\frac{1}{2}},$$

$$\nu_{iBB0} = \left(\frac{8}{3}\right)\left(2\pi k_B\right)^{\frac{1}{2}}(r_{iB}+r_B)^2\left(\frac{n_{B0}m_B}{\left(m_{iB}+m_B\right)}\right)\left[\left(\frac{T_{i0}}{m_{iB}}\right)+\left(\frac{T_{n0}}{m_B}\right)\right]^{\frac{1}{2}},$$

$$\delta_{iAA} = \left[\frac{2m_{iA}}{(m_A+m_{iA})}\right], \delta_{iBB} = \left[\frac{2m_{iB}}{(m_B+m_{iB})}\right], \delta_{iAB} = \left[\frac{2m_{iA}}{(m_B+m_{iA})}\right], \delta_{iBA} = \left[\frac{2m_{iB}}{(m_A+m_{iB})}\right]$$

are the fraction of the excess energy of a j type positively charged ion, lost in a collision with neutral j' kind of neutral atom and are dimensionless. where j and j' can be same (i.e., both carbon) or be different (i.e., one carbon and other neon)

The first term in Eq.(24) is the energy gained by ions per unit volume per unit time due to the ionization of neutral atoms, the second term is the energy gained per unit volume per unit time due to the elastic collision of ions with electrons, the third term is the energy loss per unit volume per unit time due to the sticking accretion of ions at the surface of the CNT. The last term is the energy lost per unit volume per unit time due to elastic collision with neutral species.

c) Energy balance for neutrals

The energy balance of neutrals is based on the recombination of electrons and ions, collision of neutrals with electrons and ions, neutralization of ions collected on the surface of CNT, and neutral collection current on spherical CNT tip.

$$\frac{3}{2}\left(n_A+n_B\right)k_B\left(\frac{dT_n}{d\tau}\right)=$$
$$\left[\left\{\left(\frac{3}{2}k_B\right)\left(\alpha_A n_e n_{iA}+\alpha_B n_e n_{iB}\right)\left(T_e+T_i-T_n\right)\right\}+\left(\alpha_A n_e n_{iA} I_{pA}+\alpha_B n_e n_{iB} I_{pB}\right)\right]$$
$$+\left\{\left[\left(\frac{3}{2}k_B\right)n_e\left(\nu_{eA}\delta_{eA}+\nu_{eB}\delta_{eB}\right)\left(T_e-T_n\right)\right]+\left[\left(\frac{3}{2}k_B\right)\left(\nu_{iAA}\delta_{iAA}n_{iA}+\nu_{iAB}\delta_{iAB}n_{iA}\right)\right.\right.$$
$$\left.\left.\left(T_i-T_n\right)+\left(\frac{3}{2}k_B\right)\left(\nu_{iBA}\delta_{iBA}n_{iB}+\nu_{iBB}\delta_{iBB}n_{iB}\right)\left(T_i-T_n\right)\right]\right\}$$
$$+\left\{\left(\frac{3}{2}k_B\right)n_{ct}\left[\left(1-\gamma_{iA}\right)n_{iActs}+n_{iBcts}\right]\left(T_{ct}-T_n\right)\right\}$$
$$-\left\{\left(\frac{3}{2}k_B\right)n_{ct}\left[n_{Acts}\delta_{Acts}\left(1-\gamma_A\right)\times\left(T_n-T_{ct}\right)+n_{Bcts}\delta_{Bcts}\left(T_n-T_{ct}\right)\right]\right\}-E_{diss}. \qquad (25)$$

where

I_{pA} and I_{pB} are the ionization energy (in eV) of the constituent atomic species of type A (carbon) and type B(neon),respectively,

$E_{diss}=\left(E_{A,diss}+E_{B,diss}\right)$, $E_{j,diss}$ is the energy dissipated per unit volume per unit time by neutral atoms into the surrounding atmosphere and is assumed to be equal to the difference between the temperature of the neutral atomic species and the ambient temperature.

$E_{j,diss} = E_{j,diss0}\left[\frac{\left(T_j - T_a\right)}{\left(T_{j0} - T_a\right)}\right]$ (in eV) , constant $E_{j,diss0}$ is obtained by imposing the ambient condition of the complex plasma system in Eq.(25) for both constituent neutral species[18] ,T_a is the ambient temperature.

$\delta_{Acts} = \left[\frac{2m_A}{\left(m_A + m_{cts}\right)}\right]$ and $\delta_{Bcts} = \left[\frac{2m_B}{\left(m_B + m_{cts}\right)}\right]$ are the fraction of excess energy of a neutral A(carbon) and B(neon), respectively lost in a collision with spherical CNT tip [18] and are dimensionless.

and

$m_{cts} = \frac{4}{3}\pi a^3 \rho_{cts}$ is the mass of the CNT for a spherical CNT tip , a is the radius of spherical CNT tip , and ρ_{cts} is the density of spherical CNT tip,

The first term in Eq.(25) is the power gained per unit volume by the neutral species due to recombination of electrons and positively charged ions, the second term is the rate of power gained per unit volume by neutral atoms in elastic collision with electrons and positively charged ions. The third term is the energy gained per unit volume per second due to formation of neutrals at the surface of the CNT due to ion and electron accretion. The fourth term refers to the thermal energy lost per unit volume per unit time by neutral atoms accretion on and collision with CNT tip. The last term is the energy dissipation rate per unit volume by neutral atoms to the surrounding atmosphere.

d) Energy balance for spherical CNT tip

The energy balance of CNT tip is formed based on electron, neutral and ion collection currents on CNT surface and the radiation and conduction to the host gas.

$$\frac{d}{d\tau}\left(m_{cts}C_pT_{ct}\right)=\left\{n_{ects}\left[\gamma_{es}\ \varepsilon^{s}{}_{ecs}+(1-\gamma_{es})\delta_{ects}\left[\varepsilon^{s}{}_{ecs}-\left(\frac{3}{2}k_B\right)T_{ct}\right]\right]\right\}$$
$$-\left\{\left(\frac{3}{2}k_B\right)\left\{\left(n_{Acts}\left[\gamma_A T_n+\delta_{Acts}\left(1-\gamma_A\right)\left(T_n-T_{ct}\right)\right]\right)+\left(n_{Bcts}\delta_{Bcts}\left(T_n-T_{ct}\right)\right)\right\}\right\}+$$
$$\left\{\left[n_{iActs}\left(\varepsilon^{l}{}_{iAcs}+I_{pA}\right)+n_{iBcts}\left(\varepsilon^{l}{}_{iBcs}+I_{pB}\right)\right]\right\}-\left\{\left(\frac{3}{2}k_B\right)\left[\left(1-\gamma_{iA}\right)n_{iActs}+n_{iBcts}\right]T_{ct}\right\}$$
$$-\left\{4\pi a^2\left[\varepsilon\sigma\left(T_{ct}^4-T_a^4\right)+n_A\left(\frac{8k_BT_n}{\pi m_A}\right)^{\frac{1}{2}}+n_B\left(\frac{8k_BT_n}{\pi m_B}\right)^{\frac{1}{2}}\right]k_B\left(T_{ct}-T_n\right)\right\}. \qquad (26)$$

$\varepsilon^{l}_{iAcs}(Z)=\left[\frac{2-Z\alpha_{Ai}}{1-Z\alpha_{Ai}}\right]k_BT_i$ and $\varepsilon^{l}_{iBcs}(Z)=\left[\frac{2-Z\alpha_{Bi}}{1-Z\alpha_{Bi}}\right]k_BT_i$ are the mean energy of positively charged ions (in eV), A(carbon) and B(neon),respectively (at large distance from the surface of the CNT) collected by the spherical CNT tip [18].

C_p is the specific heat of the material of the CNT at constant pressure (in ergs/gm K),

$\in$ is the emissivity of the material of the CNT and is dimensionless,

σ is the Stefan –Boltzmann constant= $5.672\text{x}10^{-5}$ erg sec^{-1} cm^{-2} K^{-4}.

The first three terms in Eq. (26) are the rate of energy transferred to the CNT tip due to sticking accretion and elastic collision by constituent species of complex plasma. The fourth term is the energy carried away by the neutral species (generated by the recombination of the accreted ions and electrons) from the spherical CNT tip per unit volume per unit time.

The last term is the rate of energy dissipation of the spherical CNT tip through radiation and conduction to the host gas [21].

G. Energy balance equation of electrons, ions and electrons and cylindrical CNT surface for growth of cylindrical CNT surface

Following the same method as in chapter 2, the energy balance equation of electrons, ions and electrons for cylindrical CNT surface case can be written as

a) Energy balance for electrons

The energy balance of electrons is accounted based on the dissociative ionization process of neutrals, the electron collection current on the CNT and its collision with CNT and the collision of electrons with neutrals and ions.

$$\left(\frac{3}{2}k_B\right)n_e\left(\frac{dT_e}{d\tau}\right)=\left[\left(\beta_A n_A\varepsilon_A+\beta_B n_B\varepsilon_B\right)-\left(\frac{3}{2}k_B\right)\left(\beta_A n_A+\beta_B n_B\right)T_e\right]-n_{ct}n_{ectcy}$$
$$\left\{\left[\gamma_{ecy}\varepsilon^{l}_{eccy}-\left(\frac{3}{2}k_B\right)T_e\right]+\delta_{ectcy}\left(1-\gamma_{ecy}\right)\left[\varepsilon^{s}_{eccy}-\left(\frac{3}{2}k_B\right)T_{ct}\right]\right\}-\left(\frac{3}{2}k_B\right)$$
$$\left\{\left(\nu_{eA}\delta_{eA}+\nu_{eB}\delta_{eB}\right)\left(T_e-T_n\right)+\left(\nu_{eAi}\delta_{eAi}+\nu_{eBi}\delta_{eBi}\right)\left(T_e-T_i\right)\right\}n_e. \quad (27)$$

where

$\varepsilon^{l}_{eccy}(Z)=k_BT_e\left[2-\left(\frac{eV_S}{k_BT_e}\right)\right]$ is the mean energy of electrons (in eV) at a large distance from the surface of cylindrical CNT surface[19].

$\varepsilon^{s}_{eccy}(Z)=2k_BT_e$ is the mean energy of electrons(in eV) collected by cylindrical CNT surface[19].

$\delta_{ectcy}\approx 2\left(\frac{m_e}{m_{ctcy}}\right)$ is the fraction of excess energy of an electron lost in a collision with cylindrical CNT surface [19]and is dimensionless.

$m_{ctcy} = \pi r^2 l \rho_{ctcy}$ is the mass of the CNT for a cylindrical CNT surface , r is the radius of cylindrical CNT surface , l is the length of cylindrical CNT surface and ρ_{ctcy} is the density of cylindrical CNT surface.

The other symbols used in Eq.(27) are explained earlier in the section F for energy balance of electrons for spherical CNT tip case.

The first term in Eq.(27) is the power gained per unit volume by electrons due to ionization of neutral atoms, the second term is the energy loss per unit volume per unit time due to the sticking accretion and elastic collisions of electron on the cylindrical CNT surface, the third term is the energy loss per unit volume per unit time due to elastic electron - atom collisions and elastic electron- ion collision.

b) Energy balance for ions

$$\left(\frac{3}{2}k_B\right)\left(n_{iA}+n_{iB}\right)\left(\frac{dT_i}{d\tau}\right)=$$

$$\left[\left(\beta_A n_A \varepsilon_{iA}+\beta_B n_B \varepsilon_{iB}\right)-\left(\frac{3}{2}k_B\right)\left(\beta_A n_A+\beta_B n_B\right)T_i\right]+\left(\frac{3}{2}k_B\right)n_e\left(\nu_{eAi}\delta_{eAi}+\nu_{eBi}\delta_{eBi}\right)$$

$$\times\left(T_e-T_i\right)-n_{ct}\left\{\left(n_{iActcy}\left[\varepsilon^l_{iAccy}-\left(\frac{3}{2}k_B\right)T_i\right]\right)+\left(n_{iBctcy}\left[\varepsilon^l_{iBccy}-\left(\frac{3}{2}k_B\right)T_i\right]\right)\right\}-\left(\frac{3}{2}k_B\right)\times$$

$$\left[\left(\nu_{iAA}\delta_{iAA}+\nu_{iAB}\delta_{iAB}\right)n_{iA}+\left(\nu_{iBA}\delta_{iBA}+\nu_{iBB}\delta_{iBB}\right)n_{iB}\right]\left(T_i-T_n\right). \quad (28)$$

where

$$\varepsilon^l_{iAccy}(Z)=k_B T_i n_{iA} rl\left(\frac{2\pi k_B T_i}{m_{iA}}\right)^{\frac{1}{2}}\left[\left(\frac{4}{\sqrt{\pi}}\right)\left(\frac{eV_S}{k_B T_i}\right)^{\frac{1}{2}}+\left(2-\left(\frac{eV_S}{k_B T_i}\right)^{\frac{1}{2}}\right)\exp\left[\frac{eV_S}{k_B T_i}\right]erfc\left[\left(\frac{eV_S}{k_B T_i}\right)^{\frac{1}{2}}\right]\right]$$

$$\varepsilon^l_{iBccy}(Z)=k_B T_i n_{iB} rl\left(\frac{2\pi k_B T_i}{m_{iB}}\right)^{\frac{1}{2}}\left[\left(\frac{4}{\sqrt{\pi}}\right)\left(\frac{eV_S}{k_B T_i}\right)^{\frac{1}{2}}+\left(2-\left(\frac{eV_S}{k_B T_i}\right)^{\frac{1}{2}}\right)\exp\left[\frac{eV_S}{k_B T_i}\right]erfc\left[\left(\frac{eV_S}{k_B T_i}\right)^{\frac{1}{2}}\right]\right]$$

are the mean energy of ions(in eV) at a large distance from the surface of cylindrical CNT surface[19] of A (carbon) and B(neon), respectively.

The other symbols used in Eq.(28) are explained earlier in the section F for energy balance of ions for spherical CNT tip case.

The first term in Eq.(28) is the energy gained by ions per unit volume per unit time due to the ionization of neutral atoms , the second term is the energy gained per unit volume per unit time due to the elastic collision of ions with electrons, the third term is the energy loss per unit volume per unit time due to the sticking accretion of ions at the cylindrical CNT surface. The last term is the energy lost per unit volume per unit time due to elastic collision of ions with neutral species.

c) Energy balance for neutrals

$$\frac{3}{2}\left(n_A+n_B\right)k_B\left(\frac{dT_n}{d\tau}\right)=$$
$$\left[\left\{\left(\frac{3}{2}k_B\right)\left(\alpha_A n_e n_{iA}+\alpha_B n_e n_{iB}\right)\left(T_e+T_i-T_n\right)\right\}+\left(\alpha_A n_e n_{iA} I_{pA}+\alpha_B n_e n_{iB} I_{pB}\right)\right]$$
$$+\left\{\left[\left(\frac{3}{2}k_B\right)n_e\left(\nu_{eA}\delta_{eA}+\nu_{eB}\delta_{eB}\right)\left(T_e-T_n\right)\right]+\left[\left(\frac{3}{2}k_B\right)\left(\nu_{iAA}\delta_{iAA}n_{iA}+\nu_{iAB}\delta_{iAB}n_{iA}\right)\right.\right.$$
$$\left.\left(T_i-T_n\right)+\left(\frac{3}{2}k_B\right)\left(\nu_{iBA}\delta_{iBA}n_{iB}+\nu_{iBB}\delta_{iBB}n_{iB}\right)\left(T_i-T_n\right)\right]\Big\}+\left\{\left(\frac{3}{2}k_B\right)n_{ct}\left[\left(1-\gamma_{iA}\right)n_{iActcy}\right.\right.$$
$$\left.+n_{iBctcy}\right]\left(T_{ct}-T_n\right)\Big\}-\left\{\left(\frac{3}{2}k_B\right)n_{ct}\left[n_{Actcy}\delta_{Actcy}\left(1-\gamma_A\right)\times\left(T_n-T_{ct}\right)+n_{Bctcy}\right.\right.$$
$$\left.\left.\delta_{Bctcy}\left(T_n-T_{ct}\right)\right]\right\}-E_{diss}. \qquad (29)$$

where

$\delta_{Actcy}=\left[\frac{2m_A}{\left(m_A+m_{ctcy}\right)}\right]$, $\delta_{Bctcy}=\left[\frac{2m_B}{\left(m_B+m_{ctcy}\right)}\right]$ are the fraction of excess energy of a neutral A(carbon) and B(neon),respectively lost in a collision with cylindrical CNT surface [19].

The other symbols used in Eq.(29) are explained earlier in the section F for energy balance of neutrals in spherical CNT tip case .

The first term in Eq.(29) is the power gained per unit volume by the neutral species due to recombination of electrons and positively charged ions, the second term is the rate of power gained per unit volume by neutral atoms in elastic collision with electrons and positively charged ions. The third term is the energy gained per unit volume per second due to formation of neutrals at the surface of the CNT due to ion and electron accretion. The fourth term refers to the thermal energy lost per unit volume per unit time by neutral atoms due to their accretion on and collision with cylindrical CNT surface. The last term is the energy dissipation rate per unit volume by neutral atoms to the surrounding atmosphere.

d) Energy balance for cylindrical CNT surface

$$\frac{d}{d\tau}\left(m_{ctcy}C_p\ T_{ct}\right)=\left\{n_{ectcy}\left[\gamma_{ecy}\ \varepsilon^{s}{}_{eccy}+\left(1-\gamma_{ecy}\right)\delta_{ectcy}\left[\varepsilon^{s}{}_{eccy}-\left(\frac{3}{2}k_B\right)T_{ct}\right]\right]\right\}$$
$$-\left\{\left(\frac{3}{2}k_B\right)\left\{\left(n_{Actcy}\left[\gamma_A T_n+\delta_{Actcy}\left(1-\gamma_A\right)\left(T_n-T_{ct}\right)\right]\right)+\left(n_{Bctcy}\delta_{Bctcy}\left(T_n-T_{ct}\right)\right)\right\}\right\}+$$
$$\left\{\left[n_{iActcy}\left(\varepsilon^{l}{}_{iAccy}+I_{pA}\right)+n_{iBctcy}\left(\varepsilon^{l}{}_{iBccy}+I_{pB}\right)\right]\right\}-\left\{\left(\frac{3}{2}k_B\right)\left[\left(1-\gamma_{iA}\right)n_{iActcy}\right.\right.$$
$$\left.\left.+n_{iBctcy}\right]\right\}T_{ct}-2\pi r\left(r+l\right)\left[\varepsilon\sigma\left(T_{ct}^{4}-T_a^{4}\right)+n_A\left(\frac{8k_BT_n}{\pi m_A}\right)^{\frac{1}{2}}+n_B\left(\frac{8k_BT_n}{\pi m_B}\right)^{\frac{1}{2}}\right]k_B\left(T_{ct}-T_n\right)\Big].$$

(30)

where

$$\varepsilon^{l}_{iAccy}(Z) = k_B T_i n_{iA} rl \left(\frac{2\pi k_B T_i}{m_{iA}}\right)^{\frac{1}{2}} \left[\left(\frac{4}{\sqrt{\pi}}\right)\left(\frac{eV_S}{k_B T_i}\right)^{\frac{1}{2}} + \left(2 - \left(\frac{eV_S}{k_B T_i}\right)^{\frac{1}{2}}\right) \exp\left[\frac{eV_S}{k_B T_i}\right] erfc\left[\left(\frac{eV_S}{k_B T_i}\right)^{\frac{1}{2}}\right]\right]$$

$$\varepsilon^{l}_{iBccy}(Z) = k_B T_i n_{iB} rl \left(\frac{2\pi k_B T_i}{m_{iB}}\right)^{\frac{1}{2}} \left[\left(\frac{4}{\sqrt{\pi}}\right)\left(\frac{eV_S}{k_B T_i}\right)^{\frac{1}{2}} + \left(2 - \left(\frac{eV_S}{k_B T_i}\right)^{\frac{1}{2}}\right) \exp\left[\frac{eV_S}{k_B T_i}\right] erfc\left[\left(\frac{eV_S}{k_B T_i}\right)^{\frac{1}{2}}\right]\right]$$

are the mean energy of ions(in eV) at a large distance from the surface of cylindrical CNT surface[19] of A (carbon) and b(neon), respectively.

C_p is the specific heat of the material of the CNT at constant pressure (in ergs/gm K),

$\in$ is the emissivity of the material of the CNT and is dimensionless,

σ is the Stefan –Boltzmann constant= 5.672×10^{-5} erg sec^{-1} cm^{-2} K^{-4}.

The first three terms in Eq. (30) are the rate of energy transferred to the CNT surface due to sticking accretion and elastic collision by constituent species of complex plasma. The fourth term is the energy carried away by the neutral species (generated by the recombination of the accreted ions and electrons) from the cylindrical CNT surface per unit volume per unit time. The last term is the rate of energy dissipation of the cylindrical CNT surface through radiation and conduction to the host gas [21].

3.4: Results and Discussions

The calculations have been carried out to study the dependence of radius of spherical CNT tip and cylindrical CNT surface, individually on the plasma parameters, i.e., electron density (n_e), electron temperature (T_e), ion density(n_i), ion temperature (T_i) and CNT number density(n_{ct}).

The plasma is composed of two types of ions, A (carbon) and B (neon) ,electrons and neutrals of A(carbon) and B(neon) . The neutral carbon and neon atom ionizes to produce carbon and neon ions and electrons. The

electron and ions of neon and carbon combines to produce neon and carbon neutrals, respectively. The process that contributes to growth is the accretion of neutral atoms and positively charged ions of carbon on the CNT.

The initial radius of spherical CNT tip (a_0) and cylindrical CNT surface (r_0) is calculated from Eqs. (5) and (6), respectively. We have simultaneously solved equations for charging of CNT, kinetics and energy balance of electrons, ions, neutrals and of spherical CNT tip and cylindrical CNT surface, separately to evaluate the evolution of radius of CNT with time for different plasma parameters.

A. Results for spherical CNT tip

The boundary conditions, at $\tau = 0$ for case of spherical CNT tip are

CNT number density $\left(n_{ct}\right)=10^{6}\text{cm}^{-3}$,ion density of carbon(type A)$\left(n_{iA0}=0.6n_{e0}\right)$, ion density of neon(typeB) $n_{iB0}=0.4n_{e0}$,neutral atom density of carbon and neon $\left(n_{A0}=n_{B0}\right)=5\times10^{11}cm^{-3}$,electron number density $\left(n_{e0}\right)=10^{12}\text{cm}^{-3}$, electron temperature $\left(T_{e0}\right)=0.6\text{eV}$,ion temperature $\left(T_{i0}\right)=2400K$, neutral temperature $\left(T_{n0}\right)=$ CNT temperature $\left(T_{ct}\right)=2000K$, mass of carbon ion $\left(m_{iA}\right)\approx$ mass of neutral carbon atom $\left(m_{A}\right)=12\text{amu}$,mass of neon ion $\left(m_{iB}\right)\approx$ mass of neon atom $\left(m_{B}\right)=20\text{amu}$,coefficient of recombination of carbon and neon with electron $\left(\alpha_{A0}\approx\alpha_{B0}\right)=10^{-7}cm^{3}/\sec$, emissivity of carbon $(\varepsilon)=0.6$, sticking coefficients of carbon ion or carbon atom $\left(\gamma_{iA}=\gamma_{A}\right)$=1,specific heat of carbon $\left(C_{p}\right)=7\times10^{6}$ergs/gm K,ionization energy of carbon $\left(I_{pA}\right)=11.26\text{eV}$,ionization energy of neon $\left(I_{pB}\right)=$ 10eV, mean energy of electron due to ionization of carbon atom $\left(\varepsilon_{A}\right)=$ 6.2eV,mean energy of electron due to ionization of neon atom $\left(\varepsilon_{B}\right)$ $=10.7\text{eV}$, mean energy of carbon ion due to ionization of carbon atom $\left(\varepsilon_{iA}\right)=7.3\text{eV}$,mean energy of neon ion due to ionization of neon atom $\left(\varepsilon_{iB}\right)=12.2\text{eV}$,energy dissipated by carbon $\left(\varepsilon_{A,diss0}\right)=42.9\text{eV}$, energy dissipated by neon $\left(\varepsilon_{B,diss0}\right)=19.6\text{eV}$,constant $(\kappa)=-1.2$, radius of CNT (a_0)= 0.7nm and density of CNT $\left(\rho_{ct}\right)$ = 4.2g/cm^3.

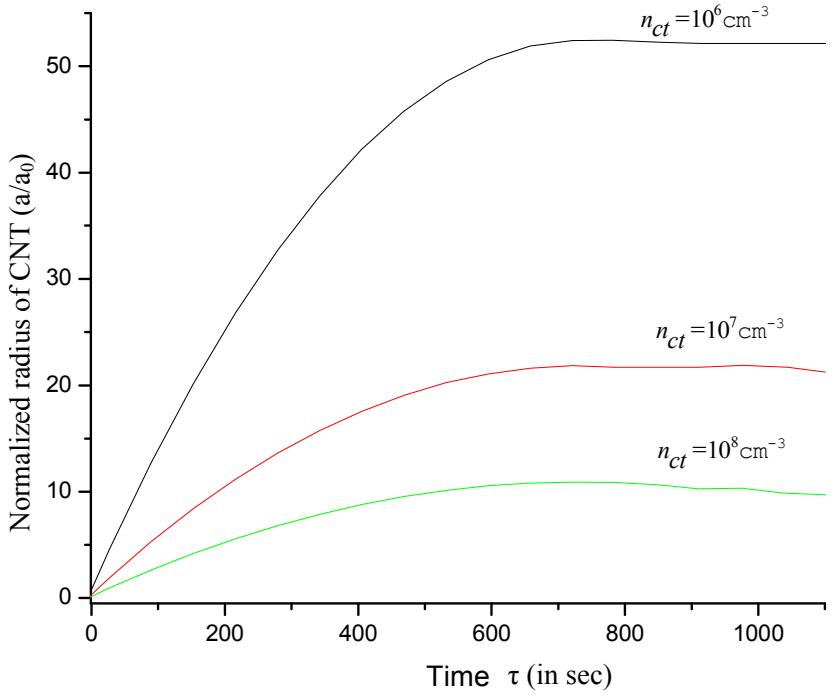

FIG.1. Shows the variation of the normalized radius a/a_0 of spherical CNT tip for different CNT number density.

In Fig. 1 the variation of normalized radius a/a_0 of spherical CNT tip with time for different CNT number density (i.e., n_{ct} = 10^6 cm^{-3}, 10^7 cm^{-3}, 10^8 cm^{-3}) and for other parameters as mentioned above, is illustrated. From Fig. 1 it can be seen that the normalized radius of CNT first increases with time and then attains a saturation value. It also shows the decrease of normalized radius a/a_0 with CNT number density n_{ct} (in cm^{-3}). This happens because for larger values of CNT number density (n_{ct}), the number of positively charged ions and neutral atoms available for accretion decreases. Since it is the accretion of neutral atoms and positively charged ions on the CNT, which leads to its growth, the decrease in their number density leads to decrease in radius of CNT.

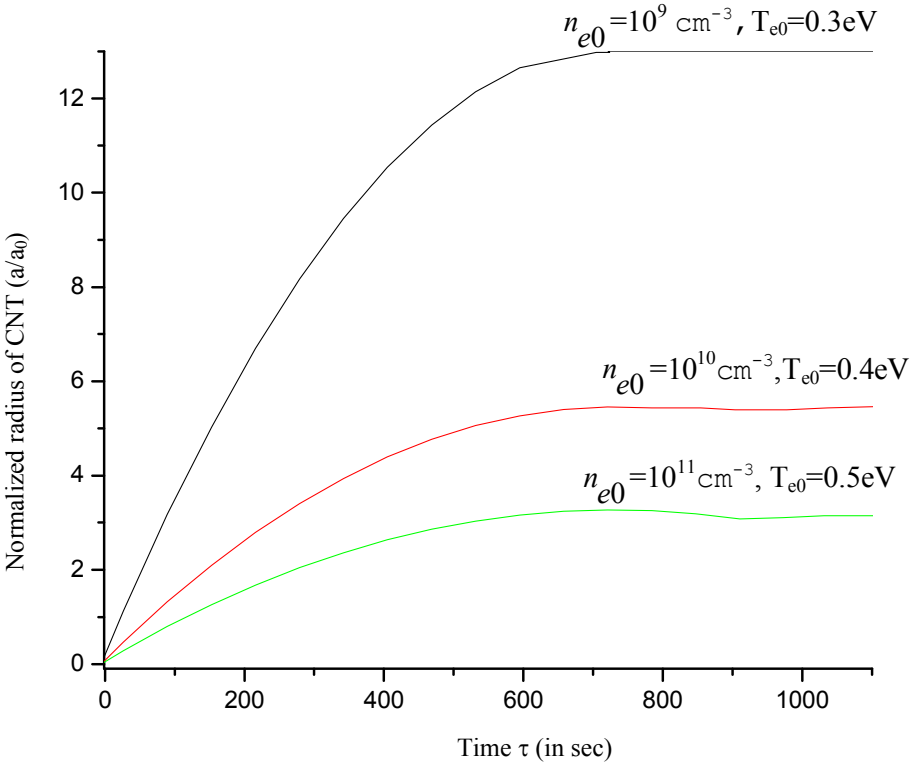

Fig. 2: Shows the variation of the normalized radius a/a_0 of spherical CNT tip for different electron number densities and electron temperatures.

In Fig. 2 the variation of normalized radius a/a_0 of spherical CNT tip with time for different electron number densities and electron temperatures (e.g., n_{e0}=10^9 cm^{-3} and T$_{e0}$=0.3eV, n_{e0}= 10^{10} cm^{-3} and T$_{e0}$=0.4eV, n_{e0}=10^{11} cm^{-3} and T$_{e0}$=0.5eV) is shown. Fig. 2 illustrates that the normalized CNT radius a/a_0 first increases with time and then attains a saturation value. It can also be seen that the normalized radius a/a_0 decreases with electron density and temperatures. The decrease of a/a_0 with electron density and temperatures is because with increase in electron densities and temperatures more and more neutral atoms ionizes to produce positively charged ions and electrons. Since the accretion of

neutral atoms on the CNT leads to its growth, the decrease in their number density because of increase in the electron density and temperature leads to decrease in radius of the CNT.

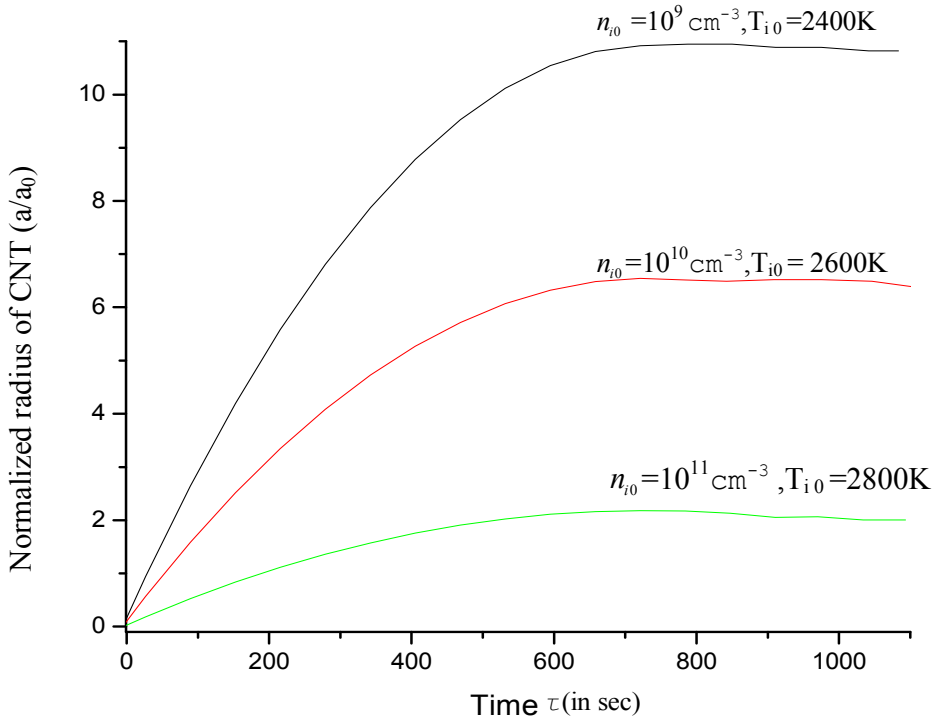

FIG. 3. Shows the variation of the normalized radius a/a$_0$ of spherical CNT tip for different ion number densities and ion temperatures

In Fig. 3 the variation of the normalized a/a$_0$ of spherical CNT tip with time for different ion number densities and ion temperatures (e.g., n_{i0}=10^9 cm^{-3}and T$_{i0}$=2400K, n_{i0}=10^{10} cm^{-3}and T$_{i0}$=2600K, n_{i0}=10^{11} cm^{-3} and T$_{i0}$=2800K) is displayed . From Fig. 3 it can be seen that the CNT radius first increases with time and then attains a saturation value. The CNT radius decreases with ion density n_{i0} (in cm^{-3}) and temperature T$_i$ (in K) can be seen. This happens because by increasing the ion density and temperatures, more and more neutral atoms ionize to produce positively

charged ions and electrons. Since it is the accretion of neutral atoms on the CNT, which leads to its growth, therefore by increasing the positively charged ion density and temperature the radius of the CNT decreases.

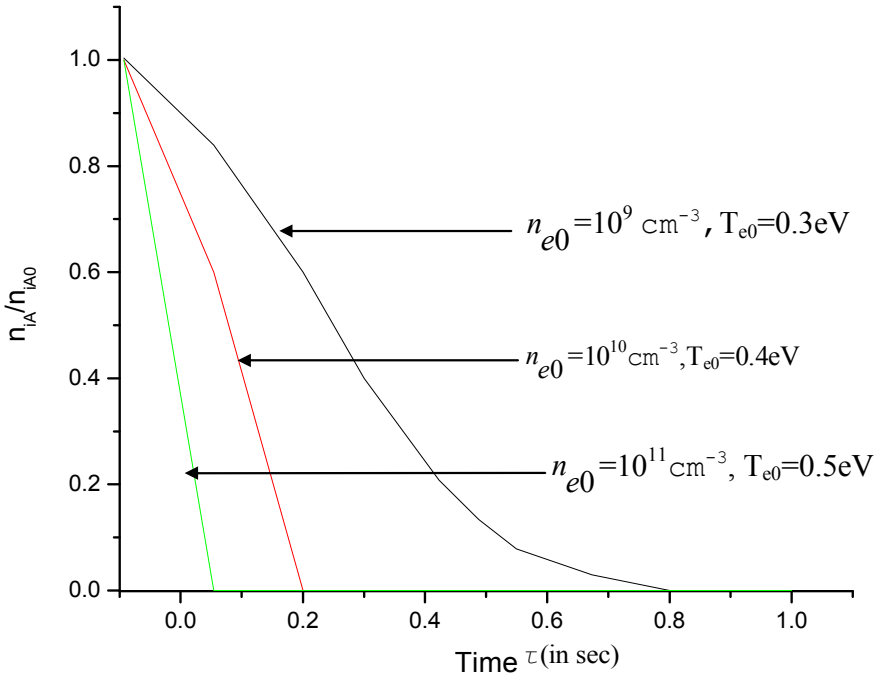

FIG.4. Shows the dependence of ionic number density of type A in plasma for different electron number densities and electron temperatures .

In Fig. 4 the variation of normalized ionic density of type A in plasma with time for different electron number densities and temperatures (e.g., n_{e0}=10^{9} cm^{-3} and T_{e0}=0.3eV, n_{e0}= 10^{10} cm^{-3} and T_{e0}=0.4eV, n_{e0}=10^{11} cm^{-3} and T_{e0}=0.5eV) is shown. It can be seen from Fig. 4 that with increasing electron density and temperature, the positively charged ion of A type decays faster.

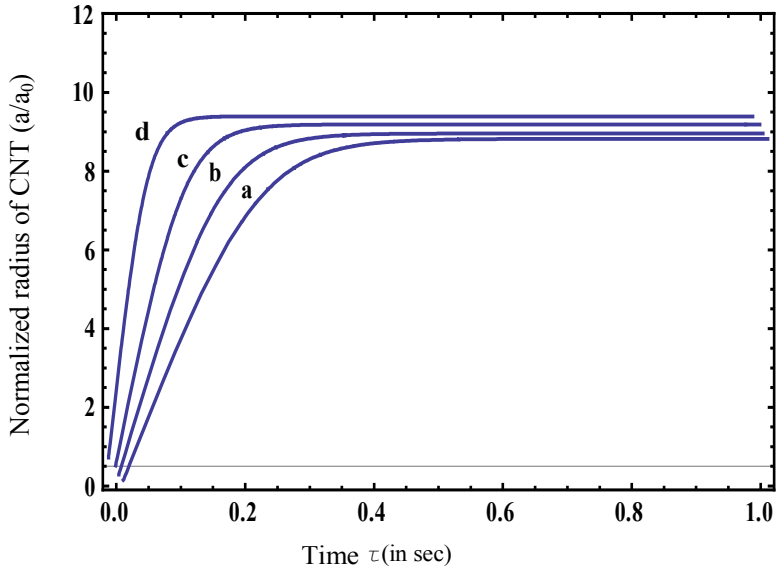

FIG. 5. Shows the variation of the normalized radius with time on the sticking coefficient of the atomic species for a, b, c, d corresponding to γ_A = 0.1, 0.3, 0.5 and 1.0, respectively.

In Fig. 5 the variation of the normalized radius a/a_0 of spherical CNT tip for different value of the sticking coefficients of atomic species(i.e., γ_A = 0.1,0.3, 0.5 & 1.0) is displayed. It can be seen from Fig. 5 that steady state is achieved faster for larger sticking coefficients of atomic species.

B. Results for cylindrical CNT surface

The boundary conditions, at $\tau = 0$ for case of cylindrical CNT surface are

CNT number density $\left(n_{ct}\right)=10^{4}\text{cm}^{-3}$,ion density of carbon(type A)$\left(n_{iA0}=0.6n_{e0}\right)$, ion density of neon(typeB) $n_{iB0}=0.4n_{e0}$,neutral atom density of carbon and neon$\left(n_{A0}=n_{B0}\right)=5\times10^{14}cm^{-3}$,electron number density$\left(n_{e0}\right)=10^{6}\text{cm}^{-3}$, electron temperature$\left(T_{e0}\right)=0.4\text{eV}$,ion temperature$\left(T_{i0}\right)=2200K$,neutral temperature $\left(T_{n0}\right)=$ CNT temperature$\left(T_{ct}\right)=2000K$,surface potential ($V_S$)= -2×10^{-4} StatV, mass of carbon ion$\left(m_{iA}\right)\approx$ mass of neutral carbon atom$\left(m_{A}\right)=12\text{amu}$,mass of neon ion $\left(m_{iB}\right)\approx$ mass of neon atom$\left(m_{B}\right)=20\text{amu}$,coefficient of recombinationof carbon and neon with electron$\left(\alpha_{A0}\approx\alpha_{B0}\right)=10^{-7}cm^{3}/\text{sec}$,emissivity of carbon $(\varepsilon)=0.6$,sticking coefficients of carbon ion or carbon atom$\left(\gamma_{iA}=\gamma_{A}\right)$=1,specific heat of carbon$\left(C_{p}\right)=7\times10^{6}$ergs/gm K,ionization energy of carbon$\left(I_{pA}\right)=11.26\text{eV}$,ionization energy of neon$\left(I_{pB}\right)=10\text{eV}$,mean energy of electron due to ionization of carbon atom$\left(\varepsilon_{A}\right)=6.2\text{eV}$,mean energy of electron due to ionization of neon atom $\left(\varepsilon_{B}\right)=10.7\text{eV}$,mean energy of carbon ion due to ionization of carbon atom$\left(\varepsilon_{iA}\right)=$ 7.3eV,mean energy of neon ion due to ionization of neon atom$\left(\varepsilon_{iB}\right)=12.2\text{eV}$, energy dissipated by carbon$\left(\varepsilon_{A,diss0}\right)=42.9\text{eV}$,energy dissipated by neon$\left(\varepsilon_{B,diss0}\right)=19.6\text{eV}$,constant$(\kappa)=-1.2$,radius of CNT($r_0$)= 8×10^{-7}cm and density of CNT$\left(\rho_{ct}\right)$ = 4.2g/cm^3.

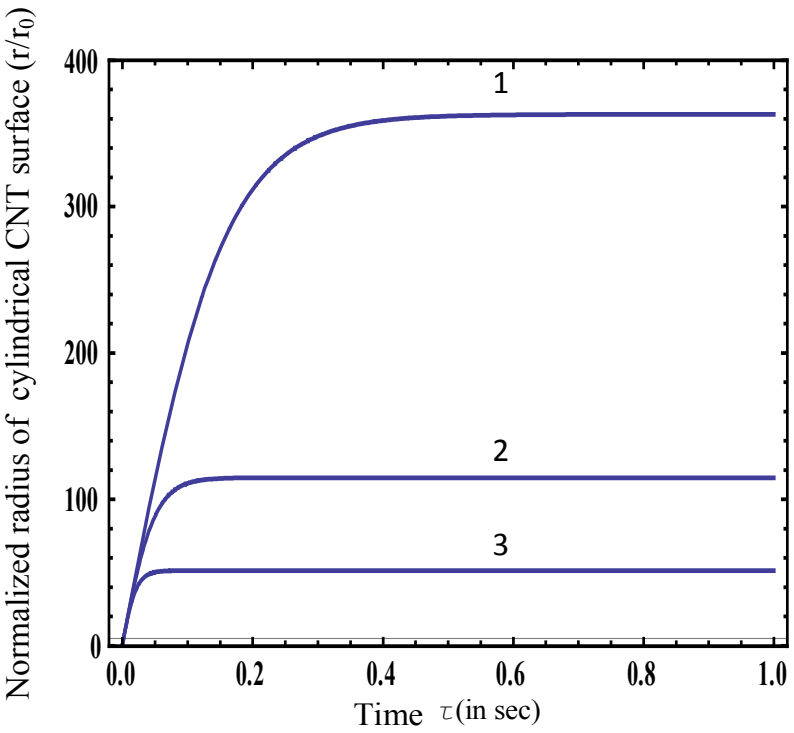

FIG. 6. Shows the variation of the normalized radius r/r_0 of cylindrical CNT with time for different CNT number density, curves 1,2 and 3 correspond to CNT density(n_{ct}) = 10^3 cm^{-3} , $1x10^4$ cm^{-3} and $5x10^4$ cm^{-3}, respectively.

In Fig.6 the variation of the normalized radius r/r_0 for cylindrical CNT surface with time for different CNT number density (i.e., n_{ct} = $10^3 cm^{-3}$, $10^4 cm^{-3}$ and $5x10^4$ cm^{-3}) and for other parameters are same as mentioned above, is plotted. From Fig. 6, it can be seen that the normalized radius of the CNT first increases with time and then attains a saturation value. It also shows the decrease of normalized radius r/r_0 with CNT number density n_{ct} (in cm^{-3}). This happens because for larger values of CNT number density $\left(n_{ct}\right)$, the number of positively charged ions, and neutral atoms available for accretion decreases. Because it is the accretion of neutral atoms and positively charged ions on the CNT, which leads to its growth, the decrease in their number density leads to decrease in radius of the CNT.

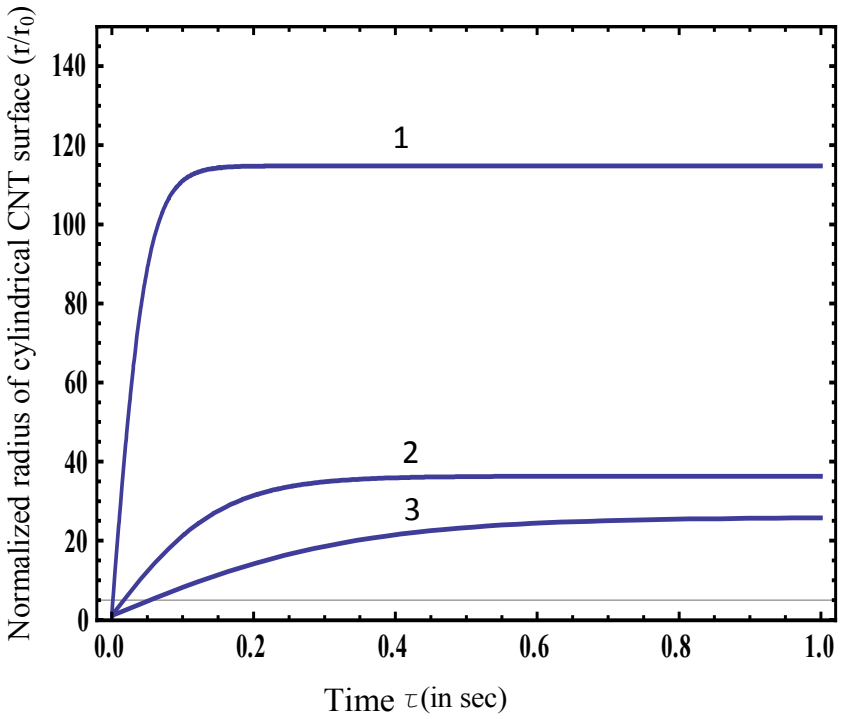

FIG.7. Shows the variation of the normalized radius r/r_0 of cylindrical CNT with time for different electron number densities and electron temperatures, curves 1,2 and 3 correspond to $n_{e0}=10^6 cm^{-3}$ and $T_{e0}=0.4eV$, $n_{e0}=10^7 cm^{-3}$ and $T_{e0}=0.5eV$ and n_{e0} $5x10^7$ cm^{-3} and $T_{e0}=0.6eV$,respectively.The other parameters are given in the text.

In Fig.7 the variation of normalized radius r/r_0 for cylindrical CNT surface with time for different electron number densities and electron temperatures (e.g., $n_{e0}=10^6$ cm^{-3} and $T_{e0}=0.4eV$, $n_{e0}=10^7 cm^{-3}$ and $T_{e0}=0.5eV$ and $n_{e0}=5x10^7$ cm^{-3} and $T_{e0}=0.6eV$) and for the CNT number density $n_{ct}=10^3$ cm^{-3}, neutral atom density as $n_{A0}=n_{B0}=10^{12}$ cm^{-3} is displayed. From Fig.7, it can be seen that the normalized CNT radius r/r_0 first increases with time and then attains a saturation value. It can also be seen that the normalized radius r/r_0 decreases with electron density and temperature. The decrease of r/r_0 with electron density and temperature occurs because with increasing electron densities and temperatures, more and more neutral atoms ionizes to produce positively charged ions and

electrons. Because the accretion of neutral atoms on the CNT leads to the growth, the decrease in their number density from an increase in the electron density and temperature leads to a decrease in radius of the CNT.

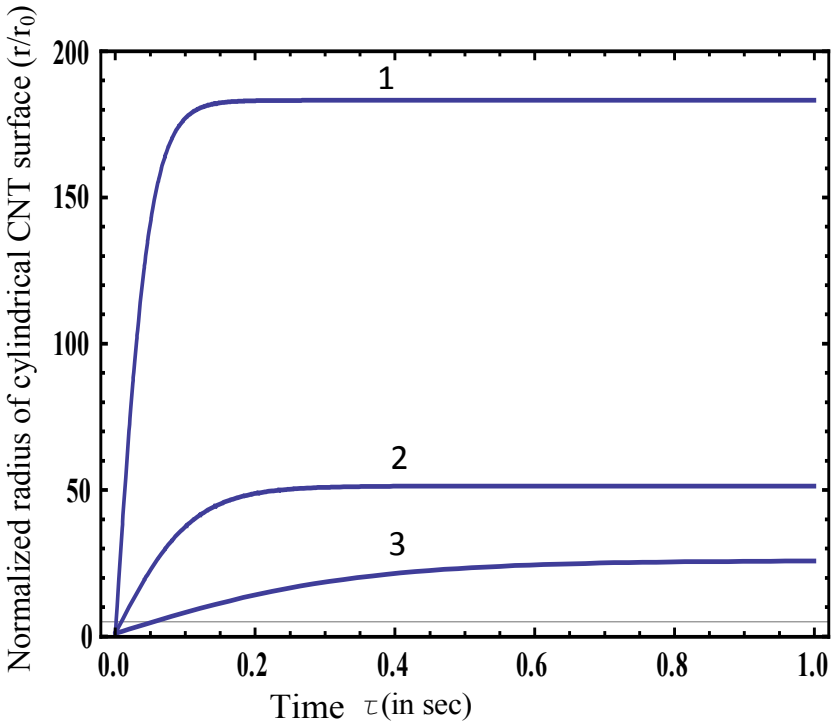

FIG. 8. Shows the variation of the normalized cylindrical radius r/r_0 of cylindrical CNT surface for different ion number densities and temperatures, curves 1,2 and 3 correspond to $n_{i0}= 10^6$ cm^{-3} and $T_{i0} =$ 2100K,$n_{i0}= 5x10^6$ cm^{-3}and T_{i0} = 2400K and $n_{i0}= 10^7$cm^{-3} and $T_{i\,0}$ = 2600K, respectively. The other parameters are given in the text.

In Fig.8, the variation of the normalized radius r/r_0 for cylindrical CNT surface with time for different ion number densities and ion temperatures (e.g., n_{i0}=10^6 cm^{-3} and T_{i0} = 2100K, n_{i0}=5x10^6 cm^{-3}and T_{i0} = 2400K and n_{i0}=10^7 cm^{-3} and $T_{i\,0}$ =2600K) and for the same parameters as Fig. 7,is shown. From Fig. 8 it can be seen that the CNT radius first increases with time and then attains a saturation value. The CNT radius decreases

with ion density n_{i0} (in cm^{-3}) and temperature T_i (in K) can also be seen. This happens because by increasing the ion density and temperature, more and more neutral atoms ionize to produce positively charged ions and electrons. Because it is the accretion of neutral atoms on the CNT, which leads to its growth, the radius of the CNT decreases with increasing positively charged ion density and temperature.

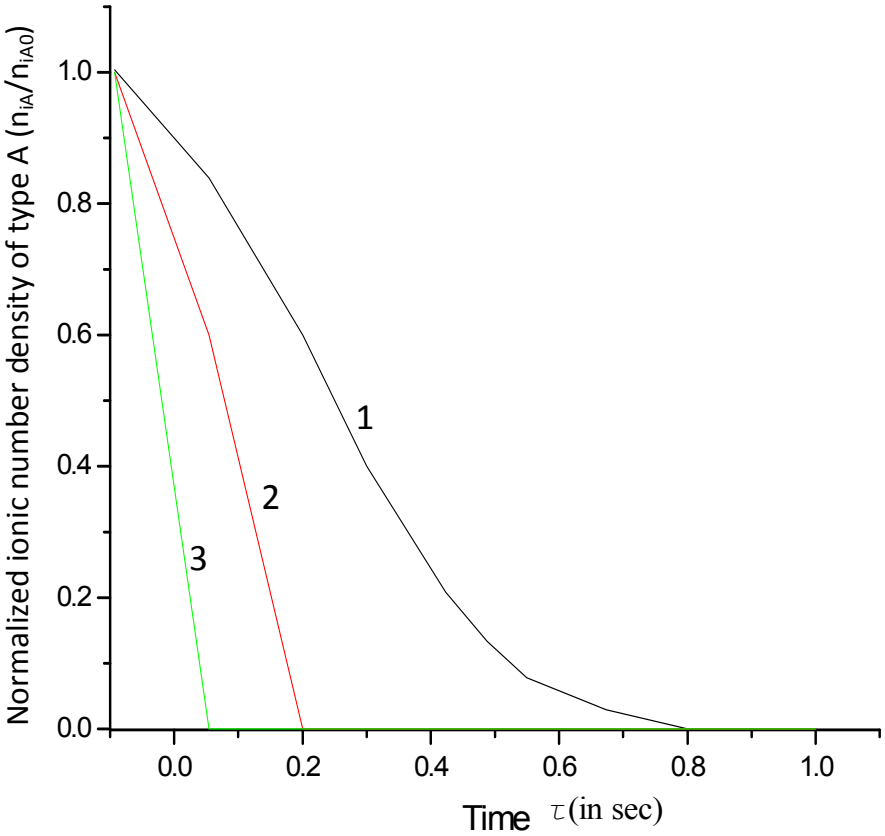

FIG. 9. Shows the dependence of ionic number density of type A in plasma for different electron number density and electron temperature, curves 1, 2 and 3 correspond to n_{e0} $=10^6 cm^{-3}$ and T_{e0}=0.4eV,n_{e0} $=10^7 cm^{-3}$ and T_{e0}=0.5eV, n_{e0} $=5x10^7$ cm^{-3} and T_{e0}=0.6eV, respectively. The other parameters are given in the text.

In Fig.9 the variation of the normalized ionic density of type A in plasma with time for different electron number densities and temperatures (e.g.,

n_{e0}=10^6cm^{-3} and T_{e0}=0.4eV, n_{e0}=10^7cm^{-3} and T_{e0}=0.5eV and n_{e0}=5x10^7 cm^{-3} and T_{e0}=0.6eV) and for the same parameters as in Figs. 6-8 is plotted. It can be seen from Fig. 9 that with increasing electron density and temperature, the positively charged A type ion decays faster.

From Figs. 4 and 9, we can infer that on increasing electron density and temperature (plasma parameters), ions of type A (carbon) decays faster, leading to a decrease in the CNT radius, which is consistent with the experimental observations of Srivastava *et al.*[6] and Lee *et a1*.[11].

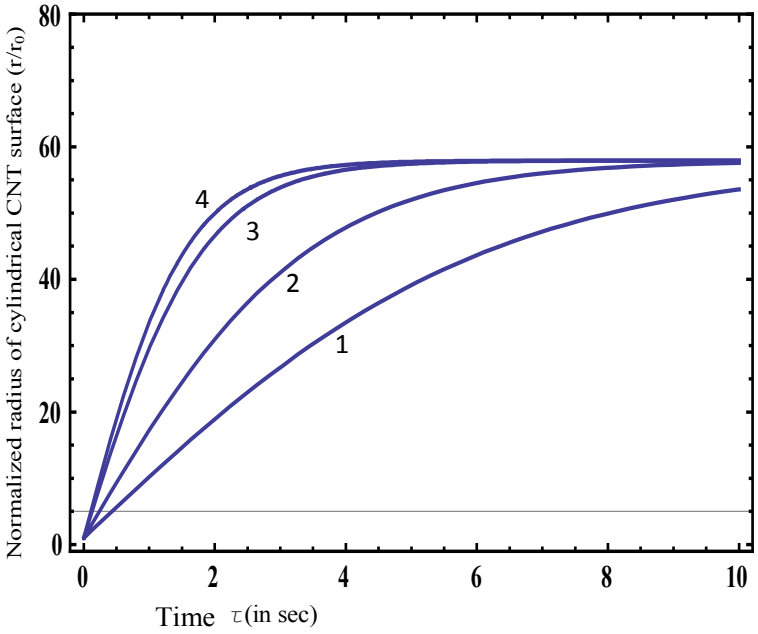

FIG. 10. Shows the variation of the normalized radius r/r_0 of cylindrical CNT with time on the sticking coefficient of the atomic species, curves 1, 2,3and 4 correspond to γ_A = 0.25, 0.45 ,0.75 and 1.0, respectively. The other parameters are given in the text.

In Fig. 10 we have plotted the variation of the normalized radius r/r_0 for the cylindrical CNT surfaces for different value of the sticking

coefficients of atomic species (γ_A = 0.25, 0.45, 0.75 and 1.0), respectively and for the same parameters as mentioned above. It can be seen from Fig. 10 that steady state is achieved faster for larger sticking coefficients of atomic species.

The work in the present chapter is evaluation of the dependence of growth profile (namely the radius) of CNT on the plasma parameters and then through the results obtained finding a rough estimate of the variation of field enhancement factor. As one knows that the field emission from CNT is always carried out in vacuum , plasma directly cannot have any influence on the field emission characteristics of CNT but since the CNT is grown in plasma and plasma parameters have huge influences on the growth of CNT , the plasma is bound to impact although indirectly, the field emission from CNT .

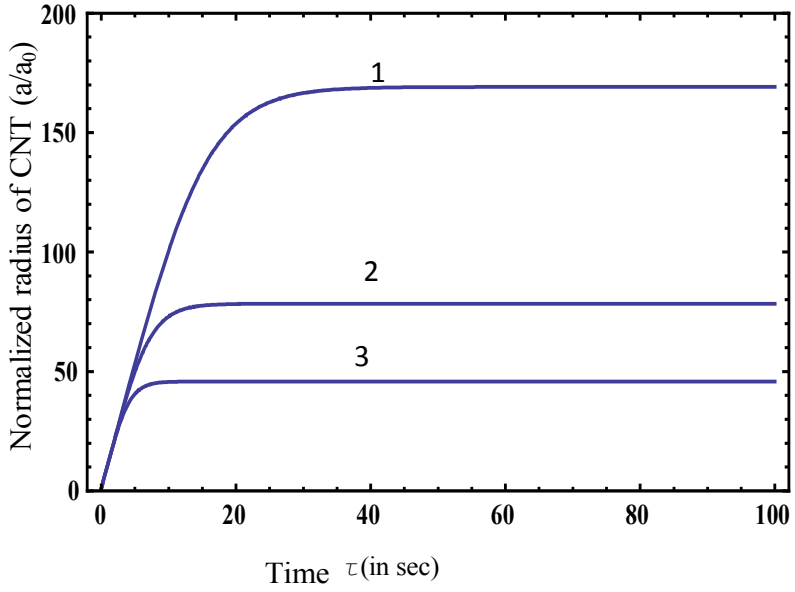

FIG.11. Shows the variation of the normalized radius a/a_0 of spherical CNT tip with time for different CNT number density, curves 1,2 and 3 correspond to n_{ct}=1x 10^3 cm^{-3}, 1x10^4 cm^{-3}, and 5x10^4 cm^{-3} ,respectively. The other parameters are given in the text.

In Fig. 11, we have plotted the normalized radius a/a_0 of spherical CNT tip for the same parameters as for cylindrical CNT surface. From Fig. 6 and 11, we can say that the normalized radius r/r_0 of the cylindrical CNT surfaces is larger than the spherical CNT tip (cf. Fig.11) for the same CNT number density. The theoretical observation can be used to validate the fact that the field enhancement factor β for spherical CNT tip will be larger in comparison to cylindrical CNT surfaces as $\left(\beta \propto r^{-\frac{1}{2}}\right)$. So a larger radius of cylindrical CNT surface would correspond to lesser field emission from them and smaller radius of spherical CNT tip would correspond to enhanced field emission from CNT tip. The above conclusion that emission from CNT tip is dominant has also been reported by Shang *et al.* [22].

Using the results obtained, the variation of the field emission factor with plasma parameters can be estimated. Since the field emission factor $\beta = \frac{l}{r}$(where l is the length of the CNT and r is the radius of the CNT). From the above discussions, it is clear that CNT radius decreases with plasma parameters (i.e., plasma density and temperature) and the CNT number density. Assuming the fixed length of CNT (l), $\beta \propto \frac{1}{r}$, so an increase in the plasma parameters should lead to a larger β. The variation of β with the CNT radius has also been experimentally verified by Xu *et al.* [23] [cf. Fig. 4(b) of Xu *et al.* [23]].

Our theoretical results are in accordance with the experimental observations of Srivastava *et al.* [6] and Lee *et a1.*[11] . The present work is motivated by important experimental investigations carried out Srivastava *et al.*[6] and Lee *et a1.*[11]. According to Srivastava *et al.*[6]

upon an increase in the microwave power, more ionization of the gas occurs, which increases the density of plasma species of relatively higher energy. Moreover, increased nucleation of graphitic clusters is expected to occur, and this leads to the formation of carbon petals of relatively smaller size and higher density at increased microwave power. Moreover, Fig.7 (a) of Srivastava *et al.* [6] reveals that the field emission current density increases with microwave power. Lee *et a1*. [11] through their experimental study predicts that the plasma treatment can modify the surface morphology and enhance the field enhancement factor of the CNT.

Moreover, the electric field emission of electrons from cylindrical surfaces has been studied in [24-26] In Ref. 26, computations have been made corresponding to Debye Shielding, e.g., potential energy of an electron of charge –e is given by $V(r) = V(a)\dfrac{\left[\ln \lambda_d / r\right]}{\left[\ln \lambda_d / a\right]} \exp\left[-\dfrac{(r-a)}{\lambda_d}\right]$,where λ_d is the Debye length of plasma and a is the plasma cylinder radius. It is seen that with a change in $ln^{\lambda_d}/_a$ by a factor of 3, the field emission current gets decreased by a factor of 5.

References

[1] A. V. Melechko, V. I. Merkulov, T. E. McKnight, M. A. Guillorn, K. L. Klein, D. H. Lowndes, and M. L. Simpson, J. Appl. Phys. **97**, 041301(2005).

[2]A. Bogaerts, E. Neyts, R. Gijbels, and J. van der Mullen, Spectrochim. Acta, Part B **57**, 609 (2002).

[3]A. Grill, *Cold Plasma in Materials Fabrication: From Fundamentals to Applications* (IEEE, New York, 1994).

[4] K. Ostrikov, *Plasma Nanoscience* (Wiley-VCH, Weinheim, 2008).

[5] Erik C. Neyts, J. Vac. Sci. Technol. B **30**, 030803(2012).

[6] S. K. Srivastava, A.K. Shukla, V. D. Vankar, and V. Kumar, Thin Solid Films **492**, 124(2005).

[7] A. F. Pal ,T. V. Rakhimova, N. V. Suetin, M.A. Timofeev, A. P. Filippov ,Plasma Phys. Rep. **33**,43 (2007).

[8] I. Levchenko, K. Ostrikov, M. Keidar, and S. Xu, J. Appl. Phys. **98**, 064304 (2005).

[9] I. Levchenko, K. Ostrikov, M. Keidar, and S. Xu, Appl. Phys. Lett. **89**, 033109 (2006).

[10] I. Levchenko, K. Ostrikov, and E. Tam, Appl. Phys. Lett. **89**, 223108 (2006).

[11] S.F. Lee, Yung-Ping Chang and Li-Ying Lee, J. Mater. Sci. Mater. Electron **20**, 851(2009).

[12] G. Zhang, W. Duan, and B. Gu, Appl. Phys.Lett. **80**, 2589 (2002).

[13] G. Zhou, W. Duan and B. Gu, Appl. Phys.Lett.**79**, 836 (2001).

[14] X. Q. Wang, M. Wang, P. M. He and Y. B. Xu, J. Appl. Phys. **96**, 6752(2004).

[15] H. S. Jang, H. R. Lee, and D.-H. Kimet, Thin Solid Films **500**, 124

(2006).

[16]S.J. Kyung, M. Voronko, J.-H. Lee, and G.-Y. Yeomet, J. Korean Phys. Soc. **47**, 818 (2005).

[17]Y. Y. Wang, S. Gupta, J. M. Garguilo, Z. J. Liu, L. C. Qin, and R. J. Nemanich, Diamond Relat. Mater. **14**, 714 (2005).

[18] M.S. Sodha , Shikha Misra, S. K. Mishra, and S. Srivastava, J. Appl. Phys.**107**,103307(2010).

[19] M. S. Sodha, S. K. Mishra and S. Misra, Phys. Plasmas **17** ,113705 (2010).

[20] M. S. Sodha and S. Guha, *Physics of Colloidal Plasmas* ,edited by A.Simon and W.B. Thomson (John Wiley and Sons, New York, 1971) p.219.

[21] M. Rosenberg, D. A. Mendis, and D. P. Sheehan, IEEE Trans. Plasma Sci. **27**, 239(1999).

[22] X.F. Shang , M.Wang ,S. Qu , Y.P. Ma , M.Q. Tan ,Y.B. Xu, and Z. H. Li , J. Appl. Phys. **102**, 054301(2007).

[23]Z. Xu, X. D. Bai and E. G. Wang, Appl. Phys. Lett. **88**, 133107(2006).

[24] M. S. Sodha and P. K. Kaw, Br. J. Appl. Phys. **2**, 1303 (1968).

[25] M. S. Sodha and A. Dixit, J. Appl. Phys. **104**, 084908 (2008).

[26] M. S. Sodha and A. Dixit, J. Appl. Phys. **105**, 034909 (2009).

CHAPTER 4

IMPACT OF NEGATIVELY CHARGED IONS ON THE GROWTH OF SPHERICAL CARBON NANOTUBE TIP IN PLASMA AND ESTIMATING FIELD EMISSION FROM THEM

4.1: Brief outline of the work in the chapter

The present chapter focuses on the impact of negatively charged ion in plasma on the growth of spherical carbon nanotube (CNT) tip and prediction of field enhancement factor of CNT from the results obtained.

4.2: Introduction

The effect of diverse component species of plasma and categorically of negatively charged ions in plasma in the growth of particles in plasmas [1-8] has attracted interest by the researchers in recent years.

Watanabe *et al*. [1] obtained particles of size 60-80 nm and 10^8-10^9 cm^{-3} in density in a helium-silane radio-frequency (RF) plasma and the particle growth rate can be explained by taking into account the contribution of radical ion and or radical fluxes. Role of negative ions in the formation of particles in low-pressure plasmas has been investigated by Choi and Kushner[2] and they reported that the negatively charged particles intermediates that are trapped in electropositive plasmas, extends the average residence time of clusters to allow the growth of critically large clusters. Relatively long residence time and chemical reactivity makes silicon (Si) containing anion to effectively trigger fast nano particle nucleation has been reported by Ostrikov [3]. Negative ions are likely precursors to the particle formation in modulated rf –

discharges[4]. Ostrikov *et al*. [5] have found that the negative fluorine ions affect the trapping and charging of particulates through alteration of sheath/ pre sheath structure. Selwyn *et al*. [6] have examined the *in-situ* laser diagnostic studies of plasma- generated particulate contamination and found that the region of particle formation and growth is coincident in time and space with a layer of negative ions and the particles that are electro- statically trapped in sheath boundary results in further clustering and growth.

The effects of growth temperature and density of participating species etc., have been extensively studied [9-13]. Other investigators [14-16] have also reported that the CNTs can be prepared self-assembled without catalyst.

4.3: MODEL

In the present chapter to investigate the role of negative ions on growth of CNT , we consider that a CNT grows in plasma containing electrons, positively charged ions of type A(carbon) and B(neon), negatively charged ions of sulphur hexafluoride (SF_6^-), neutral atoms of type A(carbon) and B(neon). The positively charged ions are assumed to be singly ionized and growth occurs through their accretion onto the embryonic CNT. In addition, we have also assumed that the shape of spherical CNT tip remains unaltered during the growth.

The initial radius of spherical CNT tip a_0 can be estimated by equating the accretion currents of electrons, negatively and positively charged ions on the CNT tip, i.e.,

$$n_{ects} + n_{-cts} = n_{iActs} + n_{iBcts} \,, \qquad (1)$$

where

$n_{ects} = \pi a^2 \left(\frac{8k_B T_e}{\pi m_e} \right)^{\frac{1}{2}} n_e \exp\left[\frac{Ze^2}{ak_B T_e} \right]$ is the electron collection current at spherical CNT tip [17] (in sec^{-1}),

$n_{ijcts} = \pi a^2 \left(\frac{8k_B T_i}{\pi m_j} \right)^{\frac{1}{2}} n_{ij} \left[1 - \frac{Ze^2}{ak_B T_i} \right]$ is the positive ion collection current on a spherical CNT tip [17] where j refers to either A (carbon) ion or B (neon) ion (in sec^{-1}), Z is the amount of charge on the CNT,

$n_{-cts} = \pi a^2 \left(\frac{8k_B T_-}{\pi m_-} \right)^{\frac{1}{2}} n_- \exp\left[\frac{Ze^2}{ak_B T_-} \right]$ is the negative ion collection current on a spherical CNT tip (in sec^{-1}).

Substituting the values of n_{ects} , n_{ijcts} (for both A (carbon)and B(neon)) and n_{-cts} (for sulphur hexafluoride) in Eq.(1) we get,

$$\pi a^2 \left(\frac{8k_B T_e}{\pi m_e} \right)^{\frac{1}{2}} n_e \exp\left[\frac{Ze^2}{ak_B T_e} \right] + \pi a^2 \left(\frac{8k_B T_-}{\pi m_-} \right)^{\frac{1}{2}} n_- \exp\left[\frac{Ze^2}{ak_B T_-} \right] = \pi a^2 \left(\frac{8k_B T_i}{\pi m_{iA}} \right)^{\frac{1}{2}} n_{iA} \left[1 - \frac{Ze^2}{ak_B T_i} \right] + \pi a^2 \left(\frac{8k_B T_i}{\pi m_{iB}} \right)^{\frac{1}{2}} n_{iB} \left[1 - \frac{Ze^2}{ak_B T_i} \right], \quad (2)$$

or

$$\left(\frac{T_e}{\pi m_e} \right)^{\frac{1}{2}} n_e \exp\left[\frac{Ze^2}{ak_B T_e} \right] + \left(\frac{T_-}{\pi m_-} \right)^{\frac{1}{2}} n_- \exp\left[\frac{Ze^2}{ak_B T_-} \right] = \left(\frac{T_i}{\pi m_{iA}} \right)^{\frac{1}{2}} n_{iA} \left[1 - \frac{Ze^2}{ak_B T_i} \right] + \left(\frac{T_i}{\pi m_{iB}} \right)^{\frac{1}{2}} n_{iB} \left[1 - \frac{Ze^2}{ak_B T_i} \right], \quad (3)$$

or

$$\left(\frac{T_e}{m_e}\right)^{\frac{1}{2}} n_e \exp\left[\frac{Ze^2}{ak_B T_e}\right] + \left(\frac{T_-}{m_-}\right)^{\frac{1}{2}} n_- \exp\left[\frac{Ze^2}{ak_B T_-}\right] = \left\{\left(\frac{T_i}{m_{iA}}\right)^{\frac{1}{2}} n_{iA}\left[1 - \frac{Ze^2}{ak_B T_i}\right]\right\} + \left\{\left(\frac{T_i}{m_{iB}}\right)^{\frac{1}{2}} n_{iB}\left[1 - \frac{Ze^2}{ak_B T_i}\right]\right\}, \tag{4}$$

For Z = -1, i.e., we assume that initially at τ=0 the CNT is negatively charged, and initial radius of CNT is a_0,

$$n_e\left(\frac{T_e}{m_e}\right)^{\frac{1}{2}} \exp\left(-\frac{e^2}{a_0 k_B T_e}\right) + n_-\left(\frac{T_-}{m_-}\right)^{\frac{1}{2}} \exp\left(-\frac{e^2}{a_0 k_B T_e}\right) = \left(1 + \frac{e^2}{a_0 k_B T_i}\right)\left[n_{iA}\left(\frac{T_i}{m_{iA}}\right)^{\frac{1}{2}} + n_{iB}\left(\frac{T_i}{m_{iB}}\right)^{\frac{1}{2}}\right]. \tag{5}$$

where

$n_e [= (1-\varepsilon_r) n_P]$ is the number density of electron (in cm^{-3}),

T_e = electron temperature (in eV),

a_0 = initial radius of spherical CNT tip (in nm),

k_B = Boltzmann's constant (in ergs/K),

T_i = positive ion temperature (in K),

$T_-(= T_e)$ is the negative ion temperature (in eV),

$n_{iA}(= n_P)$ is the number density of positive ion of type A(carbon) (in cm^{-3}),

m_{iA} = mass of positive ion of type A (carbon) (in gm),

$n_{iB}(= n_P)$ is the number density of positive ion of type B(neon)(in cm^{-3}),

m_{iB} = mass of positive ion of type B (neon) (in gm),

e = electronic charge (in Stat C),

n_- (= $\varepsilon_r n_P$) is the negatively charged ion number density (in cm^{-3}), and

m_- = mass of negatively charged ion (in gm),

$\varepsilon_r = \frac{n_{SF_6^-}}{n_{C^+}}$ (where $n_{SF_6^-}$ and n_{C^+} are the equilibrium number densities of sulphur hexafluoride and carbon ions, respectively) is the relative density of negatively charged ions and is dimensionless.

Following the model developed and processes assumed for the kinetics of plasma species in Chapter 2 and including the kinetics of negatively charged ion we write the main equations for growth of CNT in the presence of negatively charged ions in plasma.

A. Charge neutrality equation

Eq. (6) equates the net negative and positive charge on CNT to treat plasma as electrically neutral.

$$Zn_{ct} + n_{iA} + n_{iB} = n_e + n_-, \qquad (6)$$

Z= amount of charge on spherical CNT tip (dimensionless),

n_{ct} = number density of the CNT (in cm^{-3}).

B. Charging of the spherical CNT tip

$$\frac{dZ}{d\tau} = n_{iActs} + n_{iBcts} - \gamma_e n_{ects}\ , \qquad (7)$$

The first and second term in Eq.(7) denotes charge developed on the CNT due to ion collection currents of A(carbon) and B(neon) on spherical CNT tip and third term denotes the charge developed on spherical CNT tip because of electron collection current.

C. Balance equation of electron density

$$\frac{dn_e}{d\tau} = (1-\varepsilon_r)\frac{dn_P}{d\tau} = \left(\beta_A n_A + \beta_B n_B\right) - \left(\alpha_A n_e n_{iA} + \alpha_B n_e n_{iB}\right) - \gamma_e n_{ct} n_{ects} \quad ,(8)$$

β_A and β_B are the coefficients of ionization of the constituent neutral atoms of A(carbon) and B(neon) due to external agency (in sec), and $\alpha_A(T_e) = \alpha_{A0}\left(\frac{300}{T_e}\right)^k cm^3/\sec$ and $\alpha_B(T_e) = \alpha_{B0}\left(\frac{300}{T_e}\right)^k cm^3/\sec$ are the coefficients of recombination of electrons and positively charged ions [17] o f A(carbon) and B(neon),respectively where k = -1.2 is a constant , $\alpha_{A0} = \alpha_{B0} = n_{e0}\times 10^{-7}\left(\frac{1}{T_{e0}}\right)^{-1.2}$ and $n_{ects} = \pi a^2\left(\frac{8k_B T_e}{\pi m_e}\right)^{\frac{1}{2}} n_e \exp\left[\frac{Ze^2}{ak_B T_e}\right]$ is the electron collection current at the surface of spherical CNT tip [17] (in sec^{-1}) and n_{ct} is the CNT number density (in cm^{-3}) , γ_e is the sticking coefficient of electron to spherical CNT tip and is dimensionless.

The first term in Eq.(8) is the rate of gain in electron density per unit time due to ionization of neutral atoms and second term is the decrease in the electron density due to electron–ion recombination and the third term is the loss in electron density because of the electron collection current on the spherical CNT tip.

D. Balance equation of negatively charged ion density

$$\frac{dn_-}{d\tau} = \varepsilon_r \frac{dn_P}{d\tau} = \left(\beta_A n_A + \beta_B n_B\right) - \left(\alpha_A n_e n_{iA} + \alpha_B n_e n_{iB}\right) - \gamma_e n_{ct} n_{ects}, \quad (9)$$

The first term in Eq. (9) is the rate of gain in negative ion density per unit time due to ionization of neutral atoms and second term is the decrease in

the negative ion density due to electron–ion recombination. The third term is the loss in negative ion density because of the electron collection current on the spherical CNT tip.

E.Balance equation of positively charged ion density

$$\frac{dn_{iA}}{d\tau} = \beta_A n_A - \alpha_A n_e n_{iA} - n_{ct} n_{iActs}, \quad (10)$$

$$\frac{dn_{iB}}{d\tau} = \beta_B n_B - \alpha_B n_e n_{iB} - n_{ct} n_{iBcts}, \quad (11)$$

where

$$n_{iActs} = \pi a^2 \left(\frac{8k_B T_i}{\pi m_{iA}}\right)^{\frac{1}{2}} n_{iA}\left[1 - \frac{Ze^2}{ak_B T_i}\right], n_{iBcts} = \pi a^2 \left(\frac{8k_B T_i}{\pi m_{iB}}\right)^{\frac{1}{2}} n_{iB}\left[1 - \frac{Ze^2}{ak_B T_i}\right]$$

are the ion collection currents of type A(carbon) and B(neon),respectively at the surface of spherical CNT tip [17](in sec^{-1}), n_A and n_B are the neutral atom number density (in cm^{-3}).

The first term in Eqs. (10) and (11) is the gain in ion density per unit time on account of ionization of neutral atoms, the second term is the decrease in ion density due to electron-ion recombination, and the third term denotes the loss in ion density due to ion collection current on spherical CNT tip.

F. Balance equation of neutral atoms

$$\frac{dn_A}{d\tau} = \alpha_A n_e n_{iA} - \beta_A n_A + n_{ct}\left(1 - \gamma_{iA}\right) n_{iActs} - n_{ct}\gamma_A n_{Acts}, \quad (12)$$

$$\frac{dn_B}{d\tau} = \alpha_B n_e n_{iB} - \beta_B n_B + n_{ct} n_{iBcts}, \quad (13)$$

where

$$n_{Acts} = \pi a^2 \left(\frac{8k_B T_n}{\pi m_A} \right)^{\frac{1}{2}} n_A, \quad n_{Bcts} = \pi a^2 \left(\frac{8k_B T_n}{\pi m_B} \right)^{\frac{1}{2}} n_B$$

are the neutral collection currents of type A(carbon) and (neon),respectively at the surface of spherical CNT tip [17] (in sec^{-1}).

γ_A is the sticking coefficient of carbon neutrals on spherical CNT tip and γ_{iA} is the sticking coefficient of carbon ions on CNT surface, both γ_A and γ_{iA} are dimensionless.

The first term in Eqs. (12) and (13) is the gain in neutral atom density per unit time due to electron–ion recombination, the second term is the decrease in neutral density due to their ionization, the third term is the gain in neutral density due to neutralization of the ions collected on spherical CNT tip. The last term in Eq. (12) is the accretion of neutral atoms of species A (carbon) on spherical CNT tip.

G. Balance equation of the mass of spherical CNT tip

The accretion of carbon ions and neutrals on the spherical CNT tip is the main growth process.

$$\frac{dm_{ct}}{d\tau} = \left(m_A \gamma_A n_{Acts} + m_{iA} \gamma_{iA} n_{iActs} \right), \qquad (14)$$

where

$m_{ct} = \frac{4}{3}\pi a^3 \rho_{ct}$ is the mass of the CNT for a spherical CNT tip , a is the radius of spherical CNT tip , and ρ_{ct} is the density of spherical CNT tip,

The first and second term in Eq.(14) are the gain in the mass of the spherical CNT tip due to collection of atomic and ionic species A (i.e., carbon), respectively.

H. Energy balance equation of electrons

$$\left(\frac{3}{2}k_B\right)n_e\left(\frac{dT_e}{d\tau}\right)=\left[\left(\beta_A n_A\varepsilon_A+\beta_B n_B\varepsilon_B\right)-\left(\frac{3}{2}k_B\right)\left(\beta_A n_A+\beta_B n_B\right)T_e\right]-n_{ct}n_{ects}$$
$$\left\{\left[\gamma_e\varepsilon_{ecs}^{lh}-\left(\frac{3}{2}k_B\right)T_e\right]+\delta_{ect}(1-\gamma_e)\left[\varepsilon_{ecs}^{s}-\left(\frac{3}{2}k_B\right)T_{ct}\right]\right\}$$
$$-\left(\frac{3}{2}k_B\right)\left[\nu_{eA}\delta_{eA}+\nu_{eB}\delta_{eB}\right](T_e-T_n)n_e-\left(\frac{3}{2}k_B\right)\left\{\left(\nu_{eAi}\delta_{eAi}+\nu_{eBi}\delta_{eBi}\right)\left(T_e-T_i\right)\right\}n_e. \quad (15)$$

where

$\frac{3}{2}n_e k_B T_e$ is the thermal energy of electrons ,

n_e is the number density of electrons(in cm^{-3}),T_e is the electron temperature (in eV), T_{ct} is the CNT temperature (in K), and T_n is the neutral temperature (in K).

$\varepsilon_{ecs}^{lh}(Z)=\varepsilon_{ecs}^{s}(Z)-\left(\frac{Ze^2}{a}\right)$ is the mean energy of electrons (in eV) at a large distance from the surface of spherical CNT tip [17],

$\varepsilon_{ecs}^{s}(Z)=2k_B T_e$ is the mean energy of electrons (in eV) collected by spherical CNT tip [17],

$\nu_{eA}=\nu_{eA0}\left(\frac{n_A}{n_{A0}}\right)\left(\frac{T_e}{T_{e0}}\right)^{\frac{1}{2}}$ and $\nu_{eB}=\nu_{eB0}\left(\frac{n_B}{n_{B0}}\right)\left(\frac{T_e}{T_{e0}}\right)^{\frac{1}{2}}$ are the electron collision frequency (in sec^{-1}) due to elastic collisions with neutral atoms A(carbon) and B(neon), respectively [17] , and

$\nu_{eA0}=(8.3\times10^5)\pi r_A^{\,2}n_{A0}T_{e0}^{\frac{1}{2}}$ and $\nu_{eB0}=(8.3\times10^5)\pi r_B^{\,2}n_{B0}T_{e0}^{\frac{1}{2}}$,

$\nu_{eAi} = \nu_{eAi0}\left(\frac{n_{iA}}{n_{iA0}}\right)\left(\frac{T_e}{T_{e0}}\right)^{-\frac{3}{2}}$ and $\nu_{eBi} = \nu_{eBi0}\left(\frac{n_{iB}}{n_{iB0}}\right)\left(\frac{T_e}{T_{e0}}\right)^{-\frac{3}{2}}$ are the electron collision frequency (in $\sec^{-1}$) due to elastic collisions with positively charged ion of type A(carbon) and type B(neon)[17], respectively.

$\nu_{eAi0} = \left(5.5\frac{n_{e0}}{T_{e0}^{\frac{3}{2}}}\right)\ln\left(\frac{220T_{e0}}{n_{iA0}^{\frac{1}{3}}}\right)$ and $\nu_{eBi0} = \left(5.5\frac{n_{e0}}{T_{e0}^{\frac{3}{2}}}\right)\ln\left(\frac{220T_{e0}}{n_{iB0}^{\frac{1}{3}}}\right)$,

$\delta_{eA} \approx 2\left(\frac{m_e}{m_A}\right)$ and $\delta_{eB} \approx 2\left(\frac{m_e}{m_B}\right)$ are the fraction of excess energy of an electron lost in a collision with the neutral atom A(carbon) and B(neon), respectively[17] and are dimensionless,

$\delta_{eAi} \approx 2\left(\frac{m_e}{m_{iA}}\right)$ and $\delta_{eBi} \approx 2\left(\frac{m_e}{m_{iB}}\right)$ are the fraction of excess energy of an electron lost in a collision with a positively charged ion A(carbon) and B(neon), respectively [17] and are dimensionless,

$\delta_{ect} \approx 2\left(\frac{m_e}{m_{ct}}\right)$ is the fraction of excess energy of an electron lost in a collision with a CNT [17] and is dimensionless where,

$m_{ct} = \frac{4}{3}\pi a^3 \rho_{ct}$ is the mass of the CNT for a spherical CNT tip , a is the radius of spherical CNT tip , and ρ_{ct} is the density of spherical CNT tip,

The first term in Eq.(15) is the power gained per unit volume by electrons due to ionization of neutral atoms, the second term is the energy loss per unit volume per unit time due to the sticking accretion

and elastic collisions of electron at the spherical CNT tip, the third term is the energy loss per unit volume per unit time due to elastic electron - atom collisions. The fourth term is the energy loss per unit volume per unit time due to elastic electron- ion collision.

I. **Energy balance equation for negatively charged ions**

$$\frac{d}{d\tau}\left(\frac{3}{2}n_{-}k_{B}T_{e}\right)=$$
$$\left(\beta_{A}n_{A}\varepsilon_{A}+\beta_{B}n_{B}\varepsilon_{B}\right)-\left(\frac{3}{2}k_{B}\right)\left(\alpha_{A}n_{e}n_{iA}+\alpha_{B}n_{e}n_{iB}\right)T_{e}-n_{ct}n_{ects}\left\{\gamma_{e}\varepsilon_{ecs}^{lh}+\delta_{ect}\left(1-\gamma_{e}\right)\times\right.$$
$$\left.\left[\varepsilon_{ecs}^{s}-\left(\frac{3}{2}k_{B}\right)T_{ct}\right]\right\}-\left(\frac{3}{2}k_{B}\right)\left[\nu_{eA}\delta_{eA}+\nu_{eB}\delta_{eB}\right]\left(T_{e}-T_{n}\right)n_{-}-\left(\frac{3}{2}k_{B}\right)\times\left(\nu_{eAi}\delta_{eAi}+\right.$$
$$\left.\nu_{eBi}\delta_{eBi}\right)\left(T_{e}-T_{i}\right)n_{-}\ ,\qquad(16)$$

The LHS of Eq.(16) can be written as

$$\left(\frac{3}{2}k_{B}\right)n_{-}\left(\frac{dT_{e}}{d\tau}\right)+\left(\frac{3}{2}k_{B}\right)T_{e}\left(\frac{dn_{-}}{d\tau}\right)$$

Substituting the value of $\frac{dn_{-}}{d\tau}$ from Eq. (9) in the above Eq., we get

$$\left(\frac{3}{2}k_{B}\right)n_{-}\left(\frac{dT_{e}}{d\tau}\right)=$$
$$-\left(\frac{3}{2}k_{B}\right)T_{e}\left(\beta_{A}n_{A}+\beta_{B}n_{B}\right)+\left(\frac{3}{2}k_{B}\right)T_{e}\left(\alpha_{A}n_{e}n_{iA}+\alpha_{B}n_{e}n_{iB}\right)+\left(\frac{3}{2}k_{B}\right)T_{e}\gamma_{e}n_{ct}n_{ects}$$
$$+\left(\beta_{A}n_{A}\varepsilon_{A}+\beta_{B}n_{B}\varepsilon_{B}\right)-\left(\frac{3}{2}k_{B}\right)\left(\alpha_{A}n_{e}n_{iA}+\alpha_{B}n_{e}n_{iB}\right)T_{e}-n_{ct}n_{ects}\left\{\gamma_{e}\varepsilon_{ecs}^{lh}+\delta_{ect}\left(1-\gamma_{e}\right)\right.$$
$$\left.\times\left[\varepsilon_{ecs}^{s}-\left(\frac{3}{2}k_{B}\right)T_{ct}\right]\right\}-\left(\frac{3}{2}k_{B}\right)\left[\nu_{eA}\delta_{eA}+\nu_{eB}\delta_{eB}\right]\left(T_{e}-T_{n}\right)n_{-}-\left(\frac{3}{2}k_{B}\right)$$
$$\left(\nu_{eAi}\delta_{eAi}+\nu_{eBi}\delta_{eBi}\right)\left(T_{e}-T_{i}\right)n_{-},$$

On rearranging the above equation, we get

$$\left(\frac{3}{2}k_B\right)n_-\left(\frac{dT_e}{d\tau}\right)=\left[\left(\beta_A n_A\varepsilon_A+\beta_B n_B\varepsilon_B\right)-\left(\frac{3}{2}k_B\right)\left(\beta_A n_A+\beta_B n_B\right)T_e\right]-$$

$$n_{ct}n_{ects}\left\{\gamma_e\left[\varepsilon_{ecs}^{lh}-\left(\frac{3}{2}k_B\right)T_e\right]+\delta_{ect}(1-\gamma_e)\right.$$

$$\left.\left[\varepsilon_{ecs}^{s}-\left(\frac{3}{2}k_B\right)T_{ct}\right]\right\}-\left(\frac{3}{2}k_B\right)\left(\left[\nu_{eA}\delta_{eA}+\nu_{eB}\delta_{eB}\right](T_e-T_n)n_-+\right.$$

$$\left.\left(\nu_{eAi}\delta_{eAi}+\nu_{eBi}\delta_{eBi}\right)\left(T_e-T_i\right)n_-\right).$$

(17)

The first term in Eq.(17) is the power gained per unit volume by negative ion due to ionization of neutral atoms, the second term is the energy loss per unit volume per unit time due to the sticking accretion and elastic collisions of electron at the spherical CNT tip, the third term is the energy loss per unit volume per unit time due to elastic electron - atom collisions and elastic electron- ion collision.

J. Energy balance equation for positively charged ions

$$\left(\frac{3}{2}k_B\right)\left(n_{iA}+n_{iB}\right)\left(\frac{dT_i}{d\tau}\right)=$$

$$\left[\left(\beta_A n_A\varepsilon_{iA}+\beta_B n_B\varepsilon_{iB}\right)-\left(\frac{3}{2}k_B\right)\left(\beta_A n_A+\beta_B n_B\right)T_i\right]+\left(\frac{3}{2}k_B\right)n_e\left(\nu_{eAi}\delta_{eAi}+\nu_{eBi}\delta_{eBi}\right)$$

$$\times\left(T_e-T_i\right)-n_{ct}\left\{\left(n_{iActs}\left[\varepsilon_{iAcs}^{l}-\left(\frac{3}{2}k_B\right)T_i\right]\right)+\left(n_{iBcts}\left[\varepsilon_{iBcs}^{l}-\left(\frac{3}{2}k_B\right)T_i\right]\right)\right\}-\left\{\left(\frac{3}{2}k_B\right)\times\right.$$

$$\left.\left[\left(\nu_{iAA}\delta_{iAA}+\nu_{iAB}\delta_{iAB}\right)n_{iA}+\left(\nu_{iBA}\delta_{iBA}+\nu_{iBB}\delta_{iBB}\right)n_{iB}\right]\left(T_i-T_n\right)\right\}. \quad (18)$$

$\varepsilon_{iAcs}^{l}(Z)=\left[\frac{2-Z\alpha_{Ai}}{1-Z\alpha_{Ai}}\right]k_BT_i$ and $\varepsilon_{iBcs}^{l}(Z)=\left[\frac{2-Z\alpha_{Bi}}{1-Z\alpha_{Bi}}\right]k_BT_i$ are the mean energy (in eV) of positively charged ions, A(carbon) and

B(neon),respectively (at large distance from the surface of the CNT) collected by the spherical CNT tip [17].

ε_{ij} is the mean energy (in eV) of positively charged ions produced by the ionization of neutral atoms [17] and for ion A(carbon) and B(neon) are expressed as

$$\varepsilon_{iA}=\frac{3}{2}k_B T_{iA}+\frac{3k_B}{2\left(\alpha_A(T_e)\times n_{iA}\right)}\left[\left\{\nu_{iAA}\times\delta_{iAA}\times\left(T_i-T_n\right)\right\}-\left\{\nu_{eAi}\times\delta_{eAi}\times\left(T_e-T_i\right)\right\}\right]$$

$$\varepsilon_{iB}=\frac{3}{2}k_B T_{iB}+\frac{3k_B}{2\left(\alpha_B(T_e)\times n_{iB}\right)}\left[\left\{\nu_{iBB}\times\delta_{iBB}\times\left(T_i-T_n\right)\right\}-\left\{\nu_{eBi}\times\delta_{eBi}\times\left(T_e-T_i\right)\right\}\right]$$

$$\nu_{iAA}=\nu_{iAA0}\left(\frac{n_A}{n_{A0}}\right)\left(\frac{m_A T_i+m_{iA}T_n}{\left(m_A T_{i0}+m_{iA}T_{n0}\right)}\right)^{\frac{1}{2}},\nu_{iAB}=\nu_{iAB0}\left(\frac{n_B}{n_{B0}}\right)\left(\frac{m_B T_i+m_{iA}T_n}{\left(m_B T_{i0}+m_{iA}T_{n0}\right)}\right)^{\frac{1}{2}}$$

$$\nu_{iBA}=\nu_{iBA0}\left(\frac{n_A}{n_{A0}}\right)\left(\frac{m_A T_i+m_{iB}T_n}{\left(m_A T_{i0}+m_{iB}T_{n0}\right)}\right)^{\frac{1}{2}},\nu_{iBB}=\nu_{iBB0}\left(\frac{n_B}{n_{B0}}\right)\left(\frac{m_B T_i+m_{iB}T_n}{\left(m_B T_{i0}+m_{iB}T_{n0}\right)}\right)^{\frac{1}{2}}$$

are the collision frequencies(in $\sec^{-1}$) of a j type of ion with j' ion of neutral atom[17], and

$$\nu_{iAA0} = \left(\frac{8}{3}\right)\left(2\pi k_B\right)^{\frac{1}{2}} (r_{iA} + r_A)^2 \left(\frac{n_{A0} m_A}{\left(m_{iA} + m_A\right)}\right)\left[\left(\frac{T_{i0}}{m_{iA}}\right) + \left(\frac{T_{n0}}{m_A}\right)\right]^{\frac{1}{2}},$$

$$\nu_{iAB0} = \left(\frac{8}{3}\right)\left(2\pi k_B\right)^{\frac{1}{2}} (r_{iA} + r_B)^2 \left(\frac{n_{B0} m_B}{\left(m_{iA} + m_B\right)}\right)\left[\left(\frac{T_{i0}}{m_{iA}}\right) + \left(\frac{T_{n0}}{m_B}\right)\right]^{\frac{1}{2}},$$

$$\nu_{iBA0} = \left(\frac{8}{3}\right)\left(2\pi k_B\right)^{\frac{1}{2}} (r_{iB} + r_A)^2 \left(\frac{n_{A0} m_A}{\left(m_{iB} + m_A\right)}\right)\left[\left(\frac{T_{i0}}{m_{iB}}\right) + \left(\frac{T_{n0}}{m_A}\right)\right]^{\frac{1}{2}},$$

$$\nu_{iBB0} = \left(\frac{8}{3}\right)\left(2\pi k_B\right)^{\frac{1}{2}} (r_{iB} + r_B)^2 \left(\frac{n_{B0} m_B}{\left(m_{iB} + m_B\right)}\right)\left[\left(\frac{T_{i0}}{m_{iB}}\right) + \left(\frac{T_{n0}}{m_B}\right)\right]^{\frac{1}{2}},$$

$$\delta_{iAA} = \left[\frac{2m_{iA}}{(m_A + m_{iA})}\right], \delta_{iBB} = \left[\frac{2m_{iB}}{(m_B + m_{iB})}\right], \delta_{iAB} = \left[\frac{2m_{iA}}{(m_B + m_{iA})}\right], \delta_{iBA} = \left[\frac{2m_{iB}}{(m_A + m_{iB})}\right]$$

are the fraction of the excess energy of a j type positively charged ion, lost in a collision with neutral j' kind of neutral atom and are dimensionless. where j and j' can be same (i.e., both carbon) or different (i.e., one carbon and other neon).

The first term in Eq. (18) is the energy gained by ions per unit volume per unit time due to the ionization of neutral atoms , the second term is the energy gained per unit volume per unit time due to the elastic collision of ions with electrons. The third term is the energy loss per unit volume per unit time due to the sticking accretion of ions at the surface of the CNT. The last term is the energy lost per unit volume per unit time due to elastic collision with neutral species.

K. Energy balance equation for neutral atoms

$$\frac{3}{2}\left(n_A+n_B\right)k_B\left(\frac{dT_n}{d\tau}\right)=$$
$$\left[\left\{\left(\frac{3}{2}k_B\right)\left(\alpha_A n_e n_{iA}+\alpha_B n_e n_{iB}\right)\left(T_e+T_i-T_n\right)\right\}+\left(\alpha_A n_e n_{iA} I_{pA}+\alpha_B n_e n_{iB} I_{pB}\right)\right]$$
$$+\left\{\left[\left(\frac{3}{2}k_B\right)n_e\left(\nu_{eA}\delta_{eA}+\nu_{eB}\delta_{eB}\right)\left(T_e-T_n\right)\right]+\left[\left(\frac{3}{2}k_B\right)\left(\nu_{iAA}\delta_{iAA}n_{iA}+\nu_{iAB}\delta_{iAB}n_{iA}\right)\right.\right.$$
$$\left.\left(T_i-T_n\right)+\left(\frac{3}{2}k_B\right)\left(\nu_{iBA}\delta_{iBA}n_{iB}+\nu_{iBB}\delta_{iBB}n_{iB}\right)\left(T_i-T_n\right)\right]\right\}+\left\{\left(\frac{3}{2}k_B\right)n_{ct}\left[\left(1-\gamma_{iA}\right)n_{iActs}\right.$$
$$\left.+n_{iBcts}\right]\left(T_{ct}-T_n\right)\right\}-\left\{\left(\frac{3}{2}k_B\right)n_{ct}\left[n_{Acts}\delta_{Act}\left(1-\gamma_A\right)\times\left(T_n-T_{ct}\right)+n_{Bcts}\delta_{Bct}\left(T_n-T_{ct}\right)\right]\right\}$$
$$-E_{diss}. \qquad (19)$$

where

I_{pA} and I_{pB} are the ionization energy (in eV) of the constituent atomic species of type A (carbon) and type B(neon),respectively,

$E_{diss}=\left(E_{A,diss}+E_{B,diss}\right)$, $E_{j,diss}$ is the energy dissipated per unit volume per unit time by neutral atoms into the surrounding atmosphere and is assumed to be equal to the difference between the temperature of the neutral atomic species and the ambient temperature.

$E_{j,diss}=E_{j,diss0}\left[\frac{\left(T_j-T_a\right)}{\left(T_{j0}-T_a\right)}\right]$ (in eV) , constant $E_{j,diss0}$ is obtained by imposing the ambient condition of the complex plasma system in Eq.(19) for both constituent neutral species[17] ,T_a is the ambient temperature.

$\delta_{Act} = \left[\frac{2m_A}{\left(m_A + m_{ct}\right)}\right]$ and $\delta_{Bct} = \left[\frac{2m_B}{\left(m_B + m_{ct}\right)}\right]$ are the fraction of excess energy of a neutral A(carbon) and B(neon), respectively lost in a collision with spherical CNT tip [17] and are dimensionless.

and

$m_{ct} = \frac{4}{3}\pi a^3 \rho_{ct}$ is the mass of the CNT for a spherical CNT tip , a is the radius of spherical CNT tip , and ρ_{ct} is the density of spherical CNT tip,

The first term in Eq.(19) is the power gained per unit volume by the neutral species due to recombination of electrons and positively charged ions, the second term is the rate of power gained per unit volume by neutral atoms in elastic collision with electrons and positively charged ions. The third term is the energy gained per unit volume per second due to formation of neutrals at the surface of the CNT due to ion and electron accretion. The fourth term refers to the thermal energy lost per unit volume per unit time by neutral atoms accretion on and collision with CNT tip .The last term is the energy dissipation rate per unit volume by neutral atoms to the surrounding atmosphere.

L. Energy balance for spherical CNT tip

$$\frac{d}{d\tau}\left(m_{ct}C_p T_{ct}\right) = \left\{ n_{ects}\left[\gamma_e\ \varepsilon^s{}_{ecs} + \left(1-\gamma_e\right)\delta_{ect}\left[\varepsilon^s{}_{ecs} - \left(\frac{3}{2}k_B\right)T_{ct}\right]\right]\right\}$$
$$-\left\{\left(\frac{3}{2}k_B\right)\left\{\left(n_{Acts}\left[\gamma_A T_n + \delta_{Act}\left(1-\gamma_A\right)\left(T_n - T_{ct}\right)\right]\right) + \left(n_{Bcts}\delta_{Bct}\left(T_n - T_{ct}\right)\right)\right\}\right\} +$$
$$\left\{\left[n_{iActs}\left(\varepsilon^s{}_{iAcs} + I_{pA}\right) + n_{iBcts}\left(\varepsilon^s{}_{iBcs} + I_{pB}\right)\right]\right\} - \left\{\left(\frac{3}{2}k_B\right)\left[\left(1-\gamma_{iA}\right)n_{iActs} + n_{iBcts}\right]T_{ct}\right\}$$
$$-\left\{4\pi a^2\left[\varepsilon\sigma\left(T_{ct}^4 - T_a^4\right) + n_A\left(\frac{8k_B T_n}{\pi m_A}\right)^{\frac{1}{2}} + n_B\left(\frac{8k_B T_n}{\pi m_B}\right)^{\frac{1}{2}}\right]k_B\left(T_{ct} - T_n\right)\right\}. \qquad (20)$$

$$\varepsilon^{l}_{iAcs}(Z)=\left[\frac{2-Z\alpha_{Ai}}{1-Z\alpha_{Ai}}\right]k_BT_i \text{ and } \varepsilon^{l}_{iBcs}(Z)=\left[\frac{2-Z\alpha_{Bi}}{1-Z\alpha_{Bi}}\right]k_BT_i$$

are the mean energy of positively charged ions(in eV), A(carbon) and B(neon),respectively (at large distance from the surface of the CNT) collected by the spherical CNT tip [17].

C_p is the specific heat of the material of the CNT at constant pressure (in ergs/gm K),

$\in$ is the emissivity of the material of the CNT and is dimensionless,

σ is the Stefan –Boltzmann constant= $5.672\text{x}10^{-5}$ erg sec^{-1} cm^{-2} K^{-4}.

The first three terms in Eq. (20) are the rate of energy transferred to the CNT tip due to sticking accretion and elastic collision by constituent species of complex plasma. The fourth term is the energy carried away by the neutral species (generated by the recombination of the accreted ions and electrons) from the spherical CNT tip per unit volume per unit time. The last term is the rate of energy dissipation of the spherical CNT tip through radiation and conduction to the host gas [18].

4.4: Results and Discussions

In the present chapter, the calculations are performed to study the dependence of radius of spherical CNT tip (a_0) on the relative density of negative ions (n_-) i.e., ε_r. We have assumed that the shape of spherical CNT tip remains same during the growth. In addition, one important experimental observation is that the catalyst particles do not retain their original spherical or quasi-spherical shape during the growth, but are found to have truncated conical shape [19].

The values of various parameters used in the present investigation at $\tau = 0$ are,

CNT number density(n_{ct})=10^4cm^{-3}, positive ion density (n_{P0})=10^9cm^{-3}, ion density of carbon and neon(type A and B, respectively)$(n_{iA0} = n_{iB0} = n_{P0})$, negative ion density$(n_{-0})$ = $\varepsilon_r n_{P0}$, neutral atom density $(n_{A0} = n_{B0} = n_{P0})$, electron number density(n_{e0}) = $(1-\varepsilon_r)n_{P0}$, negative ion temperature(T_)=electron temperature(T_{e0})=0.6eV, ion temperature(T_{i0})=2400K, neutral temperature(T_{n0})=CNT temperature(T_{ct})=2000K.

Mass of carbon ion(m_{iA})≈mass of neutral carbon atom(m_A)=12 amu, mass of neon ion (m_{iB})≈$m$ass of neon atom(m_B)=20 amu, mass of hexaflouride (SF_6^-) negative ion(m_) = 146 amu, coefficient of recombination of carbon and neon with electron $(\alpha_{A0} \approx \alpha_{B0})$=$10^{-7}$ cm^3/sec, $e$missivity of carbon(ε)=0.6, sticking coefficients of carbon ion or carbon atom$(\gamma_{iA} = \gamma_A)$=1, specific heat of carbon(C_p)=7×10^6ergs/gm K, ionization energy of carbon(I_{pA})=11.26eV, ionization energy of neon(I_{pB})=10eV, mean energy of electron due to ionization of carbon atom(ε_A)=6.2 eV, mean energy of electron due to ionization of neon atom(ε_B)=10.7eV, mean energy of carbon ion due to ionization of carbon atom(ε_{iA})=7.3eV, mean energy of neon ion due to ionization of neon atom(ε_{iB}) =12.2eV, Energy dissipated by carbon$(\varepsilon_{A,diss0})$=42.9eV, energy dissipated by neon $(\varepsilon_{B,diss0})$=19.6 eV, constant(κ)=−1.2, radius of CNT(a_0)=12.2 nm and density of CNT (ρ_{ct}) = 4.2g/cm^3.

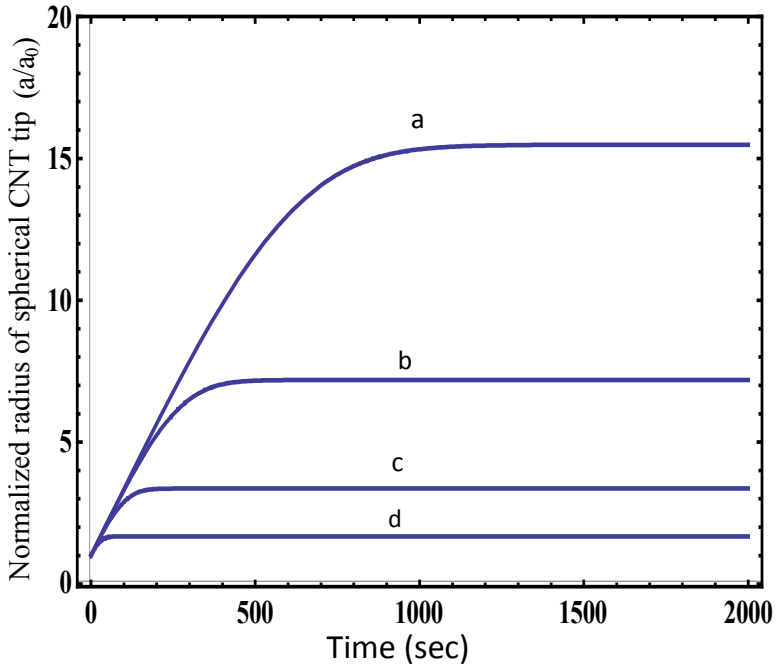

Fig.1. Shows the variation of the normalized radius a/a_0 of spherical CNT tip for different CNT number density where a, b, c and d corresponds to $n_{ct}=10^3$ cm^{-3},10^4 cm^{-3},10^5 cm^{-3},and 10^6 cm^{-3},respectively.

Fig.1 illustrates the variation of normalized radius (a/a_0) of spherical CNT tip with time for different CNT number density (i.e., $n_{ct}=10^3$ cm^{-3} ,10^4 cm^{-3}, 10^5 cm^{-3}, and 10^6 cm^{-3}) and for other parameters as mentioned above. From Fig. 1, it can be seen that the normalized radius of spherical CNT tip first increases with time and then attains a saturation value. It also shows the decrease of normalized radius a/a_0 with CNT number density n_{ct} (in cm^{-3}). This happens because for larger values of CNT number density n_{ct}, the number of positively charged ions and neutral atoms available for accretion decreases. The assumption that accretion of neutral atoms and positively charged ions on the spherical CNT tip leads to its growth, the decrease in their number density would then decrease the radius of spherical CNT tip.

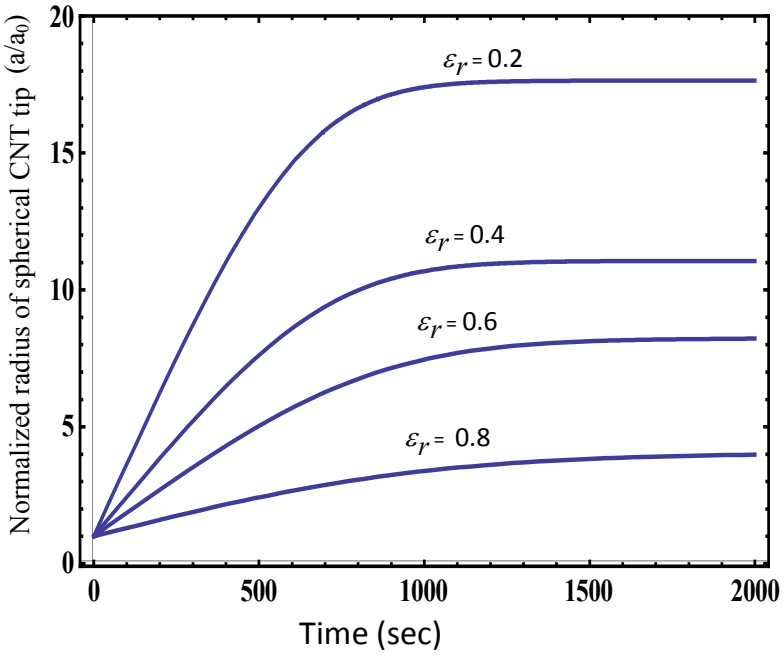

Fig. 2. Shows the variation of the normalized radius a/a_0 of spherical CNT tip for different relative density of negatively charged ions ε_r= 0.2, 0.4, 0.6 and 0.8.

Fig. 2 shows the variation of normalized radius a/a_0 of spherical CNT tip with time for different relative density of negatively charged ions(ε_r). Fig. 2 illustrates that the normalized spherical CNT tip radius a/a_0 first increases with time and then attains a saturation value. It can also be seen that the normalized radius a/a_0 decreases with relative density of negatively charged ion. The decrease of a/a_0 with relative density of negatively charged ion is implied that with increase in negative ion number density for a fixed positive ion density, more and more neutral atoms ionizes to produce positively charged ions, negatively charged ions and electrons. Since the accretion of neutral atoms on the spherical CNT tip leads to its growth, the decrease in their number density because of

increase in relative density of negatively charged ion leads to decrease in radius of the spherical CNT tip.

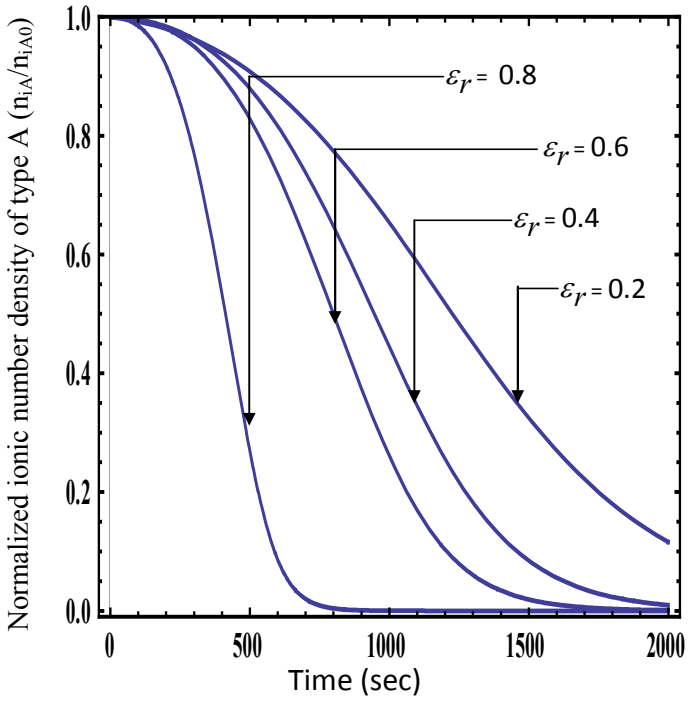

Fig. 3. Shows the dependence of ionic number density of type A(carbon) in plasma for different relative density of negatively charged ions ε_r = 0.2, 0.4, 0.6 and 0.8

Fig. 3 shows the variation of normalized ionic density of type A(carbon) in plasma with time for different relative density of negatively charged ion. It can be seen from Fig. 3 that with increasing relative density of negatively charged ion, the positively charged ion of A(carbon) decays faster.

4.4.1: Estimation of field enhancement factor

Based on the results obtained, the variation of the field emission factor with relative density of negative ions (i.e., plasma parameters) is estimated. The field emission factor is $\beta = \frac{l}{r}$(where l is the length of CNT and r is the radius of the CNT). From the results obtained in the present investigation, the radius of spherical CNT tip decreases with increase in the relative density of negatively charged ion and CNT number density. For a fixed length of CNT(l), $\beta \propto \frac{1}{r}$, so increase in negatively charged ion number density should lead to larger β. The variation of β with CNT radius has also been experimentally verified by Xu *et al.* [20]. With increase in relative density of negative ions (plasma parameters), the radius of spherical CNT tip decreases which is consistent with the experimental observations of Lee *et al.* [21] and Srivastava *et al.* [22].

References

[1] Y. Watanabe, M. Shiratani ,and M. Yamashita , Plasma Sources Sci. Technol. **2**, 35(1993).

[2] S. J. Choi and M. J. Kushner, J. Appl. Phys. **74**, 853 (1993).

[3] K.N. Ostrikov, *Plasma Nanoscience :Basic Concepts and Applications of Deterministic Nanofabrication*, (Wiley VCH, Berlin, 2008).

[4] A. A. Howling, J. L. Dorier ,and Ch. Hollenstein, Appl. Phys. Lett. **62**, 1341(1993).

[5] K. N. Ostrikov and S. Xu, *Plasma-Aided Nano Fabrification* (Wiley, Weinheim, 2007).

[6] G. S. Selwyn, J. Singh, and R. S. Benett, J. Vac. Sci. Technol. **A7**, 2758 (1989).

[7] L. Boufendi, A. Plain , J. Ph. Blondaeu, A. Bouchoule , C. Laure ,and M. Togood, Appl. Phys. Lett. **60**, 169 (1992).

[8] D. Samsonov and J. Goree, J. Vac. Sci. Technol. **A17**, 2835(1999).

[9]T. Nagai, Z. Feng, A. Kono ,and F. Shoji, Phys. Plasmas **15** ,050702 (2008).

[10] I. Levchenko, K. Ostrikov, J. Khachan, and S. V. Validimrov, Phys. Plasmas **15**,103501(2008).

[11]A. F. Pal , T. V. Rakhimova, N. V. Suetin, M.A. Timofeev, A. P. Filippov, Plasma Phys. Reports **33**,43 (2007).

[12]A.V. Melechko, V.I. Merkulov, T. E. McKnight M. A. Guillorn, K. L. Klein, D. H. Lowndes, and M. L. Simpson, J. Appl. Phys. **97**, 041301 (2005).

[13] I. Denysenko, K. Ostrikov , M.Y. Yu , and N.A. Azarenkov, J. Appl. Phys. **102**, 074308(2007).

[14] S. Botti, R. Ciardi , M.L. Terranova, S. Piccirillo V. Sessa, M. Rossi, and M. Vittori-Antisari ,Appl. Phys. Lett. **80**,1441(2002).

[15] S. Botti, R. Ciardi and L. De Dominicis, L. S. Asilyan, R. Fantoni, and T. Marolo, Chemical Phys. Lett. **378**, 117(2003).

[16] Jarrn- Horng Lin, Ching –Shiun Chen ,Hui- Ling Ma, C.-W. Chang, C.-Y. Hsu ,and H.-W. Chen, Carbon **46**, 1679(2008).

[17] M.S. Sodha , Shikha Misra, S. K. Mishra ,and S. Srivastava, J. Appl. Phys. **107**,103307(2010).

[18] M. Rosenberg, D. A. Mendis, and D. P. Sheehan, IEEE Trans. Plasma Sci.**27**, 239(1999).

[19]S. K. Srivastava, V. D. Vankar, and V. Kumar, Thin Solid Films **515**, 1552(2006).

[20] Z. Xu, X. D. Bai ,and E. G. Wang, Appl. Phys. Lett. **88**, 133107 (2006).

[21] S.F. Lee, Yung-Ping Chang ,and Li-Ying Lee, J. Mater. Sci. Mater. Electron **20**, 851(2009).

[22] S. K. Srivastava, A.K. Shukla, V. D. Vankar ,and V. Kumar, Thin Solid Films **492**, 124(2005).

CHAPTER 5

MODELING CNT GROWTH IN DIFFERENT PLASMAS AND ASSESSING FIELD EMSISSION FROM THEM

5.1: A concise blueprint of the chapter

In the present chapter, the growth of spherical carbon nanotube (CNT) tip placed over cylindrical CNT surfaces in different plasma mediums is modelled and consequent behaviour of field emission factor from them is predicted.

5.2: Introduction

The effect of plasma treatment and their consequent effects on the field emission properties of carbon nanotubes (CNT) has been an active field of research for many years.

The effect of localized lateral growth of multiwalled carbon nanotubes (MWCNTs) with ammonia (NH_3) plasma post-treatment is studied by Yau and Tsai [1], and they have shown that upon exposure to NH_3 plasma, electrical properties of CNTs is found to increase. Abdi *et al.* [2] found that as the plasma power on nickel (Ni) layer was increased, the grain size of Ni nanoparticle decreased and consequently, nanotubes of smaller diameter were obtained. Wen *et al.* [3] found that the NH_3 plasma treatment resulted in the etching effects and that more the treatment time, more the disorder in structures of carbon nanofibers. Felten *et al.* [4] have modified MWCNTs by inductively coupled radio frequency(rf)-plasma at 13.56 MHz and reported that for too high oxygen(O_2) plasma power, chemical etching occurs at the surface of CNT, thus destroying its structure.

Lee *et al.* [5] reported that the size and morphology of cobalt (Co) - catalytic seeds varied with hydrogen (H_2) plasma treatment time. Zhi *et al.* [6] have studied the field emission capability of the CNTs by hydrogen plasma treatment. Their study suggests that the hydrogen plasma treatment is a useful method for improving the field emission property of CNTs. Srivastava *et al.* [7] have reported that the oxide films without the H_2 plasma pre treatment or treated for lesser time resulted in CNT films with high percentage of carbonaceous particles and with embedded particles/nanorods distributed discontinuously in the cavity of the nanotubes.

Zhu *et al.* [8] have observed that the deposition of amorphous layer comprising carbon and fluorine during extended carbon tetra fluoride (CF_4) plasma treatment, may hamper the field emission from CNT films.

Ahn *et al.* [9] have demonstrated external rf plasma irradiation of argon (Ar) gas to well-aligned MWCNTs to modify any structural defects and vaporize contamination of the MWCNTs grown at temperature of 400 ^{0}C. In this case, it was seen that there was a structural enhancement in the MWCNTs that resulted in a reduction of the turn on fields from 1.65 V/ μm to 0.93 V/ μm and an increase in the field emission current. Jaehyeong *et al*. [10] studied the influence of various plasma treatments on the properties of CNTs for composite applications and found that the long plasma treatment time changed the CNT morphology dramatically.

Feng *et al.* [11] have studied the effects of plasma treatment on microstructure and electron field emission (FE) properties of screen-printed carbon nanotube films and found that on H_2, nitrogen (N_2) and NH_3 plasma treatment, the plasma treated CNT films had superior FE

behaviour with emission site density (ESD) increasing from 10^3 to $10^6/cm^2$.

Lee *et al.* [12] have studied the plasma treatment effects on the surface morphology and field emission characteristics of CNTs and found that CNTs treated with the H_2, Ar and CF_4 have a higher density of defect and small average diameter as compared with that of untreated CNTs, reflecting the etching effects of plasma treatment. They also reported that the field emission is highest for CNTs treated with H_2 plasma.

5.3: MODEL

Following the model developed in Chapter 2 , we now consider a CNT with spherical tip placed over the cylindrical surface grown (without catalyst) in the presence of plasma containing electrons, positively charged ions of type A and B, neutral atoms of type A and B as shown in Fig.1

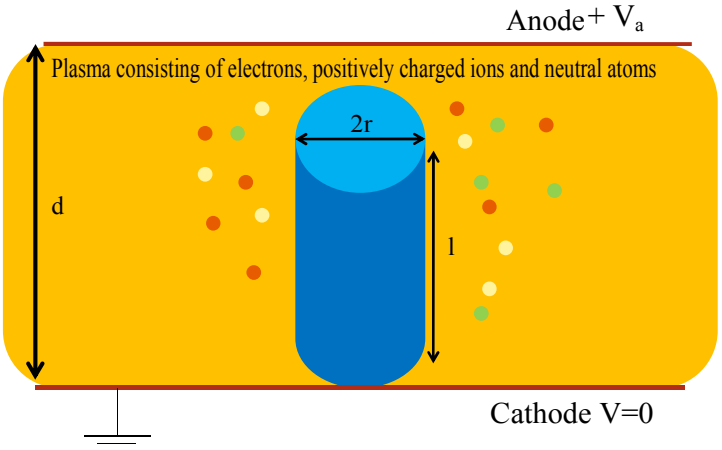

Fig. 1. Shows the spherical CNT tip placed over cylindrical CNT surface in a plasma containing electrons, positively charged ions and neutral atoms.

The initial radius of CNT r_0 (same for spherical tip and cylindrical surface) can be estimated by equating the accretion of electrons and positively charged ions on the CNT, i.e.,

$$n_{ects} + n_{ectys} = n_{iActs} + n_{iBcts} + n_{iActy} + n_{iBcty} \tag{1}$$

where

a) $n_{ects} = \pi r^2 \left(\frac{8k_B T_e}{\pi m_e} \right)^{\frac{1}{2}} n_e \exp\left[Z\alpha_e \right]$ is the electron collection current at the surface of spherical CNT tip [13] (in $\sec^{-1}$) and $\alpha_e = \left(\frac{e^2}{rk_B T_e} \right)$.

b) $n_{ijcts} = \pi r^2 \left(\frac{8k_B T_i}{\pi m_{ij}} \right)^{\frac{1}{2}} n_{ij} \left[1 - Z\alpha_i \right]$ is the ion collection current of a spherical CNT tip [13] (in $\sec^{-1}$) and $\alpha_i = \left(\frac{e^2}{rk_B T_i} \right)$

c) $n_{ectcys} = n_e rl \left(\frac{2\pi k_B T_e}{m_e} \right)^{\frac{1}{2}} \exp\left[\frac{eV_s}{k_B T_e} \right]$ is the electron collection current at the surface of cylindrical CNT [14] (in $\sec^{-1}$) .

d) $n_{ijctcys} = n_{ij} rl \left(\frac{2\pi k_B T_i}{m_{ij}} \right)^{\frac{1}{2}} \left\{ \frac{2}{\sqrt{\pi}} \left(\frac{eV_s}{k_B T_i} \right)^{\frac{1}{2}} + \exp\left[\frac{eV_s}{k_B T_i} \right] erfc\left[\left(\frac{eV_s}{k_B T_i} \right)^{\frac{1}{2}} \right] \right\}$ is the ion collection current of a cylindrical CNT [14] (in $\sec^{-1}$) ,

where j refers to either A(carbon) or B (H_2^+ in hydrogen plasma, Ar^+ in argon plasma, CH_4^+ in methane plasma and CF_4^+ in carbon tetra fluoride plasma)

Substituting the above values for $n_{ects}, n_{ijcts}, n_{ectcys}, n_{ijctcys}$ in Eq.(1) we get

$$\pi r^2\left(\frac{8k_BT_e}{\pi m_e}\right)^{\frac{1}{2}} n_e \exp\left[\frac{Ze^2}{rk_BT_e}\right] + n_e rl\left(\frac{2\pi k_BT_e}{m_e}\right)^{\frac{1}{2}} \exp\left[\frac{eV_s}{k_BT_e}\right] = \pi r^2\left(\frac{8k_BT_i}{\pi m_{iA}}\right)^{\frac{1}{2}} n_{iA}\left[1-\frac{Ze^2}{rk_BT_i}\right] +$$
$$\pi r^2\left(\frac{8k_BT_i}{\pi m_{iB}}\right)^{\frac{1}{2}} n_{iB}\left[1-\frac{Ze^2}{rk_BT_i}\right] + n_{iA} rl\left(\frac{2\pi k_BT_i}{m_{iA}}\right)^{\frac{1}{2}}\left\{\frac{2}{\sqrt{\pi}}\left(\frac{eV_s}{k_BT_i}\right)^{\frac{1}{2}} + \exp\left[\frac{eV_s}{k_BT_i}\right] erfc\left[\left(\frac{eV_s}{k_BT_i}\right)^{\frac{1}{2}}\right]\right\}$$
$$+ n_{iB} rl\left(\frac{2\pi k_BT_i}{m_{iB}}\right)^{\frac{1}{2}}\left\{\frac{2}{\sqrt{\pi}}\left(\frac{eV_s}{k_BT_i}\right)^{\frac{1}{2}} + \exp\left[\frac{eV_s}{k_BT_i}\right] erfc\left[\left(\frac{eV_s}{k_BT_i}\right)^{\frac{1}{2}}\right]\right\}, \qquad (2)$$

$$2\pi r^2\left(\frac{T_e}{\pi m_e}\right)^{\frac{1}{2}} n_e \exp\left[\frac{Ze^2}{rk_BT_e}\right] + n_e rl\left(\frac{\pi T_e}{m_e}\right)^{\frac{1}{2}} \exp\left[\frac{eV_s}{k_BT_e}\right] = 2\pi r^2\left(\frac{T_i}{\pi m_{iA}}\right)^{\frac{1}{2}} n_{iA}\left[1-\frac{Ze^2}{rk_BT_i}\right] +$$
$$2\pi r^2\left(\frac{T_i}{\pi m_{iB}}\right)^{\frac{1}{2}} n_{iB}\left[1-\frac{Ze^2}{rk_BT_i}\right] + n_{iA} rl\left(\frac{\pi T_i}{m_{iA}}\right)^{\frac{1}{2}}\left\{\frac{2}{\sqrt{\pi}}\left(\frac{eV_s}{k_BT_i}\right)^{\frac{1}{2}} + \exp\left[\frac{eV_s}{k_BT_i}\right] erfc\left[\left(\frac{eV_s}{k_BT_i}\right)^{\frac{1}{2}}\right]\right\}$$
$$+ n_{iB} rl\left(\frac{\pi T_i}{m_{iB}}\right)^{\frac{1}{2}}\left\{\frac{2}{\sqrt{\pi}}\left(\frac{eV_s}{k_BT_i}\right)^{\frac{1}{2}} + \exp\left[\frac{eV_s}{k_BT_i}\right] erfc\left[\left(\frac{eV_s}{k_BT_i}\right)^{\frac{1}{2}}\right]\right\}, \qquad (3)$$

For Z = -1, i.e., initially the CNT is negatively charged and radius of CNT is r_0,

$$2\pi r_0^2\left(\frac{T_e}{\pi m_e}\right)^{\frac{1}{2}} n_e \exp\left[\frac{-e^2}{r_0 k_B T_e}\right] + n_e r_0 l\left(\frac{\pi T_e}{m_e}\right)^{\frac{1}{2}} \exp\left[\frac{eV_s}{k_B T_e}\right] = \left\{2\pi r_0^2\left[1+\frac{e^2}{r_0 k_B T_i}\right]\left(\left(\frac{T_i}{\pi m_{iA}}\right)^{\frac{1}{2}} n_{iA} + \left(\frac{T_i}{\pi m_{iB}}\right)^{\frac{1}{2}} n_{iB}\right)\right\} + \left(r_0 l\left\{\frac{2}{\sqrt{\pi}}\left(\frac{eV_s}{k_B T_i}\right)^{\frac{1}{2}} + \exp\left[\frac{eV_s}{k_B T_i}\right] erfc\left[\left(\frac{eV_s}{k_B T_i}\right)^{\frac{1}{2}}\right]\right\}\left(n_{iA}\left(\frac{\pi T_i}{m_{iA}}\right)^{\frac{1}{2}} + n_{iB}\left(\frac{\pi T_i}{m_{iB}}\right)^{\frac{1}{2}}\right)\right) \quad (4)$$

where

l = length of CNT(in μm),

V_s = the surface potential on the cylindrical CNT (in Stat V),

n_e = number density of electron (in cm^{-3}),

T_e = electron temperature (in eV),

k_B = Boltzmann's constant (in ergs/K),

T_i = ion temperature (in K),

n_{iA} = number density of ion A where A refers to carbon in all plasmas considered (in cm^{-3}),

m_{iA} = mass of ion A(in gm),

n_{iB} = number density of ion B where B refers to H_2^+ in hydrogen plasma, Ar^+ in argon plasma, CH_4^+ in methane plasma and CF_4^+

in carbon tetra fluoride plasma (in cm^{-3}),

m_{iB} = mass of ion B (in gm),

e = electronic charge(in Stat C).

Following the model developed in Chapter 2 and using the terms for spherical tip and cylindrical surface from chapter 3, we write the equations for growth of CNT with spherical tip placed over cylindrical surface as:

A. Charge neutrality equation

The Eq.(5) equates the net negative and positive charge on CNT to render plasma as electrically neutral.

$$Zn_{ct} + n_{iA} + n_{iB} = n_e, \qquad (5)$$

Z= amount of charge on spherical tip placed over cylindrical surface (dimensionless),

n_{ct} = the number density of the CNT(in cm^{-3}),

n_{iA} = number density of ion A (in cm^{-3}) ,

n_{iB} = number density of ion B(in cm^{-3}).

B. Charging of the CNT

This equation describes the charge developed on the CNT with spherical tip placed over cylindrical surface due to accretion of electrons and positively charged ions on the surface of CNT.

$$\frac{dZ}{d\tau} = n_{iActs} + n_{iActcys} + n_{iBcts} + n_{iBctcys} - \gamma_e\left(n_{ects} + n_{ectcys}\right), \qquad (6)$$

where γ_e is the sticking coefficient of electrons on CNT surface.

The first and second term in Eq.(6) denotes charge developed on the CNT due to ion collection currents of A(carbon) , third and fourth term

denotes charge developed on the CNT due to ion collection currents of B(either hydrogen, argon, methane, or carbon tetra fluoride), on spherical tip over cylindrical surface. The last term denotes charge developed on spherical tip placed over cylindrical surface because of electron collection current.

C. Growth rate equation of electron density

The growth rate equation of electron density accounts for ionization of neutral into ions and electrons and recombination of electrons and ions to form neutrals.

$$\frac{dn_e}{d\tau} = \left(\beta_A n_A + \beta_B n_B\right) - \left(\alpha_A n_e n_{iA} + \alpha_B n_e n_{iB}\right) - \gamma_e n_{ct}\left(n_{ects} + n_{ectcys}\right) \quad ,(7)$$

β_A and β_B are the coefficients of ionization of the constituent neutral atoms of A(carbon) and B(either hydrogen, argon, methane, or carbon tetra fluoride) due to external agency (in sec), and

$\alpha_A(T_e) = \alpha_{A0}\left(\frac{300}{T_e}\right)^k cm^3/\sec$ and $\alpha_B(T_e) = \alpha_{B0}\left(\frac{300}{T_e}\right)^k cm^3/\sec$ are the coefficients of recombination of electrons and positively charged ions [13] of A(carbon) and B(hydrogen, argon, methane, or carbon tetra fluoride) where $\alpha_{A0} = \alpha_{B0} = n_{e0}\times 10^{-7}\left(\frac{1}{T_{e0}}\right)^{-1.2}$ and

n_{ects}, n_{ectcys} are the electron collection current at the surface of spherical CNT tip[13] and cylindrical CNT surface [14], respectively (in sec^{-1}) and n_{ct} is the CNT number density (in cm^{-3}) , γ_e is the sticking coefficient of electron to spherical tip placed over cylindrical CNT surface and is dimensionless.

The first term in Eq.(7) is the rate of gain in electron density per unit time due to ionization of neutral atoms and second term is the decrease in the electron density due to electron–ion recombination and the third term is the loss in electron density because of the electron collection current on the spherical tip placed over cylindrical CNT surface.

D. Growth rate equation of positively charged ion density

The number density balance equation of ions is developed assuming processes such as ionization of neutrals to produce ions and electrons and the electron and ion recombination to form neutrals.

$$\frac{dn_{iA}}{d\tau} = \beta_A n_A - \alpha_A n_e n_{iA} - n_{ct}\left(n_{iActs} + n_{iActcys}\right), \tag{8}$$

$$\frac{dn_{iB}}{d\tau} = \beta_B n_B - \alpha_B n_e n_{iB} - n_{ct}\left(n_{iBcts} + n_{iBctcys}\right), \tag{9}$$

$$n_{iActs} = \pi r^2 \left(\frac{8k_B T_i}{\pi m_{iA}}\right)^{\frac{1}{2}} n_{iA}\left[1 - \frac{Ze^2}{rk_B T_i}\right], n_{iBcts} = \pi r^2 \left(\frac{8k_B T_i}{\pi m_{iB}}\right)^{\frac{1}{2}} n_{iB}\left[1 - \frac{Ze^2}{rk_B T_i}\right]$$

are the ion collection currents at spherical CNT tip [13](in sec^{-1}) for A(carbon) and B (either hydrogen, argon, methane, or carbon tetra fluoride),respectively.

$$n_{iActcys} = n_{iA} r l \left(\frac{2\pi k_B T_i}{m_{iA}}\right)^{\frac{1}{2}} \left\{\frac{2}{\sqrt{\pi}}\left(\frac{eV_s}{k_B T_i}\right)^{\frac{1}{2}} + \exp\left[\frac{eV_s}{k_B T_i}\right] erfc\left[\left(\frac{eV_s}{k_B T_i}\right)^{\frac{1}{2}}\right]\right\},$$

$$n_{iBctcys} = n_{iB} r l \left(\frac{2\pi k_B T_i}{m_{iB}}\right)^{\frac{1}{2}} \left\{\frac{2}{\sqrt{\pi}}\left(\frac{eV_s}{k_B T_i}\right)^{\frac{1}{2}} + \exp\left[\frac{eV_s}{k_B T_i}\right] erfc\left[\left(\frac{eV_s}{k_B T_i}\right)^{\frac{1}{2}}\right]\right\}$$

are the ion collection currents at the cylindrical CNT surface [14](in sec^{-1}) for A(carbon) and B (either hydrogen, argon, methane, or carbon tetra fluoride),respectively.

The first term in Eqs. (8) and (9) is the gain in ion density per unit time on account of ionization of neutral atoms, the second term is the decrease in ion density due to electron-ion recombination, and the third term denotes the loss in ion density due to ion collection current to the spherical tip placed over cylindrical CNT surface.

E. Growth rate equation of neutral atoms

$$\frac{dn_A}{d\tau} = \alpha_A n_e n_{iA} - \beta_A n_A + n_{ct}\left(1-\gamma_{iA}\right)\left(n_{iActs} + n_{iActcys}\right) - n_{ct}\gamma_A\left(n_{Acts} + n_{Actcys}\right), \tag{10}$$

$$\frac{dn_B}{d\tau} = \alpha_B n_e n_{iB} - \beta_B n_B + n_{ct}\left(n_{iBcts} + n_{iBctcys}\right), \tag{11}$$

where

$$n_{Acts} = \pi r^2 \left(\frac{8k_B T_n}{\pi m_A}\right)^{\frac{1}{2}} n_A, \quad n_{Bcts} = \pi r^2 \left(\frac{8k_B T_n}{\pi m_B}\right)^{\frac{1}{2}} n_B$$

are the neutral collection currents at the surface of spherical CNT tip [13] (in sec^{-1}), and

$$n_{Actcys} = \pi rl \left(\frac{2k_B T_n}{m_A}\right)^{\frac{1}{2}} n_A, \quad n_{Bctcys} = \pi rl \left(\frac{2k_B T_n}{m_B}\right)^{\frac{1}{2}} n_B$$

are the neutral collection currents at the cylindrical CNT surface [14](in sec^{-1}),n_A and n_B are the neutral atom number density (in cm^{-3}).

γ_A is the sticking coefficient of carbon neutrals on spherical tip placed over cylindrical CNT surface and γ_{iA} is the sticking coefficient of carbon ions on CNT surface, both γ_A and γ_{iA} are dimensionless.

The first term in Eqs. (10) and (11) is the gain in neutral atom density per unit time due to electron–ion recombination, the second term is the decrease in neutral density due to their ionization, the third term is the gain in neutral density due to neutralization of the ions collected on spherical tip placed over cylindrical CNT surface. The last term in Eq. (10) is the accretion of neutral atoms of species A (carbon) on spherical tip placed over cylindrical CNT surface.

F. Growth rate equation of the mass of CNT

The accretion of ions and neutrals on CNT surface is the main process contributing to growth of CNT.

$$\frac{dm_{ct}}{d\tau} = \left[m_A \gamma_A \left(n_{Acts} + n_{Actcys} \right) + m_{iA} \gamma_{iA} \left(n_{iActs} + n_{iActcys} \right) \right], \qquad (12)$$

$m_{ct} = \frac{4}{3}\pi r^3 \rho_{ct} + \pi r^2 l \rho_{ct}$ is the mass of the entire CNT, ρ_{ct} is the density of CNT, r is the radius and l is the length of entire CNT.

The first and second term in Eq.(12) is the gain in the mass of the spherical tip placed over cylindrical CNT surface, respectively due to collection of atomic and ionic species A (i.e., carbon), respectively.

G. Energy balance equation of electrons

$$\frac{d}{d\tau}\left(\frac{3}{2}n_e k_B T_e\right)$$

$$=\left(\beta_A n_A \varepsilon_A+\beta_B n_B \varepsilon_B\right)-\left(\frac{3}{2}k_B\right)\left(\alpha_A n_e n_{iA}+\alpha_B n_e n_{iB}\right)T_e-n_{ct}n_{ectcys}$$

$$\left\{\gamma_e \varepsilon_{eccy}^{lh}+\delta_{ect}(1-\gamma_e)\left[\varepsilon_{eccy}^{s}-\left(\frac{3}{2}k_B\right)T_{ct}\right]\right\}-$$

$$n_{ct}n_{ects}\left\{\gamma_e \varepsilon_{ecs}^{lh}+\delta_{ect}(1-\gamma_e)\left[\varepsilon_{ecs}^{s}-\left(\frac{3}{2}k_B\right)T_{ct}\right]\right\}-\left(\frac{3}{2}k_B\right)$$

$$\left[\nu_{eA}\delta_{eA}+\nu_{eB}\delta_{eB}\right](T_e-T_n)n_e-\left(\frac{3}{2}k_B\right)\times\left(\nu_{eAi}\delta_{eAi}+\nu_{eBi}\delta_{eBi}\right)\left(T_e-T_i\right)n_e\ ,$$

(13)

The LHS of Eq.(13) can be rewritten as

$$\left(\frac{3}{2}k_B\right)n_e\left(\frac{dT_e}{d\tau}\right)+\left(\frac{3}{2}k_B\right)T_e\left(\frac{dn_e}{d\tau}\right)$$

Substituting the value of $\frac{dn_e}{d\tau}$ from Eq. (7) in the above Eq., we get

$$\left(\frac{3}{2}k_B\right)n_e\left(\frac{dT_e}{d\tau}\right)=$$

$$-\left(\frac{3}{2}k_B\right)T_e\left(\beta_A n_A+\beta_B n_B\right)+\left(\frac{3}{2}k_B\right)T_e\left(\alpha_A n_e n_{iA}+\alpha_B n_e n_{iB}\right)+\left(\frac{3}{2}k_B\right)T_e\gamma_e n_{ct}n_{ects}$$

$$+\left(\frac{3}{2}k_B\right)T_e\gamma_e n_{ct}n_{ectcys}+\left(\beta_A n_A \varepsilon_A+\beta_B n_B \varepsilon_B\right)-\left(\frac{3}{2}k_B\right)\left(\alpha_A n_e n_{Ai}+\alpha_B n_e n_{Bi}\right)T_e-$$

$$n_{ct}n_{ectcys}\left\{\gamma_e \varepsilon_{eccy}^{l}+\delta_{ect}(1-\gamma_e)\left[\varepsilon_{eccy}^{s}-\left(\frac{3}{2}k_B\right)T_{ct}\right]\right\}$$

$$-n_{ct}n_{ects}\left\{\gamma_e \varepsilon_{ecs}^{l}+\delta_{ect}(1-\gamma_e)\left[\varepsilon_{ecs}^{s}-\left(\frac{3}{2}k_B\right)T_{ct}\right]\right\}-$$

$$\left(\frac{3}{2}k_B\right)\left[\nu_{eA}\delta_{eA}+\nu_{eB}\delta_{eB}\right](T_e-T_n)n_e-\left(\frac{3}{2}k_B\right)\times\left(\nu_{eAi}\delta_{eAi}+\nu_{eBi}\delta_{eBi}\right)\left(T_e-T_i\right)n_e\ ,$$

(14)

On rearranging the above equation, we get

$$\left(\frac{3}{2}k_B\right)n_e\left(\frac{dT_e}{d\tau}\right)= \left\{\left[\left(\beta_A n_A \varepsilon_A+\beta_B n_B \varepsilon_B\right)-\left(\frac{3}{2}k_B\right)\left(\beta_A n_A+\beta_B n_B\right)T_e\right]\right\}-\left\{n_{ct}n_{ectcys}\right.$$
$$\left\{\left[\gamma_e \varepsilon^{l}_{eccy}-\left(\frac{3}{2}k_B\right)T_e\right]+\delta_{ect}\left(1-\gamma_e\right)\left[\varepsilon^{s}_{eccy}-\left(\frac{3}{2}k_B\right)T_{ct}\right]\right\}-n_{ct}n_{ects}$$
$$\left\{\left[\gamma_e \varepsilon^{l}_{ecs}-\left(\frac{3}{2}k_B\right)T_e\right]+\delta_{ect}\left(1-\gamma_e\right)\left[\varepsilon^{s}_{ecs}-\left(\frac{3}{2}k_B\right)T_{ct}\right]\right\}\right\}-\left\{\left(\frac{3}{2}k_B\right)\right.$$
$$\left.\left\{\left[\nu_{eA}\delta_{eA}+\nu_{eB}\delta_{eB}\right]\left(T_e-T_n\right)+\left(\nu_{eAi}\delta_{eAi}+\nu_{eBi}\delta_{eBi}\right)\left(T_e-T_i\right)\right\}n_e\right\}. \qquad (15)$$

where

$\frac{3}{2}n_e k_B T_e$ is the thermal energy of electrons ,

n_e is the number density of electrons(in cm^{-3}),T_e is the electron temperature (in eV), T_{ct} is the CNT temperature (in K), and T_n is the neutral temperature (in K).

$\varepsilon^{l}_{ecs}(Z)=\varepsilon^{s}_{ecs}(Z)-\left(\frac{Ze^2}{r}\right)$ is the mean energy of electrons (in eV) at a large distance from the surface of spherical CNT tip [13],

$\varepsilon^{s}_{ecs}(Z)=2k_B T_e$ is the mean energy of electrons (in eV) collected by spherical CNT tip [13],

$\varepsilon^{l}_{eccy}(Z)=k_B T_e\left[2-\left(\frac{eV_s}{k_B T_e}\right)\right]$ is the mean energy of electrons (in eV) at a large distance from the surface of cylindrical CNT surface[14],

$\varepsilon^{s}_{eccy}(Z)=2k_B T_e$ is the mean energy of electrons(in eV) collected by cylindrical CNT surface[14],

$\nu_{eA}=\nu_{eA0}\left(\frac{n_A}{n_{A0}}\right)\left(\frac{T_e}{T_{e0}}\right)^{\frac{1}{2}}$ and $\nu_{eB}=\nu_{eB0}\left(\frac{n_B}{n_{B0}}\right)\left(\frac{T_e}{T_{e0}}\right)^{\frac{1}{2}}$ are the electron collision frequency (in sec^{-1}) due to elastic collisions with neutral

atoms A(carbon) and B(either hydrogen, argon, methane, or carbon tetra fluoride), respectively [13] , and

$\nu_{eA0} = (8.3\times10^5)\pi r_A{}^2 n_{A0} T_{e0}{}^{\frac{1}{2}}$ and $\nu_{eB0} = (8.3\times10^5)\pi r_B{}^2 n_{B0} T_{e0}{}^{\frac{1}{2}}$,

$\nu_{eAi} = \nu_{eAi0}\left(\frac{n_{iA}}{n_{iA0}}\right)\left(\frac{T_e}{T_{e0}}\right)^{-\frac{3}{2}}$ and $\nu_{eBi} = \nu_{eBi0}\left(\frac{n_{iB}}{n_{iB0}}\right)\left(\frac{T_e}{T_{e0}}\right)^{-\frac{3}{2}}$ are the electron collision frequency (in sec^{-1}) due to elastic collisions with positively charged ion of type A(carbon) and type B(either hydrogen, argon, methane, or carbon tetra fluoride)[13],

$\nu_{eAi0} = \left(5.5\frac{n_{e0}}{T_{e0}{}^{\frac{3}{2}}}\right)\ln\left(\frac{220T_{e0}}{n_{iA0}{}^{\frac{1}{3}}}\right)$ and $\nu_{eBi0} = \left(5.5\frac{n_{e0}}{T_{e0}{}^{\frac{3}{2}}}\right)\ln\left(\frac{220T_{e0}}{n_{iB0}{}^{\frac{1}{3}}}\right)$,

$\delta_{eA} \approx 2\left(\frac{m_e}{m_A}\right)$ and $\delta_{eB} \approx 2\left(\frac{m_e}{m_B}\right)$ are the fraction of excess energy of an electron lost in a collision with the neutral atom A(carbon) and B(either hydrogen, argon, methane, or carbon tetra fluoride),respectively[13] and are dimensionless,

$\delta_{eAi} \approx 2\left(\frac{m_e}{m_{iA}}\right)$ and $\delta_{eBi} \approx 2\left(\frac{m_e}{m_{iB}}\right)$ is the fraction of excess energy of an electron lost in a collision with a positively charged ion A(carbon) and B(either hydrogen, argon, methane, or carbon tetra fluoride), respectively [13] and is dimensionless,

$\delta_{ect} \approx 2\left(\frac{m_e}{m_{ct}}\right)$ is the fraction of excess energy of an electron lost in a collision with a CNT [13] and is dimensionless where,

$m_{ct} = \frac{4}{3}\pi r^3 \rho_{ct} + \pi r^2 l \rho_{ct}$ is the mass of the entire CNT and ρ_{ct} is the density of CNT.

The first term in Eq. (15) is the power gained per unit volume by electrons due to ionization of neutral atoms, the second term is the energy loss per unit volume per unit time due to the sticking accretion and elastic collisions of electron at the spherical CNT tip. The third term is the energy loss per unit volume per unit time due to elastic electron - atom collisions and elastic electron- ion collision.

H. Energy balance equation for positively charged ions

$$\frac{d}{d\tau}\left[\frac{3}{2}\left(n_{iA}+n_{iB}\right)k_B T_i\right]$$

$$=\left(\beta_A n_A \varepsilon_{iA}+\beta_B n_B \varepsilon_{iB}\right)+\left(\frac{3}{2}k_B\right)n_e\left[\nu_{eAi}\delta_{eAi}+\nu_{eBi}\delta_{eBi}\right]\left(T_e-T_i\right)-$$
$$\left(\frac{3}{2}k_B\right)\left(\alpha_A n_e n_{iA}+\alpha_B n_e n_{iB}\right)T_i - n_{ct}\left[\left(n_{iActs}\varepsilon^l_{iAcs}+n_{iBcts}\varepsilon^l_{iBcs}\right)\right.$$
$$\left.+\left(n_{iActcys}\varepsilon^l_{iAccys}+n_{iBctcys}\varepsilon^l_{iBccys}\right)\right]-\left(\frac{3}{2}k_B\right)\left[\left(\nu_{iAA}\delta_{iAA}+\nu_{iAB}\delta_{iAB}\right)n_{iA}\right.$$
$$\left.+\left(\nu_{iBA}\delta_{iBA}+\nu_{iBB}\delta_{iBB}\right)n_{iB}\right]\left(T_i-T_n\right), \qquad (16)$$

The LHS of Eq.(16) can be rewritten as

$$\left(\frac{3}{2}k_B\right)\left(n_{iA}+n_{iB}\right)\left(\frac{dT_i}{d\tau}\right)+\left(\frac{3}{2}k_B\right)T_i\left(\frac{d\left(n_{iA}+n_{iB}\right)}{d\tau}\right)$$

Substituting the value of $\frac{dn_i}{d\tau}$ from Eqs.(8) and (9) in Eq.(16), we get

$$\left(\frac{3}{2}k_B\right)\left(n_{iA}+n_{iB}\right)\left(\frac{dT_i}{d\tau}\right)=$$

$$-\left(\frac{3}{2}k_B\right)\left(\beta_A n_A+\beta_B n_B\right)+\left(\frac{3}{2}k_B\right)\left(\alpha_A n_e n_{iA}+\alpha_B n_e n_{iB}\right)+\left(\frac{3}{2}k_B\right)n_{ct}\left[\left(n_{iActs}+n_{iActcys}\right)+\left(n_{iBcts}+n_{iBctcys}\right)\right]+\left(\beta_A n_A\varepsilon_{iA}+\beta_B n_B\varepsilon_{iB}\right)+\left(\frac{3}{2}k_B\right)n_e\left[\nu_{eAi}\delta_{eAi}+\nu_{eBi}\delta_{eBi}\right]\left(T_e-T_i\right)-\left(\frac{3}{2}k_B\right)\left(\alpha_A n_e n_{iA}+\alpha_B n_e n_{iB}\right)T_i-n_{ct}\left[\left(n_{iActs}\varepsilon^l_{iAcs}+n_{iBcts}\varepsilon^l_{iBcs}\right)+\left(n_{iActcys}\varepsilon^l_{iAccys}+n_{iBctcys}\varepsilon^l_{iBccys}\right)\right]-\left(\frac{3}{2}k_B\right)\left[\left(\nu_{iAA}\delta_{iAA}+\nu_{iAB}\delta_{iAB}\right)n_{iA}+\left(\nu_{iBA}\delta_{iBA}+\nu_{iBB}\delta_{iBB}\right)n_{iB}\right]\left(T_i-T_n\right),$$

(17)

On rearranging the above equation, we get

$$\left(\frac{3}{2}k_B\right)\left(n_{iA}+n_{iB}\right)\left(\frac{dT_i}{d\tau}\right)=$$

$$\left[\left(\beta_A n_A\varepsilon_{iA}+\beta_B n_B\varepsilon_{iB}\right)-\left(\frac{3}{2}k_B\right)\left(\beta_A n_A+\beta_B n_B\right)T_i\right]+\left(\frac{3}{2}k_B\right)n_e\left[\nu_{eAi}\delta_{eAi}+\nu_{eBi}\delta_{eBi}\right]\left(T_e-T_i\right)-n_{ct}\left\{\left[\left(n_{iActs}\left[\varepsilon^l_{iAcs}-\left(\frac{3}{2}k_B\right)T_i\right]\right)+\left(n_{iBcts}\left[\varepsilon^l_{iBcs}-\left(\frac{3}{2}k_B\right)T_i\right]\right)\right]+\left[\left(n_{iActcys}\left[\varepsilon^l_{iAccys}-\left(\frac{3}{2}k_B\right)T_i\right]\right)+\left(n_{iBctcys}\left[\varepsilon^l_{iBccys}-\left(\frac{3}{2}k_B\right)T_i\right]\right)\right]\right\}-\left(\frac{3}{2}k_B\right)\left[\left(\nu_{iAA}\delta_{iAA}+\nu_{iAB}\delta_{iAB}\right)n_{iA}+\left(\nu_{iBA}\delta_{iBA}+\nu_{iBB}\delta_{iBB}\right)n_{iB}\right]\left(T_i-T_n\right),$$

(18)

where

$\frac{3}{2}\left(n_{iA}+n_{iB}\right)k_B T_i$ is the thermal energy of ions ,

n_{iA} and n_{iB} are the number density of positively charged ions of type A(carbon) and type B(either hydrogen, argon, methane, or carbon tetra

fluoride), respectively(in cm^{-3}),T_i is the ion temperature (in K), T_n is the temperature of neutral (in K).

$\varepsilon^{l}_{iAcs}(Z)=\left[\frac{2-Z\alpha_{Ai}}{1-Z\alpha_{Ai}}\right]k_BT_i$ and $\varepsilon^{l}_{iBcs}(Z)=\left[\frac{2-Z\alpha_{Bi}}{1-Z\alpha_{Bi}}\right]k_BT_i$ are the mean energy (in eV) of positively charged ions, A(carbon) and B(either hydrogen, argon, methane, or carbon tetra fluoride), respectively (at large distance from the surface of the CNT) collected by the spherical CNT tip [13] ,

$$\varepsilon^{l}_{iAccys}(Z)=k_BT_in_{iA}rl\left(\frac{2\pi k_BT_i}{m_{iA}}\right)^{\frac{1}{2}}\left[\left(\frac{4}{\sqrt{\pi}}\right)\left(\frac{eV_S}{k_BT_i}\right)^{\frac{1}{2}}+\left(2-\left(\frac{eV_S}{k_BT_i}\right)^{\frac{1}{2}}\right)\exp\left[\frac{eV_S}{k_BT_i}\right]erfc\left[\left(\frac{eV_S}{k_BT_i}\right)^{\frac{1}{2}}\right]\right]$$

$$\varepsilon^{l}_{iBccys}(Z)=k_BT_in_{iB}rl\left(\frac{2\pi k_BT_i}{m_{iB}}\right)^{\frac{1}{2}}\left[\left(\frac{4}{\sqrt{\pi}}\right)\left(\frac{eV_S}{k_BT_i}\right)^{\frac{1}{2}}+\left(2-\left(\frac{eV_S}{k_BT_i}\right)^{\frac{1}{2}}\right)\exp\left[\frac{eV_S}{k_BT_i}\right]erfc\left[\left(\frac{eV_S}{k_BT_i}\right)^{\frac{1}{2}}\right]\right]$$

are the mean energy of ions(in eV) at a large distance from the surface of cylindrical CNT surface[14] of A (carbon) and B(either hydrogen, argon, methane, or carbon tetra fluoride), respectively.

ε_{ij} is the mean energy (in eV) of positively charged ions produced by the ionization of neutral atoms [13] and for ion A(carbon) and B(either hydrogen, argon, methane, or carbon tetra fluoride) are expressed as

$$\varepsilon_{iA}=\frac{3}{2}k_BT_{iA}+\frac{3k_B}{2\left(\alpha_A(T_e)\times n_{iA}\right)}\left[\left\{\nu_{iAA}\times\delta_{iAA}\times\left(T_i-T_n\right)\right\}-\left\{\nu_{eAi}\times\delta_{eAi}\times\left(T_e-T_i\right)\right\}\right]$$

$$\varepsilon_{iB}=\frac{3}{2}k_BT_{iB}+\frac{3k_B}{2\left(\alpha_B(T_e)\times n_{iB}\right)}\left[\left\{\nu_{iBB}\times\delta_{iBB}\times\left(T_i-T_n\right)\right\}-\left\{\nu_{eBi}\times\delta_{eBi}\times\left(T_e-T_i\right)\right\}\right]$$

$$\nu_{iAA}=\nu_{iAA0}\left(\frac{n_A}{n_{A0}}\right)\left(\frac{m_AT_i+m_{iA}T_n}{\left(m_AT_{i0}+m_{iA}T_{n0}\right)}\right)^{\frac{1}{2}},\nu_{iAB}=\nu_{iAB0}\left(\frac{n_B}{n_{B0}}\right)\left(\frac{m_BT_i+m_{iA}T_n}{\left(m_BT_{i0}+m_{iA}T_{n0}\right)}\right)^{\frac{1}{2}}$$

$$\nu_{iBA}=\nu_{iBA0}\left(\frac{n_A}{n_{A0}}\right)\left(\frac{m_AT_i+m_{iB}T_n}{\left(m_AT_{i0}+m_{iB}T_{n0}\right)}\right)^{\frac{1}{2}},\nu_{iBB}=\nu_{iBB0}\left(\frac{n_B}{n_{B0}}\right)\left(\frac{m_BT_i+m_{iB}T_n}{\left(m_BT_{i0}+m_{iB}T_{n0}\right)}\right)^{\frac{1}{2}}$$

are the collision frequencies(in $\sec^{-1}$) of a j type of ion with j' ion of neutral atom[13], and

$$\nu_{iAA0}=\left(\frac{8}{3}\right)\left(2\pi k_B\right)^{\frac{1}{2}}(r_{iA}+r_A)^2\left(\frac{n_{A0}m_A}{\left(m_{iA}+m_A\right)}\right)\left[\left(\frac{T_{i0}}{m_{iA}}\right)+\left(\frac{T_{n0}}{m_A}\right)\right]^{\frac{1}{2}},$$

$$\nu_{iAB0}=\left(\frac{8}{3}\right)\left(2\pi k_B\right)^{\frac{1}{2}}(r_{iA}+r_B)^2\left(\frac{n_{B0}m_B}{\left(m_{iA}+m_B\right)}\right)\left[\left(\frac{T_{i0}}{m_{iA}}\right)+\left(\frac{T_{n0}}{m_B}\right)\right]^{\frac{1}{2}},$$

$$\nu_{iBA0}=\left(\frac{8}{3}\right)\left(2\pi k_B\right)^{\frac{1}{2}}(r_{iB}+r_A)^2\left(\frac{n_{A0}m_A}{\left(m_{iB}+m_A\right)}\right)\left[\left(\frac{T_{i0}}{m_{iB}}\right)+\left(\frac{T_{n0}}{m_A}\right)\right]^{\frac{1}{2}},$$

$$\nu_{iBB0}=\left(\frac{8}{3}\right)\left(2\pi k_B\right)^{\frac{1}{2}}(r_{iB}+r_B)^2\left(\frac{n_{B0}m_B}{\left(m_{iB}+m_B\right)}\right)\left[\left(\frac{T_{i0}}{m_{iB}}\right)+\left(\frac{T_{n0}}{m_B}\right)\right]^{\frac{1}{2}},$$

$$\delta_{iAA}=\left[\frac{2m_{iA}}{(m_A+m_{iA})}\right],\delta_{iBB}=\left[\frac{2m_{iB}}{(m_B+m_{iB})}\right],\delta_{iAB}=\left[\frac{2m_{iA}}{(m_B+m_{iA})}\right],\delta_{iBA}=\left[\frac{2m_{iB}}{(m_A+m_{iB})}\right]$$

are the fraction of the excess energy of a j type positively charged ion, lost in a collision with neutral j' kind of neutral atom and are dimensionless. where j and j' can be same (i.e., both carbon or both either hydrogen, argon, methane, or carbon tetra fluoride) or different

(i.e., one carbon and other either hydrogen, argon, methane, or carbon tetra fluoride).

The first term in Eq.(18) is the energy gained by ions per unit volume per unit time due to the ionization of neutral atoms , the second term is the energy gained per unit volume per unit time due to the elastic collision of ions with electrons. The third term is the energy loss per unit volume per unit time due to the sticking accretion of ions at the surface of the CNT. The last term is the energy lost per unit volume per unit time due to elastic collision with neutral species.

I. Energy balance equation for neutral atoms

$$\frac{d}{d\tau}\left[\frac{3}{2}\left(n_A+n_B\right)k_BT_n\right]=$$
$$\left[\left(\frac{3}{2}k_B\right)\left(\alpha_An_en_{iA}+\alpha_Bn_en_{iB}\right)\left(T_e+T_i\right)+\left(\alpha_An_en_{iA}I_{pA}+\alpha_Bn_en_{iB}I_{pB}\right)\right]+\left(\frac{3}{2}k_B\right)$$
$$\left[n_e\left(\nu_{eA}\delta_{eA}+\nu_{eB}\delta_{eB}\right)\left(T_e-T_n\right)+\left[\left(\nu_{iAA}\delta_{iAA}+\nu_{iAB}\delta_{iAB}\right)n_{iA}\left(T_i-T_n\right)\right.\right.$$
$$\left.\left.+\left(\nu_{iBA}\delta_{iBA}+\nu_{iBB}\delta_{iBB}\right)n_{iB}\left(T_i-T_n\right)\right]\right]+$$
$$\left(\frac{3}{2}k_B\right)n_{ct}\left(\left[\left(1-\gamma_{iA}\right)n_{iActs}+n_{iBcts}\right]T_{ct}+\left(\left[\left(1-\gamma_{iA}\right)n_{iActcys}+n_{iBctcys}\right]T_{ct}\right)\right)$$
$$-\left(\frac{3}{2}k_B\right)n_{ct}\left[n_{Acts}\left[\gamma_AT_n+\delta_{Act}\left(1-\gamma_A\right)\left(T_n-T_{ct}\right)\right]+n_{Bcts}\delta_{Bct}\left(T_n-T_{ct}\right)\right]$$
$$-\left(\frac{3}{2}k_B\right)n_{ct}\left[n_{Actcys}\left[\gamma_AT_n+\delta_{Act}\left(1-\gamma_A\right)\left(T_n-T_{ct}\right)\right]+n_{Bctcys}\delta_{Bct}\left(T_n-T_{ct}\right)\right]$$
$$-\left(\frac{3}{2}k_B\right)\left(\beta_An_A+\beta_Bn_B\right)T_n-E_{diss}, \qquad (19)$$

The LHS of Eq.(19) can be rewritten as

$$\frac{3}{2}\left(n_A+n_B\right)k_B\left(\frac{dT_n}{d\tau}\right)+\frac{3}{2}k_BT_n\left(\frac{d\left(n_A+n_B\right)}{d\tau}\right)$$

Substituting the value of $\frac{d\left(n_A+n_B\right)}{d\tau}$ from Eqs. (10) and (11) and multiplying by $\frac{3}{2}k_BT_n$ in Eq.(19) we get,

$$\frac{3}{2}\left(n_A+n_B\right)k_B\left(\frac{dT_n}{d\tau}\right)=$$
$$-\left(\frac{3}{2}k_B\right)T_n\left(\alpha_An_en_{iA}+\alpha_Bn_en_{iB}\right)+\left(\frac{3}{2}k_B\right)T_n\left(\beta_An_A+\beta_Bn_B\right)-\left(\frac{3}{2}k_B\right)T_nn_{ct}$$
$$\left[\left[\left(1-\gamma_{iA}\right)\left(n_{iActs}+n_{iActys}\right)\right]+\left(n_{iBcts}+n_{iBctcys}\right)\right]+\left(\frac{3}{2}k_B\right)n_{ct}\gamma_A\left(n_{Acts}+n_{Actcys}\right)$$
$$+\left[\left(\frac{3}{2}k_B\right)\left(\alpha_An_en_{iA}+\alpha_Bn_en_{iB}\right)\left(T_e+T_i\right)+\left(\alpha_An_en_{iA}I_{pA}+\alpha_Bn_en_{iB}I_{pB}\right)\right]+\left(\frac{3}{2}k_B\right)$$
$$\left[n_e\left(\nu_{eA}\delta_{eA}+\nu_{eB}\delta_{eB}\right)\left(T_e-T_n\right)+\left[\left(\nu_{iAA}\delta_{iAA}+\nu_{iAB}\delta_{iAB}\right)n_{iA}\left(T_i-T_n\right)\right.\right.$$
$$\left.\left.+\left(\nu_{iBA}\delta_{iBA}+\nu_{iBB}\delta_{iBB}\right)n_{iB}\left(T_i-T_n\right)\right]\right]+$$
$$\left(\frac{3}{2}k_B\right)n_{ct}\left(\left[\left(1-\gamma_{iA}\right)n_{iActs}+n_{iBcts}\right]T_{ct}+\left(\left[\left(1-\gamma_{iA}\right)n_{iActcys}+n_{iBctcys}\right]T_{ct}\right)\right)$$
$$-\left(\frac{3}{2}k_B\right)n_{ct}\left[n_{Acts}\left[\gamma_AT_n+\delta_{Act}\left(1-\gamma_A\right)\left(T_n-T_{ct}\right)\right]+n_{Bcts}\delta_{Bct}\left(T_n-T_{ct}\right)\right]$$
$$-\left(\frac{3}{2}k_B\right)n_{ct}\left[n_{Actcys}\left[\gamma_AT_n+\delta_{Act}\left(1-\gamma_A\right)\left(T_n-T_{ct}\right)\right]+n_{Bctcys}\delta_{Bct}\left(T_n-T_{ct}\right)\right]$$
$$-\left(\frac{3}{2}k_B\right)\left(\beta_An_A+\beta_Bn_B\right)T_n-E_{diss}, \tag{20}$$

On rearranging the above equation, we get

$$\frac{3}{2}\left(n_A+n_B\right)k_B\left(\frac{dT_n}{d\tau}\right)=$$
$$\left[\left\{\left(\frac{3}{2}k_B\right)\left(\alpha_A n_e n_{iA}+\alpha_B n_e n_{iB}\right)\left(T_e+T_i-T_n\right)\right\}+\left(\alpha_A n_e n_{iA} I_{pA}+\alpha_B n_e n_{iB} I_{pB}\right)\right]$$
$$+\left\{\left[\left(\frac{3}{2}k_B\right)n_e\left(\nu_{eA}\delta_{eA}+\nu_{eB}\delta_{eB}\right)\left(T_e-T_n\right)\right]+\left[\left(\frac{3}{2}k_B\right)\left(\nu_{iAA}\delta_{iAA}n_{iA}+\nu_{iAB}\delta_{iAB}n_{iA}\right)\left(T_i-T_n\right)+\right.\right.$$
$$\left.\left.\left(\frac{3}{2}k_B\right)\left(\nu_{iBA}\delta_{iBA}n_{iB}+\nu_{iBB}\delta_{iBB}n_{iB}\right)\left(T_i-T_n\right)\right]\right\}+\left\{\left(\left(\frac{3}{2}k_B\right)n_{ct}\left[\left(1-\gamma_{iA}\right)n_{iActs}+n_{iBcts}\right]\left(T_{ct}-T_n\right)\right)\right.$$
$$\left.+\left(\left(\frac{3}{2}k_B\right)n_{ct}\left[\left(1-\gamma_{iA}\right)n_{iActcys}+n_{iBctcys}\right]\left(T_{ct}-T_n\right)\right)\right\}-\left\{\left(\left(\frac{3}{2}k_B\right)\left[n_{Acts}\delta_{Act}\left(1-\gamma_A\right)\times\left(T_n-T_{ct}\right)\right.\right.\right.$$
$$\left.\left.\left.+n_{Bcts}\delta_{Bct}\left(T_n-T_{ct}\right)\right]\right)+\left\{\left(\left(\frac{3}{2}k_B\right)n_{ct}\left[n_{Actcys}\delta_{Act}\left(1-\gamma_A\right)\times\left(T_n-T_{ct}\right)\ +n_{Bctcys}\delta_{Bct}\left(T_n-T_{ct}\right)\right]\right)\right\}\right\}$$
$$-E_{diss}. \qquad (21)$$

where

I_{pA} and I_{pB} are the ionization energy (in eV) of the constituent atomic species of type A (carbon) and type B(either hydrogen, argon, methane, or carbon tetra fluoride),respectively,

$E_{diss}=\left(E_{A,diss}+E_{B,diss}\right)$, $E_{j,diss}$ is the energy dissipated per unit volume per unit time by neutral atoms into the surrounding atmosphere and is assumed to be equal to the difference between the temperature of the neutral atomic species and the ambient temperature.

$E_{j,diss}=E_{j,diss0}\left[\frac{\left(T_j-T_a\right)}{\left(T_{j0}-T_a\right)}\right]$ (in eV) , constant $E_{j,diss0}$ is obtained by imposing the ambient condition of the complex plasma system in Eq.(21) for both constituent neutral species[13] ,T_a is the ambient temperature.

$\delta_{Act} = \left[\frac{2m_A}{\left(m_A + m_{ct}\right)}\right]$ and $\delta_{Bct} = \left[\frac{2m_B}{\left(m_B + m_{ct}\right)}\right]$ are the fraction of excess energy of a neutral A(carbon) and B(either hydrogen, argon, methane, or carbon tetra fluoride), respectively lost in a collision with CNT [13] and are dimensionless.

The first term in Eq.(21) is the power gained per unit volume by the neutral species due to recombination of electrons and positively charged ions, the second term is the rate of power gained per unit volume by neutral atoms in elastic collision with electrons and positively charged ions. The third term is the energy gained per unit volume per second due to formation of neutrals at the surface of the CNT due to electron and ion accretion. The fourth term refers to the thermal energy lost per unit volume per unit time by neutral atoms due to their accretion on and collision with CNT surface. The last term is the energy dissipation rate per unit volume by neutral atoms to the surrounding atmosphere.

J. Energy balance for spherical CNT tip placed over cylindrical surfaces

$$\frac{d}{d\tau}\left(m_{ct}C_pT_{ct}\right)=\left\{\left(n_{ects}\left[\gamma_e\varepsilon^s{}_{ecs}+\left(1-\gamma_e\right)\delta_{ect}\left[\varepsilon^s{}_{ecs}-\left(\frac{3}{2}k_B\right)T_{ct}\right]\right]\right)+\left(n_{ectcy}\left[\gamma_e\varepsilon^s{}_{eccy}\right.\right.\right.$$

$$\left.\left.\left.+\left(1-\gamma_e\right)\delta_{ect}\left[\varepsilon^s{}_{eccy}-\left(\frac{3}{2}k_B\right)T_{ct}\right]\right]\right)\right\}-\left\{\left[\left(\frac{3}{2}k_B\right)\left(\left[n_{Acts}\left[\gamma_AT_n+\delta_{Act}\left(1-\gamma_A\right)\times\left(T_n-T_{ct}\right)\right]\right.\right.\right.$$

$$\left.\left.\left.+n_{Bcts}\delta_{Bct}\left(T_n-T_{ct}\right)\right)\right]+\left[\left(\frac{3}{2}k_B\right)\left(\left[n_{Actcys}\left[\gamma_AT_n+\delta_{Act}\left(1-\gamma_A\right)\times\left(T_n-T_{ct}\right)\right]\right.\right.\right.$$

$$\left.\left.\left.+n_{Bctcys}\delta_{Bct}\left(T_n-T_{ct}\right)\right)\right]\right]\right\}+\left\{\left(\left[n_{iActs}\left(\varepsilon^s{}_{iAcs}+I_{pA}\right)+n_{iBcts}\left(\varepsilon^s{}_{iBcs}+I_{pB}\right)\right]+\right.\right.$$

$$\left.\left.\left[n_{iActcys}\left(\varepsilon^s{}_{iAccys}+I_{pA}\right)+n_{iBctcys}\left(\varepsilon^s{}_{iBccys}+I_{pB}\right)\right]\right)\right\}-$$

$$\left\{\left(\left(\frac{3}{2}k_B\right)\left[\left(\left(1-\gamma_{iA}\right)n_{iActs}+n_{iBcts}\right)+\left(\left(1-\gamma_{iA}\right)n_{iActcys}+n_{iBctcys}\right)\right]T_{ct}\right)\right\}$$

$$-\left\{\left(4\pi r^2+2\pi rl\right)\left[\varepsilon\sigma\left(T_{ct}{}^4-T_a{}^4\right)+\left[n_A\left(\frac{8k_BT_n}{\pi m_A}\right)^{\frac{1}{2}}+n_B\left(\frac{8k_BT_n}{\pi m_B}\right)^{\frac{1}{2}}\right]k_B\left(T_{ct}-T_n\right)\right]\right\}. \tag{22}$$

$\varepsilon^l_{iAcs}(Z)=\left[\frac{2-Z\alpha_{Ai}}{1-Z\alpha_{Ai}}\right]k_BT_i$ and $\varepsilon^l_{iBcs}(Z)=\left[\frac{2-Z\alpha_{Bi}}{1-Z\alpha_{Bi}}\right]k_BT_i$ are the mean energy (in eV) of positively charged ions, A(carbon) and B(either hydrogen, argon, methane, or carbon tetra fluoride),respectively (at large distance from the surface of the CNT) collected by the spherical CNT tip [13] .

$$\varepsilon^l_{iAccys}(Z)=k_BT_in_{iA}rl\left(\frac{2\pi k_BT_i}{m_{iA}}\right)^{\frac{1}{2}}\left[\left(\frac{4}{\sqrt{\pi}}\right)\left(\frac{eV_s}{k_BT_i}\right)^{\frac{1}{2}}+\left(2-\left(\frac{eV_s}{k_BT_i}\right)^{\frac{1}{2}}\right)\exp\left[\frac{eV_s}{k_BT_i}\right]erfc\left[\left(\frac{eV_s}{k_BT_i}\right)^{\frac{1}{2}}\right]\right]$$

$$\varepsilon^l_{iBccys}(Z)=k_BT_in_{iB}rl\left(\frac{2\pi k_BT_i}{m_{iB}}\right)^{\frac{1}{2}}\left[\left(\frac{4}{\sqrt{\pi}}\right)\left(\frac{eV_s}{k_BT_i}\right)^{\frac{1}{2}}+\left(2-\left(\frac{eV_s}{k_BT_i}\right)^{\frac{1}{2}}\right)\exp\left[\frac{eV_s}{k_BT_i}\right]erfc\left[\left(\frac{eV_s}{k_BT_i}\right)^{\frac{1}{2}}\right]\right]$$

are the mean energy of ions(in eV) at a large distance from the surface of cylindrical CNT surface[14] of A (carbon) and B (either hydrogen, argon, methane, or carbon tetra fluoride), respectively.

C_p is the specific heat of the material of the CNT at constant pressure (in ergs/gm K),

$\in$ is the emissivity of the material of the CNT and is dimensionless,

σ is the Stefan –Boltzmann constant= 5.672×10^{-5} erg sec^{-1} cm^{-2} K^{-4}.

The first three terms in Eq. (22) are the rate of energy transferred to the CNT tip due to sticking accretion and elastic collision by constituent species of complex plasma. The fourth term is the energy carried away by the neutral species (generated by the recombination of the accreted ions and electrons) from the spherical CNT tip per unit volume per unit time. The last term is the rate of energy dissipation of the spherical CNT tip through radiation and conduction to the host gas [15].

K. Field enhancement factor

Using the expression for field enhancement factor β as obtained by Wang *et al.* [16]

$$\beta = \frac{h}{\rho} + 3.5 \tag{23}$$

where,

h = the height of CNT and ρ = the radius of CNT.

5.4: Results and Discussion

Our main interest in the present chapter is to observe the effect of different plasmas, especially of heavy ion plasma such as carbon tetraflouride (CF_4) and methane (CH_4), light ion plasma such as hydrogen (H_2) and of neutral plasmas such as argon (Ar), on the growth of the CNT. Since in the present model it is assumed that the accretion of neutral atoms and positively charged ions on the CNT causes its growth;

the different plasmas being investigated for growth presently will cause changes in the morphology of the CNT.

We have solved Eq. (4) to calculate the initial radius of CNT by feeding the parameters corresponding to various plasmas and then equations for charging of the CNT, kinetics and energy balance of electrons, ions, neutrals and of the spherical CNT tip placed over cylindrical CNT surface are simultaneously solved for different plasmas considered, by using MATHEMATICA software with appropriate boundary conditions.

(1) For H_2 plasma, boundary conditions $\tau = 0$,

CNT number density (n_{ct}) =10^6 cm^{-3}, ion number density of type A (n_{iA0}=$0.8\,n_{e0}$), ion number density of type B ($n_{iB0} = 0.2 n_{e0}$), neutral atom number density of type A and B $\left(n_{A0} = n_{B0}\right) = 1\times10^{14}$ cm^{-3} ,electron number density $\left(n_{e0}\right) = 10^6$ cm^{-3}, electron temperature T_{e0}=0.5eV, ion temperature (T_{i0}) = 2000 K , neutral temperature (T_{n0}) = CNT temperature $\left(T_{ct}\right)$=1950K, mass of ion A $\left(m_{iA}\right) \approx$ mass of neutral atom A $\left(m_A\right)$ = 12 amu (carbon) ,mass of ion B $\left(m_{iB}\right) \approx$ mass of neutral atom B $\left(m_B\right)$ =2 amu (hydrogen (H_2)), coefficient of recombination of electrons and positive ion of type A and B $\left(\alpha_{A0} \approx \alpha_{B0}\right)$ =10^{-7}cm^3/sec, emissivity of material of CNT (ε)=0.6 , the sticking coefficient of ion A and neutral atom A $\left(\gamma_{iA} = \gamma_A\right)$=1, specific heat of CNT $\left(C_p\right) = 7\times10^6$ ergs/gm K, the ionization energy of neutral atom A $\left(I_{pA}\right) = 5.26$ eV, the ionization energy of neutral atom B $\left(I_{pB}\right) = 7$ eV ,

ε_A=4.69 eV, ε_B=6.7 eV, the mean energy of positively charged ions produced by the ionization of neutral atom A(ε_{iA})=4.78 eV, the mean energy of positively charged ions produced by the ionization of neutral atom B (ε_{iB})= 7.03 eV, the dissipation energy of neutral atom A ($\varepsilon_{A,diss0}$) =1820.9eV, the dissipation energy of neutral atom B($\varepsilon_{B,diss0}$) =799.6 eV, constant(κ)= -1.2, initial radius (r_0) = 1.80 nm, and density of the CNT (ρ_{ct})= 4.2g/cm^3.

(2) For CH_4 plasma, using values from Herrebout *et al*. [17] , boundary conditions $\tau = 0$, n_{ct}=10^6 cm^{-3} , n_{iA0}=$0.6n_{e0}$, $n_{iB0} = 0.4n_{e0}$ n_{A0}= n_{B0}=1x10^{15} cm^{-3}, n_{e0}= 1.12x10^{10} cm^{-3},T_{e0}= 1.15 eV, $T_{i0} = 2100\,\mathrm{K}$, $T_{n0} = T_{ct} = 2000\,\mathrm{K}$, $m_{iA} \approx m_A$=12 amu (carbon), $m_{iB} \approx m_B$=16 amu (methane (CH_4)), $\alpha_{A0} \approx \alpha_{B0}$=1.12x10^{-7}cm^3/sec, ε =0.6 , γ_{iA}=γ_A=1, ϕ=5 eV (Carbon), $C_p = 7\times10^6$ ergs/gm K, $I_{pA} = 8.16$ eV, $I_{pB} = 9.43$ eV , ε_A=9.59 eV, ε_B=6.79 eV, ε_{iA}=5.15 eV, ε_{iB}= 9.50 eV ,$\varepsilon_{A,diss0}$ =1964.1 eV, $\varepsilon_{B,diss0}$=608.5eV,κ=-1.2, r_0= 1.66 nm, and ρ_{ct}= 4.2g/cm^3.

(3) For Ar plasma, using values of plasma parameters from Chai *et al*. [18] , boundary conditions $\tau = 0$,
n_{ct}=10^6 cm^{-3}, n_{iA0}=$0.6n_{e0}$, $n_{iB0} = 0.4n_{e0}$,n_{A0}= n_{B0}=1.03x10^{15} cm^{-3}, n_{e0}=1.2x10^9 cm^{-3},T_{e0}= 1.3 eV, T_{i0}=2200 K, $T_{n0} = T_{ct} = 2000\,\mathrm{K}$, $m_{iA} \approx m_A$ =12amu(carbon), $m_{iB} \approx m_B$=40amu(argon(Ar)), $\alpha_{A0} \approx \alpha_{B0}$ 1.02x10^{-7}cm^3/sec, ε =0.6 , γ_{iA}=γ_A=1, $C_p = 7\times10^6$ ergs/gm K, I_{pA} =

9.56 eV, I_{pB} = 10.97 eV , ε_A=13.58 eV, ε_B=8.62 eV, ε_{iA}=7.51 eV, ε_{iB}= 9.24 eV , $\varepsilon_{A,diss0}$=2055.61 eV, $\varepsilon_{B,diss0}$=416.5 eV, κ = -1.2, r_0= 1.62 nm, and ρ_{ct} = 4.2g/cm^3.

(4) For CF_4 plasma, using values of plasma parameters from Kim *et al.* [19] boundary conditions $\tau = 0$,

n_{ct} =10^6 cm^{-3} , n_{iA0}=0.6 n_{e0}, $n_{iB0} = 0.4 n_{e0}$, $n_{A0} = n_{B0} = 5\times10^{11}$ cm^{-3} ,n_{e0}=3.5x10^{10} cm^{-3}, T_{e0}=1.5 eV, $T_{i0} = 2400$ K, $T_{n0} = T_{ct} = 2000$ K. $m_{iA} \approx m_A$=12 amu (carbon), $m_{iB} \approx m_B$=84 amu (carbon tetra fluoride (CF_4)) , $\alpha_{A0} \approx \alpha_{B0}$=3.5x 10^{-7}cm^3/sec, ε =0.6 , γ_{iA}=γ_A=1, $C_p = 7\times10^6$ ergs/gm K, I_{pA} = 10.26 eV, I_{pB} = 12.3 eV , ε_A= 675.71 eV, ε_B=119.5 eV, ε_{iA}=542.15 eV, ε_{iB}= 359.35eV , $\varepsilon_{A,diss0}$ = 2251.7 eV, $\varepsilon_{B,diss0}$ =214.11 eV, κ = -1.2, r_0= 4.80nm, and ρ_{ct} = 4.2g/cm^3

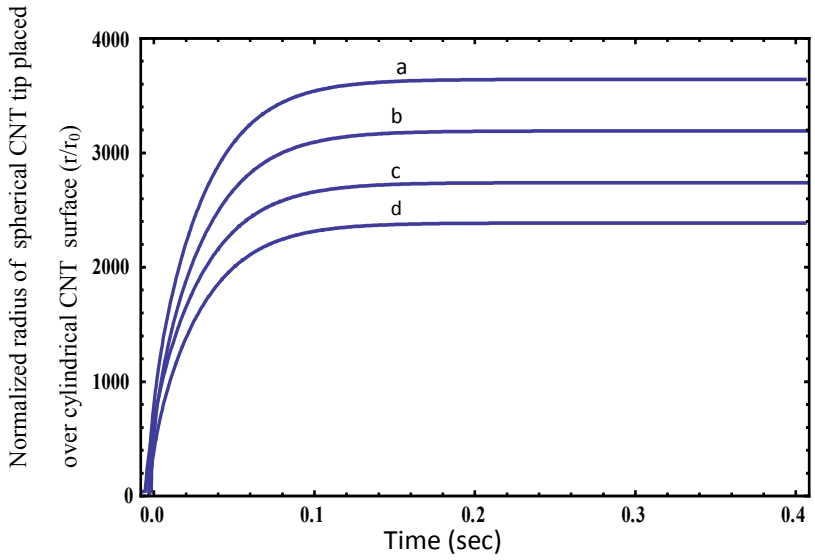

Fig.2. Shows the variation of the normalized radius (r/r_0) with time of spherical CNT tip placed over cylindrical CNT surface for different plasmas, where a, b, c and d corresponds to CF_4, Ar, CH_4 and H_2 plasmas, respectively.

Fig. 2 illustrates the variation of normalized radius of the spherical CNT tip placed over the cylindrical CNT surface (r/r_0) with time for different plasma parameters taken for respective plasmas considered. It can be seen from Fig. 2 that the radius of spherical CNT tip placed over cylindrical CNT surface decreases as (r/r_0 for CF_4)> (r/r_0 for Ar)>(r/r_0 for CH_4)> (r/r_0 for H_2). The radius for all plasma first increases and then attains a saturation value. The main parameters that determine the growth pattern going into plateau region are the values of sticking coefficients of neutral atoms and ions of type A, and the charge developed on the CNT. As the value of sticking coefficients of neutral atoms and ions increases, the steady state is achieved faster. Also, as more and more neutral atoms and positively charged ions stick on the CNT surface, the negative charge on the CNT decreases, which further stops the accretion of ions and

neutral atoms on the surface of CNT and CNT radius saturates. Nagai *et al.* [20], Hayashi *et al.* [21] and Courteille *et al.* [22] have reported a similar kind of growth pattern of CNT and nanoparticles in plasma.

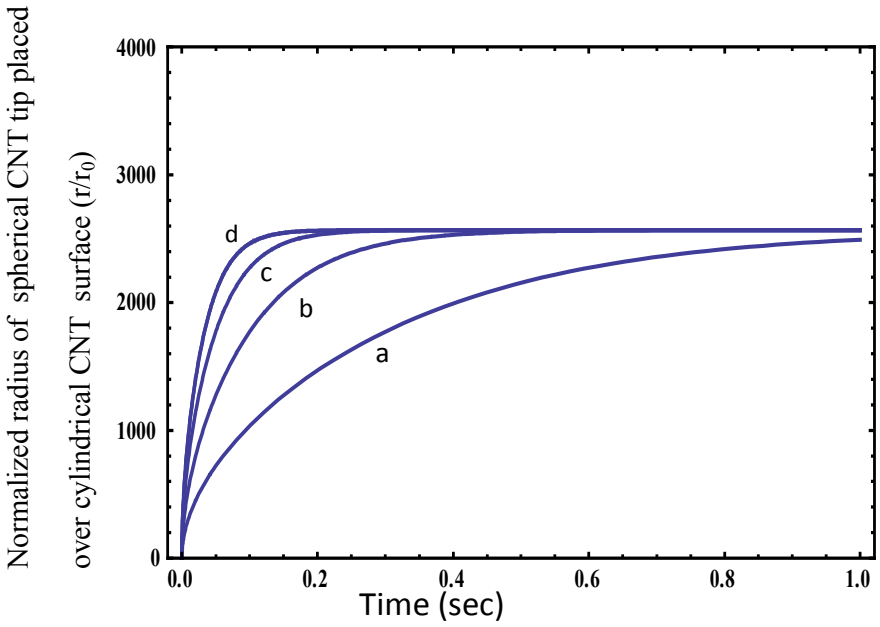

Fig.3. Shows the variation of the normalized radius (r/r_0) with time for spherical CNT tip placed over cylindrical CNT surface for H_2 plasma for different values of the atomic sticking coefficients, where a, b, c and d corresponds to γ_A = 0.1,0.3, 0.6 and 0.9, respectively.

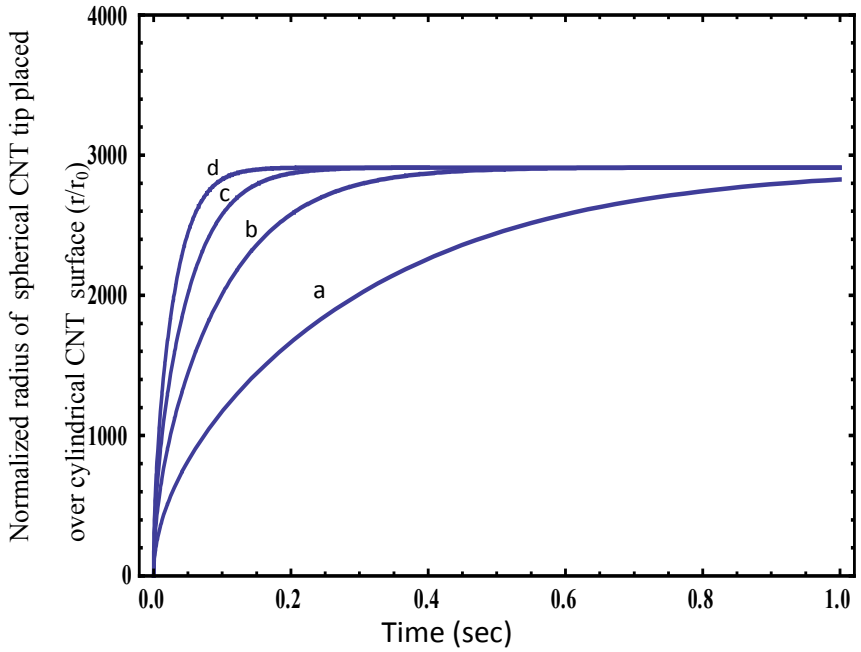

Fig.4. Shows the variation of the normalized radius (r/r_0) with time for spherical CNT tip placed over cylindrical CNT surface for CH_4 plasma for different values of the atomic sticking coefficients, where a, b, c and d corresponds to γ_A = 0.1,0.3, 0.6 and 0.9,respectively.

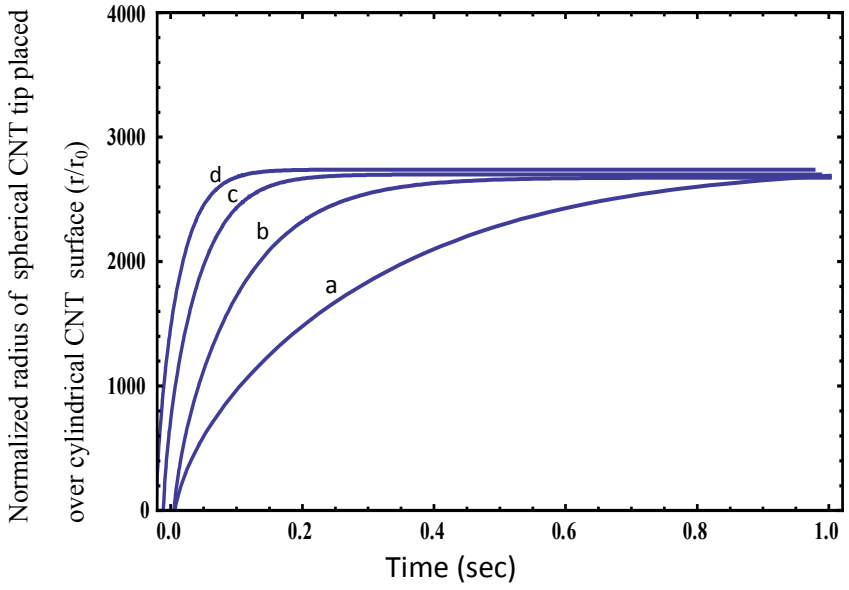

Fig. 5. Shows the variation of the normalized radius (r/r_0) with time for spherical CNT tip placed over cylindrical CNT surface for Ar plasma for different values of the atomic sticking coefficients, where a, b, c and d corresponds to γ_A = 0.1,0.3, 0.6 and 0.9, respectively.

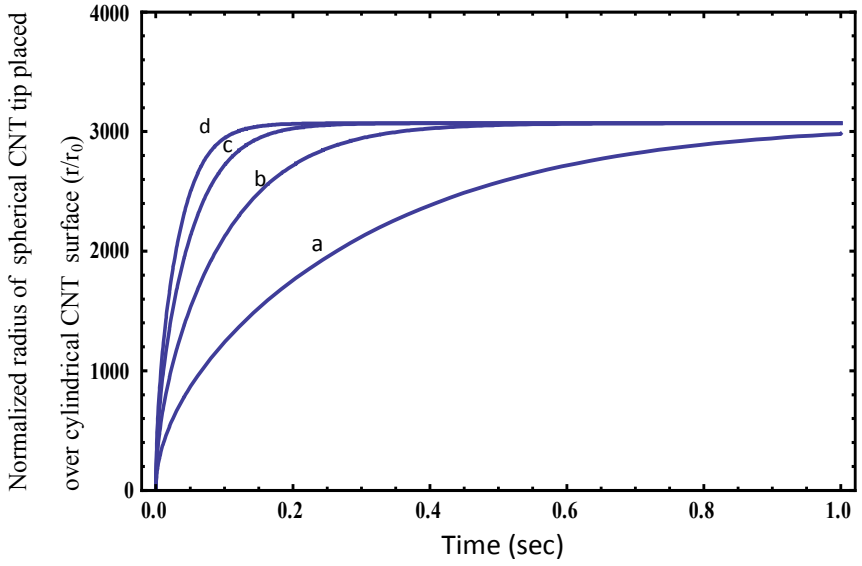

Fig. 6. Shows the variation of the normalized radius (r/r_0) with time for spherical CNT tip placed over cylindrical CNT surface for CF_4 plasma for different values of the atomic sticking coefficients, where a, b, c and d corresponds to γ_A = 0.1,0.3, 0.6 and 0.9, respectively.

Fig. 3 to 6 illustrates the variation of normalized radius with the time of the spherical CNT tip placed over cylindrical CNT surface in H_2 , CH_4 , Ar and CF_4 plasmas for different values of the atomic sticking coefficients γ_A = 0.1,0.3, 0.6 and 0.9. It can be seen that the steady state is achieved faster as the value of atomic sticking coefficients is increased but the effect is more pronounced in CF_4 (cf. Fig. 6) which is valid because the nanotube of maximum radius grows in CF_4 plasma.

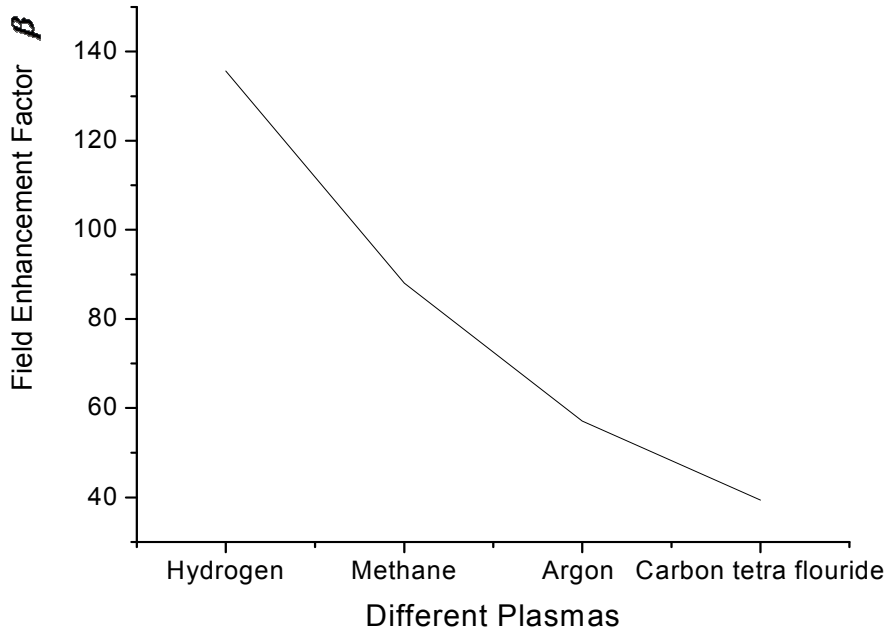

Fig. 7. Shows the field enhancement factor β for different plasmas i.e., for CF_4, Ar, CH_4 and H_2.

Using Eq. (23), we have plotted in Fig. 7 the variation in the field enhancement factor for CNTs grown in all four different types of plasmas. We calculate the radius of the CNT in all different types of plasmas as 113.5 nm in H_2, 220nm in CH_4, 280nm in Ar and 360nm in CF_4 , height of the CNT was fixed at 15 μm, the field enhancement factor are obtained as 135.658 in H_2, 71.6 in CH_4 , 57.07 in Ar, 45.166 in CF_4 . From the Fig. 7 it can be concluded that the field emission is maximum for H_2 plasma, followed by CH_4, then Ar and minimum for CF_4. The variation of field enhancement factor with radius is also validated by Xu *et al.* [23].

The possible physical explanation for the above observed behaviour may be that the plasma causes etching of the CNTs and thereby reduces the radius of the CNT. Since for the H_2 plasma, the radius of the CNT is least,

means that H_2 plasma causes maximum etching, and thereby opening up more field emission sites of the CNT tip as well as cylindrical surfaces and causing maximum field emissions from the CNT grown in H_2 plasma. The above result obtained has also been experimentally verified by Zhu *et al.* [8] and Lee *et al.* [12].

Zhu *et al.* [8] have also stated that CF_4 plasma treatment may hamper the field emission from CNT films. Also Lee *et al.* [12] have reported that the field emission current density is maximum for the H_2 plasma followed by Ar plasma , the CF_4 plasma treated CNTs films and is least for the untreated CNT (cf. Fig. 5 of Lee *et al*. [12]). Hence, our theoretical results comply with the experimental observations.

References

[1] W.H. Yau and C.H. Tsai, Surf. Interface Anal. **44**,535 (2012).

[2] Y. Abdi, E. Arzi and S. Mohajerzadeh, NanoMat. & Nanotech**. 44**, 149(2008).

[3] H. C. Wen, K. Yang , K.-L. Ou, W.-F. Wu , C. P. Chou, , R. C. Luo, and Y. M. Chang, Surf. Coatings Tech. **200**, 166(2006).

[4] A. Felten, C. Bittencourt, J. J. Pireaux , G.Van Lier, and J. C Charlier , J. Appl. Phys. **98**, 074308(2005).

[5] Ho Lee, Youn-Seon Kang, Paul S Lee and Jai-Young Lee , J. Alloys Comp. **330**, 569(2002).

[6] C. Y. Zhi, X.D. Bai and E. G. Wang, Appl. Phys. Lett. **81**, 1690 (2002).

[7]S. K. Srivastava, V. D. Vankar, V. Kumar, Nano-Micro Lett.**2**, 46 (2010).

[8] Y.W. Zhu, F.C. Cheong, T. Yu, X.J. Xu, C.T. Lim, J.T.L. Thong, Z.X. Shen, C.K. Ong, Y.J. Liu, A.T.S. Wee, C.H. Sow, Carbon **43**, 395(2005).

[9] K. S Ahn, J. S Kim, C. O.Kim, J. P. Hong, Carbon **41,** 2481(2003).

[10] Jaehyeong Lee, Donggun Lim, Wonseok Choi, and S. Dimitrijev , J. Nanosc. Nanotech.**12**,1507(2012).

[11] T. Feng, J. Zhang , Q. Li, Physica E. **36**, 28(2007).

[12] S. F. Lee, Yung-Ping Chang and Li-Ying Lee , J. Mater. Sci. Mater. Electron **20**, 851(2009).

[13] M.S. Sodha , Shikha Misra, S. K. Mishra, and S. Srivastava, J. Appl. Phys.**107**,103307(2010).

[14] M. S. Sodha, S. K. Mishra and S. Misra, Phys. Plasmas **17** ,113705

(2010).

[15] M. Rosenberg, D. A. Mendis, and D. P. Sheehan, IEEE Trans. Plasma Sci. **27**, 239(1999).

[16] X.Q Wang, M. Wang, P.M. He and Y.B. Xu, J. Appl. Phys **96**, 6752 (2004).

[17] D. Herrebout, A. Bogaerts, M. Yan ,and R. Gijbels, J. Appl. Phys. **90**,570(2001).

[18] K. B. Chai, C. R. Seon, C. W. Chung, N. S. Yoon and W. Choe, J. Appl. Phys. **109** ,013312(2011).

[19] J. H. Kim, K.-H. Chung, and Y.- S. Yoo,, J. Korean Phys. Soc. **47** ,249 (2005).

[20]T. Nagai, Z. Feng, A. Kono and F. Shoji, Phys. Plasmas **15**, 050702 (2008).

[21] Y. Hayashi and K. Tachibana , Jpn. J. Appl. Phys. **33**,476(1994).

[22]C. Courteille, C. Hollenstein , J. L. Dorier, P. Gay, W Schwarzenbach, A. A Howling, E. Bertran , G. Viera, R. Martins, and A. Macarico, J. Appl. Phys. **80**, 2069(1996).

[23] Zhi Xu, X. D. Bai and E. G. Wang, Appl. Phys. Lett. **88**,133107 (2006).

CHAPTER 6

INVESTIGATIONS ON THE EFFECT OF DIFFERENT PLASMA COMPOSITIONS ON GROWTH OF SPHERICAL CARBON NANOTUBE (CNT) TIP AND ESTIMATING FIELD EMISSION FROM THEM

6.1: A brief outline of the work in the chapter

The present chapter details the growth of CNT under different plasma compositions and predicting their field emission properties from the results obtained.

6.2: Introduction

The role of plasma compositions is set up to be an important parameter in growth of CNT and other nanostructure over the years.

Srivastava *et al*. [1] have studied the effect of plasma composition on the growth and microstructure of CNTs. The morphology and microstructure of nanotubes were found to be strongly dependent on plasma compositions and different shapes of CNTs were observed for different plasma compositions.

Han *et al.* [2] have studied the effect of growth parameters such as composition of reactant gases on growth of carbon nanotubes (CNTs) and proposed that the growth of CNTs is dependent on the total flow rate, but the diameter of CNTs is mainly determined by the ratio of ammonia (NH_3) to acetylene (C_2H_2) and plasma intensity rather than the total flow rate.

Bell *et al.* [3] have studied the effect of plasma composition during plasma-enhanced chemical vapor deposition (PECVD) of CNTs and observed that different plasma compositions of C_2H_2/NH_3 produces different shapes of CNT.

Teo *et al.* [4] have reported that varied C_2H_2/NH_3 ratio , morphology of the unpatterned silicon (Si) area clearly changes from being etched at a low C_2H_2/NH_3 ratio to being covered by a thick, delaminating amorphous carbon film for high C_2H_2/NH_3 ratios.

Kiang *et al.* [5] have shown that the nanotube diameter distributions are modified by the addition of the heavy metals such as bismuth(Bi) ,lead (Pb). They further suggest that a more efficient synthesis of tubules with a wider range of diameters will facilitate investigations of nanotube properties and applications that depend on the diameter, such as electric conductivity and hydrogen storage media.

Chen *et al.* [6] have grown CNT in methane (CH_4)/ carbon-dioxide (CO_2) gas mixture and found that the compositions of plasma significantly affect the reaction mechanism in CNTs growth and the highest yield of CNT was obtained at 70% ratio of CH_4/CO_2 .

Xiong *et al.* [7] studied growth of double walled CNT (DWCNT) under different combinations of methane(CH_4) to hydrogen(H_2) (i.e., at 300/0, 300/6, and 300/12) and found that concentration of hydrogen affects DWCNT growth and optimum growth was recorded for CH_4/H_2 ratio of 300/6.

6.3: MODEL

In view of the cited literature in the present chapter, we consider CNT growth in plasma containing electrons, positively charged ions of type A (carbon) and B (cesium), neutral atoms of type A (carbon) and B

(cesium). The two ions have considerable differences in their masses such that we consider ion A to be a light and ion B to be a heavy ion. The ratio of heavy to light ion masses is 11.5. The number density of both light and heavy ions is related to positive ion density (n_{p0}) as number density of light positive ion A (carbon) $n_{ilA} = \alpha_l n_{p0}$, number density of heavy positive ion B (cesium) $n_{ihB} = \alpha_h n_{p0}$, α_l and α_h are the fractional concentrations of light and heavy positive ions, respectively where $\alpha_h = 1 - \alpha_l$.

The initial radius of spherical CNT tip can be estimated by equating the accretion of electrons and positively charged ions on the CNT tip , i.e., electron collection current on the CNT(n_{ect}) is equal to total ion collection at CNT (n_{ilAct}+n_{ihBct})

$$n_{ect} = n_{ilAct} + n_{ihBct} \quad , \qquad (1)$$

where

$n_{ect} = \pi a^2 \left(\frac{8k_B T_e}{\pi m_e} \right)^{\frac{1}{2}} n_e \exp\left[\frac{Ze^2}{ak_B T_e} \right]$ is the electron collection current at the surface of spherical CNT tip (in sec^{-1}) [8] ,

$n_{ilAct} = \pi a^2 \left(\frac{8k_B T_i}{\pi m_{ilA}} \right)^{\frac{1}{2}} n_{ilA} \left[1 - \frac{Ze^2}{ak_B T_i} \right]$ is the light ion collection current on a spherical CNT tip (in sec^{-1}) [8] ,

$n_{ihBct} = \pi a^2 \left(\frac{8k_B T_i}{\pi m_{ihB}} \right)^{\frac{1}{2}} n_{ihB} \left[1 - \frac{Ze^2}{ak_B T_i} \right]$ is the heavy ion collection current on a spherical CNT tip (in sec^{-1}) [8] ,

Substituting the values of n_{ect} ,n_{ilAct} (for carbon) and n_{ihBct} (for cesium) in Eq.(1) we get,

$$\pi a^2\left(\frac{8k_BT_e}{\pi m_e}\right)^{\frac{1}{2}} n_e \exp\left[\frac{Ze^2}{ak_BT_e}\right] = \pi a^2\left(\frac{8k_BT_i}{\pi m_{ilA}}\right)^{\frac{1}{2}} n_{ilA}\left[1-\frac{Ze^2}{ak_BT_i}\right] + \pi a^2\left(\frac{8k_BT_i}{\pi m_{ihB}}\right)^{\frac{1}{2}} n_{ihB}\left[1-\frac{Ze^2}{ak_BT_i}\right], \tag{2}$$

or

$$\left(\frac{8k_BT_e}{\pi m_e}\right)^{\frac{1}{2}} n_e \exp\left[\frac{Ze^2}{ak_BT_e}\right] = \left(\frac{8k_BT_i}{\pi m_{ilA}}\right)^{\frac{1}{2}} n_{ilA}\left[1-\frac{Ze^2}{ak_BT_i}\right] + \left(\frac{8k_BT_i}{\pi m_{ihB}}\right)^{\frac{1}{2}} n_{ihB}\left[1-\frac{Ze^2}{ak_BT_i}\right], \tag{3}$$

or

For Z = -1, i.e., we assume that initially at τ=0 the CNT is negatively charged, and initial radius of CNT tip is a_0,

$$\left(\frac{T_e}{m_e}\right)^{\frac{1}{2}} n_e \exp\left[-\frac{e^2}{a_0k_BT_e}\right] = \left(\frac{T_i}{m_{ilA}}\right)^{\frac{1}{2}} n_{ilA}\left[1+\frac{e^2}{a_0k_BT_i}\right] + \left(\frac{T_i}{m_{ihB}}\right)^{\frac{1}{2}} n_{ihB}\left[1+\frac{e^2}{a_0k_BT_i}\right], \tag{4}$$

or

$$n_e\left(\frac{T_e}{m_e}\right)^{\frac{1}{2}} \exp\left(-\frac{e^2}{a_0k_BT_e}\right) = \left(1+\frac{e^2}{a_0k_BT_i}\right)\left[n_{ilA}\left(\frac{T_i}{m_{ilA}}\right)^{\frac{1}{2}} + n_{ihB}\left(\frac{T_i}{m_{ihB}}\right)^{\frac{1}{2}}\right], \tag{5}$$

where

$n_{e0} = n_{p0}$ = number density of electron (in cm^{-3}),

n_{p0} = plasma density (in cm^{-3}),

T_e = electron temperature(in eV),

a_0 = initial radius of spherical CNT tip (in nm),

k_B = Boltzmann's constant(in ergs/K),

T_i = ion temperature(in K),

$n_{ilA} = \alpha_l n_{p0}$ = number density of light positive ion A(in cm^{-3}),

m_{ilA} = mass of light positive ion A(in gm),

$n_{ihB} = \alpha_h n_{p0}$ = number density of heavy positive ion B(in cm^{-3}),

α_l and α_h are the fractional concentrations of light and heavy positive ions, respectively and $\alpha_h = 1 - \alpha_l$, both α_l and α_h are dimensionless,

m_{ihB} = mass of heavy positive ion B(in gms),

m_e=mass of electron(in gm),

e = electronic charge (in Stat C).

A. Charge neutrality equation

Eq. (6) equates the net negative and positive charge in the plasma on the spherical CNT tip to make plasma as electrically neutral.

$$Zn_{ct} + n_{ilA} + n_{ihB} = n_e, \qquad (6)$$

Z= amount of charge on spherical CNT tip (dimensionless) ,

n_{ct} = the number density of the CNT(in cm^{-3}).

B. Charging of the CNT

Eq. (7) describes the charge developed on the CNT due to accretion of electrons and positively charged ions on the surface of the CNT.

$$\frac{dZ}{d\tau} = n_{ilAct} + n_{ihBct} - \gamma_e n_{ect}, \tag{7}$$

where γ_e is the sticking coefficient of electrons on CNT surface and is dimensionless.

The first and second term in Eq.(7) denotes charge developed due to ion collection currents of type A(carbon) and B(cesium) on spherical CNT tip and third term denotes the denotes charge developed on spherical CNT tip because of electron collection current.

C. Growth rate equation of electron density

The growth rate equation of electron density considers ionization of neutrals into ions and electrons ,recombination of electrons and ions to form neutrals and the electron collection current to CNT tip.

$$\frac{dn_e}{d\tau} = \left(\beta_A n_{lA} + \beta_B n_{hB}\right) - \left(\alpha_A n_e n_{ilA} + \alpha_B n_e n_{ihB}\right) - \gamma_e n_{ct} n_{ect}, \tag{8}$$

where

β_A and β_B are the coefficients of ionization of the constituent neutral atoms of A(carbon) and B(cesium) due to external agency (in sec)[8], and

$\alpha_A(T_e) = \alpha_{A0}\left(\frac{300}{T_e}\right)^k cm^3/\sec$ and $\alpha_B(T_e) = \alpha_{B0}\left(\frac{300}{T_e}\right)^k cm^3/\sec$ are the coefficients of recombination of electrons and positively charged ions [8] , of A(carbon) and B(cesium),respectively where $k = -1.2$ is a constant

, $\alpha_{A0} = \alpha_{B0} = n_{e0} \times 10^{-7} \left(\frac{1}{T_{e0}} \right)^{-1.2}$ and n_{ct} is the CNT number density (in cm^{-3}).

The first term in Eq.(8) is the rate of gain in electron density per unit time due to ionization of neutral atoms and second term is the decrease in the electron density due to electron–ion recombination and the third term is the loss in electron density because of the electron collection current on the spherical CNT tip.

D. Growth rate equation of positively charged ion density

The number density balance equation of ions is developed considering processes such as ionization of neutrals to produce ions and electrons, electron and ion recombination to form neutrals, and ion collection current to CNT tip.

$$\frac{dn_{ilA}}{d\tau} = \beta_A n_{lA} - \alpha_A n_e n_{ilA} - n_{ct} n_{ilAct}, \quad (9)$$

$$\frac{dn_{ihB}}{d\tau} = \beta_B n_{hB} - \alpha_B n_e n_{ihB} - n_{ct} n_{ihBct}, \quad (10)$$

where

$$n_{ilAct} = \pi a^2 \left(\frac{8k_B T_i}{\pi m_{ilA}} \right)^{\frac{1}{2}} n_{ilA} \left[1 - \frac{Ze^2}{ak_B T_i} \right], n_{ihBct} = \pi a^2 \left(\frac{8k_B T_i}{\pi m_{ihB}} \right)^{\frac{1}{2}} n_{ihB} \left[1 - \frac{Ze^2}{ak_B T_i} \right]$$

are the ion collection currents at the surface of spherical CNT tip [8](in sec^{-1}), n_{lA} and n_{hB} are the neutral atom number densities (in cm^{-3})of A (carbon) and B(cesium),respectively..

The first term in Eqs. (9) and (10) is the gain in ion density per unit time on account of ionization of neutral atoms, the second term is the decrease

in ion density due to electron-ion recombination, and the third term denotes the loss in ion density due to ion collection current on spherical CNT tip.

E. Growth rate equation of neutral atoms

The processes such as recombination of electrons and ions, ionization of neutrals , accretion of neutrals and ions on the CNT surface are accounted in the balance equation of neutral atom density.

$$\frac{dn_{lA}}{d\tau} = \alpha_A n_e n_{ilA} - \beta_A n_{lA} + n_{ct}\left(1-\gamma_{ilA}\right) n_{ilAct} - n_{ct}\gamma_{lA} n_{lAct} \,, \qquad (11)$$

$$\frac{dn_{hB}}{d\tau} = \alpha_B n_e n_{ihB} - \beta_B n_{hB} + n_{ct} n_{ihBct} \quad , \qquad (12)$$

where

$$n_{lAct} = \pi a^2 \left(\frac{8k_B T_n}{\pi m_{lA}}\right)^{\frac{1}{2}} n_{lA}, \;\; n_{hBct} = \pi a^2 \left(\frac{8k_B T_n}{\pi m_{hB}}\right)^{\frac{1}{2}} n_{hB}$$

are the neutral collection currents at the surface of spherical CNT tip [8] (in sec^{-1}) for A(carbon) and B(cesium),respectively.

γ_{lA} is the sticking coefficient of carbon neutrals on spherical CNT tip and γ_{ilA} is the sticking coefficient of carbon ions on spherical CNT tip, both γ_{lA} and γ_{ilA} are dimensionless.

The first term in Eqs. (11) and (12) is the gain in neutral atom density per unit time due to electron–ion recombination, the second term is the decrease in neutral density due to their ionization, the third term is the gain in neutral density due to neutralization of the ions collected on spherical CNT tip. The last term in Eq. (11) is the accretion of neutral atoms of species A(carbon) on spherical CNT tip.

F. Growth rate equation of the mass of CNT

The accretion of ions and neutrals of carbon on the surface of CNT are the main growth processes considered in the present model.

$$\frac{dm_{ct}}{d\tau} = \left(m_{lA}\gamma_{lA} n_{lAct} + m_{ilA}\gamma_{ilA} n_{ilAct} \right), \tag{13}$$

where

$m_{ct} = \frac{4}{3}\pi a^3 \rho_{ct}$ is the mass of the CNT for a spherical CNT tip , a is the radius of spherical CNT tip , and ρ_{ct} is the density of spherical CNT tip,

The first and second term in Eq.(13) is the gain in the mass of the spherical CNT tip due to collection of atomic and ionic species of A (i.e., carbon), respectively.

G. Energy balance equation of electrons

$$\left(\frac{3}{2}k_B\right) n_e \left(\frac{dT_e}{d\tau}\right) = \left[\left(\beta_A n_{lA} \varepsilon_{lA} + \beta_B n_{hB} \varepsilon_{hB}\right) - \left(\frac{3}{2}k_B\right)\left(\beta_A n_{lA} + \beta_B n_{hB}\right) T_e \right] - n_{ct} n_{ect}$$
$$\left\{ \left[\gamma_e \varepsilon_{ecs}^{lh} - \left(\frac{3}{2}k_B\right) T_e \right] + \delta_{ect}(1-\gamma_e) \left[\varepsilon_{ecs}^{S} - \left(\frac{3}{2}k_B\right) T_{ct} \right] \right\}$$
$$- \left(\frac{3}{2}k_B\right) \left[\nu_{elA}\delta_{elA} + \nu_{ehB}\delta_{ehB} \right] (T_e - T_n) n_e - \left(\frac{3}{2}k_B\right) \left\{ \left(\nu_{elAi}\delta_{elAi} + \nu_{ehBi}\delta_{ehBi} \right) \left(T_e - T_i \right) \right\} n_e. \tag{14}$$

where

$\frac{3}{2} n_e k_B T_e$ is the thermal energy of electrons ,

n_e is the number density of electrons(in cm^{-3}), T_e is the electron temperature (in eV), T_{ct} is the CNT temperature (in K), and T_n is the neutral temperature (in K).

$\varepsilon_{ecs}^{lh}(Z) = \varepsilon_{ecs}^{s}(Z) - \left(\frac{Ze^2}{a}\right)$ is the mean energy of electrons (in eV) at a large distance from the surface of spherical CNT tip [8],

$\varepsilon_{ec}^{s}(Z) = 2k_B T_e$ is the mean energy of electrons (in eV) collected by spherical CNT tip [8],

$\nu_{elA} = \nu_{elA0}\left(\frac{n_{lA}}{n_{lA0}}\right)\left(\frac{T_e}{T_{e0}}\right)^{\frac{1}{2}}$ and $\nu_{ehB} = \nu_{ehB0}\left(\frac{n_{hB}}{n_{hB0}}\right)\left(\frac{T_e}{T_{e0}}\right)^{\frac{1}{2}}$ are the electron collision frequencies (in sec^{-1}) due to elastic collisions with neutral atoms of A(carbon) and B(cesium), respectively [9] , and

$\nu_{elA0} = (8.3\times10^5)\pi r_A{}^2 n_{lA0} T_{e0}{}^{\frac{1}{2}}$ and $\nu_{ehB0} = \left(8.3\times10^5\right)\pi r_B{}^2 n_{hB0} T_{e0}{}^{\frac{1}{2}}$,

$\nu_{elAi} = \nu_{elAi0}\left(\frac{n_{ilA}}{n_{ilA0}}\right)\left(\frac{T_e}{T_{e0}}\right)^{-\frac{3}{2}}$ and $\nu_{ehBi} = \nu_{ehBi0}\left(\frac{n_{ihB}}{n_{ihB0}}\right)\left(\frac{T_e}{T_{e0}}\right)^{-\frac{3}{2}}$ are the electron collision frequencies (in sec^{-1}) due to elastic collisions with positively charged ion of type A(carbon) and type B(cesium)[9],

$\nu_{elAi0} = \left(5.5\frac{n_{e0}}{T_{e0}{}^{\frac{3}{2}}}\right)\ln\left(\frac{220T_{e0}}{n_{ilA0}{}^{\frac{1}{3}}}\right)$ and $\nu_{ehBi0} = \left(5.5\frac{n_{e0}}{T_{e0}{}^{\frac{3}{2}}}\right)\ln\left(\frac{220T_{e0}}{n_{ihB0}{}^{\frac{1}{3}}}\right)$,

$\delta_{elA} \approx 2\left(\frac{m_e}{m_{lA}}\right)$ and $\delta_{ehB} \approx 2\left(\frac{m_e}{m_{hB}}\right)$ are the fraction of excess energy of an electron lost in a collision with the neutral atom A(carbon) and B(cesium), respectively[8] and are dimensionless,

$\delta_{elAi} \approx 2\left(\frac{m_e}{m_{ilA}}\right)$ and $\delta_{ehBi} \approx 2\left(\frac{m_e}{m_{ihB}}\right)$ is the fraction of excess energy of an electron lost in a collision with a positively charged ion A(carbon) and B(cesium), respectively [8] and are dimensionless,

$\delta_{ect} \approx 2\left(\frac{m_e}{m_{ct}}\right)$ is the fraction of excess energy of an electron lost in a collision with a CNT [8] and is dimensionless where,

$m_{ct} = \frac{4}{3}\pi a^3 \rho_{ct}$ is the mass of the CNT for a spherical CNT tip , a is the radius of spherical CNT tip , and ρ_{ct} is the density of spherical CNT tip,

The first term in Eq.(14) is the power gained per unit volume by electrons due to ionization of neutral atoms, the second term is the energy loss per unit volume per unit time due to the sticking accretion and elastic collisions of electron at the spherical CNT tip. The third and fourth term is the energy loss per unit volume per unit time due to elastic electron - atom collisions and elastic electron- ion collision,respectively.

H. Energy balance equation for positively charged ions

$$\left(\frac{3}{2}k_B\right)\left(n_{ilA}+n_{ihB}\right)\left(\frac{dT_i}{d\tau}\right) =$$

$$\left[\left(\beta_A n_{lA}\varepsilon_{ilA}+\beta_B n_{hB}\varepsilon_{ihB}\right)-\left(\frac{3}{2}k_B\right)\left(\beta_A n_{lA}+\beta_B n_{hB}\right)T_i\right]+\left(\frac{3}{2}k_B\right)n_e\left(\nu_{elAi}\delta_{elAi}+\nu_{ehBi}\delta_{ehBi}\right)$$
$$\times\left(T_e-T_i\right)-n_{ct}\left\{\left(n_{ilAct}\left[\varepsilon^{l}_{ilAcs}-\left(\frac{3}{2}k_B\right)T_i\right]\right)+\left(n_{ihBct}\left[\varepsilon^{l}_{ihBcs}-\left(\frac{3}{2}k_B\right)T_i\right]\right)\right\}-\left\{\left(\frac{3}{2}k_B\right)\times\right.$$
$$\left.\left[\left(\nu_{ilAlA}\delta_{ilAlA}+\nu_{ilAhB}\delta_{ilAhB}\right)n_{ilA}+\left(\nu_{ihBlA}\delta_{ihBlA}+\nu_{ihBhB}\delta_{ihBhB}\right)n_{ihB}\right]\left(T_i-T_n\right)\right\}. \quad (15)$$

where

$\frac{3}{2}\left(n_{ilA}+n_{ihB}\right)k_B T_i$ is the thermal energy of ions ,

n_{ilA} and n_{ihB} are the number densities of positively charged ions of type A(carbon) and type B(cesium), respectively(in cm^{-3}),T_i is the ion temperature (in K), T_n is the temperatures of neutral (in K).

$\varepsilon^{l}_{ilAcs}(Z)=\left[\frac{2-Z\alpha_{Ai}}{1-Z\alpha_{Ai}}\right]k_BT_i$ and $\varepsilon^{l}_{ihBcs}(Z)=\left[\frac{2-Z\alpha_{Bi}}{1-Z\alpha_{Bi}}\right]k_BT_i$ are the mean energy (in eV) of positively charged ions, A(carbon) and B(cesium),respectively (at large distance from the surface of the CNT) collected by the spherical CNT tip [8] .

ε_{ilA} andε_{ihB} is the mean energy(in eV) of positively charged ions produced by the ionization of neutral atoms [8] and for ion A(carbon) and B(cesium),respectively and are expressed as

$$\varepsilon_{ilA}=\frac{3}{2}k_BT_i+\frac{3k_B}{2\left(\alpha_A(T_e)\times n_{ilA}\right)}\left[\left\{\nu_{ilAlA}\times\delta_{ilAlA}\times\left(T_i-T_n\right)\right\}-\left\{\nu_{elAi}\times\delta_{elAi}\times\left(T_e-T_i\right)\right\}\right]$$

$$\varepsilon_{ihB}=\frac{3}{2}k_BT_i+\frac{3k_B}{2\left(\alpha_B(T_e)\times n_{ihB}\right)}\left[\left\{\nu_{ihBhB}\times\delta_{ihBhB}\times\left(T_i-T_n\right)\right\}-\left\{\nu_{ehBi}\times\delta_{ehBi}\times\left(T_e-T_i\right)\right\}\right]$$

$$\nu_{ilAlA}=\nu_{ilAlA0}\left(\frac{n_{lA}}{n_{lA0}}\right)\left(\frac{m_{lA}T_i+m_{ilA}T_n}{\left(m_{lA}T_{i0}+m_{ilA}T_{n0}\right)}\right)^{\frac{1}{2}},\nu_{ilAhB}=\nu_{ilAhB0}\left(\frac{n_{hB}}{n_{hB0}}\right)\left(\frac{m_{hB}T_i+m_{ilA}T_n}{\left(m_{hB}T_{i0}+m_{ilA}T_{n0}\right)}\right)^{\frac{1}{2}}$$

$$\nu_{ihBlA}=\nu_{ihBlA0}\left(\frac{n_{lA}}{n_{lA0}}\right)\left(\frac{m_{lA}T_i+m_{ihB}T_n}{\left(m_{lA}T_{i0}+m_{ihB}T_{n0}\right)}\right)^{\frac{1}{2}},\nu_{ihBhB}=\nu_{ihBhB0}\left(\frac{n_{hB}}{n_{hB0}}\right)\left(\frac{m_{hB}T_i+m_{ihB}T_n}{\left(m_{hB}T_{i0}+m_{ihB}T_{n0}\right)}\right)^{\frac{1}{2}}$$

are the collision frequencies (in sec^{-1}) of a j type of ion with j' ion of neutral atom[8],and

$$\nu_{ilAlA0} = \left(\frac{8}{3}\right)\left(2\pi k_B\right)^{\frac{1}{2}}(r_{ilA}+r_{lA})^2\left(\frac{n_{lA0}m_{lA}}{\left(m_{ilA}+m_{lA}\right)}\right)\left[\left(\frac{T_{i0}}{m_{ilA}}\right)+\left(\frac{T_{n0}}{m_{lA}}\right)\right]^{\frac{1}{2}},$$

$$\nu_{ilAhB0} = \left(\frac{8}{3}\right)\left(2\pi k_B\right)^{\frac{1}{2}}(r_{ilA}+r_{hB})^2\left(\frac{n_{hB0}m_{hB}}{\left(m_{ilA}+m_{hB}\right)}\right)\left[\left(\frac{T_{i0}}{m_{ilA}}\right)+\left(\frac{T_{n0}}{m_{hB}}\right)\right]^{\frac{1}{2}},$$

$$\nu_{ihBlA0} = \left(\frac{8}{3}\right)\left(2\pi k_B\right)^{\frac{1}{2}}(r_{ihB}+r_{lA})^2\left(\frac{n_{lA0}m_{lA}}{\left(m_{ihB}+m_{lA}\right)}\right)\left[\left(\frac{T_{i0}}{m_{ihB}}\right)+\left(\frac{T_{n0}}{m_{lA}}\right)\right]^{\frac{1}{2}},$$

$$\nu_{ihBhB0} = \left(\frac{8}{3}\right)\left(2\pi k_B\right)^{\frac{1}{2}}(r_{ihB}+r_{hB})^2\left(\frac{n_{hB0}m_{hB}}{\left(m_{ihB}+m_{hB}\right)}\right)\left[\left(\frac{T_{i0}}{m_{ihB}}\right)+\left(\frac{T_{n0}}{m_{hB}}\right)\right]^{\frac{1}{2}},$$

$$\delta_{ilAlA} = \left[\frac{2m_{ilA}}{(m_{lA}+m_{ilA})}\right], \delta_{ihBhB} = \left[\frac{2m_{ihB}}{(m_{hB}+m_{ihB})}\right], \delta_{ilAhB} = \left[\frac{2m_{ilA}}{(m_{hB}+m_{ilA})}\right],$$

$$\delta_{ihBlA} = \left[\frac{2m_{ihB}}{(m_{lA}+m_{ihB})}\right]$$

are the fraction of the excess energy of a j type positively charged ion, lost in a collision with neutral j' kind of neutral atom and are dimensionless. where j and j' can be same (i.e., both carbon) or be different (i.e., one carbon and other cesium)

The first term in Eq.(15) is the energy gained per unit volume per unit time by the positively charged ions due to the ionization of neutral atoms , the second term is the energy gained per unit volume per unit time due to the elastic collision of ions with electrons. The third term is the energy loss per unit volume per unit time due to the sticking accretion of ions at

the surface of the CNT. The last term is the energy lost per unit volume per unit time due to elastic collision with neutral species.

I. Energy balance equation for neutral atoms

$$\frac{3}{2}\left(n_{lA}+n_{hB}\right)k_B\left(\frac{dT_n}{d\tau}\right)=$$

$$\left[\left\{\left(\frac{3}{2}k_B\right)\left(\alpha_A n_e n_{ilA}+\alpha_B n_e n_{ihB}\right)\left(T_e+T_i-T_n\right)\right\}+\left(\alpha_A n_e n_{ilA}I_{pA}+\alpha_B n_e n_{ihB}I_{pB}\right)\right]$$

$$+\left\{\left[\left(\frac{3}{2}k_B\right)n_e\left(\nu_{elA}\delta_{elA}+\nu_{ehB}\delta_{ehB}\right)\left(T_e-T_n\right)\right]+\left[\left(\frac{3}{2}k_B\right)\left(\nu_{ilAlA}\delta_{ilAlA}n_{ilA}+\nu_{ilAhB}\delta_{ilAhB}n_{ilA}\right)\right.\right.$$

$$\left.\left(T_i-T_n\right)+\left(\frac{3}{2}k_B\right)\left(\nu_{ihBlA}\delta_{ihBlA}n_{ihB}+\nu_{ihBhB}\delta_{ihBhB}n_{ihB}\right)\left(T_i-T_n\right)\right]\right\}+$$

$$\left\{\left(\frac{3}{2}k_B\right)n_{ct}\left[\left(1-\gamma_{ilA}\right)n_{ilAct}+n_{ihBct}\right]\left(T_{ct}-T_n\right)\right\}$$

$$-\left\{\left(\frac{3}{2}k_B\right)n_{ct}\left[n_{lAct}\delta_{lAct}\left(1-\gamma_A\right)\times\left(T_n-T_{ct}\right)+n_{hBct}\delta_{hBct}\left(T_n-T_{ct}\right)\right]\right\}-E_{diss}. \qquad (16)$$

where

I_{pA} and I_{pB} are the ionization energy (in eV) of the constituent atomic species of type A (carbon) and type B(cesium),respectively,

$E_{diss}=\left(E_{A,diss}+E_{B,diss}\right)$, $E_{j,diss}$ is the energy dissipated per unit volume per unit time by neutral atoms into the surrounding atmosphere and is assumed to be equal to the difference between the temperature of the neutral atomic species and the ambient temperature.

$E_{j,diss}=E_{j,diss0}\left[\frac{\left(T_j-T_a\right)}{\left(T_{j0}-T_a\right)}\right]$ (in eV) , constant $E_{j,diss0}$ is obtained by imposing the ambient condition of the complex plasma system in Eq.(16) for both constituent neutral species[8] ,T_a is the ambient temperature.

$\delta_{lAct} = \left[\frac{2m_{lA}}{\left(m_{lA}+m_{ct}\right)}\right]$ and $\delta_{hBct} = \left[\frac{2m_{hB}}{\left(m_{hB}+m_{ct}\right)}\right]$ are the fraction of excess energy of a neutral A(carbon) and B(cesium), respectively lost in a collision with spherical CNT tip [8] and are dimensionless.

The first term in Eq.(16) is the power gained per unit volume by the neutral species due to recombination of electrons and positively charged ions, the second term is the rate of power gained per unit volume by neutral atoms in elastic collision with electrons and positively charged ions. The third term is the energy gained per unit volume per second due to formation of neutrals at the surface of the CNT due to electron and ion accretion. The fourth term refers to the thermal energy lost per unit volume per unit time by neutral atoms accretion on and collision with CNT tip. The last term is the energy dissipation rate per unit volume by neutral atoms to the surrounding atmosphere.

J) Energy balance for spherical CNT tip

$$\frac{d}{d\tau}\left(m_{ct}C_pT_{ct}\right)=\left\{n_{ect}\left[\gamma_e\ \varepsilon^s{}_{ecs}+(1-\gamma_e)\delta_{ect}\left[\varepsilon^s{}_{ecs}-\left(\frac{3}{2}k_B\right)T_{ct}\right]\right]\right\}$$
$$-\left\{\left(\frac{3}{2}k_B\right)\left\{\left(n_{lAct}\left[\gamma_AT_n+\delta_{lAct}\left(1-\gamma_A\right)\left(T_n-T_{ct}\right)\right]\right)+\left(n_{hBct}\delta_{hBct}\left(T_n-T_{ct}\right)\right)\right\}\right\}+$$
$$\left\{\left[n_{ilAct}\left(\varepsilon^s{}_{ilAcs}+I_{pA}\right)+n_{ihBct}\left(\varepsilon^s{}_{ihBcs}+I_{pB}\right)\right]\right\}-\left\{\left(\frac{3}{2}k_B\right)\left[\left(1-\gamma_{ilA}\right)n_{ilAct}+n_{ihBct}\right]T_{ct}\right\}$$
$$-\left\{4\pi a^2\left[\varepsilon\sigma\left(T_{ct}^4-T_a^4\right)+n_{lA}\left(\frac{8k_BT_n}{\pi m_{lA}}\right)^{\frac{1}{2}}+n_{hB}\left(\frac{8k_BT_n}{\pi m_{hB}}\right)^{\frac{1}{2}}\right]k_B\left(T_{ct}-T_n\right)\right\}. \qquad (17)$$

$\varepsilon^{l}_{ilAcs}(Z)=\left[\frac{2-Z\alpha_{Ai}}{1-Z\alpha_{Ai}}\right]k_BT_i$ and $\varepsilon^{l}_{ihBcs}(Z)=\left[\frac{2-Z\alpha_{Bi}}{1-Z\alpha_{Bi}}\right]k_BT_i$ are the mean energy(in eV) of positively charged ions, A(carbon) and B(cesium),respectively (at large distance from the surface of the CNT) collected by the spherical CNT tip [8] ,

C_p is the specific heat of the material of the CNT at constant pressure (in ergs/gm K),

$\in$ is the emissivity of the material of the CNT and is dimensionless,

σ is the Stefan –Boltzmann constant= $5.672\text{x}10^{-5}$ erg sec^{-1} cm^{-2} K^{-4}.

The first three terms in Eq. (17) are the rate of energy transferred to the CNT tip due to sticking accretion and elastic collision by constituent species of complex plasma. The fourth term is the energy carried away by the neutral species (generated by the recombination of the accreted ions and electrons) from the spherical CNT tip per unit volume per unit time. The last term is the rate of energy dissipation of the spherical CNT tip through radiation and conduction to the host gas [9].

6.4: Results and Discussions

In the present chapter, we have carried out calculations to study the dependence of radius of spherical CNT tip on the various compositions of ions in plasma i.e., of n_{ilA0} and n_{ihB0} . The accretion of neutral atoms and positively charged ions on the CNT is considered as the main growth process. Different plasma compositions signify different concentrations of participating ions. In the present investigation, we have varied the fractional concentration of light positively charged ion and studied its effect on radius of spherical CNT tip. We have solved equations for charging of CNT, kinetics and energy balance of light and heavy

positively charged ions, electrons, ions, neutrals and of spherical CNT tip with appropriate boundary conditions, viz., at

CNT number density $\left(n_{ct}\right)=10^{6}\text{cm}^{-3}$,ion density of carbon(type A)$\left(n_{ilA0}=0.8n_{e0}\right)$, ion density of cesium(typeB) $n_{ihB0}=0.2n_{e0}$,neutral atom density of carbon and cesium$\left(n_{lA0}=n_{hB0}\right)=1\times10^{14}cm^{-3}$,electron number density$\left(n_{e0}\right)=10^{6}\text{cm}^{-3}$, electron temperature$\left(T_{e0}\right)=0.5\text{eV}$,ion temperature$\left(T_{i0}\right)=2100K$, neutral temperature$\left(T_{n0}\right)=$ CNT temperature$\left(T_{ct}\right)=1950K$, mass of carbon ion$\left(m_{ilA}\right)$ $\approx$ mass of neutral carbon atom$\left(m_{lA}\right)=12$ amu,mass of cesium ion $\left(m_{ihB}\right)\approx$ mass of cesium atom$\left(m_{hB}\right)=132.905$ amu,coefficient of recombination of carbon and cesium with electron$\left(\alpha_{A0}\approx\alpha_{B0}\right)=10^{-7}cm^{3}/\text{sec}$,emissivity of carbon$(\varepsilon)=0.6$,sticking coefficients of carbon ion or carbon atom$\left(\gamma_{ilA}=\gamma_{lA}\right)$ =1,specific heat of carbon$\left(C_{p}\right)=7\times10^{6}$ergs/gm K,ionization energy of carbon $\left(I_{pA}\right)=15.26$ eV,ionization energy of cesium$\left(I_{pB}\right)=10$ eV, mean energy of electron due to ionization of carbon atom$\left(\varepsilon_{lA}\right)=6.2\text{eV}$,mean energy of electron due to ionization of cesium atom$\left(\varepsilon_{hB}\right)=18.7\text{eV}$, mean energy of carbon ion due to ionization of carbon atom$\left(\varepsilon_{ilA}\right)=17.3\text{eV}$,mean energy of cesium ion due to ionization of cesium atom$\left(\varepsilon_{ihB}\right)=12.2\text{eV}$,energy dissipated by carbon$\left(\varepsilon_{A,diss0}\right)$ $=42.9\text{eV}$,energy dissipated by cesium$\left(\varepsilon_{B,diss0}\right)=19.6\text{eV}$,constant$(\kappa)=-1.2$, radius of CNT($a_0$)= 0.07nm and density of CNT$\left(\rho_{ct}\right)=4.2\text{g/cm}^{3}$.

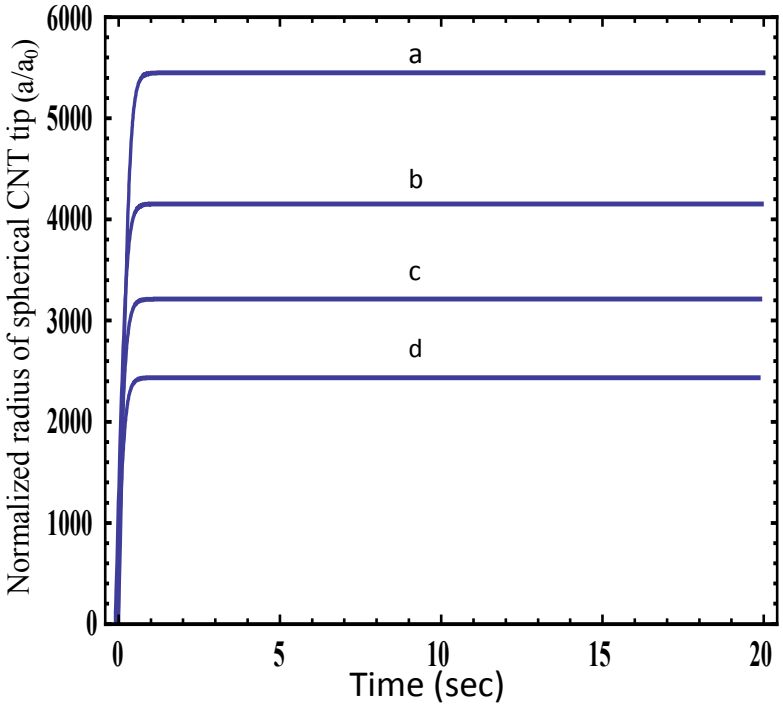

Fig.1. Shows the variation of the normalized radius a/a_0 of spherical CNT tip for different fractional concentrations of light positively charged ions (α_l) where a, b, c and d correspond to α_l=0.1,0.3,0.6, and 0.9, respectively.

Fig. 1 illustrates the variation of normalized radius a/a_0 of spherical CNT tip with time for different fractional concentrations of light positively charged ions (i.e.,α_l= 0.1,0.3,0.6 ,and 0.9) and for other parameters as mentioned above. From Fig. 1 it can be seen that the normalized radius of CNT first increases with time and then attains a saturation value. It also shows the decrease of normalized radius a/a_0 with fractional concentrations of light positively charged ions. As the light ion number density i.e., α_l increases in plasma then that would mean that a lot of neutral carbon atom dissociated to produce that many number of carbon ions in plasma. In addition, because the main growth

process in present model is the accretion of neutral atoms on the CNT, there reduced number would imply a smaller radius of CNT.

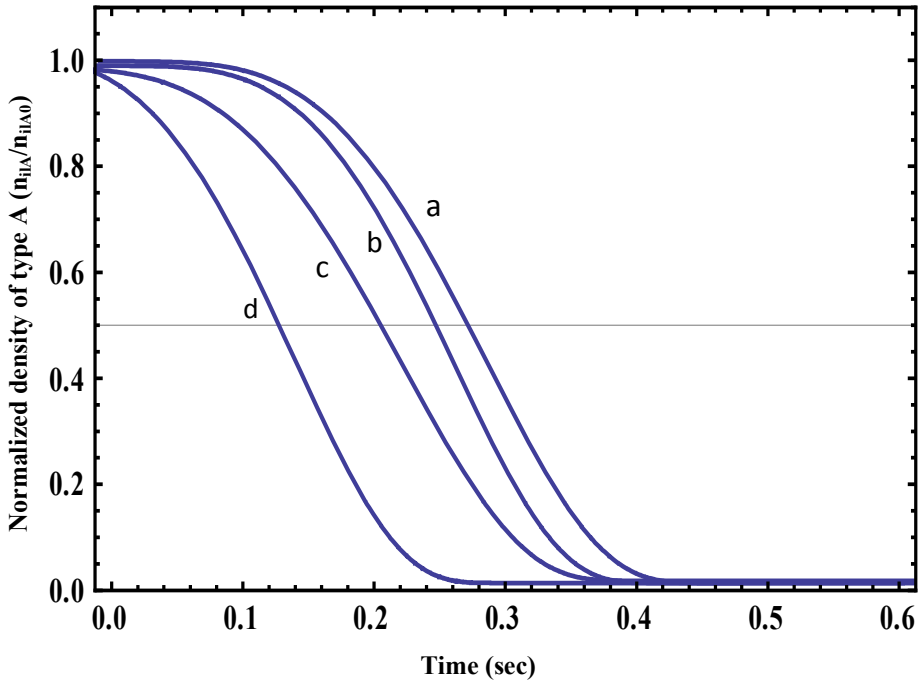

Fig. 2: Shows the variation of the normalized ionic density of type A with time on the sticking coefficient of the atomic species for a, b ,c ,and d corresponding to γ_{lA} = 0.1, 0.3, 0.5, and 1.0, respectively.

Fig. 2 shows the variation of normalized ionic density of type A in plasma with time for different values of sticking coefficients γ_{lA} = 0.1, 0.3, 0.5 and 1.0 and for other parameters as mentioned above. It can be seen from Fig. 2 that with increasing atomic sticking coefficients , the positively charged ion of A type decays faster.

The above results are in line with the observations of Srivastava *et al*. [1], Han *et al.*[2], Kiang *et al.* [5] ,and Lee *et a1*.[10] where different plasma compositions leads to modifications in structure of CNTs.

6.4.1: Estimating field emission from CNT

On the basis of results obtained we can infer that larger light ion concentration gives CNT with smaller radius and since field enhancement factor [11] is

$$\beta = \frac{h}{\rho} + 3.5 \quad , \tag{18}$$

where

h = the height of CNT and ρ = the radius of CNT ,

Assuming a fixed height of CNT, the Eq. (18) shows that the field enhancement factor is inversely proportional to the radius of CNT. From the results of the present chapter one can see that larger light ion concentration leads to smaller radius of CNT, hence better field emission from CNT is expected from the CNTs grown in plasma containing higher concentrations of lighter ions.

References

[1]S. K. Srivastava, V. D. Vankar and Vikram Kumar, Thin Solid Films **515**, 1552(2006).

[2]Jae-Hee Han , Sun Hong Choi , Tae Young Lee , Ji-Beom Yoo , Chong-Yun Park , Ha Jin Kim , In-Taek Han , SeGi Yu , Whikun Yi , Gyeong Soo Park , Minho Yang , Nae Sung Lee , J.M. Kim, Thin Solid Films **409** ,126 (2002).

[3] M. S. Bell, R.G. Lacerda, K. B. K. Teo, N. L. Rupesinghe, M. Chhowalla, Appl. Phys. Lett. **85**, 7(2004).

[4] K. B. K. Teo, M. Chhowalla, G. A. J. Amaratunga, W. I. Milne, D. G. Hasko, G. Pirio, P. Legagneux, F. Wyczisk, and D. Pribat, Appl. Phys. Lett. **79**,1534(2001).

[5] Ching-hwa Kiang, William A. Goddard , Robert Beyers, Jesse R. Salem and Donald S. Bethune, J. Phys. Chem. Solids **57**, 35(1996).

[6] Mi Chen, Chieng-Ming Chen, and Chia-Fu Chen, Thin Solid Films **420**, 230 (2002).

[7] GY Xiong, Y Suda, D Z Wang, J Y Huang ,and Z F Ren, Nanotechnology **16** ,532 (2005).

[8]M. S. Sodha , Shikha Misra, S. K. Mishra, Sweta Srivastava, J. Appl. Phys. **107**,103307(2010).

[9] M. Rosenberg, D. A. Mendis, and D. P. Sheehan, IEEE Trans. Plasma Sci.**27**, 239(1999).

[10]S. F. Lee, Yung-Ping Chang, Li-Ying Lee, J. Mater. Sci. Mater. Electron **20**, 851(2009).

[11] X.Q Wang, M. Wang, P.M. He and Y.B. Xu, J. Appl. Phys **96**, 6752 (2004)

CHAPTER 7

MODELING CARBON NANOTUBE GROWTH ON THE CATALYST-SUBSTRATE SURFACE SUBJECTED TO REACTIVE PLASMA

7.1: A Brief outline of the work done in the chapter

The present chapter details the model for the growth of carbon nanotube (CNT) on a catalyst-substrate surface in reactive plasma. The complex processes during growth of CNT assisted by catalyst in reactive plasma are accounted in the present chapter and the effects of process and plasma parameters on the growth profiles of CNT are studied.

7.2: Introduction

Low temperature plasmas are beneficial to the synthesis of carbon-based nanostructures. For nanofabrication, either solid particle float in the plasma or some nanoscale objects grow on a solid surface exposed to plasma. The second method is the area of pursuit in recent years where plasma assisted synthesis of nanostructures has been the major area of concern. In plasma-assisted synthesis of nanostructures, the particles in ionized gas phase nucleate, crystallize, and are taken through the plasma sheath, eventually to deposit on the surface. [1]

Numerous works have been performed to study the CNT growth in plasma, the consequent effects of radio frequency (rf) power density, temperature, gas flow rate on the growth rate, and dimensions of resulting CNTs [2–7].

Choi *et al.* [2] have established that the growth rate and the density of CNTs increase with the reduction of the rf power density when vertically aligned CNTs were grown on nickel (Ni) coated silicon (Si) substrates using microwave plasma-enhanced chemical vapor deposition (MPECVD) technique.

Aksak *et al.* [3] have demonstrated that at temperatures over and above 850 ^{0}C, the CNT formation with average radius distribution decreases while their length increases with temperature. They also noticed that the temperature affected the as-grown CNTs diameter inversely.

Loffler *et al.* [4] have optimized the growth of the CNT by plasma enhanced chemical vapor deposition (PECVD) for field emitters and observed the effect of growth parameters on the growth rate of the CNT. They confirmed that CNTs are better aligned at high power, but the etch rate increased due to strong ion bombardment. As a result, the catalytic particle is sputtered during the PECVD process so that the diameter of the CNT decreases and hence this effect can be used to sharpen the tip of the CNT by an adapted growth time.

Abdi *et al.* [5] have studied the effects of plasma powers on the growth of carbon nanotubes via PECVD method and found that as the plasma power of the Ni layer was increased, the grain size of Ni nanoparticle decreased and consequently, nanotubes of smaller diameter were obtained.

Cho *et al.* [6] have investigated the effect of ammonia (NH_3) gas on the growth of the CNTs using thermal CVD. They observed that the CNT length increased while CNT radius decreased with the NH_3 flow (cf. Fig. 5 of Cho *et al.* [6]). Moreover, the CNTs were etched back by direct current (dc) plasma of nitrogen (N_2) to reduce the population density and

radius of curvatures of CNTs, which resulted in a considerable improvement of the field emission characteristics.

Srivastava *et al.* [7] have studied the effect of hydrogen (H_2) plasma treatment on oxide films on the growth and microstructures of multi walled carbon nanotubes (MWCNTs). They reported that the oxide films without H_2 plasma pretreatment or treated for lesser time resulted in CNT films with the high percentage of carbonaceous particles, and with embedded particles/ nanorods distributed discontinuously in the cavity of the nanotubes.

Many theoretical models have evolved to study the nanostructure growth in plasma. Plasma environment processes, such as ion bombardment, atomic hydrogen effects, electron number density, sheath thickness, and surface potential on the growth rate, have been extensively examined [8–12].

Denysenko *et al.* [8] have studied the growth of single walled carbon nanotubes (SWCNTs) in a PECVD process using the surface deposition model. In this case, it was shown that at low substrate temperatures (1000 K), the atomic hydrogen and ion fluxes from the plasma could strongly affect the nanotube growth.

Levchenko *et al.* [9] have suggested that the plasma-aided process, in comparison to the neutral flux deposition, is a very efficient tool to control the nanotube aspect ratio. They highlight that an increased influx and controllable deposition of ionic building blocks (BBs) directly onto the nanotube lateral surfaces can be used to deterministically control the geometric configuration of the nanotips.

Mehdipour *et al.* [10] have analytically studied the effect of electron number density, sheath thickness, gas pressure, surface potentials, etching

gas density on the growth rate of carbon nanofibres. They calculated the exact temperature of the catalyst nanoparticle with respect to the substrate temperature. They also established that the growth parameters like (total gas pressure), the relative concentrations of hydrocarbon and etching gas can be used to obtain nanostructures with high aspect ratio (i.e., ratio of height of CNT to radius of CNT).

Ostrikov *et al.* [11] have highlighted the plasma based process during nanostructures growth, including sheath effects and the various processes involved during nanostructure growth like an ion induced dissociation, ion decomposition, hydrogen recombination, ion induced neutralization, adsorption of hydrogen atoms, adsorption and desorption of hydrocarbon radicals, and surface diffusion of carbon atoms and several others.

In recent years, most of the research publications on nanostructure synthesis do feature information on field emission properties. This partly may be ascribable to the reason that carbon nanostructures have emerged as potential field emitter devices [12–17].

Despite the available experimental literature on the growth of CNTs in plasma there are a very few theoretical models that describe the exact processes during the CNT growth in a plasma environment where innumerable complex processes take place. Thus, in the present chapter we try to model the CNT growth on the catalyst-substrate surface in reactive plasma by including sheath kinetics, the balance equation of the various plasma species like neutrals, ions, electrons and finally numerically solve for the radius and height of the CNT due to accretion and surface diffusion processes.

7.3: MODEL

In the present chapter, we consider the growth of carbon nanotube (CNT) on the catalyst-substrate surface subjected to reactive plasma containing electrons, positively charged ions of methane (CH_3^+, CH_2^+) denoted as ions A and hydrogen ions (H^+) denoted as ions B, neutral atoms of type A methane (CH_4) and neutral atoms of type B hydrogen (H_2). The nickel (Ni) catalyst is placed over the silicon (Si) substrate. The reactive plasma of Ar+ H_2+CH_4 is considered and CH_4 acts as a carbon source gas. Since catalyst-substrate surface is in contact with the plasma, we shall consider sheath kinetics in our present study. The electric field created due to charge separation within the sheath region is taken along *x*-axis.

The sheath equations are:

Firstly, the continuity equation [18]

$$\frac{\partial n}{\partial \tau} + \nabla.(nu) = G - L,$$

where G and L are the left over terms of collisions part of the Boltzmann equation (Eq. 2.3.3 of Libermann *et al.*[18]) when integrated over velocities. They denote collisions that create or destroy particles, respectively, i.e., either recombination or ionization where $G = \nu_{iz} n_e$ and L= volume loss rate

Finally, the continuity equation reduces to [18]

$$\nabla.(nu) = \nu_{iz} n_e \tag{1}$$

n_e= number density of electron (in cm^{-3}),

ν_{iZ} = ionization frequency (in sec^{-1}),

n and u denote the number density (in cm^{-3}), and fluid velocity (in cm/sec) of electrons, CH_3^+, CH_2^+, Ar^+ and H^+.

Secondly, ion momentum balance equation [18]

$$Mn_j u_j \frac{du_j}{dx} = en_j E - Mn_j \nu_{jn} u_j, \quad (2)$$

where M is the mass of ions in plasma(in gm), u_j are their fluid velocity(in cm/sec), n_j is their number density (in cm^{-3}), ν_{jn} is the collision frequency(in sec^{-1}) and E is the electric field (in Stat V/cm).

For determining potential within the sheath, we use Poisson's equation [10]

$$\frac{d^2\phi}{dx^2} = -4\pi \sum q_j \delta_j n_j, \quad (3)$$

where $\delta_j = \left(\frac{n_{ij}}{n_e}\right)$ is the j^{th} ion to electron number density ratio and is dimensionless and ϕ is the electrostatic potential , and $\sum_j \delta_j = 1$ and $0 < \delta_j < 1$ as electron density is greater in plasma bulk than in sheath[18].

For the CNT growth over the catalyst-substrate surface in plasma, the following steps are assumed in the model:

1. Firstly, the applied plasma power dissociates the catalyst particle thereby forming catalyst nanoparticle.
2. The ions of methyl (CH_3^+, CH_2^+) adsorb on the catalyst-substrate surface with adsorption flux J_{aij} [19].
3. Some of the ions desorp with desorption energy ε_{ai} with desorption flux $J_{desorptionj}$ [19].
4. Then, there is thermal dehydrogenation (removal of hydrogen) of ion induced dissociated methyl ions to produce carbon ions.

5. While a big fraction of carbon atoms diffuses into catalyst particle contributing to nanotube growth, some of the carbon atoms evaporate from the surface with evaporation energy ε_{ev}.
6. Ultimately, the growth of CNT occurs due to two main processes, surface diffusion of carbon ions into the catalyst surface and sticking of neutrals onto the catalyst surface. The hydrogen ions effectively shape nanoparticles tip by etching effects.

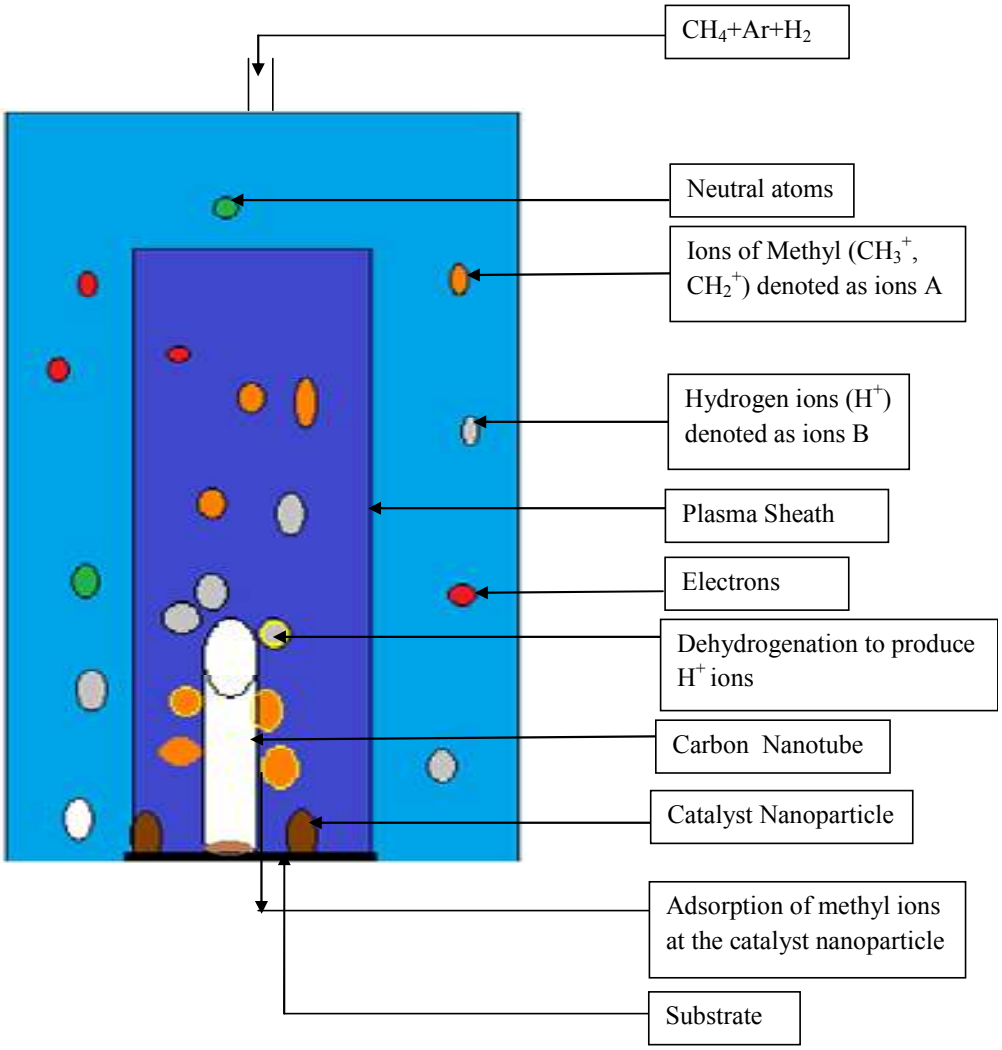

FIG.1. Schematic of the processes involved during the carbon nanotube growth on the catalyst substrate surface in reactive plasma.

A. Charging of the CNT

The equation describes the charge developed on the entire CNT (i.e., spherical tip over cylindrical surface), due to accretion of electrons and diffusion of positively charged ions on the surface of the CNT (spherical tip over cylindrical surface).

$$\frac{dZ}{d\tau} = n_{iActs} + n_{iActcys} + n_{iBcts} + n_{iBctcys} - \gamma_e\left(n_{ects} + n_{ectcys}\right), \qquad (4)$$

where,

Z is the amount of charge over the entire CNT (i.e., spherical tip and cylindrical surface) and is dimensionless,

$n_{ects} = \pi r_{ct}^2 \left(\frac{8k_B T_e}{\pi m_e}\right)^{\frac{1}{2}} n_e(x) \exp\left[Z\alpha_e + \frac{eU_s}{k_B T_s}\right]$ is the electron collection current at the surface of the spherical CNT tip (in sec^{-1}) and $\alpha_e = \left(\frac{e^2}{r_{ct} k_B T_e}\right)$, r_{ct} is the nanoparticle radius (in nm), U_s is the substrate bias (in V) and k_B is the Boltzmann's constant (in ergs/K),

$n_e(x) = n_{e0} \exp\left[\frac{|e|\phi(x)}{k_B T_e}\right]$ is the electron density in plasma sheath(in cm^{-3}) , $\phi(x)$ is the electrostatic potential (in StatV), n_{e0} is plasma density in bulk(in cm^{-3}) and it decreases towards the substrate, and T_e is the electron temperature(in eV),

$\phi(x) = \phi_0 \exp\left(-\frac{|x|}{\lambda_d}\right)$ is the negative potential at the surface, and λ_d is the plasma Debye length[1] .

$$n_{ectcys} = n_e(x) r_{ct} h \left(\frac{2\pi k_B T_e}{m_e} \right)^{\frac{1}{2}} \exp\left[\frac{eV_s}{k_B T_e} + \frac{eU_s}{k_B T_s} \right]$$ is the electron

collection current on the cylindrical surface of the CNT(in sec^{-1}) and V_s is the surface potential on the cylindrical surface of the CNT(in StatV) and h is the height of cylindrical surface of the CNT (in μm), m_e is the mass of electron (in gm),

$$n_{ijctcys} = n_{ij}(x) r_{ct} h \left(\frac{2\pi k_B T_i}{m_{ij}} \right)^{\frac{1}{2}} \left\{ \frac{2}{\sqrt{\pi}} \left(\frac{eV_s}{k_B T_i} \right)^{\frac{1}{2}} + \exp\left[\frac{eV_s}{k_B T_i} \right] erfc \left[\left(\frac{eV_s}{k_B T_i} \right)^{\frac{1}{2}} \right] \right\}$$

$$\exp\left[-\frac{E_b}{k_B T_s} \right] \exp\left[-\frac{eU_s}{k_B T_s} \right]$$

is the ion collection current on the cylindrical surface of CNT(in sec^{-1}), T_i is the ion temperature (in K), m_{ij} is the ion mass (in gm) (j refers to either A(hydrocarbon) or B(hydrogen) positively charged ion), E_b is the energy barrier for bulk diffusion $(\approx 1.6eV)$, T_s is the substrate or catalyst temperature ,

$$n_{ijcts} = \pi r_{ct}^2 \left(\frac{8k_B T_i}{\pi m_{ij}} \right)^{\frac{1}{2}} n_{ij}(x) \left[1 - Z\alpha_i \right] \exp\left[-\frac{E_b}{k_B T_s} \right] \exp\left[-\frac{eU_s}{k_B T_s} \right]$$

is the ion collection current to spherical CNT(in sec^{-1}), where

$n_{ij}(x) = n_{ij0} \left(1 - \frac{2e\phi(x)}{m_{ij} v_{ij0}^2} \right)^{\frac{1}{2}}$ is the ion density in plasma sheath [18](in cm^{-3}) ,

v_{ij0} is the ion velocity at any point within the plasma (in cm/sec) and

$$\alpha_i \left(= \frac{e^2}{r_{ct} k_B T_i} \right)$$

Substrate bias is an essential factor because when the charge on CNT is increasing the negative substrate bias leads to more negative charge developing on the CNT surface that finally results an increase in the thickness of plasma sheath [1]. Moreover, increasing the negative substrate bias accelerates the positive ion species.

B. Balance equation of electron density

The equation describes the balance of electron number density in the plasma bulk

$$\frac{dn_e}{d\tau} = \left(\beta_A n_A + \beta_B n_B\right) - \left(\alpha_A n_e n_{iA} + \alpha_B n_e n_{iB}\right) - \gamma_e n_{ct}\left(n_{ects} + n_{ectcys}\right), \tag{5}$$

where

β_A and β_B are the coefficients of ionization of the constituent neutral atoms of A(hydrocarbon) and B(hydrogen) due to external agency (in sec), and $\alpha_A(T_e) = \alpha_{A0}\left(\frac{300}{T_e}\right)^k cm^3/\sec$ and $\alpha_B(T_e) = \alpha_{B0}\left(\frac{300}{T_e}\right)^k cm^3/\sec$ are the coefficients of recombination of electrons and positively charged ions [20] of A(hydrocarbon) and B(hydrogen),respectively where k =-1.2 is a constant $\alpha_{A0} = \alpha_{B0} = n_{e0} \times 10^{-7}\left(\frac{1}{T_{e0}}\right)^{-1.2}$ and n_{ct} is the CNT number density (in cm^{-3}).

The terms on the right side of Eq. (5) are the rate of gain in electron density per unit time on account of ionization of neutral atoms, the decaying rate of the electron density due to electron–ion recombination

and the electron collection current at the surface of the CNT (spherical tip over cylindrical surface).

C. Balance equation of positively charged ion density

The equation describes the balance of positively charged ions in plasma bulk

$$\frac{dn_{iA}}{d\tau} = \beta_A n_A - \alpha_A n_e n_{iA} - n_{ct}\left(n_{iActs} + n_{iActcys}\right) - J_{aiA} + J_{desorptionA} \quad ,(6)$$

$$\frac{dn_{iB}}{d\tau} = \beta_B n_B - \alpha_B n_e n_{iB} - n_{ct}\left(n_{iBcts} + n_{iBctcys}\right) - J_{aiB} + J_{desorptionB} + J_{th} \quad ,(7)$$

$J_{aij} = \frac{P_i}{\left(2\pi m_{ij} k_B T_{ij}\right)^{\frac{1}{2}}} \times \frac{n_{ij}}{j_{ij}}$ is the adsorption flux onto the catalyst -substrate surface (in cm^{-3} sec^{-1}), P_i is the partial pressure of adsorbing species [19],

$J_{desorptionj} = n_{ij}\nu \exp\left(\frac{-\varepsilon_{ai}}{k_B T_{ij}}\right)$ is the desorption flux from the catalyst – substrate surface (in cm^{-3} sec^{-1}), j refers to either A or B ions, ν is the thermal vibrational frequency (in sec^{-1}) , ε_{ai} is the adsorption energy (in eV)[19],

$J_{th} = n_{iB}\nu \exp\left(\frac{-\delta\varepsilon_{th}}{k_B T_S}\right)$ is the flux of type B ion (namely hydrogen) on account of thermal dehydrogenation(in cm^{-3} sec^{-1}). $\delta\varepsilon_{th}$ is the activation energy of thermal dehydrogenation.

The first term in Eqs. (6) and (7) is the gain in ion number density per unit time on account of ionization of neutral atoms, the second term is the

electron-ion recombination, the third term is the ion collection current to the surface of the CNT (spherical tip over cylindrical surface). The fourth term is the loss of ions on account of their adsorption to the catalyst - substrate surface and fifth term is the gain of ion density due to their desorption from the catalyst -substrate surface into the plasma. The last term in Eq. (7) describes the increase of hydrogen ion number density in plasma because of thermal dehydrogenation.

D. Balance equation of neutral atoms

The equation describes the balance of neutral atoms in plasma

$$\frac{dn_A}{d\tau} = \alpha_A n_e n_{iA} - \beta_A n_A + n_{ct}\left(1-\gamma_{iA}\right)\left(n_{iActs} + n_{iActys}\right) - n_{ct}\gamma_A\left(n_{Acts} + n_{Actcys}\right) \quad ,(8)$$

$$\frac{dn_B}{d\tau} = \alpha_B n_e n_{iB} - \beta_B n_B + n_{ct}\left(1-\gamma_{iB}\right)\left(n_{iBcts} + n_{iBctcys}\right) - n_{ct}\gamma_B\left(n_{Bcts} + n_{Bctcys}\right) \quad (9)$$

where

$n_{jcts} = \pi r_{ct}^2 \left(\frac{8k_B T_n}{\pi m_j}\right)^{\frac{1}{2}} n_j$ is the neutral collection current at the surface of spherical CNT tip (in sec^{-1}),

$n_{jctcys} = \pi r_{ct} h \left(\frac{2k_B T_n}{m_j}\right)^{\frac{1}{2}} n_j$ is the neutral collection current on the cylindrical surface of CNT (in sec^{-1}).

γ_{iA} and γ_{iB} are the ion sticking coefficients and $\gamma_A$and γ_B are the neutral atom sticking coefficients, and both γ_{iA} and γ_{iB} and $\gamma_A$and γ_B are dimensionsionless. n_j is the neutral atom density (in

cm^{-3}), T_n is the neutral atom temperature (in K) , n_j is the neutral atom density (in cm^{-3}) and m_j is the neutral atom mass (in gm).

The first term in Eqs. (8) and (9) is the gain in neutral atom density per unit time due to electron–ion recombination, the second term is the decrease in neutral density due to ionization, the third term is the gain in neutral density due to neutralization of the particles collected at the surface of the CNT. The last term denotes the loss in neutral density due to accumulation of neutral atoms of species A and B on the surface of the CNT.

E. Rate equation for energy of catalyst particle

The basis of our assumption for developing Eq.(10) follows from Srivastava *et al*. [24] where they have suggested an increase in the density of energetic plasma species with the applied power.

$$rfpower = C_p T_S \frac{d}{d\tau}\left(m_p\right) = \left[n_{iActP}\left(\varepsilon^s{}_{iAc} + I_{pA} \right) + n_{iBctP}\left(\varepsilon^s{}_{iBc} + I_{pB} \right) \right] - \left(\frac{3}{2} k_B\right)\left[\left(1-\gamma_{iA}\right) n_{iActP} + n_{iBctP}\right] T_S, \tag{10}$$

where

$m_P = \frac{4}{3}\pi {r_P}^3 \rho_P$ is the mass of catalyst particle, r_p is the radius of catalyst particle [10] whose initial value is 50 nm. ρ_P is the mass density of catalyst particle(in gm/cm^3). C_p is the specific heat of catalyst particle (Ni) and is 0.44KJ/Kg ^{0}K and T_s is the substrate temperature (in ^{0}C). I_{pA} and I_{pB} are the ionization energies of atoms A and B, respectively (in eV),

$\varepsilon^s_{ijc}(Z) = \left(\left(\frac{\left(2 - Z\gamma_{ji}\right)}{\left(1 - Z\gamma_{ji}\right)} \right) - Z\gamma_{ji} \right) k_B T_{ij}$ are the mean energy (in eV) collected by

the ions j (where, j refers to ion A or B) at the surface of the catalyst particle and $\gamma_{ji} = \left(\frac{e^2}{r_P k_B T_{ij}} \right)$,

$n_{ijctP} = \pi r_P^2 \left(\frac{8 k_B T_i}{\pi m_{ij}} \right)^{\frac{1}{2}} n_{ij}(x) \left[1 - Z\gamma_i \right] \exp\left[-\frac{E_b}{k_B T_s} \right] \exp\left[-\frac{eU_s}{k_B T_s} \right]$ is the ion collection current at the surface of catalyst particle (in sec^{-1}), (where, j refers to ion A(hydrocarbon) or B(hydrogen)) .

The Eq. (10) denotes the influence of rf power on the mass of catalyst particle for constant specific heat and substrate temperature. The first term on the right side of Eq. (10) is the rate of energy transferred to the catalyst particle due to the ions collected at the surface of catalyst particle because of ionization of neutral atoms A and B and mean energy collected by the ions at the surface of catalyst particle. The second term is due to the sticking accretion of ion A and B at the catalyst particle site.

We assume in the present model that as the applied rf power increases, it ionizes the gas more which creates more energetic ions which thereby increases the density of plasma species of relatively higher energy, i.e., the number density and temperature of ion A and B increases. We also assume that the rf power affects the radius of catalyst particle and the temperature ,and specific heat are unaffected by applying rf power because many researches done highlight the variation of size of particles with rf power only such as Abdi *et al.* [5] and Srivastava *et al*. [24].

In Solving Eq. (10), we consider different rf power, i.e., 50 W, 100W, 150W, and 200W. The substrate temperature T_S is taken as 500 ^{0}C ,

Substrate bias U_s= -50V. n_{iB0}= n_{iA0}=10^8 cm^{-3},T_{i0}=1900K , ε_{iAc}^{s}= ε_{iBc}^{s} =2.648 eV , I_{pA}=10.27eV and I_{pB} =12eV. Substituting all the above value for a fixed rf power at 50W, we can calculate n_{iActP}, n_{iBctP}. Now, for higher plasma power we consider slightly different ion density and ion temperature and calculate n_{iActP} and n_{iBctP} and consequently the catalyst particle radius (r_p).The other parameters are same as mentioned in result and discussion section.ϵ_{iAc}^{s}

The resulting value of catalyst nanoparticle at time τ serves as the initial radius of nanotube (r_{ct}).

F. Growth rate equation of the curved surface area of CNT

Following, Denysenko *et al.* [8], Mehdipour *et al.* [10], and Denysenko *et al.* [25], we develop Eqs. (11 and 12) that traces the development of the CNT on catalyst nanoparticle. The height of CNT is obtained from Eq. (11) in which we consider the growth of the cylindrical part of the CNT and the value of the height of the cylindrical part of the CNT at the time τ is then fed into Eq. (12) to determine the CNT radius (r_{ct}). The Eq. (12) specifically calculates the curved surface area of spherical CNT tip.

$$r_{ct}\frac{d(2\pi h)}{d\tau}=\left(\left\{2n_{CH}\nu\exp\left(\frac{-\delta E_t}{k_BT_s}\right)+2\theta_{CH}j_{iA}y_d+2j_{iA}+\frac{j_{iA}\sigma_{ads}j_{iB}}{\nu}+j_c\right\}m_c+\left\{j_{iA}(1-\theta_t)+\frac{j_{iA}\sigma_{ads}j_H}{\nu}+j_{iA}\exp\left(\frac{-\delta E_t}{k_BT_s}\right)\right\}m_{iA}\right)$$
$$\times\frac{D_s\times 2\pi r_{ct}}{\pi r_{ct}^2\rho_{ct}}\left(\frac{1}{n_{iActcys}}\right)+\gamma_{CH_4}\pi r_{ct}^2 n_{CH_4ctcys} \quad ,(11)$$

$$\frac{d(4\pi r_{ct}^2)}{d\tau}=\left(j_{iB}\exp\left(\frac{-E_b}{k_BT_s}\right)+j_{iB}\exp\left(\frac{-\delta E_{th}}{k_BT_s}\right)+j_{iB}(1-\theta_t)+j_{iB}+\theta_{CH}\left(j_{iB}y_d+\nu_0\nu\exp\left(\frac{-\delta E_i}{k_BT_s}\right)\right)\right)\frac{h(\tau)}{n_{iB}}, \quad ,(12)$$

where

The explanation for all the symbols used in Eq. (11) is given in Table 1.

The explanation for all the symbols used in Eq. (12) is given in Table 2.

The explanation for all the terms used in Eq. (11) is given in Table 3.

The explanation for all the terms used in Eq. (12) is given in Table 4.

Table 1. Explanation for all the symbols used in Eq.(11)

S.No.	**The notation of various symbols used in Eq.(11)**	**The explanation for symbols in Eq.(11)**
1.	$n_{CH} = \theta_{CH} \nu_0$ (in cm^{-2})	The number density or concentration of CH (CH denotes CH_4 species) [10]
2.	$\nu_0 \approx 1.3 \times 10^{15} cm^{-2}$	The number of adsorption sites per unit area[8]
3.	$j_c = n_c v_{thc}/4$ (in cm^{-2} sec^{-1})	Ion flux of carbon atoms[10]
4.	v_{thc} (in cm/sec)	Thermal velocity of carbon atoms[10]
5.	$j_{iA} = n_{iA}(k_B T_i / m_{iA})^{1/2}$ (in cm^{-2} sec^{-1}) and $j_{iB} = n_{iB}(k_B T_i / m_{iB})^{1/2}$ (in cm^{-2} sec^{-1})	Ion flux of type A and B, respectively
6.	$y_d \approx \varepsilon_{icH} / \varepsilon_{dis}$ (dimensionless)	Ratio of kinetic energy associated with the motion of hydrocarbon ions impinging on the substrate to dissociation energy of CH_4 [10]
7.	n_{iB} (in cm^{-3})	Number density of type B ions i.e., hydrogen ions

8.	ε_{icH} (in eV)	Kinetic energy associated with the motion of hydrocarbon ions impinging on the substrate[8]
9.	ε_{dis} (in eV)	Dissociation energy of CH_4
10.	$\sigma_{ads} \approx 6.8\times10^{-16} cm^2$	Cross section area for the reactions of atomic hydrogen with adsorbed particles[10]
12	D_s and $\left[D_S = D_{s0}\exp(-E_S/k_B T_S)\right]$ $D_{s0} = \nu a_0^2$ is a constant (in $nm^2 sec^{-1}$)	Surface diffusion coefficient[8]
13.	E_s=0.3eV	Energy barrier for diffusion of carbon (C) on the catalyst[8]
14.	a_0 =0.34 nm	Inter atomic distance between carbon atoms
15.	θ_t (dimensionless)	Total surface coverage[10]
16.	$\delta\varepsilon_t$ =1.3eV	Energy due to thermal dissociation[8]
17.	γ_{CH_4} (dimensionless)	Sticking coefficient of CH_4 neutrals[20]
18.	m_c =12 amu	Mass of a carbon atom
19.	m_{iA} =15 amu for CH_3^+ = 14 amu for CH_2^+	Mass of type A(methyl) ions

20.	$h(\tau)$ (in μm)	Height of CNT at time τ
21.	n_{iB}(in cm^{-3})	Number density of type B ions i.e., hydrogen ions
22.	$n_{CH4ctcys}$ (in sec^{-1})	Methane neutral atom collection current at the surface of cylindrical CNT[20]
23.	k_B=1.38x10^{-16} ergs/K	Boltzmann's constant
24.	T_s=550^{0}C	Substrate temperature
25.	r_P=50nm	Initial radius of catalyst particle
26.	$\rho_{ct} = 8.908 g/cm^3$	Density of nickel (Ni)
27.	$\nu = 10^{13}$ Hz	Thermal vibrational frequency[8]
28.	$n_{iActcys}$(in sec^{-1})	Ion collection current of hydrocarbon(i.e., A) the surface of cylindrical CNT [20]

Table 2. Explanation for all the symbols used in Eq.(12)

S.No.	**The notation of various symbols used in Eq.(12)**	**The explanation for symbols in Eq.(12)**
1.	$j_{iB} = n_{iB}(k_B T_i / m_{iB})^{1/2}$(in cm^{-2} sec^{-1})	Ion flux of type B ion (hydrogen ion)
2.	T_i (in K)	Ion temperature
3.	$E_b \approx 1.6eV$	Energy barrier for bulk diffusion[10]
4.	δE_{th} (in eV)	Energy due to dehydrogenation of CH_4 [8]

5.	θ_t (dimensionless)	Total surface coverage[10]
6.	h(τ) (in μm)	Height of CNT at time τ
7.	r_{ct} (in nm)	Radius of spherical CNT tip

Table 3. Explanation for all the terms used in Eq.(11)

S. No.	**The mathematical Expression for terms in Eq.(11)**	**The detailed explanation for terms in Eq.(11)**
1.	$2n_{CH}\nu\exp\left(\frac{-\delta E_t}{k_B T_s}\right)$	The generation of carbon atoms on the catalyst surface due to thermal dissociation of methyl ions[8]
2.	$2\theta_{CH}\, j_{iA}\, y_d$	Ion -Induced dissociation of CH_4 [8]
3.	$2j_{iA}$	Decomposition of positively charged hydrocarbon ions
4.	$\frac{j_{iA}\sigma_{ads} j_{iB}}{\nu}$	Interaction of hydrocarbon ions with hydrogen ions[10]
5.	j_C	Incoming flux of carbon atoms
6.	j_{iA}	Incoming flux of hydrocarbon ions per unit time onto the catalyst particle
7.	$\frac{j_{iA}\sigma_{ads} j_H}{\nu}$	Interaction of adsorbed type A ions with atomic hydrogen from plasma[8]
8.	$j_{iA}(1-\theta_t)$	Adsorption of hydrocarbon ions onto the catalyst-substrate surface[10]
9.	$j_{iA}\exp\left(\frac{-\delta E_t}{k_B T_s}\right)$	Thermal dissociation of CH_4 [8]

10.	$\frac{D_S \times 2\pi r_{ct}}{\pi r_{ct}^2 \rho_{ct}}$	The surface diffusion of various species across the catalyst nanoparticle per unit area per unit mass density[8]
11.	$\gamma_{CH_4} \pi r_{ct}^2 n_{CH_4} ctcys$	Accretion of neutral methane atoms to the cylindrical surface of CNT[20]

Table 4. Explanation for all the terms used in Eq.(12)

S.No.	**The Mathematical Expression for terms in Eq.(12)**	**The detailed explanation for terms for terms in Eq.(12)**
1.	$j_{iB} \exp\left(\frac{-E_b}{k_B T_s}\right)$	Hydrogen atom diffusing into catalyst - substrate surface [8]
2.	$j_{iB} \exp\left(\frac{-\delta E_{th}}{k_B T_s}\right)$	Incoming flux of hydrogen due to the dehydrogenation of CH_4[10]
3.	$j_{iB}(1-\theta_t)$	Adsorption of hydrogen ions to the catalyst - substrate surface[8]
4.	j_{iB}	Decomposition of hydrogen ions
5.	$\theta_{CH} j_{iB} y_d$	Ion induced dissociation of CH_4 [10]
6.	$\theta_{CH} \nu_0 \nu \exp\left(\frac{-\delta E_i}{k_B T_s}\right)$	Incorporation of hydrogen ions due to thermal decomposition of hydrocarbon ions[8]
7.	$h(\tau)$	Height of CNT at time τ
8.	n_{iB}	Number density of type B ions i.e., hydrogen ions

7.4: Numerical Result and Discussions

This chapter introduces a theoretical model for the intellect of the CNT growth on the catalyst-substrate surface in reactive plasma. Reactive Plasma is composed of multiple reactive species that continually transform into each other and new species because of numerous chemical reactions in ionized form. Since during nanostructure synthesis there are numerous processes involved like ionization, recombination, dissociation, etc. we, therefore, consider reactive plasma in our present model instead of the multi component plasma.

We assume that firstly the applied plasma power creates active species plasma, which dissociates the catalyst particle into nano clusters needed for CNTs nucleation and growth. In a plasma medium, processes such as ionization (in which a neutral atom gives rise to an ion) and recombination (of an ion with an electron results in a neutral molecule), adsorption (absorption on the surface), desorption of ionic species, thermal dehydrogenation (removal of hydrogen), evaporation and their diffusion (surface) into catalyst surface and sticking of neutral atoms to the CNT surface takes place. The substrate-catalyst surface is in contact with the plasma, therefore the inevitable plasma sheath is molded close to the surface in contact with the plasma. Due to plasma sheath, the electric field is directed from plasma bulk towards the surface that accelerates the ions towards the surface, and then the effect of sheath on electron and ion collection current to the CNT surface has been taken into account in the present model.

The calculations have been formed to investigate the dependence of the height and radius of the CNT on the plasma parameters (i.e., ion density and temperature of both type A and B ions) by simultaneous solution of Eqs.1 to 12 at appropriate boundary conditions viz.,

For CH_4 plasma, using values from Herrebout *et al*. [21], boundary conditions

$\tau = 0$, ion number density (n_{iA0}=0. $6n_{e0}$) and $n_{iB0} = 0.4n_{e0}$, neutral atom density (n_{A0}=n_{B0}= $1x10^{15}$ cm^{-3}), electron number density (n_{e0} =$1.12x10^{10}$ cm^{-3}), electron temperature (T_{e0}) =1.15eV, ion temperature (T_{i0}) =2100K, neutral temperature (T_{n0}) =2000 K, mass of ion A m_{iA}=14 amu and 15 amu (e.g., Methyl (CH_3^+ or CH_2^+), mass of ion B $\left(m_{iB}\right)$ =1amu, coefficient of recombination of electrons and ions$\left(\alpha_{A0} \approx \alpha_{B0}\right)$ =$1.12X10^{-7}cm^3$/sec, ,κ= -1.2 and density of Ni$\left(\rho_P\right)$= 8.908 g/cm^3. Other parameters used in the calculation are substrate temperature (T_s) =500 ^{0}C, thermal energy barrier on the catalyst surface $\delta\varepsilon_t$ =1.3eV, energy barrier for bulk diffusion E_b=1.6eV, energy due to thermal decomposition of methyl ions $\delta\varepsilon_i$ =300eV , dissociation energy ε_{dis} = 4.35eV of C_2H_2 (Mehdipour *et al.*[10]) or CH_4 in our case.

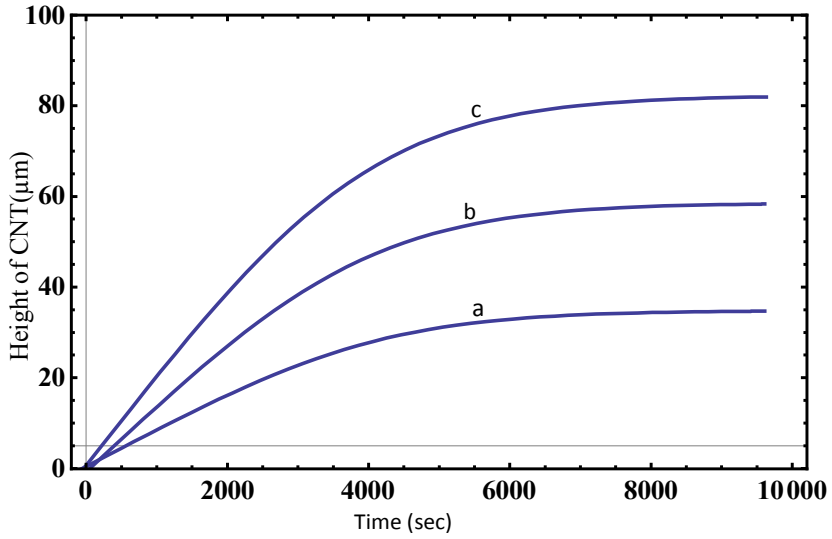

FIG.2. Depicts the time evolution of the height of CNT for different ion density and temperature of type A (hydrocarbon) (where a, b and c corresponds to n_{iA0}= 10^9 $cm^{-3}$and T_{i0} =1800K, n_{iA0}= $5x10^{10}$ $cm^{-3}$and T_{i0} =2000K and n_{iA0}= 10^{11} $cm^{-3}$and T_{i0} = 2100K,respectively). The other parameters are given in the text.

Fig.2 illustrates the time evolution of the height of CNT for different ion density and temperature of type A (hydrocarbon) (i.e., n_{iA0}= 10^9 cm^{-3} and T_{i0} = 1800K, n_{iA0}= $5x10^{10}$ cm^{-3} and T_{i0} = 2000K, and n_{iA0}= 10^{11} cm^{-3} and T_{i0} = 2100K). The Fig. 2 indicates that the height of CNT ncreases as ion density and temperature increases. This is imputable to the fact that as temperature T_{i0} and density n_{i0} increases, the plasma sheath thickness increases and ions gain more energy on communicating through the sheath, consequently the energized ion diffusion to catalyst particle increase thereby increasing the height of CNT. The similar pattern of variance of the height of CNT with time as obtained in Fig.2 has also been obtained by Futaba *et al*. [22] (cf. Fig.2a of Futaba *et al.* [22]) and Loffler *et al*. [4] (cf. Fig.4 of Loffler *et al.* [4]).The observations of Fig.2 are in principle with the experimental observations of Aksak *et al*. [3].

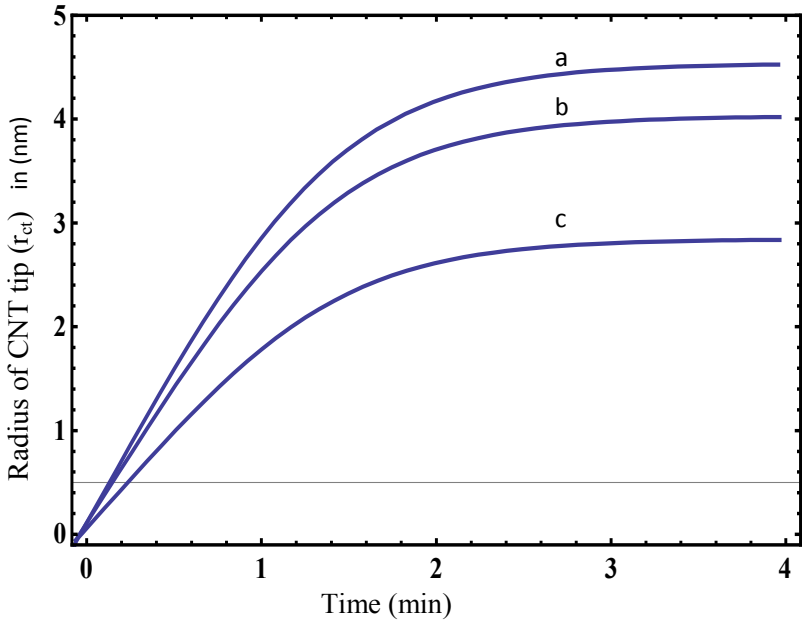

FIG.3. Depicts the time evolution of the radius of the CNT tip for different ion density and temperature of type B(hydrogen) (where a, b and c corresponds to n_{iB0}= 10^9 $cm^{-3}$and T_{i0} =1800K, n_{iB0}= $5x10^{10}$ $cm^{-3}$and T_{i0} = 2000K and n_{iB0}= 10^{11} $cm^{-3}$and $T_{i\,0}$ = 2100K, respectively).

Fig.3 illustrates the time evolution of the radius of the spherical CNT tip for the different ion density and temperature of type B (hydrogen) ions (i.e., n_{iB0}= 10^9 cm^{-3} and T_{i0} = 1800K, n_{iB0}= $5x10^{10}$ cm^{-3} and T_{i0} =2000K ,and n_{iB0}= $10^{11}cm^{-3}$ and T_{i0} = 2100K). The Fig.3 indicates that the radius of CNT decreases as ion density and temperature of hydrogen ions increases. This is imputable to the fact that the tip of CNT is bombarded by incoming hydrogen ions, which etches up the tip of CNT, and thus shortening the radius of the spherical CNT tip. At higher temperatures and density, energy is sufficient to dissociate methane gas into carbon and hydrogen ions, where carbon contributes to the length of CNTs, hydrogen effectively shapes the nanoparticle tip radius. The reason why we have not looked at the surface diffusion of hydrogen onto catalyst nanoparticle is that the activation energy for surface diffusion of hydrogen to Ni is

greater than the activation energy in PECVD (~0.23 eV) (Hoffmann *et al.*[23]). The results of Fig.3 comply with the works of Denysenko *et al.* [8], Mehdipour *et al.* [12].

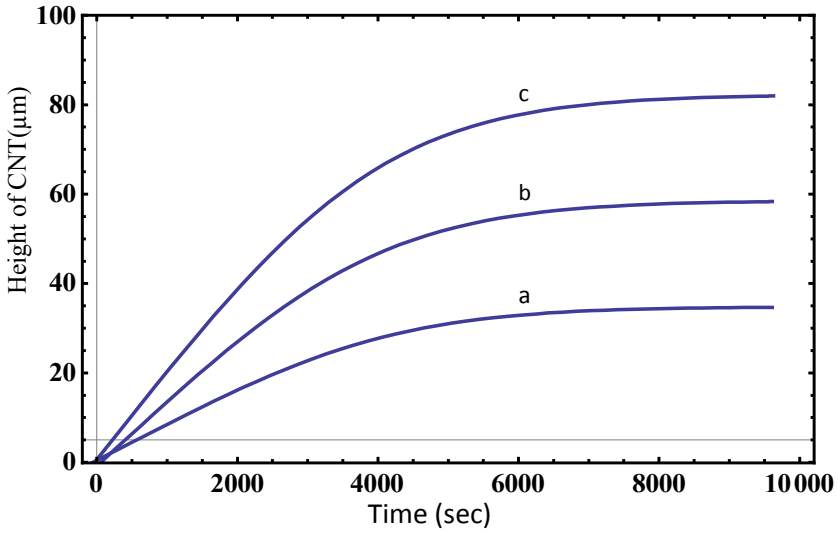

FIG.4. Depicts the time evolution of the height of CNT for different substrate bias (where a, b and c corresponds to U_s = -50V,-100Vand-200V, respectively).

Fig.4 illustrates the time evolution of the height of CNT for different substrate bias (U_s) (i.e., U_s = -50V, -100Vand -200V). As the negative substrate bias is increased, more negative charge develops on the CNT (see Fig. 5 of the present discussion) which in turn thickens the plasma sheath and therefore increases the diffusion and accretion of ions on CNT surface.

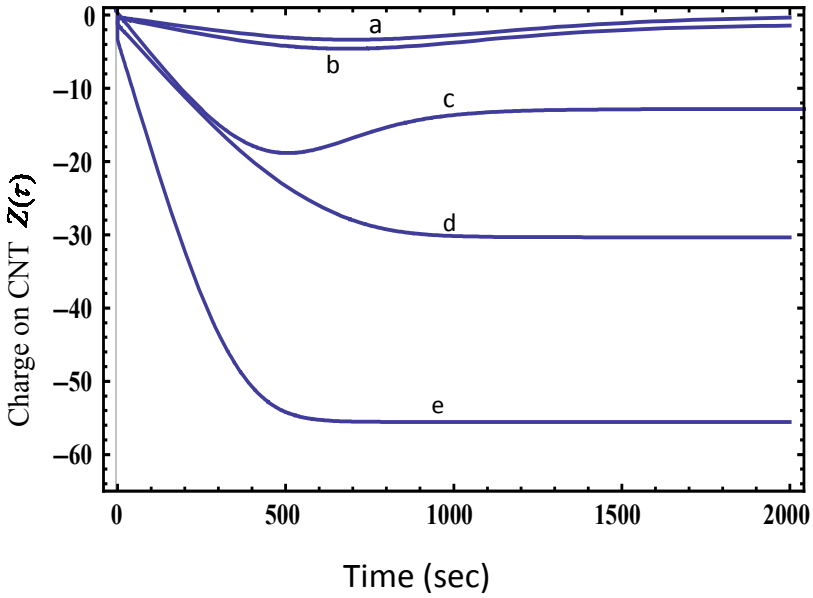

FIG. 5. Depicts the time evolution of charge on CNT for different substrate bias (where a, b, c, d and e corresponds to U_s = -25V, -50V, - 100V,-150V and –200V ,respectively).

Fig. 5 depicts the time evolution of charge on CNT for different substrate bias (e.g., U_S = -25V, -50V, -100V, -150V and -200V). From the Fig. 5 we see that the charge developed on the CNT increases with the substrate bias. Ostrikov *et al.* [26] have also discussed the importance of charge variation effects on particles in plasma.

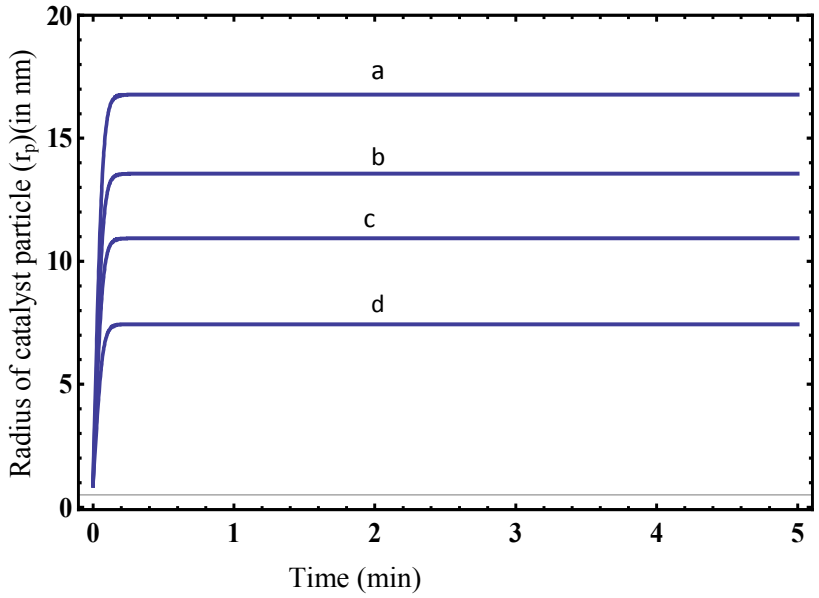

FIG. 6. Depicts the time evolution of the radius of catalyst particle for different rf plasma power (where a, b, c and d corresponds to rf power = 50W, 100W , 150W and 200 W).

Fig. 6 illustrates the variation of the radius of catalyst particle with rf power (i.e. rf power = 50W, 100W, 150W and 200 W). It shows that as the rf power is increased catalyst nanoparticle of smaller radii is observed. The fluctuation may be that with increasing plasma power the electric field in the plasma sheath increases, which in turn increases the ion bombardment to catalyst particle and thereby etching up catalyst particle. The increased plasma power dissociates the hydrocarbon gas in the plasma bulk rather than at the catalyst particle site. The above observation has been validated by the works of Abdi *et al.* [5] and Srivastava *et al*. [24] .

As, plasma treatments better the field emission characteristics[12-13], from the present study, we can conclude that by suitably varying ion density and temperature ,and substrate bias, we can obtain more heighted

and lesser radii nanotubes i.e., CNTs with high aspect ratio. Hence, the results can be extended to better the field emission characteristics of CNTs.

References

[1] K. Ostrikov and S. Xu, *Plasma Aided Nanofabrication* (Wiley-VCH Verlag GmbH & Co. KGaA, 2007).

[2]Young Chul Choi, Young Min Shin, Young Hee Lee and Byung Soo Lee Gyeong-Su Park W. B. Choi, N.S. Lee, and J. M. Kim, Appl. Phys. Lett. **76**, 2367(2000).

[3] M. Aksak, S. Kir and Y. Selamet, J. Optoelectronics &Adv. Mat. Symposia **1**, 281(2009).

[4] R. Loffler, M. Haffner, G. Visanescu, H. Weigand, X. Wang, D. Zhang, M. Fleischer, A. J. Meixner, J. Fortagh, and D. P. Kern, Carbon **49**, 4197 (2011).

[5]Y. Abdi, E. Arzi and S. Mohajerzadeh, NanoMat. Nanotech. **44**, 149 (2008).

[6] H. Jin Cho , N. Lee ,I. Jang , H. Soo Uh and J. Pyo Hong, J. Korean Phys. Soc. **50**,1848(2007).

[7] S.K. Srivastava , V.D. Vankar, V. Kumar , Nano-Micro Lett. **2**,46(2010).

[8] I. Denysenko, K. Ostrikov, M. Y. Yu, and N. A. Azarenkov, J. Appl. Phys.**102**, 074308 (2007).

[9] I. Levchenko, K. Ostrikov, J. Khachan, S. V.Validimrov, Phys. Plasmas **15**, 103501(2008).

[10] H. Mehdipour, K. Ostrikov and A. E. Rider, Nanotech. **21**, 455605 (2010).

[11] K. Ostrikov, E.C. Neyts and M. Meyyappan, Adv. Phys. **62**,113 (2013).

[12] T Feng, J. Zhang ,Q. Li , Physica E. **36**, 28 (2007).

[13] S.F. Lee, Yung-Ping Chang and Li-Ying Lee, J. Mater. Sci. Mater.

Electron **20**, 851(2009).

[14] V. I. Merkulov, D. H. Lowndes, Y. Y. Wei, G. Eres, and E. Voelkl, Appl. Phys. Lett. **76**, 3555 (2000).

[15] Walt A. de Heer, A. Chatelain, D. Ugarte, Science **270**, 5239(1995).

[16] Jong Min Kim, Won Bong Choi , Nae Sung Lee, Jae Eun Jung, Diamond and Related Mat. **9**, 1184 (2000).

[17] Li Yukui, Zhu Changchun, Liu Xinghui, Diamond and Related Materials **11,**1845(2002).

[18] M.A. Liberman and A.J. Litchenberg, *Principles of Plasma Discharge sand Materials Processing*(Wiley Interscience publication, U.S.A. , 1994).

[19] O. A. Louchev, C. Dussarrat and Y. Sato, J. Appl. Phys. **86**,1736(1999).

[20] M. S. Sodha , Shikha Misra, S. K. Mishra, Sweta Srivastava, J. Appl. Phys. **107**,103307(2010).

[21] D. Herrebout , A. Bogaerts , M. Yan and R. Gijbels ,J Appl. Phys. **90**,570 (2001).

[22] Don N. Futaba, K. Hata, T. Yamada, KK. Mizuno, M. Yumura and S. Iijima, Phys. Rev. Lett. **95**, 056104 (2005).

[23] S. Hofmann, C. Ducati, J. Robertson and B. Kleinsorge, Appl. Phys. Lett. **83**, 135 (2003).

[24] S. K. Srivastava, A. K. Shukla, V. D. Vankar, and V. Kumar, Thin Solid Films **492**, 124 (2005).

[25] I.Denysenko and K. Ostrikov, J. Phys. D: Appl. Phys. **42**, 015208 (2009).

[26] K. N. Ostrikov, M. Y. Yu, S. V. Vladimirov, and O. Ishihara, Phys. Plasmas **6**, 737 (1999).

CHAPTER 8

THEORETICAL MODELING OF TEMPERATURE DEPENDENT CATALYST-ASSISTED GROWTH OF CONICAL CARBON NANOTUBE TIP BY PLASMA ENHANCED CHEMICAL VAPOR DEPOSITION PROCESS

8.1: A brief outline of the work done in the present chapter

The present chapter examines the effect of substrate temperature on the growth of the carbon nanotube (CNT) with conical tip assisted by the catalyst in reactive plasma. The model developed in chapter 7 is employed to underline the importance of substrate temperature on the growth of CNT. The work aims to investigate the mechanism by which feedstock gas in PECVD chamber leads to an increase in substrate temperature and the effect of increase of substrate temperature on the growth rate of CNTs.

8.2: Introduction

Carbon nanotubes (CNTs) prepared by PECVD are vertically aligned [1-2] which can be either free standing or forest like. CNTs are expected to have lesser growth temperatures than those by chemical vapor deposition (CVD) as in PECVD the plasma dissociates the feedstock gas, so more and more number of carbon radicals and higher stable hydrocarbons become readily available for nanotube growth [3]. In recent years, during the growth of CNTs by PECVD, an external heating source beneath the substrate has been used for substrate heating [1, 2, 4]. There have been works, where the external source for the substrate heating was not used [5-7]. Teo *et al.* [7] have synthesized straight and well-aligned carbon

nanofibres (CNF) by a substrate exposed to the plasma in a simple, parallel plate dc PECVD reactor for nanotube growth and it heats up to high temperatures (700 °C) without the aid of an external heater.

The temperature has been identified to play an important role in the catalyst-assisted growth of CNTs. Numerous works have been done to highlight the role of temperature on the growth of CNTs [8-15].

Han *et al.* [8] have demonstrated that as the growth temperature increases, the average diameter of CNTs increased from 40 nm to110nm and the growth rate was enhanced from 2 μm/h to 15 μm/h. Baratunde *et al.* [9] have shown that as the growth temperature was decreased, the associated decrease in CNT density and average CNT diameter resulted in an increased thermal resistance at the interface. Lee *et al.* [10] have demonstrated that the growth rate and the average diameter increase nonlinearly with temperature. The growth rate enhances from 1.6 μm/min by a factor of 18 and the average diameter increases from 20 to 150 nm for the temperature rise of 800 to 1100 °C.

Loffler *et al.* [11] have shown that at higher temperatures of the substrate and catalyst the hydrocarbon gas dissociates faster, aided by the catalyst. A higher diffusion rate of carbon atoms through the catalytic particle can be expected, which results in considerably longer CNTs at the same growth time.

The motivation for the work in the present chapter stems from the recent studies where the dependence of growth rate of nanostructures on various parameters including substrate temperatures, electron and ion densities, the flux ratio of etching and hydrocarbon ions etc. has been widely investigated [12-15].

Denysenko *et al.* [12] have shown that at low substrate temperatures (1000 K), the atomic hydrogen and ion fluxes from the plasma could strongly influence CNT growth. Mehdipour *et al.* [13] have studied the growth rate of carbon nanofibre as a function of substrate temperature for different electron and ion temperatures. They have observed that the growth rate as a function of substrate temperature increases as ion and electron temperatures are increased. Denysenko and Ostrikov [14] have described the plasma-assisted growth of carbon nanofibres (CNFs) that accounts for the nanostructure heating by ion and etching gas fluxes from the plasma. They have shown that fluxes from the plasma environment can substantially increase the temperature of the catalyst nanoparticle located on the top of the CNF with respect to the substrate temperature. Burmaka *et al.* [15] have shown that the growth rates of SWCNT array and the film between the nanotubes, as well as the length of SWCNTs can be successfully controlled by adjusting neutral and ion fluxes to the nanotubes, SWCNT surface temperature and the penetration depths of the neutral and ionic species.

Tips of CNT grown by PECVD are seen to have various shapes. Conical tip CNTs have been obtained by many researchers. [16-18].

Srivastava *et al.* [16] have obtained films containing randomly oriented conical CNTs with varying length and density grown on silicon (Si) substrates by microwave plasma enhanced chemical vapor deposition (MPECVD) process at relatively low temperature by judicious control of the process parameters such as microwave power and growth time.

A model describing the mechanism of the growth of carbon nanotube in a plasma medium assisted by the catalyst–substrate surface was developed in Chapter 7. In the previous chapter, the substrate temperature was taken

as a constant during the growth process. In the present chapter, we shall investigate the effect of substrate temperatures on the catalyst-assisted growth of the CNT (both the cylindrical CNT surface and conical CNT tip) in the reactive plasma medium.

The equations and the underlying physics behind the equations would be same as in Chapter 7 except that instead of spherical tip of CNT we shall now consider conical CNT tip and substrate temperature would not be a constant.

8.3: MODEL

Consider a catalyst particle of nickel (Ni) over the substrate of Si in a plasma chamber. The plasma is composed of ions of acetylene (C_2H_2) and hydrogen (H_2), neutrals of acetylene and hydrogen, and electrons. The ions of acetylene and hydrogen are designated as A and B ions, respectively. In Argon (Ar) + H_2+C_2H_2 plasma, C_2H_2 acts as a carbon source gas, H_2 acts as etching gas and Ar is the carrier gas.

The main processes for the CNT growth over the catalyst-substrate surface in plasma that are considered in the present model are detailed below:

1. It is assumed that the applied plasma power ionizes the gas within the chamber, thereby creating plasma species of relatively higher energy. These highly energetic ions initiate the fragmentation of catalyst particle to form catalyst nanoparticle, which then seed nanotube growth on them.
2. The acetylene ions traverses through the plasma sheath to the catalyst-substrate surface and then thermal dissociation, ion induced dissociation, decomposition of positively charged ions, interaction of adsorbed acetylene ions with atomic hydrogen from

plasma , and thermal dissociation of carbon source gas of acetylene ion and other processes, occurs to finally result in the adsorption , surface diffusion and accretion of acetylene neutrals to determine the height of growing CNT.

3. Then, there is decomposition of positively charged hydrogen ions, incorporation of hydrogen ions due to thermal dissociation of acetylene ions, and the accretion of hydrogen ions into catalyst - substrate surface. The hydrogen ions effectively shape the nanoparticle tip due to etching effects.

In Table 1 , the assumed processes in the model that occur during CNT growth in a PECVD chamber with their corresponding terms are given.

Table 1. Outline of the main processes during the growth of catalyst-assisted CNT in the plasma medium, considered in the present model.

Assumed processes in the model that occur during CNT growth in a PECVD chamber	**Corresponding Terms**
1.Thermal dissociation of C_2H_2 ions [13]	$2n_{CH}\nu\exp\left(\frac{-\delta E_t}{k_B T_s}\right)$
2. Ion induced dissociation of C_2H_2 [13]	$2\theta_{CH} j_{iA} y_d$
3. Decomposition of positively charged acetylene ions [13]	$2j_{iA}$
4. Interaction of acetylene ions with atomic hydrogen [14]	$\frac{j_{iA}\sigma_{ads} j_{iB}}{\nu}$
5. Incoming flux of carbon atoms [13]	j_c
6. Adsorption of C_2H_2 ions to the catalyst-substrate surface [13]	$j_{iA}(1-\theta_t)$
7. Thermal dissociation of C_2H_2 [13]	$j_{iA}\exp\left(\frac{-\delta E_t}{k_B T_s}\right)$
8. Accretion of neutral acetylene atoms to the cylindrical surface of CNT	$\gamma_{C_2H_2}\pi r_P^2 n_{C_2H_2} ctcys$

9. Diffusion of hydrogen atom into catalyst-substrate surface[13]	$j_{iB}\exp\left(\frac{-E_b}{k_B T_s}\right)$
10. Incoming flux of hydrogen due to the dehydrogenation of C_2H_2[13]	$j_{iB}\exp\left(\frac{-\delta E_{th}}{k_B T_s}\right)$
11. Adsorption of hydrogen ions to the catalyst-substrate surface[14]	$j_{iB}(1-\theta_t)$
12. Decomposition of hydrogen ions[14]	j_{iB}
13. Ion induced dissociation of hydrogen [13]	$\theta_{CH} j_{iB} y_d$
14. Incorporation of hydrogen ions due to thermal decomposition of acetylene ions[13]	$\theta_{CH}\nu_0\nu\exp\left(-\frac{\delta E_i}{k_B T_s}\right)$
15. Accretion of neutral acetylene atoms to the conical tip of CNT	$\gamma_{C_2H_2}\pi r_{conct}^2 n_{C_2H_2 conct}$
16. Adsorption flux of acetylene ions and hydrogen ions to catalyst-substrate surface[19]	$J_{aij}=\frac{P_i}{\left(2\pi m_{ij}k_B T_{ij}\right)^{\frac{1}{2}}}\times\frac{n_{ij}}{j_{ij}}$
17. Desorption flux of acetylene ions and hydrogen ions from catalyst-substrate surface[19]	$J_{desorptionj}=n_{ij}\nu\left(-\frac{\varepsilon_{ai}}{k_B T_{ij}}\right)$
18. Ion collection current to the CNT(both conical tip and cylindrical surface)	$n_{iBconcts}+n_{iBcysct}$ or $n_{iAconcts}+n_{iAcysct}$
19. Neutral collection current to the CNT(both conical tip and cylindrical surface)	$n_{Bconcts}+n_{Bcysct}$ or $n_{Aconcts}+n_{Acysct}$

A. The sheath equations

The electric field is directed towards z- axis.

i) The continuity equation,

$$\left(\hat{i}\frac{\partial}{\partial x}+\hat{j}\frac{\partial}{\partial y}+\hat{k}\frac{\partial}{\partial z}\right).\hat{k}(n_j u_j)=\nu_{iz}n_e, \qquad (1)$$

where

n_e= number density of electron (in cm^{-3}),

ν_{iz}= ionization frequency (in sec^{-1}),

u_j = fluid velocity of electrons, $C_2H_2^+$, Ar^+ and H^+ (in cm/sec),

n_j = number density of electrons, $C_2H_2^+$, Ar^+ and H^+(in cm^{-3}),

ii) The ion momentum balance equation

$$Mn_j u_j \frac{du_j}{dz} = en_j E - Mn_j \nu_{jn} u_j, \tag{2}$$

where M is the mass of ions in plasma (in gm), ν_{jn} is the collision frequency (in sec^{-1}) and E is the electric field (in StatV/cm) .

iii) Using Poisson's equation, we determine potential within the sheath

$$\frac{d^2\phi}{dz^2} = -4\pi \sum q_j \delta_j n_j, \tag{3}$$

where $\delta_j = \left(\frac{n_{ij}}{n_e}\right)$ is the j[th] ion to electron number density ratio and is dimensionless and ϕ is the electrostatic potential , $\sum_j \delta_j = 1$,and $0 < \delta_j < 1$ as electron density is greater in plasma bulk than in the sheath.

B. Energy balance equation for catalyst particle

Initially, a catalyst particle nickel (Ni) of radius 30 nm is considered to be placed over a silicon (Si) substrate surface. It is assumed that the applied rf power creates plasma species of higher energy such that these highly energetic ions then accretes at the surface of catalyst particle and any increase in their number density and temperature results in catalyst particles of smaller radii. Therefore, the Eq. (4) describes the

fragmentation of a catalyst particle into catalyst nanoparticle of smaller radii.

The basis of our assumption for developing Eq.(4) follows from Srivastava *et al*. [20] as they have highlighted that an increase in microwave power causes more ionization of the gas, which increases the density of plasma species of relatively higher energy. Following experimental results of Srivastava *et al*. [20], we assume that as the applied rf power increases, it ionizes the gas more which creates more energetic ions, which implies that plasma species of relatively higher energy are created. Since, energy of ions corresponds to the number density and temperature of ions so we assume that with an increase in rf power the number density and temperature of plasma species increases.

$$rf\ power = \frac{d}{d\tau}\left(C_p m_p T_S\right) = \left[n_{iActP}\left(\varepsilon^S{}_{iAc} + I_{pA}\right) + n_{iBctP}\left(\varepsilon^S{}_{iBc} + I_{pB}\right)\right] - \left(\frac{3}{2}k_B\right)\left[\left(1-\gamma_{iA}\right)n_{iActP} + n_{iBctP}\right]T_S - 4\pi r_P^2 \varepsilon\sigma(T_s^4 - T_a^4), \tag{4}$$

where

$m_P\left(=\frac{4}{3}\pi r_P^3 \rho_P\right)$ is the mass of catalyst particle (in gm), r_p is the radius of catalyst particle (in nm). ρ_P is the mass density of catalyst particle(in gm/cm^3), C_p is the specific heat of catalyst particle (Ni) and is 0.44KJ/Kg^{0}K and T_s is the substrate temperature (in ^{0}C) . I_{pA} and I_{pB} are the ionization energies of atoms A (acetylene) and B (hydrogen), respectively and (in eV). T_a is the ambient temperature and (in K). ε is the emissivity of the material of the catalyst (dimensionless) and σ is the Stefan–Boltzmann constant and (in erg cm^{-2} s^{-1}K^{-4}).

In the present chapter we assume, that the applied rf power not only ionizes the feedstock gas in the chamber but also heats up the substrate as well and Eq.(4) governs the variation of substrate temperature. The substrate and catalyst temperature are assumed to be the same.

$\varepsilon_{ijc}^{s}(Z)\left\{=\left[\left(\frac{2-Z\gamma_{ji}}{1-Z\gamma_{ji}}\right)-Z\gamma_{ji}\right]k_B T_{ij}\right\}$ are the mean energy(in eV) collected by the ions j (where, j refers to ion A (acetylene) or B (hydrogen)) at the surface of the catalyst particle [21], $\gamma_{ji}=\left(\frac{e^2}{r_P k_B T_{ij}}\right)$ and is dimensionless ,and e being the electronic charge (in StatC).

$$n_{ijctP}=\pi r_P^2\left(\frac{8k_B T_i}{\pi m_{ij}}\right)^{\frac{1}{2}} n_{ij}(z)\left[1-Z\gamma_{ji}\right]\exp\left[-\frac{E_b}{k_B T_s}\right]\exp\left[-\frac{eU_s}{k_B T_s}\right]$$

is the ion collection current at the surface of catalyst particle, (where, j refers to ion A or B) [22] (in sec^{-1}) .

In Solving Eq. (4), we consider that at rf power of 100W, and at τ=0 the ion densities (n_{iB0}= n_{iA0}) =$10^9 cm^{-3}$, ion temperature (T_{i0}) =2100 K, T_s= 550 ^{0}C, energy barrier for bulk diffusion (E_b) =1.6 eV , substrate bias (U_s) = -50V, and catalyst particle radius (r_{P0})= 30 nm in expression for n_{iActP} and n_{iBctP}, we can calculate n_{iActP0}, n_{iBctP0}.

Now, by using the calculated values of n_{iActP0} and n_{iBctP0} and the other parameters i.e., ε_{iAc}^{s} = 8.2 eV, ε_{iBc}^{s} = 13.2 eV, I_{pA}=11.87eV, and I_{pB} =9.7eV in Eq. (4) we can get the value of catalyst particle radius r_P (in nm) and its temperature T_s (in ^{0}C) at any time τ (in sec).

The Eq. (4) denotes the influence of rf power on the mass of catalyst particle for specific heat and substrate temperature. The first term on the

right side of Eq. (4) is the rate of energy transferred to the catalyst particle due to the ions collected at the surface of catalyst particle because of ionization of neutral atoms A and B and mean energy collected by the ions at the surface of catalyst particle. The second term is due to the sticking accretion of ion A (acetylene) and B (hydrogen) at the catalyst particle site. The last term on the right side of Eq. (4) is the rate of energy dissipation of the catalyst particle through radiation and conduction to the host gas.

The resulting value of catalyst nanoparticle at time τ serves as the initial base radius of the cylindrical part of nanotube.

C. Growth rate equation of the curved surface area of CNT

$$r_P \frac{d(2\pi h)}{d\tau} = \left(\left\{ 2n_{CH} \nu \exp\left(\frac{-\delta E_t}{k_B T_s}\right) + 2\theta_{CH} j_{iA} y_d + 2j_{iA} + \frac{j_{iA}\sigma_{ads} j_{iB}}{\nu} + j_c \right\} m_c + \right.$$

$$\left. \left\{ j_{iA}(1-\theta_t) + \frac{j_{iA}\sigma_{ads} jH}{\nu} + j_{iA} \exp\left(\frac{-\delta E_t}{k_B T_s}\right) \right\} m_{iA} \right) \times \frac{D_S \times 2\pi r_P}{\pi r_P^2 \rho_{ct}} \left(\frac{1}{n_{iActcys}} \right) +$$

$$\gamma_{C_2H_2} \pi r_P^2 \, n_{C_2H_2 ctcys}, \tag{5}$$

$$\frac{d(\pi r_{conct} l)}{d\tau} = \left(j_{iB} \exp\left(\frac{-E_b}{k_B T_s}\right) + j_{iB} \exp\left(\frac{-\delta E_{th}}{k_B T_s}\right) + j_{iB}(1-\theta_t) + j_{iB} + \theta_{CH} \left(j_{iB} y_d + \nu_0 \nu \exp\left(\frac{-\delta E_i}{k_B T_s}\right) \right) \right) \frac{h(\tau)}{n_{iB}} +$$

$$\gamma_{C_2H_2} \pi r_{conct}^2 \, n_{C_2H_2 conct}, \tag{6}$$

Since the opening angle (θ) [23] of conical CNT tip is 45^0 the slanted length (l) of conical CNT tip becomes

$$l = \left(h'^2 + r_{conct}^2 \right)^{\frac{1}{2}}$$

h' is the height of conical CNT tip

$$\tan\theta = \frac{r_{conct}}{h'}$$

Since θ is 45^0,

$$l = \sqrt{2r^2_{conct}} = \sqrt{2}\, r_{conct},$$

The symbols and terms in Eq.(5) are described in Table 2 and 4, respectively.

The symbols and terms in Eq.(6) are described in Table 3 and 5, respectively.

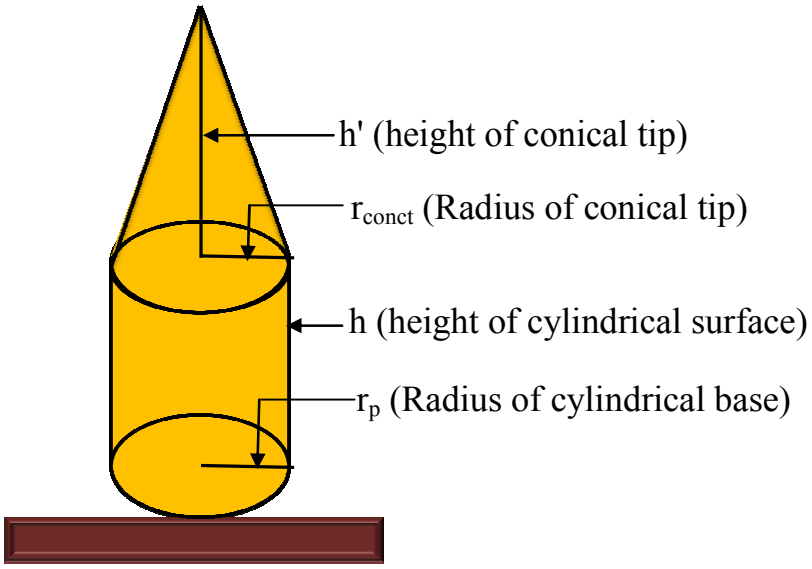

Fig. 1. Schematic of cylindrical CNT with conical tip

Table 2. Explanation for all the symbols used in Eq. (5)

S.No.	The notation of various symbols used in Eq.(5)	The explanation for symbols in Eq.(5)
1.	$n_{CH} = \theta_{CH}\nu_0$ (in cm^{-2})	The number density or concentration of CH (CH denotes C_2H_2 species) [13]
2.	$\nu_0 \approx 1.3\times10^{15} cm^{-2}$	The number of adsorption sites per

		unit area[14]
3.	$j_c=n_c v_{thc}/4$ (in cm^{-2} sec^{-1})	Ion flux of carbon atoms[13]
4.	v_{thc} (in cm/sec)	Thermal velocity of carbon atoms[14]
5.	$j_{iA}=n_{iA}(k_B T_i/ m_{iA})^{1/2}$ (in cm^{-2} sec^{-1}) and $j_{iB}=n_{iB}(k_B T_i/ m_{iB})^{1/2}$(in cm^{-2} sec^{-1})	Ion flux of type A(hydrocarbon) and B(hydrogen), respectively
6.	$y_d \approx \varepsilon_{icH} / \varepsilon_{dis}$ (dimensionless)	Ratio of kinetic energy associated with the motion of hydrocarbon ions impinging on the substrate to dissociation energy of C_2H_2 [13]
7.	n_{iB} (in cm^{-3})	Number density of type B ions i.e., hydrogen ions
8.	ε_{icH} (in eV)	Kinetic energy associated with the motion of hydrocarbon ions impinging on the substrate[13]
9.	ε_{dis}(in eV)	Dissociation energy of C_2H_2
10.	$\sigma_{ads} \approx 6.8 \times 10^{-16} cm^2$	Cross section for the reactions of atomic hydrogen with adsorbed particles[14]
11.	D_s and $\left[D_S = D_{s0} \exp(-E_S / k_B T_S)\right]$ $D_{s0} = \nu a_0^2$ is a constant (in $nm^{-2}sec^{-1}$)	Surface diffusion coefficient[13]
12.	E_s=0.3eV	Energy barrier for diffusion of carbon (C) on the catalyst[14]
13.	a_0 =0.34 nm	Inter atomic distance between carbon atoms
14.	θ_t (dimensionless)	Total surface coverage[13]
15.	$\delta\varepsilon_t$ =1.3eV	Energy due to thermal dissociation [14]
16.	$\gamma_{C_2H_2}$(dimensionless)	Sticking coefficient of C_2H_2 neutrals

17.	m_c =12 amu	Mass of a carbon atom
18.	m_{iA} = 26 amu	Mass of type A $C_2H_2^+$ (acetylene) ions
19.	h(τ) (in μm)	Height of CNT at time τ
20.	n_{iB} (in cm^{-3})	Number density of type B ions i.e., hydrogen ions
21.	$n_{C2H2ctcys}$ (in sec^{-1})	Acetylene neutral atom collection current at the surface of cylindrical CNT
22.	k_B=1.38x10^{-16} ergs/K	Boltzmann's constant
23.	T_s=500^0C	Substrate temperature
24.	r_{ct}=30nm	Initial radius of catalyst particle
25.	$\rho_{ct} = 8.908 g/cm^3$	Density of nickel (Ni)
26.	$\nu = 10^{13}$ Hz	Thermal vibrational frequency[13]
27.	$n_{iActcys}$ (in sec^{-1})	Ion collection current of hydrocarbon(i.e., A) the surface of cylindrical CNT

Table 3. Explanation for all the symbols used in Eq.(6)

S.No.	**The notation of various symbols used in Eq.(6)**	**The explanation for symbols in Eq.(6)**
1.	$j_{iB} = n_{iB}(k_B T_i / m_{iB})^{1/2}$ (in $cm^{-2} sec^{-1}$)	Ion flux of hydrogen (B ion)
2.	T_i (in K)	Ion temperature
3.	$E_b \approx 1.6eV$	Energy barrier for bulk diffusion[13]
4.	δE_{th} (in eV)	Energy due to dehydrogenation of C_2H_2 [10]
5.	θ_t (dimensionless)	Total surface coverage[13]
6.	h(τ) (in μm)	Height of CNT at time τ
7.	r_{conct}(in nm)	Radius of conical CNT tip

Table 4. Explanation for all the terms used in Eq.(5)

S. No.	The mathematical Expression for terms in Eq.(5)	The detailed explanation for terms in Eq.(5)
1.	$2n_{CH}\nu\exp\left(\frac{-\delta E_t}{k_B T_s}\right)$	The generation of carbon atoms on the catalyst surface due to thermal dissociation of acetylene ions[13]
2.	$2\theta_{CH}{}^{j}{}_{iA}{}^{y}d$	Ion -Induced dissociation of C_2H_2 [14]
3.	$2j_{iA}$	Decomposition of positively charged hydrocarbon ions
4.	$\frac{j_{iA}\sigma_{ads}j_{iB}}{\nu}$	Interaction of hydrocarbon ions with hydrogen ions[13]
5.	j_C	Incoming flux of carbon atoms
6.	j_{iA}	Incoming flux of hydrocarbon ions per unit time onto the catalyst particle
7.	$\frac{j_{iA}\sigma_{ads}j_H}{\nu}$	Interaction of adsorbed type A ions with atomic hydrogen from plasma[13]
8.	$j_{iA}(1-\theta_t)$	Adsorption of hydrocarbon ions onto the catalyst-substrate surface[14]
9.	$j_{iA}\exp\left(\frac{-\delta E_t}{k_B T_s}\right)$	Thermal dissociation of C_2H_2[13]
10.	$\frac{D_S\times 2\pi r_P}{\pi r_P^2 \rho_P}$	The surface diffusion of various species onto the catalyst surface across the catalyst nanoparticle per unit area per unit mass density[13]
11.	$\gamma_{C_2H_2}\pi r_P^2 n_{C_2H_2}{}^{ctcys}$	Accretion of neutral acetylene atoms to the cylindrical surface of CNT[20]

Table 5. Explanation for all the terms used in Eq.(6)

S.No.	The Mathematical Expression for terms in Eq.(6)	The detailed explanation for terms for terms in Eq.(6)
1.	$j_{iB}\exp\left(\frac{-E_b}{k_B T_s}\right)$	Hydrogen atom diffusing into catalyst - substrate surface [13]
2.	$j_{iB}\exp\left(\frac{-\delta E_{th}}{k_B T_s}\right)$	Incoming flux of hydrogen due to the dehydrogenation of C_2H_2[14]
3.	$j_{iB}(1-\theta_t)$	Adsorption of hydrogen ions to the catalyst - substrate surface[13]
4.	j_{iB}	Decomposition of hydrogen ions
5.	$\theta_{CH} j_{iB} y_d$	Ion induced dissociation of C_2H_2 [13]
6.	$\theta_{CH}\nu_0\nu\exp\left(\frac{-\delta E_i}{k_B T_s}\right)$	Incorporation of hydrogen ions due to thermal decomposition of hydrocarbon ions[13]
7.	$h(\tau)$	Height of CNT at time τ
8.	n_{iB}	Number density of type B ions i.e., hydrogen ions
9.	$\gamma_{C_2H_2}\pi r_{conct}^2 n_{C_2H_2 conct}$	Sticking of neutrals of acetylene on the conical tip of CNT.

D.Charge kinetics of the CNT surface

The positive hydrocarbon and hydrogen ion and electron currents at the surface of the CNT contribute to the charge developing on the CNT surface. Over a period of time, the initial negative charge on the CNT would be affected by the accretion of the positive ion and electron collection currents. As expected the positive ion accretion on CNT would decrease the negative charge and after some time the CNT would be positively charged such that further accretion of positive ions on CNT surface increases the positive charge on CNT surface whereas electron

current would depreciate charge on CNT surface. Eq. (7) describes the charge developed on the entire CNT (i.e., the conical tip over the cylindrical surface).

$$Z'[\tau] = n_{iAconcts} + n_{iAcysct} + n_{iBconcts} + n_{iBcysct} - \gamma_e \left(n_{econcts} + n_{ecysct} \right), \tag{7}$$

where

Z is the amount of charge over the entire CNT (i.e., conical tip and cylindrical surface) (dimensionless).

a) For electron on the conical CNT tip:

$n_{econcts} = \pi r_{conct}\, l \left(\frac{8 k_B T_e}{\pi m_e} \right)^{\frac{1}{2}} n_e(z) \exp\left[\frac{Z\alpha_e}{k_B T_e} + \frac{eU_s}{k_B T_s} \right]$ is the electron collection current at the surface of the conical CNT tip (in sec^{-1}) and, r_{conct} is the radius of conical CNT tip (in nm), l is the slant height of conical CNT and $\alpha_e = eV_{con}(z)$ (in eV),

where

$$V_{con}(z) = \sigma \left(\frac{3\sqrt{h'^2 - 2h'z + 2z^2} + (-2h' + 4z) Log\left[\frac{-2h' + 4z + 2\sqrt{2}\sqrt{h'^2 - 2h'z + 2z^2}}{\sqrt{2}} \right]}{4\sqrt{2}\varepsilon_0} \right)$$

Following [23] the potential at a point on the surface of a cone (V_{con} (z)) can be derived by considering a conical surface with uniform surface charge density σ , radius r_{conct} , height h' and slant height l.

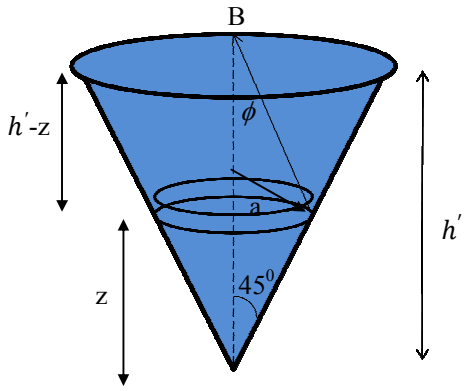

Fig.2. Geometry of the conical tip in the present problem

Considering a small disc at height z with differential height dz, the surface area of disc would be d$a = 2\pi adl$, since the opening angle of disc is 45^0, $\frac{dz}{dl} = Cos\ \frac{\pi}{4}\ or\ dl =\ \sqrt{2}$ dz, the elemental charge on the disc is $dq = \sigma da = 2\sqrt{2}\pi\sigma adz$

The differential electric field, along z-axis at point B due to the disc is given as in [23]

$$dE_{con} = \frac{1}{4\pi\varepsilon_0}\frac{dq}{|r|^2}\hat{r} \tag{8}$$

or

$$dE_{con} = \frac{1}{4\pi\varepsilon_0}\frac{2\sqrt{2}\,\pi\sigma adz}{|r|^2}\hat{r} \tag{9}$$

Now $|r| = \sqrt{(h'-z)^2 + a^2}$ and since cone has opening angle of 45^0 , a=z such that Eq.(9) can be rewritten as

$$dE_{con} = \frac{1}{4\pi\varepsilon_0}\frac{2\sqrt{2}\pi\sigma z dz}{\left((h'-z)^2+z^2\right)} \tag{10}$$

Now, the radial part of the electric field cancel each other and only the vertical component remains such that

$$dE_{conz} = dECos\phi = \frac{1}{4\pi\varepsilon_0}\frac{2\sqrt{2}\pi\sigma z(h'-z)dz}{\left((h'-z)^2+z^2\right)^{\frac{3}{2}}} \tag{11}$$

Integrating Eq. (11) over the entire cone surface

$$E_{con}\,\hat{z} = \frac{\sigma}{\sqrt{2}\varepsilon_0}\int\frac{2\sqrt{2}\pi\sigma z(h'-z)dz}{\left((h'-z)^2+z^2\right)^{\frac{3}{2}}}\,\hat{z} \tag{12}$$

Solving Eq. (12), we get,

$$E_{con}\,\hat{z} = \frac{\sigma\left(-2h'+4z-\sqrt{2}\sqrt{h'^2-2h'z+2z^2}\,Log\left[-2h'+4z-2\sqrt{2}\sqrt{h'^2-2h'z+2z^2}\right]\right)}{4\sqrt{2}\sqrt{h'^2-2h'z+2z^2}}. \tag{13}$$

Now, solving for potential on the surface of a cone

$$V_{con}(z) = -\int_{\infty}^{z} E.dz$$

or

$$V_{con}(z)=\sigma\left(\frac{3\sqrt{h'^2-2h'z+2z^2}+(-2h'+4z)Log\left[\frac{-2h'+4z+2\sqrt{2}\sqrt{h'^2-2h'z+2z^2}}{\sqrt{2}}\right]}{4\sqrt{2}\varepsilon_0}\right)$$

(14)

Moreover,

$n_e(z)=n_{e0}\exp\left[\frac{|e|\phi(z)}{k_BT_e}\right]$ is the electron density in plasma sheath(in cm^{-3}) , $\phi(z)$ is the electrostatic potential (in StatV), n_{e0} is plasma density in bulk(in cm^{-3}) and it decreases towards the substrate, and T_e is the electron temperature(in eV), $\phi(z)=\phi_0\exp\left(-\frac{|z|}{\lambda_d}\right)$ is the negative potential at the surface, and λ_d is the plasma Debye length .

b) For electrons on cylindrical surface:

$n_{ecysct}=n_e(z)\ r_P h\left(\frac{2\pi k_BT_e}{m_e}\right)^{\frac{1}{2}}\exp\left[\frac{eV_S}{k_BT_e}+\frac{eU_S}{k_BT_S}\right]$ is the electron collection current on the cylindrical surface of the CNT(in sec^{-1}) and V_s is the surface potential on the cylindrical surface of the CNT(in StatV) and h is the height of cylindrical surface of the CNT(in μm), m_e is the mass of electron(in gm).

c) For ions on the cylindrical surface:

$$n_{ijcysct}=n_{ij}(z)\ r_P\ h\left(\frac{2\pi k_BT_{ij}}{m_{ij}}\right)^{\frac{1}{2}}\left\{\frac{2}{\sqrt{\pi}}\left(\frac{eV_S}{k_BT_{ij}}\right)^{\frac{1}{2}}+\exp\left[\frac{eV_S}{k_BT_{ij}}\right]erfc\left[\left(\frac{eV_S}{k_BT_{ij}}\right)^{\frac{1}{2}}\right]\right\}$$

$$\exp\left[-\frac{E_b}{k_BT_S}\right]\exp\left[-\frac{eU_S}{k_BT_S}\right]$$

is the ion collection current on the cylindrical surface of CNT(in sec $^{-1}$), T_i is the ion temperature (in K), m_{ij} is the ion mass (j refers to either A or B positively charged ion as explained earlier)(in gm) , E_b is the energy barrier for bulk diffusion $(\approx 1.6eV)$, T_s is the substrate or catalyst temperature (in ^{0}C).

d) For ions on the conical tip surface:

$$n_{ijconcts} = \pi\, r_{conct}\, l \left(\frac{8k_B T_i}{\pi m_{ij}}\right)^{\frac{1}{2}} n_{ij}(z)\left[1-\frac{Z\alpha_i}{k_B T_{ij}}\right]\exp\left[-\frac{E_b}{k_B T_s}\right]\exp\left[-\frac{eU_s}{k_B T_s}\right]$$

is the ion collection current on the conical CNT tip (in sec^{-1}),

$n_{ij}(z) = n_{ij0}\left(1-\frac{2e\phi(z)}{m_{ij}v_{ij0}^2}\right)^{\frac{-1}{2}}$ where $n_{ij}(z)$ is the ion density in plasma sheath (in cm^{-3}) , v_{ij0} is the ion velocity at any point within the plasma (in cm/sec) and $\alpha_i = eV_{con}(z)$

In Eq.(7) , first and second term denotes charge developed on the entire CNT (i.e., the conical tip over cylindrical surface) due to accretion of positively charged ions of acetylene, third and fourth term denotes the charge developed on the entire CNT (i.e., the conical tip over cylindrical surface) due to accretion of positively charged ions of hydrogen. The last term describes the loss in charge due to electron collection current at the surface of the CNT (i.e., the conical tip over cylindrical surface).

E. Stability equation of electron number density

The Eq. (15) represents that the dissociative ionization of neutrals produces ions and electrons hence it increases the number density of electrons in the plasma , whereas recombination of electrons and ions to

produce neutrals and electron collection current to CNT would decrease the electron number density in plasma.

$$\frac{dn_e}{d\tau} = \left(\beta_A n_A + \beta_B n_B\right) - \left(\alpha_A n_e n_{iA} + \alpha_B n_e n_{iB}\right) - \gamma_e n_{ct}\left(n_{econcts} + n_{ecysct}\right)$$

, (15)

where

β_A and β_B are the coefficients of ionization of the constituent neutral atoms of A(hydrocarbon) and B(hydrogen) due to external agency (in sec), and are the coefficients of recombination of electrons and positively charged ions [21] of A(hydrocarbon) and B(hydrogen),respectively where k = -1.2 is a constant ,

$\alpha_A(T_e) = \alpha_{A0}\left(\frac{300}{T_e}\right)^k cm^3/\sec$ and $\alpha_B(T_e) = \alpha_{B0}\left(\frac{300}{T_e}\right)^k cm^3/\sec$,

$\alpha_{A0} = \alpha_{B0} = n_{e0}\times 10^{-7}\left(\frac{1}{T_{e0}}\right)^{-1.2}$ and n_{ct} is the CNT number density (in cm^{-3}).

The terms on the right side of Eq. (15) are the rate of gain in electron density per unit time on account of ionization of neutral atoms, the decaying rate of the electron density due to electron–ion recombination and the electron collection current at the surface of the CNT (conical tip over cylindrical surface).

F. Stability equation of positively charged ion number density

For the positive ions within the plasma , the process considered are that the dissociative ionization of neutrals produces ions and electrons ,thereby the ion's number density increases in plasma bulk , the recombination of ions and electrons to produce neutrals decreases ion number density in plasma bulk. Moreover, the ions collected on the CNT

surface would decrease their number density in plasma bulk, the adsorption of ions on the catalyst-substrate surface decreases their number density in plasma bulk and the ions that are desorped from the catalyst –substrate surface contributes to ion density in plasma bulk.

$$\frac{dn_{iA}}{d\tau} = \beta_A n_A - \alpha_A n_e n_{iA} - n_{ct}\left(n_{iAconcts} + n_{iAcysct}\right) - J_{aiA} + J_{desorptionA}, \tag{16}$$

$$\frac{dn_{iB}}{d\tau} = \beta_B n_B - \alpha_B n_e n_{iB} - n_{ct}\left(n_{iBconcts} + n_{iBcysct}\right) - J_{aiB} + J_{desorptionB} + J_{th}, \tag{17}$$

The first term in Eqs. (16) and (17) is the gain in ion number density per unit time on account of ionization of neutral atoms, the second term is the electron-ion recombination, the third term is the ion collection current to the surface of the CNT (conical tip over cylindrical surface). The fourth term is the loss of ion density because of their adsorption to the catalyst - substrate surface and fifth term is the gain of ion density due to the desorption of ions from the catalyst-substrate surface into plasma. The last term in Eq. (17) describes the increase of hydrogen ion number density in plasma because of thermal dehydrogenation.

G. Stability equation of neutral atom number density

The Eqs. (18) and (19) describes the balance of neutral species in plasma considering that the recombination of electrons-ions increases the neutral density in plasma bulk, ionization of neutral molecules to produce ions and electrons decreases neutral density in plasma bulk, and neutral collection current on the CNT surface would decrease their density in plasma bulk.

$$\frac{dn_A}{d\tau} = \alpha_A n_e n_{iA} - \beta_A n_A + n_{ct}\left(1-\gamma_{iA}\right)\left(n_{iAconcts} + n_{iAcysct}\right) - n_{ct}\gamma_A\left(n_{Aconcts} + n_{Acysct}\right), \tag{18}$$

$$\frac{dn_B}{d\tau} = \alpha_B n_e n_{iB} - \beta_B n_B + n_{ct}\left(1-\gamma_{iB}\right)\left(n_{iBconcts} + n_{iBcysct}\right) - n_{ct}\gamma_B\left(n_{Bconcts} + n_{Bcysct}\right), \tag{19}$$

where

$n_{jconcts} = \pi r_{conct}{}^{l}\left[\frac{8k_B T_n}{\pi m_j}\right]^{\frac{1}{2}} n_j$ is the neutral collection current at the surface of conical CNT tip (in sec^{-1}),

$n_{jcysct} = \pi r_P{}^{h}\left[\frac{2k_B T_n}{m_j}\right]^{\frac{1}{2}} n_j$ is the neutral collection current on the cylindrical surface of CNT (in sec^{-1}).

γ_{iA} and γ_{iB} are the ion sticking coefficients and γ_A and γ_B are the neutral atom sticking coefficients, and both γ_{iA} and γ_{iB} and γ_A and γ_B are dimensionsionless. n_j is the neutral atom density (in cm^{-3}), T_n is the neutral atom temperature (in K) , n_j is the neutral atom density (in cm^{-3}) and m_j is the neutral atom mass (in gm).

The first term in Eqs. (18) and (19) is the gain in neutral atom density per unit time due to electron–ion recombination, the second term is the decrease in neutral density due to ionization, the third term is the gain in neutral density due to neutralization of the particles collected at the surface of the CNT. The last term is the accumulation of neutral atoms of species A and B on the surface of the CNT.

8.4: NUMERICAL RESULT AND DISCUSSIONS

The work in the present chapter investigates the role of substrate temperature on the growth of carbon nanotubes by PECVD process. In the present model, we assume the inhomogeneous deposition of ions on CNT growing in a plasma medium assisted by catalyst. The calculations have been formed to investigate the dependence of the height of cylindrical CNT surface and radius of the conical CNT tip as a function of substrate temperature for different ion density and ion temperature by simultaneous solution of Eqs. 1 to 7 and 15 to 19 at appropriate boundary conditions.

The values of height and radius of the CNT as obtained by Eqs. (5) and (6) are obtained at different times as a function of temperature. But since we are interested in studying the variation in height and radius of the CNT as a function of substrate temperature, the value of height and radius of CNT are plotted for a fixed time interval i.e., τ = 0 min to 30 min for varying substrate temperature.

For Ar plasma, using the values of ion number density and temperature from Chai *et al*. [24], the initial boundary conditions for the present calculations are at

$\tau = 0$, ion number density (n_{iA0}=0. 6 n_{e0} and n_{iB0}=0. 4 n_{e0}) , neutral atom density ($n_{A0}=n_{B0}=1x10^{14}$ cm^{-3}), electron number density (n_{e0} $=1.12x10^{9}cm^{-3}$), electron temperature(T_{e0})=1.5eV, ion temperature (T_{iA0}) =2200K, neutral temperature(T_{n0}) = 2000K, mass of ion A m_{iA}= 26 amu (acetylene ($C_2H_2^+$)), mass of ion B $\left(m_{iB}\right)$=1amu(H^+), coefficient of

recombination of electrons and ions$\left(\alpha_{A0} \approx \alpha_{B0}\right)$=1.12 x 10^{-7}cm^3/sec, ,κ = -1.2 and density of Ni$\left(\rho_P\right)$= 8.908 g/cm^3.

Other parameters used in the calculation are substrate temperature(T_s)=550 ^{0}C,energy barrier for bulk diffusion E_b=1.6eV, energy due to thermal decomposition of acetylene ions $\delta\varepsilon_i$ =300eV ,dissociation energy of C_2H_2 (Mehdipour *et al.*[13]) ε_{dis} =4.35eV, Ionization energies of neutral atom A (I_{pA}) = 8.76 eV, Ionization energies of neutral atom B (I_{pB}) = 6.56 eV, the mean energy collected by the ion A at the surface of catalyst particle (ε_{iA})= 5.915 eV, the mean energy collected by the ion B at the surface of catalyst particle ($\varepsilon_{iB)}$= 9.80 eV.

Substituting all the above values in Eqs. 1 to 7 and 15 to 19, we simultaneously solve the first order differential Eqs. 1 to 7 and 15 to 19 using MATHEMATICA software to investigate the dependence of height and radius of CNT for different substrate temperature (T_s), and ion density and temperature of either acetylene (n_{iA0} and T_{iA0}) or hydrogen ions (n_{iB0} and T_{iB0}).

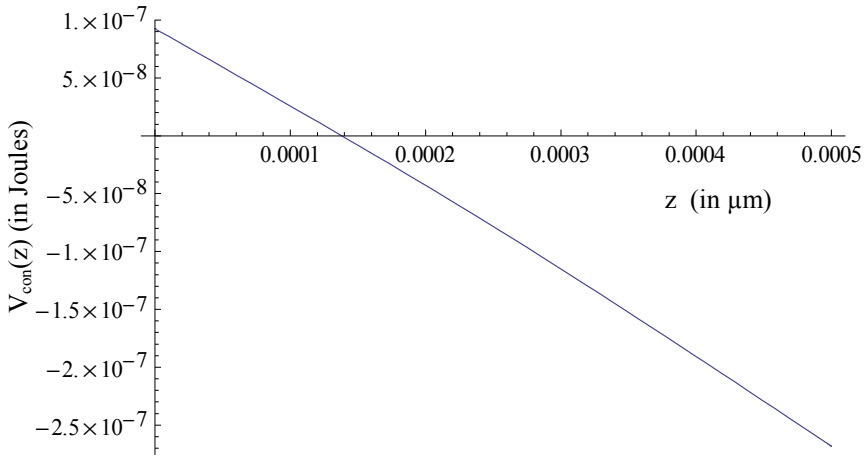

FIG.3. Sketches the variation of potential of conical CNT tip with axial distance.

Fig. 3 sketches the variation of potential at a conical surface ($V_{con}(z)$) as a function of axial distance (z). It can be seen from Fig. 3 that the potential on the conical surface decreases with the axial distance (z). The decrease in the potential at a conical surface (V_{con} (z)) with axial distance (z) follows the same trend as the electrostatic potential at the surface behaves as the distance from the surface is increased. The electrostatic potential at the surface decreases as the distance from the surface is increased.

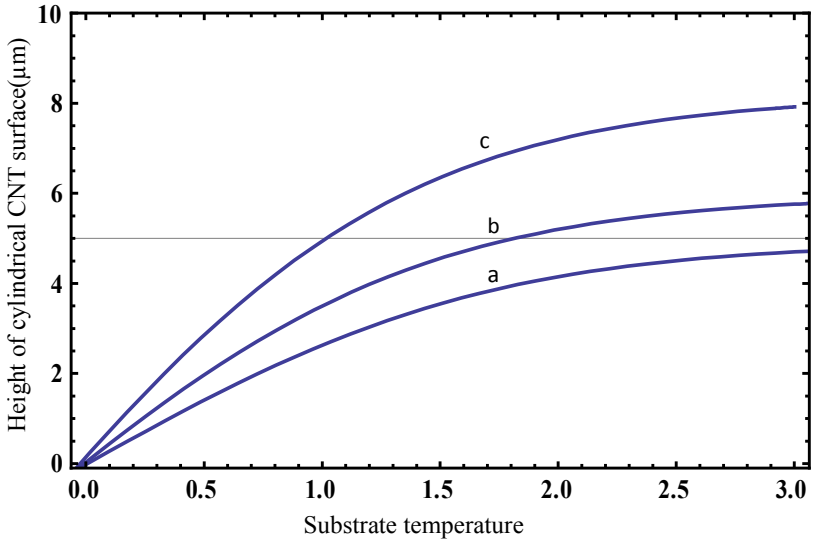

FIG. 4. Depicts the evolution of the height of cylindrical CNT surface as a function of substrate temperature for different ion density and temperature of type A ions (where a, b and c corresponds to n_{iA0}= 10^9 cm^{-3},T_{iA0}=2250K; n_{iA0}= $2x10^{10}cm^{-3}$,T_{iA0}=2300K and n_{iA0}= 3 $x10^{11}$ cm^{-3} ,T_{iA0}=2400K). The other parameters are given in the text.

Fig. 4 traces the evolution of the height of the cylindrical part of the CNT as a function of substrate temperature for different ion densities of type A and temperatures (e.g., n_{iA0}= 10^9 cm^{-3} ,T_{iA0}=2250 K; n_{iA0}= $2x10^{10}$ cm^{-3} ,T_{iA0} =2300 K ,and n_{iA0}= 3 x 10^{11} cm^{-3} ,T_{iA0} =2400 K). It can be seen from the Fig. 4 that as substrate temperature is increased for a fixed ion density and temperature of type A ion (i.e., acetylene ion) the height of the CNT increases. This is because with increasing substrate temperature, the hydrocarbon gas dissociates faster, leading to higher diffusion of carbon through catalyst particle thereby giving enhanced growth rates. Moreover, with increasing ion density and temperature of type A ions, the effective carbon flux to the catalyst surface increases which results in better CNTs growth.

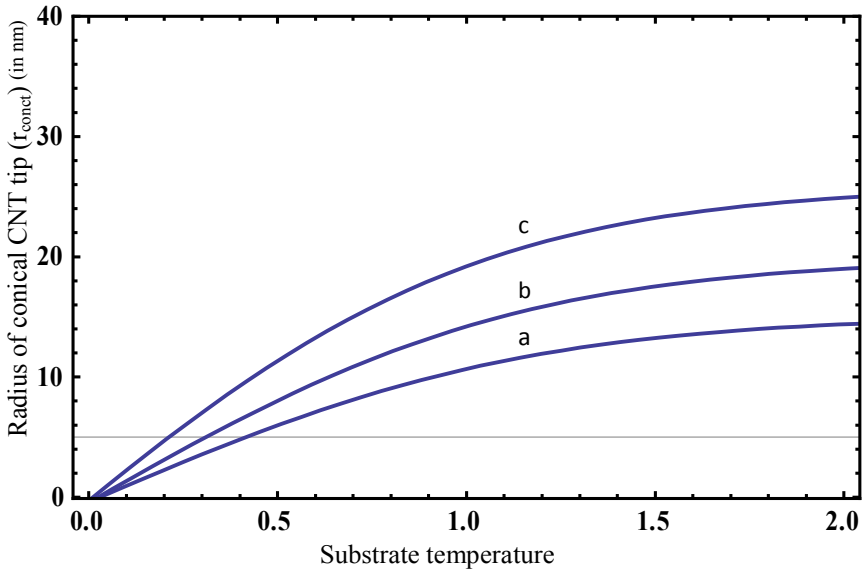

FIG. 5. Depicts the time evolution of the radius of the conical CNT tip for different density and temperature of type A ions (where a, b and c corresponds to $n_{iA0}= 10^9$ cm^{-3} ,T_{iA0}=2250K; $n_{iA0}= 2x10^{10}$cm^{-3} ,T_{iA0}=2300K and $n_{iA0}= 3 \times 10^{11}$ cm^{-3} ,T_{iA0}=2400K). The other parameters are given in the text.

Fig. 5 traces the evolution of the radius of the conical CNT tip as a function of substrate temperature for different ion densities and temperatures of type A (i.e. , $n_{iA0}= 10^9$ cm^{-3} ,T_{iA0}=2250K; $n_{iA0}= 2x10^{10}$ cm^{-3} ,T_{iA0}=2300K ,and $n_{iA0}= 3 \times 10^{11}$ cm^{-3} ,T_{iA0}=2400K). It can be seen from Fig. 5 that as substrate temperature is increased for a fixed ion density and temperature of type A ion (i.e., acetylene ion), the radius of the conical CNT tip increases. This is because with increasing substrate temperature, the hydrocarbon gas dissociates faster, leading to higher diffusion of carbon through catalyst particle thereby giving larger radius. In addition, as the ion density and temperature of type A ions (i.e., acetylene ion) is increased, the effective carbon flux to the catalyst surface increases which results in a larger radius of the CNT tip.

The observations of Figs. 4 and 5, i.e., the enhanced growth rate of the CNT with substrate temperatures are in principle with the experimental

observations of Han *et al.* [8] , Baratunde *et al.* [9] , Lee *et al.* [10] , Loffler *et al.* [11] , and theoretical findings of Mehdipour *et al.* [13] .

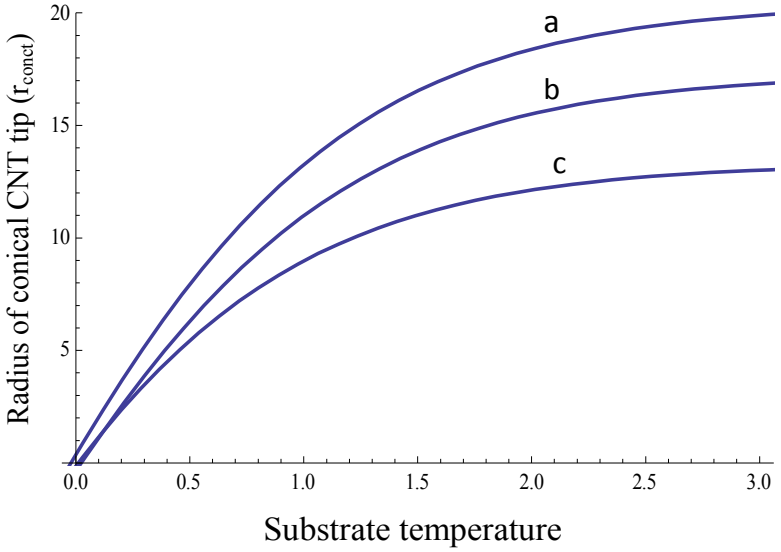

FIG. 6. Illustrates the evolution of the radius of the conical CNT tip as a function of substrate temperature for different ion density and temperature of type B ions (where a, b and c corresponds to $n_{iB0}= 10^9$ cm^{-3},T_{iB0}=2300K; $n_{iB0}= 5x10^{10}$ cm^{-3},T_{iB0}= 2350K and $n_{iB0}= 4 \times 10^{11}$ cm^{-3} ,T_{iB0}=2400K).

Fig. 6 traces the evolution of the radius of the conical CNT tip as a function of substrate temperature for the different ion density and temperature of type B ions (i.e., $n_{iB0}= 10^9$ cm^{-3},T_{iB0}=2300K; $n_{iB0}= 5x\ 10^{10}$ cm^{-3} ,T_{iB0}= 2350K and $n_{iB0}= 4 \times 10^{11}$ cm^{-3} ,T_{iB0}=2400K). It can be seen from Fig. 6 that as substrate temperature is increased for a fixed ion density and temperature of the type B ion (i.e., hydrogen ion), the radius of CNT increases. This is imputable to the fact that as the substrate temperature is increased for a fixed ion density and temperature of type B ions (i.e., hydrogen ion) the radius of the conical CNT tip increases because with increasing substrate temperature, the feedstock gas dissociates more and consequently, a larger number of carbon radicals and higher stable hydrocarbons become easily available for CNT growth.

However, as the density of type B ion (i.e., hydrogen ion) increases, the radius of the conical CNT tip decreases because of etching effects of hydrogen. The results of Fig. 6 comply with works of Mehdipour *et al.* [13] and Denysenko *et al.*[14].

References

[1] Lance Delzeit, Ian McAninch, Brett A. Cruden, David Hash, Bin Chen, Jie Han and M. Meyyappan, J. Appl. Phys. **91**, 6027 (2002).

[2] V. I. Merkulov, D. H. Lowndes, Y. Y. Wei, G. Eres and E. Voelkl, Appl. Phys. Lett. **76**, 3555 (2000).

[3]M. Meyyappan, L. Delzeit, A. Cassell, D. Hash, Plasma Sources Sci. Technol. **12**, 205 (2003).

[4] M. Chhowalla, K. B. Teo, C. Ducati, N. L. Rupesinghe, G. A. J. Amaratunga, A. C. Ferrari, D. Roy, J. Robertson, W. I. Milne, J. Appl. Phys. **90**, 5308(2001).

[5] Y. C. Choi , D. J Bae, Y. H. Lee, B. S. Lee, G. S. Park, W.B. Choi, N. S. Lee, J. M. Kim, J. Vac. Sci. Technol. A **18**, 1864 (2000).

[6] J. I. B Wilson, N. Scheerbaum, S. Karim, N. Polwart, P. John, Y. Fan, A. G. Fitzgerald, Diamond Relat. Mater. **11**,918 (2002).

[7] Kenneth B. K. Teo, David B. Hash, Rodrigo G. Lacerda, Nalin L. Rupesinghe, Martin S. Bell, Sharvari H. Dalal, Deepak Bose, T. R. Govindan, Brett A. Cruden, Manish Chhowalla, Gehan A. J. Amaratunga,M. Meyyappan, and William I. Milne, Nano Lett. **4**, 921(2004).

[8] Jae-Hee Han , Sun Hong Choi , Tae Young Lee, Ji-Beom Yoo, Chong-Yun Park , Ha Jin Kim ,In-Taek Han , SeGi Yu , Whikun Yi , Gyeong Soo Park , Minho Yang , Nae Sung Lee, J.M. Kim, Thin Solid Films **409**,126 (2002).

[9]A. Cola Baratunde, B. Amama Placidus , Xu Xianfan, S. Fisher Timothy, J. Heat Transfer **130**, 114503(2008).

[10]Yun Tack Lee ,Jeunghee Park, Young Sang Choi, Hyun Ryu and

Hwack Joo Lee , J. Phys. Chem. B, **106***,* 7614 (2002) .

[11]R. Loffler, M. Haffner, G. Visanescu, H. Weigand, X. Wang, D. Zhang, M. Fleischer, A. J. Meixner, J. Fortagh, and D. P. Kern, Carbon **49**, 4197 (2011).

[12] I. B. Denysenko, K. Ostrikov, M. Y. Yu, and N. A. Azarenkov, J. Appl. Phys.**102**, 074308 (2007).

[13] H. Mehdipour, K. Ostrikov, and A. E. Rider, Nanotechnology **21**, 455605 (2010).

[14] I. B. Denysenko and K. Ostrikov, J. Phys. D: Appl. Phys. **42,** 015208 (2009).

[15]G. Burmaka, I. B. Denysenko, K. Ostrikov, I. Levchenko, N. A. Azarenkov, Plasma Process. Polym. **11**, 798(2014).

[16]Sanjay Kumar Srivastava , Vasant D. Vankar , Vikram Kumar, Nanoscale Res Lett **3**,25 (2008).

[17] Sumio Iijima, P. M. Ajayan, and T. Ichihashi, Phys. Rev. Lett. **69**, 3100 (1992).

[18] D. L. Carroll, P. Redlich, P. M. Ajayan, J. C. Charlier, X. Blase, A. De Vita, and R. Car, Phys. Rev. Lett. **78**, 2811(1997).

[19] O. A. Louchev, C. Dussarrat and Y. Sato, J. Appl. Phys. **86**,1736 (1999).

[20] Sanjay K. Srivastava , A.K. Shukla , V.D. Vankar , V. Kumar, Thin Solid Films **492**,124(2005).

[21] M. S. Sodha , Shikha Misra, S. K. Mishra, Sweta Srivastava, J. Appl. Phys. **107**,103307(2010).

[22] M. S. Sodha, S.K. Mishra and S. Misra, Phys. Plasmas **16**, 123701 (2009).

[23]http://www2.warwick.ac.uk/fac/sci/physics/current/teach/module_ho

me/ px 263/assignments/assignment1_soln.pdf.

[24] K. B. Chai, C. R. Seon , C.W. Chung, , N. S.Yoon, and W. Choe, J. Appl. Phys. **109**, 013312 (2011).

CHAPTER 9

INVESTIGATIONS ON THE EFFECT OF DIFFERENT CARRIER GASES AND THEIR FLOW RATES ON THE GROWTH OF CARBON NANOTUBES

9.1: Brief Outline of the work done

The present chapter investigates the effect of different carrier gases and their flow rates on the growth of carbon nanotubes (CNTs). The model developed for the growth of CNT assisted by catalyst in a plasma medium is extended to a case where three different carrier gases i.e., argon (Ar), ammonia (NH_3) and nitrogen (N_2) are considered. The flow rates of all the three carrier gas are varied individually, keeping the flow rates of hydrocarbon and hydrogen gas constant; to investigate the variations in the number densities of hydrocarbon and hydrogen ions in the plasma and their consequent effects on the height and radius of CNT.

9.2: Introduction

Plasma-enhanced chemical vapor deposition (PECVD) has recently emerged as promising carbon nanostructure growth technique [1–5]. PECVD has the advantage of producing low-temperature and vertically aligned carbon nanotubes (CNTs). The main parameters during PECVD process are the growth temperature, substrate bias, externally applied power, growth time, type of catalyst, type of substrate, composition of gases in PECVD, types of feed gas or reducing gas or carrier gas and their respective flow rates among several others.

Different carrier gases like argon (Ar), ammonia (NH_3), nitrogen (N_2), and hydrogen (H_2) are found to have different effects on the growth density of CNT. [6-11].

Kayastha *et al.* [6] have found that the addition of specific carrier gases could critically modify the growth rate and growth density of multiwall carbon nanotubes (MWCNTs). In particular, the addition of Ar to acetylene (C_2H_2) increases the growth density of MWCNTs, while the addition of hydrogen (H_2) and nitrogen (N_2) gases decreases the growth density.

Mi *et al.* [7] have investigated the effects of ammonia (NH_3) and nitrogen (N_2) as carrier gases on the structure and morphology of CNTs. They observed that the diameter of the CNTs synthesized in NH_3 was larger than that in N_2. Moreover, the alignment of the CNTs grown in NH_3 was better than that in N_2.

Jung *et al.* [8] have investigated the growth behaviors in various gas environments of N_2 , H_2 , Ar, NH_3 and their mixtures. It was observed that in NH_3 environment much enhanced CNT growth occurs than in the mixture of N_2 and H_2 environment.

Yap *et al.* [9] found that carrier gas could change the growth rate, growth density, and structures of MWCNTs. They investigated the growth of CNT under different conditions e.g., (a) pure C_2H_2, (b) C_2H_2 and Ar, (c) C_2H_2 and H_2, (d) C_2H_2 and N_2. The addition of Ar dilutes C_2H_2 and reduces the number of C_2H_2 molecules reacting on the iron (Fe) catalyst surface. Both H_2 and N_2 reduce the growth density of MWCNTs.

Mi and Jia [10] have grown CNTs arrays on macro porous substrate for different time in the ammonia and nitrogen carrier gases by floating

catalyst method. They observed that the CNTs diameter is smaller in N_2 than that grown in NH_3.

Qian *et al.* [11] found that the size and distribution of carbon spheres become smaller as the ratio of Ar to H_2 in the carrier gas decreases. Also, pure argon favors the growth of carbon spheres while pure hydrogen does not.

Studies have been done to investigate the effects of flow rate of carrier gases on the growth of CNTs. It is seen that increasing the flow rate of carrier gases affects the growth density and growth rate of CNTs [12-14].

Toussi *et al.* [12] have investigated three different flow rates of Ar carrier gas (i.e., 50 mL/min, 100 mL/min and 150 mL/min) on the growth of carbon nanotubes. It was seen that as the flow rate of Ar carrier gas was increased, the yield of carbon nanotubes increased.

Malgas *et al.* [13] studied the effect of mixture ratios and nitrogen carrier gas flow rates on the morphology of carbon nanotube structures and reported that at the constant temperature of 750 °C and the higher carrier gas flow rates of N_2 resulted in CNTs with smaller diameters.

Reynolds *et al.* [14] have investigated the effects of hydrogen (H_2) flow rate on CNT growth and observed that at a constant methane (CH_4) flow rate of 700 sccm and by varying flow rate of H_2 as 100 and 200 sccm, few CNTs were produced.

Denysenko *et al.*[15] have developed a spatially averaged global discharge model to study the densities and fluxes of the radical neutrals and charged species, the effective electron temperature, methane conversion factor under various growth conditions. They observed that the densities of molecular and atomic hydrogen decrease with flow rate of

argon (J_{Ar}), whereas the densities of hydrocarbon neutrals grow with flow rate of argon (J_{Ar}).

The vertically aligned and low–temperature CNT so produced by PECVD process have found applications in vertical transistors [16], field emission devices [17-21] and field ionization applications [22] among others.

The above works that have been cited [6-14] to study the effects of different carrier gases and their flow rates on the growth of CNT do mention the effects of different carrier gases but do not sufficiently underline the exact processes behind the observed effects. Moreover, they have considered various routes of CNT growth like catalytic chemical vapor deposition[6] , pyrolysis of ferrocene and C_2H_2 mixture [7], chemical vapor deposition (CVD)[8], thermal CVD[9], floating catalyst method[10], non-catalytic CVD[11]. In the present study, we try to present the possible reasons behind the different observed behaviors of different carrier gases and their consequent ramifications on the growth of CNT. We try to explain the behavior of various carrier gases during CNT growth through a PECVD process by the number density profile of hydrocarbon and hydrogen species created in different carrier gas environments and their repercussions on growing CNT.

9.3. Model

Using the model developed in chapter 7 and following Denysenko *et al.* [15], a cylindrical stainless steel reactor chamber of the plasma source which has the inner diameter (R) =16 cm and length (L) =23 cm is considered. The plasma contains ions of methyl (CH_3^+), methane (CH_4^+) denoted as ions A and hydrogen ions ($H^+/H_2^+/H_3^+$) denoted as ions B, and carrier gas ions of argon(Ar), nitrogen(N_2) and ammonia (NH_3) (i.e., $Ar^+/ N_2^+ /NH_3^+$, respectively) are denoted as ions C. A substrate of

silicon (Si) over which catalyst of nickel (Ni) is placed is considered in the present chapter. In the reactive plasma so considered CH_4 acts as a carbon source gas and the growth of CNT occurs through the process assumed as listed below:

1. Plasma containing methyl, methane, hydrogen, and either of argon, nitrogen and ammonia ions is considered.
2. Electric field is directed towards *x*-direction.
3. Negative substrate potential is applied to the substrate.
4. A cylindrical stainless steel reactor chamber of the plasma source which has the inner diameter (R) = 16 cm and length (L) = 23 cm is considered following Denysenko *et al.* [15]
5. Plasma power ionizes the gas (hydrocarbon, hydrogen and carrier gas) and highly energetic hydrocarbon, hydrogen and carrier gas ions initiates the dissociation of catalyst particle to form catalyst nanoparticle, which then seed nanotube growth on them.
6. These hydrocarbon, hydrogen and carrier gas ion then travel through the plasma sheath undergoing recombination, adsorption, desorption ,loss to the walls and various other processes to eventually diffuse and accrete on catalyst nanoparticle to form CNT.

Denysenko *et al.* [15] have considered a large number of possible hydrocarbons in their study but we in the present investigation limit ourselves to a limited number of hydrocarbons. Moreover, Sode *et al.* [23] have considered various possible combinations of ions in H_2-Ar plasma like Ar^+, H^+, H_2^+, H_3^+, and ArH^+ but the present problem considers CH_3^+, CH_4^+ , H^+, H_2^+, H_3^+ , and either of Ar^+, N_2^+ and NH_3^+.

The present study is therefore, applicable to the cases where higher hydrocarbons and a varied combinations of ions in plasma are not considered.

A.The sheath equations

Following (Mehdipour *et al.* [24]) and Lieberman and Lichtenberg [25], the sheath equations are:

1. The continuity equation

$$\left(\hat{i}\frac{\partial}{\partial x}+\hat{j}\frac{\partial}{\partial y}+\hat{k}\frac{\partial}{\partial z}\right).\hat{i}\left(n_l u_{lx}\right)=\nu_l n_e, \tag{1}$$

2. The ion momentum balance equation

$$m_l n_l u_{lx}\frac{du_{lx}}{dx}=en_l E-m_l n_l \nu_{ln} u_{lx}, \tag{2}$$

3. Poisson's equation (Mehdipour *et al*.[24])

$$\frac{d^2\phi(x)}{dx^2}=-4\pi\sum q_l\delta_l n_l, \tag{3}$$

where l refers to either electron (e), CH_3^+, CH_4^+, H^+, H_2^+, H_3^+ ,and either of $Ar^+/N_2^+/ NH_3^+$.

m_l is the mass of species l (in gm), n_l is their number density (in cm^{-3}), u_{lx} is the fluid velocity of the particle l (in cm/sec) ,

$\phi(x)$ is the sheath potential (in Stat V), ν_l is the ionization frequency(in sec^{-1}),

υ_{ln} is the collision frequency with the neutrals(in sec^{-1}) and q_l is the charge of species l (in StatC) ,

δ_l is the l^{th} ion to electron number density ratio and is dimensionless ,

$\sum_l \delta_l = 1$ and $0 < \delta_l < 1$ as electron density is greater in plasma bulk than in sheath.

Now by using Child Sheath law in cases where the high voltage is applied over longer time scales [26], the plasma sheath width (λ_s) is given as

$\lambda_S = \frac{\sqrt{3}}{2}\lambda_d \left(\frac{2U_S}{k_B T_e}\right)^{\frac{3}{4}}$, where $\lambda_d \left(= \sqrt{\frac{k_B T_e}{n_e e^2}}\right)$ is the Debye length of the plasma.

and U_s is the substrate bias (in V), k_B is the Boltzmann constant (in ergs/K) and T_e is electron temperature (in eV).

The ion- neutral collisions have been taken into account in the present model and these collisions attain significance at higher pressures. However, our model did not undertake pressure effects into account but it has been reported that the sheath width decreases as neutral pressure is increased. [24]

B.Charging of the CNT

The equation describes the charge developed on the entire CNT (i.e., spherical tip placed over cylindrical surface), due to accretion of electrons and positively charged hydrocarbon, hydrogen, and carrier gas ions on the surface of the CNT (i.e., spherical tip over cylindrical surface).

$$\frac{dZ}{d\tau} = I_{iActs} + I_{iActcys} + I_{iBcts} + I_{iBctcys} + I_{iCcts} + I_{iCctcys} - \gamma_e \left(I_{ects} + I_{ectcys}\right), \quad (4)$$

where

Z is the amount of charge over the entire CNT (i.e., spherical tip and cylindrical surface) and is dimensionless,

$I_{ects} = \pi r_{ct}^2 \left(\frac{8k_B T_e}{\pi m_e} \right)^{\frac{1}{2}} n_e(x) \exp\left[Z\alpha_e + \frac{eU_S}{k_B T_S} \right]$ is the electron collection current at the surface of the spherical CNT tip(in sec^{-1}) and $\alpha_e \left(= \frac{e^2}{r_{ct} k_B T_e} \right)$(in eV), r_{ct} is the CNT tip radius (in nm),

$n_e(x) = n_{e0} \exp\left[\frac{|e|\phi(x)}{k_B T_e} \right]$ is the electron density in plasma sheath (in cm^{-3}) [27],

$\phi(x)$ is the electrostatic potential(in StatV). γ_e is the sticking coefficient of electrons and is dimensionless, $\phi(x) = \phi_0 \exp\left(-\frac{|x|}{\lambda_d} \right)$, ϕ_0 is the negative potential at the surface (in StatV),

$I_{ectcys} = n_e(x) r_{ct} h \left(\frac{2\pi k_B T_e}{m_e} \right)^{\frac{1}{2}} \exp\left[\frac{eV_S}{k_B T_e} + \frac{eU_S}{k_B T_S} \right]$ is the electron collection current on the cylindrical surface of the CNT(in sec^{-1}) , V_s is the surface potential on the cylindrical surface of the CNT(in StatV) , h is the height of cylindrical surface of the CNT(in μm) and m_e is the mass of electron(in gm),

$$I_{ijctcys} = n_{ij}(x) r_{ct} h \left(\frac{2\pi k_B T_i}{m_{ij}} \right)^{\frac{1}{2}} \left\{ \frac{2}{\sqrt{\pi}} \left(\frac{eV_S}{k_B T_i} \right)^{\frac{1}{2}} + \exp\left[\frac{eV_S}{k_B T_i} \right] erfc\left[\left(\frac{eV_S}{k_B T_i} \right)^{\frac{1}{2}} \right] \right\} \exp\left[-\frac{E_b}{k_B T_S} \right] \exp\left[-\frac{eU_S}{k_B T_S} \right]$$

is the ion collection current on the cylindrical surface of CNT(in sec^{-1}), T_i is the ion temperature(in K), m_{ij} is the ion mass (j refers to either A, B or

C positively charged ions) (in gms), E_b is the energy barrier for bulk diffusion $(\approx 1.6eV)$, T_s is the substrate or catalyst temperature (in ^{0}C),

$I_{ijcts} = \pi r_{ct}{}^2 \left(\frac{8k_B T_i}{\pi m_{ij}} \right)^{\frac{1}{2}} n_{ij}(x)\left[1 - Z\alpha_i\right] \exp\left[-\frac{E_b}{k_B T_s} \right] \exp\left[-\frac{eU_s}{k_B T_s} \right]$ is the ion collection current on the spherical CNT tip (in sec^{-1}),

$n_{ij}(x) = n_{ij0}\left(1 - \frac{2e\phi(x)}{m_{ij} v_{ij0}^2} \right)^{\frac{-1}{2}}$,where $n_{ij}(x)$ is the ion density in plasma sheath (in cm^{-3}) , v_{ij0} is the ion velocity at any point within the plasma (in cm/sec) and $\alpha_i = \left(\frac{e^2}{r_{ct} k_B T_i} \right)$

The following assumptions were considered for solving the currents:

1. Maxwellian distribution of electrons and ions was considered.
2. $e\phi(x) << k_B T_e$
3. $T_e << U_s$ i.e., temperature of electrons is lesser than the substrate potential.
4. The mean free path of the ions is greater than the distance *x* in the sheath.
5. For the sheath to perform its function and repel electrons the potential must be monotonically decreasing with increasing *x*. This will occur if $n_i(x) > n_e(x)$ for all *x* in the sheath [26].
6. The high voltage is considered to be applied over longer time scales therefore, the ions would be accelerated by the electric field [26].

C.Balance equation of electron density

The Eq. (5) describes the balance of electron number density in the plasma bulk. The processes such as dissociative ionization of neutrals to produce electrons and ions increases electron number density , recombination of electrons with ions reduces electron density in plasma bulk, electron collection current to the CNT surface reduces electron density in plasma bulk , and loss of electrons to discharge wall are considered.

$$\frac{dn_e}{d\tau} = \left(\beta_A n_A + \beta_B n_B + \beta_C n_C\right) - \left(\alpha_A n_e n_{iA} + \alpha_B n_e n_{iB} + \alpha_C n_e n_{iC}\right) - \gamma_e n_{ct}\left(I_{ects} + I_{ectcys}\right) - K_{wall}^{e} n_e, \tag{5}$$

where

β_A , β_B and β_C are the coefficients of ionization of the constituent neutral atoms of A(hydrocarbon) ,B(hydrogen) and C(carrier gas) due to external agency (in sec),

$\alpha_A(T_e) = \alpha_{A0}\left(\frac{300}{T_e}\right)^k cm^3/\sec$, $\alpha_B(T_e) = \alpha_{B0}\left(\frac{300}{T_e}\right)^k cm^3/\sec$ and $\alpha_C(T_e) = \alpha_{C0}\left(\frac{300}{T_e}\right)^k cm^3/\sec$ are the coefficients of recombination of electrons

positively charged ions [33] of A(hydrocarbon) ,B(hydrogen) ,and C(carrier gas), respectively where k =-1.2 is a constant , n_{ct} is the CNT number density (in cm^{-3})

and $\alpha_{A0} = \alpha_{B0} = \alpha_{C0} = n_{e0} \times 10^{-7}\left(\frac{1}{T_{e0}}\right)^{-1.2}$.

I_{ects} and I_{ectcys} are electron collection currents to spherical CNT tip and cylindrical CNT surface (in sec^{-1}),respectively.

$K^{e}_{wall} n_e \left(= \frac{\gamma_e v_{the} S_{surf} n_e}{4V} \right)$ is the number of electrons lost on the discharge wall per unit time per unit volume (in cm^{-3} sec^{-1}), where γ_e is the sticking coefficients of electrons and is dimensionless,

$v_{the} \left(= \sqrt{\frac{8T_e}{\pi m_e}} \right)$ is the average thermal velocity of electrons[15] (in cm/sec), S_{surf} is the chamber surface area(in cm^2), and V is the volume of the PECVD chamber (in cm^3) whose inner diameter R= 16 cm and length L =23 cm is considered [15].

The first term on the right side of Eq. (5) is the rate of gain in electron density per unit time because of dissociative ionization of neutral atoms; the second term is the decaying rate of the electron density due to the electron–ion recombination. The third term is the electron collection current at the surface of the CNT (spherical tip placed over the cylindrical surface). The last term denotes the loss of the electrons to the discharge wall [15].

D.Balance equation of positively charged ion density

The Eqs. (6) to (8) describes the balance of positively charged ions in plasma bulk considering dissociative ionization of neutral atoms, recombination of electrons and ions, ion collection current at CNT surface, their adsorption, desorption, thermal dehydrogenation and loss to the discharge wall.

$$\frac{dn_{iA}}{d\tau} = \beta_A n_A - \alpha_A n_e n_{iA} - n_{ct}\left(I_{iActs} + I_{iActcys}\right) - J_{aiA} + J_{desorptioniA} - K_{wall}^{iA} n_{iA} + \sum_i k_{i1} n_A n_{iC},$$

(6)

$$\frac{dn_{iB}}{d\tau} = \beta_B n_B - \alpha_B n_e n_{iB} - n_{ct}\left(I_{iBcts} + I_{iBctcys}\right) - J_{aiB} + J_{desorptioniB} + J_{th} - K_{wall}^{iB} n_{iB} + \sum_i k_{i2} n_B n_{iC},$$

(7)

$$\frac{dn_{iC}}{d\tau} = \beta_C n_C - \alpha_C n_e n_{iC} - n_{ct}\left(I_{iCcts} + I_{iCctcys}\right) - J_{aiC} + J_{desorptioniC} - K_{wall}^{iC} n_{iC} + \sum_i k_{i1} n_A n_{iC} + \sum_i k_{i2} n_B n_{iC},$$

(8)

$J_{aij} = \frac{Pi}{\left(2\pi m_{ij} k_B T_{ij}\right)^{\frac{1}{2}}} \times \frac{n_{ij}}{j_{ij}}$ is the adsorption flux onto the catalyst –substrate surface (in cm^{-3} sec^{-1}), P_i is the partial pressure of adsorbing species [28],

$J_{desorptionij} = n_{ij}\nu \exp\left(\frac{-\varepsilon_{ai}}{k_B T_{ij}}\right)$ is the desorption flux of ions from the catalyst – substrate surface (in cm^{-3} sec^{-1}), j refers to either A ,B or C ions, ν is the thermal vibrational frequency $\approx 3\times10^{13}$ Hz , ε_{ai} is the adsorption energy [28] (in eV), n_{ij} is the ion number density at the catalyst substrate surface (in cm^{-3}).

$J_{th} = n_H \nu \exp\left(\frac{-\delta\varepsilon_{th}}{k_B T_S}\right)$ is the flux of type B ion (namely hydrogen) on account of thermal dehydrogenation (in cm^{-3} sec^{-1}). $\delta\varepsilon_{th}$ is the activation energy of thermal dehydrogenation (in eV), n_H is the hydrogen ion number density at the catalyst- substrate surface (in cm^{-3}).

$K_{wall}^{ij} = \frac{\gamma_{ij} v_{thij} S_{surf}}{4V}$ denotes the loss of ions j on the discharge wall per unit time per unit volume(in sec^{-1}), γ_{ij} is the sticking coefficients of ions and is dimensionless , $v_{thij} = \sqrt{\frac{8T_{ij}}{\pi m_{ij}}}$ is the average thermal velocity of ions A ,B or C (in cm/sec).

The first term in Eqs. (6), (7) and (8) is the gain in ion density per unit time because of ionization of neutral atoms, the second term is loss of ion density in plasma bulk due to electron-ion recombination. The third term is loss of ion density in plasma bulk due to the ion collection current to the surface of the CNT (spherical tip over the cylindrical surface). The fourth term is the loss of ions because of their adsorption to the catalyst - substrate surface and fifth term is the gain of ion density due to the desorption of ions from the catalyst -substrate surface into plasma bulk. The term J_{th} in Eq. (7) describes the increase of hydrogen ion number density in plasma because of thermal dehydrogenation. The $K_{wall}^{ij} n_{ij}$ in Eqs.(6) ,(7) and (8) denotes the loss of the ions to the discharge wall [15]. The last term in Eqs. (6) ,(7) and (8) is the gain in ion number density due to neutral/ion reactions[15]. The rate of reaction [29] $k_{i1} = 1.05 \times 10^{-10}$ cm^3/s and rate of reaction [30] $k_{i2} = 2.7 \times 10^{-10}$ cm^3/s.

E. Balance equation of neutral atoms

The Eqs. (9), (10), and (11) describes the balance of neutral species in plasma due to recombination of electrons and ions, dissociative ionization

of neutral molecules, ion and neutral collection current on the CNT surface, inflow and outflow into and from the chamber and neutral/ion reactions.

$$\frac{dn_A}{d\tau} = \alpha_A n_e n_{iA} - \beta_A n_A + n_{ct}\left(1-\gamma_{iA}\right)\left(I_{iActs} + I_{iActys}\right) - n_{ct}\gamma_A\left(I_{Acts} + I_{Actcys}\right) + I_A - O_A - \sum_i k_i n_A n_{iC}, \quad (9)$$

$$\frac{dn_B}{d\tau} = \alpha_B n_e n_{iB} - \beta_B n_B + n_{ct}\left(1-\gamma_{iB}\right)\left(I_{iBcts} + I_{iBctcys}\right) - n_{ct}\gamma_B\left(I_{Bcts} + I_{Bctcys}\right) + I_B - O_B - \sum_i k_i n_B n_{iC}, \quad (10)$$

$$\frac{dn_C}{d\tau} = \alpha_C n_e n_{iC} - \beta_C n_C + n_{ct}\left(1-\gamma_{iC}\right)\left(I_{iCcts} + I_{iCctcys}\right) - n_{ct}\gamma_C\left(I_{Ccts} + I_{Cctcys}\right) + I_C - O_C - \sum_i k_i n_A n_{iC} - \sum_i k_i n_B n_{iC}, \quad (11)$$

$I_{jcts} = \pi r_{ct}^2 \left(\frac{8k_B T_n}{\pi m_j}\right)^{\frac{1}{2}} n_j$ is the neutral collection current at the surface of the spherical CNT tip (in sec^{-1}) ,

$I_{jctcys} = \pi r_{ct} h \left(\frac{2k_B T_n}{m_j}\right)^{\frac{1}{2}} n_j$ is the neutral collection current on the cylindrical surface of CNT(in sec^{-1}).

$\gamma_{ij} = 1$ is the ion sticking coefficient and $\gamma_j =$ lis the neutral atom

sticking coefficient and are dimensionless, T_n is the neutral atom temperature (in K), n_j is the neutral atom density (in cm^{-3}) and m_j is the neutral atom mass (in gm).

$I_j\left(\frac{cm^{-3}}{s}\right)=\frac{4.4\times10^{17}J_j[sccm]}{V}$ is the inflow i.e., the rate at which species j enter the chamber. J_j is the gas inlet flow rate[15] (in standard cubic centimeter per minute).

$O_j\left(\frac{cm^{-3}}{s}\right)=\frac{\nu_{pump}\,n_j}{V}$ is the outflow i.e., the rate at which species j leave the chamber [15].

ν_{pump} is the pumping rate (in cm^3/s) . n_j is the number density of species j (in cm^{-3}) and V is the volume of the chamber (cm^3) [15]. j can either be neutrals of CH_4 ,H_2 or $Ar/N_2/NH_3$.

The first term in Eqs. (9), (10) and (11) is the gain in neutral atom density per unit time due to electron–ion recombination; the second term is the decrease in neutral density due to dissociative ionization. The third term is the gain in neutral density due to neutralization of the particles collected at the surface of the CNT. The fourth term is the accumulation of neutral atoms of species A and B on the surface of the CNT. The fifth term denotes the increase of neutral density in plasma bulk due to their inflow into the chamber and sixth term denotes the decrease of neutral density in plasma bulk due to their outflow from the chamber [15]. The last terms denotes the loss in number density due to neutral and ion reactions [15].

F. Rate equation for Energy of catalyst particle

Initially, a catalyst particle nickel (Ni) of radius 30 nm is considered to be placed over a silicon (Si) substrate surface.

As, Srivastava *et al*. [31] have highlighted in their experimental findings that an increase in microwave power causes more ionization of the gas, which increases the density of plasma species of relatively higher energy. Following experimental results of Srivastava *et al*. [31], we assume that as the applied rf power increases, it ionizes the gas more which creates more energetic ions, which implies that plasma species of relatively higher energy are created. Since, energy of ions corresponds to the number density and temperature of ions so we assume that with an increase in rf power the number density and temperature of plasma species increases. A catalyst particle of nickel (Ni) of radius 30 nm is considered to be placed over a silicon (Si) substrate surface which on the increase of rf power fragments into catalyst nanoparticle due to generation of more energetic plasma species.

$$rfpower = C_p T_S \frac{d}{d\tau}\left(m_p\right) = \left[I_{iActP}\left(\varepsilon^S{}_{iAc} + I_{pA} \right) + I_{iBctP}\left(\varepsilon^S{}_{iBc} + I_{pB} \right) + I_{iCctP}\left(\varepsilon^S{}_{iCc} + I_{pC} \right) \right] - \left(\frac{3}{2} k_B \right) \left[\left(1-\gamma_{iA}\right) I_{iActP} + \left(1-\gamma_{iB}\right) I_{iBctP} + \left(1-\gamma_{iC}\right) I_{iCctP} \right] T_S, \quad (12)$$

where

$m_P = \frac{4}{3}\pi r_P{}^3 \rho_P$ is the mass of catalyst particle (in gm), r_p is the radius of catalyst particle(in nm).

ρ_P is the mass density of catalyst particle (in gm/cm^3), C_p is the specific heat of catalyst particle (Ni) and is 0.44KJ/Kg^{0}K and T_s is the substrate

temperature (in ^{0}C). I_{pA} , I_{pB} and I_{pC} are the ionization energies of atoms A (methane) ,B (hydrogen) and C (either Ar/NH_3/N_2), respectively (in eV) . In the present problem, we have assumed the substrate and catalyst temperature to be the same. However, Denysenko and Azarenkov [32] have considered the substrate and catalyst temperature to be different in their study and concluded that the substrate-holding platform temperature differs from that of the catalyst nanoparticle temperature mainly due to the temperature variation along the Si substrate.

$\varepsilon_{ijc}^{s}(Z)=\left(\left(\frac{\left(2-Z\gamma_{ji}\right)}{\left(1-Z\gamma_{ji}\right)}\right)-Z\gamma_{ji}\right)k_BT_{ij}$ are the mean energy collected by the ions j (in eV) (where, j refers to ion A, B or C) at the surface of the catalyst particle [33] and $\gamma_{ji}=\left(\frac{e^2}{r_Pk_BT_{ij}}\right)$

$$I_{ijctP}=\pi r_P{}^2\left(\frac{8k_BT_i}{\pi m_{ij}}\right)^{\frac{1}{2}}n_{ij}(x)\left[1-Z\gamma_{ji}\right]\exp\left[-\frac{E_b}{k_BT_s}\right]\exp\left[-\frac{eU_s}{k_BT_s}\right]$$

is the ion collection current at the surface of catalyst particle, j (where, j refers to ion A, B or C) (in sec^{-1})**.**

In Solving Eq. (12), we consider that at rf power of 100W, and at τ=0 feeding ion density (n_{iB0}= n_{iA0})=10^9cm^{-3} ,ion temperature T_{i0} =2100K, substrate temperature T_s =550 ^{0}C, energy for bulk diffusion E_b =1.6eV, substrate bias U_s = -50V and catalyst particle radius r_{P0} =30nm in expression for ion collection currents (I_{iActP} , I_{iBctP} and I_{iCctP}), we can calculate I_{iActP0}, I_{iBctP0} and I_{iCctP0} .

Feeding I_{iActP0}, I_{iBctP0} and I_{iCctP0} and the other parameters i.e., ε_{iAC}^{s}

=13.2 eV , ε_{iBC}^{s}= 13.2 eV and ε_{iCC}^{s} =13.2 eV, I_{pA}=11.87eV , I_{pB} =10.7eV and I_{pC}=12.21eV in Eq. (12), we can get the value of catalyst particle radius r_P at any time τ for T_s= 550^0C .

The terms on the right side of Eq. (12) is the rate of energy transferred to the catalyst particle due to the ions collected at the surface of catalyst particle because of ionization of neutral atoms A , B and C and mean energy collected by the ions at the surface of catalyst particle, and due to the accretion of ions A , B and C at the catalyst particle site.

The resulting value of catalyst nanoparticle at time τserves as the initial base radius of the cylindrical part of nanotube.

G. Growth rate equation of the curved surface area of CNT

$$r_P \frac{d(2\pi h)}{d\tau} = \left(\left\{ 2n_{CH} \nu \exp\left(\frac{-\delta E_t}{k_B T_s}\right) + 2\theta_{CH} j_{iA} y_d + 2 j_{iA} + \frac{j_{iA}\sigma_{ads} j_{iB}}{\nu} + j_{carbon} \right\} m_{carbon} \right.$$

$$\left. + \left\{ j_{iA} + \frac{j_{iA}\sigma_{ads} j_H}{\nu} + j_{iA} \exp\left(\frac{-\delta E_t}{k_B T_s}\right) \right\} m_{iA} \right) \times \frac{D_S \times 2\pi r_p}{\pi r_p^2 \rho_p} \left(\frac{1}{I_{iActcys}} \right) +$$

$$\gamma_{CH_4} \pi r_P^2 I_{CH_4 ctcys} + \gamma_C \pi r_P^2 I_{Cctcys}$$

,(13)

$$\frac{d(\pi r_{ct}^2)}{d\tau} = \left\{ j_{iB} \exp\left(\frac{-E_b}{k_B T_s}\right) + j_{iB} \exp\left(\frac{-\delta E_{th}}{k_B T_s}\right) + j_{iB}(1-\theta_t) + j_{iB} + \theta_{CH} \left(j_{iB} y_d + \nu_0 \nu \exp\left(\frac{-\delta E_i}{k_B T_s}\right) \right) \right\} \frac{h(\tau)}{n_{iB}} +$$

$$\gamma_C \pi r_{ct}^2 I_{Ccts}.$$

(14)

The Eqs. (13 and 14) traces the development of the CNT on the catalyst nanoparticle. The height of cylindrical CNT surface is obtained from Eq. (13) in which we consider the growth of the cylindrical part of the CNT and the value of the height of the cylindrical CNT surface at time τ is then fed into Eq. (14) to determine the radius of spherical CNT tip (r_{ct}). The Eq. (14) specifically calculates the curved surface area of the spherical CNT tip.

The Eq. (14) accounts only for the nanoparticle tip radius as bottom area is already determined by the catalyst nanoparticle because they seed nanoparticle growth on them. $h(\tau)$ is the height of the CNT at a time τ .

The explanation for all the symbols used in Eq. (13) is given in Table 1.

The explanation for all the symbols used in Eq. (14) is given in Table 2.

The explanation for all the terms used in Eq.(13) is given in Table 3.

The explanation for all the terms used in Eq.(14) is given in Table 4.

Table 1. Explanation for all the symbols used in Eq.(13)

S.No.	**The notation of various symbols used in Eq.(13)**	**The explanation for symbols in Eq.(13)**
1.	$n_{CH} = \theta_{CH} \nu_0$ (in cm^{-2})	The number density or concentration of CH (CH denotes CH_4 species)[24]
2.	$\nu_0 \approx 1.3 \times 10^{15} cm^{-2}$	The number of adsorption sites per unit area [34]
3.	$j_{carbon}=n_{carbon}v_{thcarbon}/4$ (in cm^{-2} sec^{-1})	Ion flux of carbon atoms[24]
4.	$v_{thcarbon}$ (in cm sec^{-1})	The thermal velocity of carbon atoms[24]
5.	$j_{iA} =n_{iA}(k_B T_i/ m_{iA})^{1/2}$ (in cm^{-2}	Ion flux of type A and B,

	sec^{-1}) and $j_{iB} = n_{iB}(k_B T_i / m_{iB})^{1/2}$ (in cm^{-2} sec^{-1})	respectively
6.	$y_d \approx \varepsilon_{icH} / \varepsilon_{dis}$ (dimensionless)	Ratio of kinetic energy associated with the motion of hydrocarbon ions impinging on the substrate to dissociation energy of CH_4 [24]
7.	n_{iB} (in cm^{-3})	Number density of type B ions i.e., hydrogen ions
8.	ε_{icH} (in eV)	Kinetic energy associated with the motion of hydrocarbon ions impinging on the substrate [34]
9.	ε_{dis}(in eV)	Dissociation energy of CH_4
10.	$\sigma_{ads} \approx 6.8 \times 10^{-16} cm^2$	Cross section for the reactions of atomic hydrogen with adsorbed particles[24]
11.	n_{iC} (in cm^{-3})	Number density of C ions(i.e., carrier ions)
12	D_s and $\left[D_s = D_{s0} \exp(-E_s / k_B T_s)\right]$ $D_{s0} = \nu a_0^2$ is a constant (in nm^{-2} sec^{-1})	Surface diffusion coefficient [34]
13.	E_s= 0.3 eV	Energy barrier for diffusion

		of carbon (C) on the catalyst [34]
14.	a_0 =0.34 nm	Inter atomic distance between carbon atoms
15.	θ_t (dimensionless)	Total surface coverage[24]
16.	$\delta\varepsilon_t$ =1.3eV	Energy due to thermal dissociation[34]
17.	γ_{CH_4} (dimensionless)	Sticking coefficient of CH_4 neutrals
18.	γ_C (dimensionless)	Sticking coefficient of carrier gas i.e., of either $Ar/N_2/NH_3$
19.	m_{carbon} =12 amu	The mass of a carbon atom
20.	m_{iA} =15 amu for CH_3^+ = 16 amu for CH_4^+	The mass of type A(methyl) ions The mass of type A(methane) ions
21.	$h(\tau)$(in μm)	Height of CNT at time τ
22.	n_{iB} (in cm^{-3})	Number density of type B ions i.e., hydrogen ions
23.	$I_{CH4ctcys}$ (in sec^{-1})	Methane neutral atom collection current at the surface of cylindrical CNT
24.	I_{Cctcys}(in sec^{-1})	Carrier gas neutral atom collection current at the surface of cylindrical CNT

25.	k_B=1.38x10^{-16} ergs/K	Boltzmann's constant
26.	T_s=550 ^{0}C	Substrate temperature
27.	r_p=30 nm	Initial radius of catalyst particle
28.	ρ_P = 8.908 g/cm^3	Density of nickel (Ni)
29.	θ_{CH} (dimensionless)	Surface coverages of CH_4 species[24]
30.	ν= 10^{13} Hz	Thermal vibrational frequency[34]
31.	$I_{iActcys}$(in sec^{-1})	Ion collection current of hydrocarbon(i.e., A) the surface of cylindrical CNT

Table 2. Explanation for all the symbols used in Eq. (14)

S. No.	**The notation of various symbols used in Eq.(14)**	**The explanation for symbols in Eq.(14)**
1.	j_{iB} =$n_{iB}(k_BT_i/ m_{iB})^{1/2}$(in cm^{-2} sec^{-1})	Ion flux of hydrogen (B ion)
2.	T_i (in K)	Ion temperature
3.	$E_b \approx 1.6eV$	Energy barrier for bulk diffusion[24]
4.	$\delta\varepsilon_{th}$ (in eV)	Energy due to dehydrogenation of CH_4 [34]
5.	θ_t (dimensionless)	Total surface coverage [24]
6.	$h(\tau)$(in μm)	Height of CNT at time τ
7.	r_{ct}(in nm)	Radius of spherical CNT tip

Table 3. Explanation for all the terms used in Eq.(13)

S.No.	The mathematical Expression for terms in Eq.(13)	The detailed explanation for terms in Eq.(13)
1.	$2n_{CH}\nu\exp\left(\frac{-\delta E_t}{k_B T_s}\right)$	The generation of carbon atoms on the catalyst surface due to thermal dissociation of methyl ions[24]
2.	$2\theta_{CH} j_{iA} y_d$	Ion -Induced dissociation of CH_4 [24]
3.	$2 j_{iA}$	Decomposition of positively charged hydrocarbon ions
4.	$\frac{j_{iA}\sigma_{ads} j_{iB}}{\nu}$	Interaction of hydrocarbon ions with hydrogen ions [34]
5.	j_{carbon}	Incoming flux of carbon atoms
6.	j_{iA}	Incoming flux of hydrocarbon ions per unit time onto the catalyst particle
7.	$\frac{j_{iA}\sigma_{ads} j_H}{\nu}$	Interaction of adsorbed type A ions with atomic hydrogen from plasma[24]
8.	$j_{iA}(1-\theta_t)$	Adsorption of hydrocarbon ions onto the catalyst-substrate surface[34]
9.	$j_{iA}\exp\left(\frac{-\delta E_t}{k_B T_s}\right)$	Thermal dissociation of CH_4[34]

10.	$\frac{D_S \times 2\pi r_p}{\pi r_p^2 \rho_p}$	The surface diffusion of various species onto the catalyst surface across the catalyst nanoparticle per unit area per unit mass density[34]
11.	$\gamma_{CH_4} \pi r_P^2 I_{CH_4} ctcys$	Accretion of neutral methane atoms to the cylindrical surface of CNT
12.	$\gamma_C \pi r_P^2 I_{Cctcys}$	Accretion of neutral carrier gas atoms to the cylindrical surface of CNT

Table 4. Explanation for all the terms used in Eq.(14)

S.No.	**The Mathematical Expression for terms in Eq.(14)**	**The detailed explanation for terms in Eq.(14)**
1.	$j_{iB} \exp\left(\frac{-E_b}{k_B T_s}\right)$	Hydrogen atom diffusing into catalyst - substrate surface [34]
2.	$j_{iB} \exp\left(\frac{-\delta E_{th}}{k_B T_s}\right)$	Incoming flux of hydrogen due to the dehydrogenation of CH_4[24]
3.	$j_{iB}(1-\theta_t)$	Adsorption of hydrogen ions to the catalyst - substrate surface[34]
4.	j_{iB}	Decomposition of hydrogen ions
5.	$\theta_{CH} j_{iB} y_d$	Ion induced dissociation of CH_4[24]
6.	$\theta_{CH} \nu_0 \nu \exp\left(\frac{-\delta E_i}{k_B T_s}\right)$	Incorporation of hydrogen ions due to thermal decomposition of hydrocarbon ions[24]
7.	$h(\tau)$	Height of CNT at time τ
8.	n_{iB}	Number density of type B ions i.e.,

		hydrogen ions
9.	$\gamma_C \pi r_{ct}^2 I_{Ccts}$	Accretion of neutral carrier gas atoms at the spherical CNT tip

9.4: Numerical Result and Discussions

In the present chapter, we are studying the effect of different carrier gases and their flow rates on the growth of CNT through the PECVD process. In a PECVD process, the applied power dissociates the feedstock gas (e.g., methane CH_4) and the dissociated species traverse through the plasma sheath following the decomposition of a hydrocarbon gas on the surface of the catalyst and bulk diffusion of carbon into the catalyst particle until saturation to eventually, form carbon nanostructures.

Ions from plasma do usually deposit inhomogeneously on CNTs growing as a forest as reported in Burmaka *et al.* [35]. Therefore, in the present model, we assume the inhomogeneous deposition of ions on CNT growing in a reactive plasma medium assisted by the catalyst.

In a PECVD chamber, there are three input gases: hydrocarbon gas, carrier gas and hydrogen gas. In the present analysis, we investigate the effects of carrier gases on the growth of CNT in a reactive plasma medium. The three different carrier gases e.g., argon (Ar), ammonia (NH_3) and nitrogen (N_2) are considered. The flow rates of all the three carrier gases are varied individually keeping the flow rate of hydrocarbon and hydrogen gas constant.

The calculations have been formed to investigate the dependence of hydrocarbon and hydrogen number density, the height of cylindrical CNT surface and radius of the spherical CNT tip with time for different flow

rates of carrier gases by simultaneous solution of Eqs. 1 to 14 at appropriate boundary conditions.

The initial boundary conditions for the present calculations are at $\tau = 0$, ion number density (n_{iA0}=0.5 ne0, n_{iB0}=0.5 ne0 and n_{iC0}=0.5 ne0) ,neutral atom density ($n_{A0}=n_{B0}=n_{C0}=1x10^{14}$ cm^{-3}), electron number density ($n_{e0}=1.12x10^{9}$ cm^{-3}), electron temperature (T_{e0}) =1.5eV, ion temperature (T_{iA0}) =2200K, neutral temperature(T_{n0}) = 2000K, mass of ion A $\left(m_{iA}\right)$= 15 amu (methyl ion CH_3^+) and 16 amu (methane ion CH_4^+), mass of ion B $\left(m_{iB}\right)$= 1amu for (H^+) , 2 amu for(H_2^+) and 3 amu for (H_3^+), mass of ion C $\left(m_{iC}\right)$=40 amu for Ar^+,17 amu for NH_3^+ and 28 amu for N_2^+, coefficient of recombination of electrons and ions $\left(\alpha_{A0} \approx \alpha_{B0} \approx \alpha_{C0}\right)$ =$1.12x10^{-7}cm^3/sec$, constant κ = -1.2 and density of Ni $\left(\rho_P\right)$= $8.908g/cm^3$.

Other parameters used in the calculation are substrate temperature (T_s) =550^0C, energy barrier for bulk diffusion (E_b)=1.6eV, energy due to thermal decomposition of methyl ions $\delta\varepsilon_i$ =300eV ,dissociation energy of CH_4 (ε_{dis}) =4.2eV, Ionization energies of neutral atom A (I_{pA}) = 8.96 eV, Ionization energies of neutral atom B (I_{pB}) =6.86 eV, the mean energy collected by the ion A at the surface of catalyst particle (ε_{iA}) = 6 eV, the mean energy collected by the ion B at the surface of catalyst particle (ε_{iB}) = 11eV, sticking coefficient of electron (γ_e) = 1, sticking coefficient of ion (γ_{ij}) =1 , chamber surface area (S_{surf}) = 3918.72 cm^2 , average thermal velocity of electrons (v_{the}) = 6.48×10^6 cm/s, chamber

volume (V) = 18488.32 cm^3 ,and average thermal velocity of ions (v_{thij}) $=3.67\times10^6$ cm/s.

The flow rate of CH_4 (J_{CH4}) and H_2 (J_{H2}) is fixed at 6.0 sccm (standard cubic centimeter per minute) and 12 sccm, respectively. Three different carrier gases N_2, NH_3 and Ar are considered and their flow rates are individually varied to study the effects of all the three carrier gases and their flow rates on the growth of the CNT by PECVD process. Flow rate of carrier gas (J_C) is varied as 10sccm, 20sccm, and 30sccm.

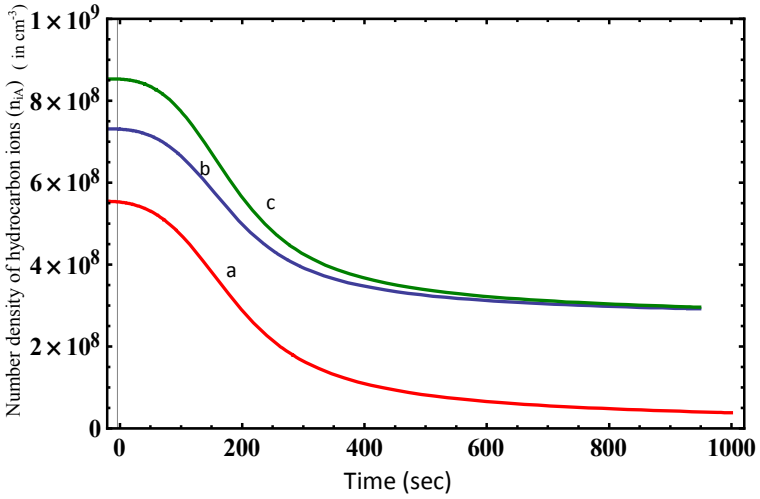

Fig. 1. Depicts the time evolution of number density of hydrocarbon ions (in cm^{-3}) for different flow rate of argon carrier gas (where a, b and c corresponds to J_{Ar}= 10sccm, 20sccm and 30sccm,respectively). The other parameters are given in text.

Fig. 1 displays the variation of the number density of hydrocarbon ions (in cm^{-3}) with time for different flow rates of argon (Ar) carrier gas (i.e. J_{Ar}= 10sccm, 20sccm and 30sccm). It can be seen from Fig. 1 that as the flow rate of carrier gas is increased the number density of hydrocarbon ions increases. This may be ascribed to the fact that with increasing the

carrier gas flow rate , the ions of carrier gas increases and they then react with neutrals of methane giving rise to ions of methyl, thereby increasing their number density within the plasma. The possible governing equation [15] for the above process is

Ar^{+}(Argon) + CH_4 (Methane) $\rightarrow$ CH_3^{+} (Methyl) + H (Hydrogen) + Ar(Argon)

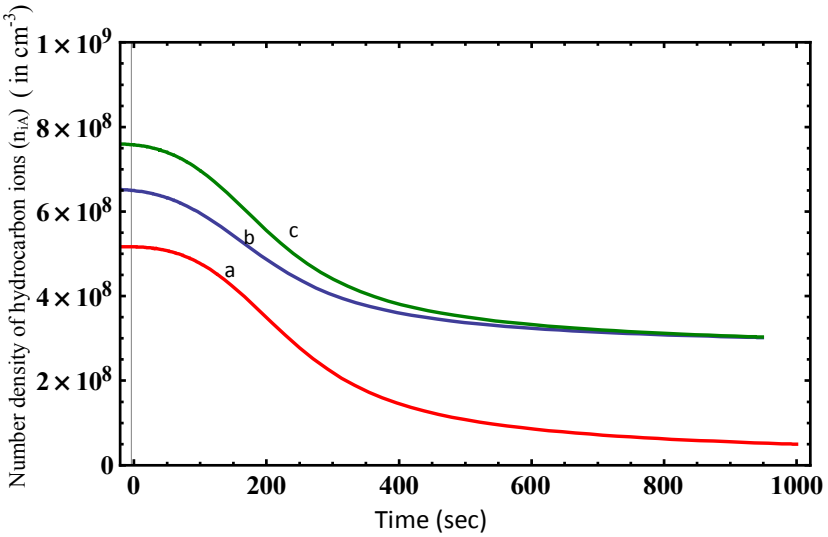

Fig. 2. Depicts the time evolution of number density of hydrocarbon ions (in cm^{-3}) for different flow rate of ammonia carrier gas (where a, b and c corresponds to J_{NH3}= 10sccm, 20sccm and 30sccm,respectively). The other parameters are given in the text.

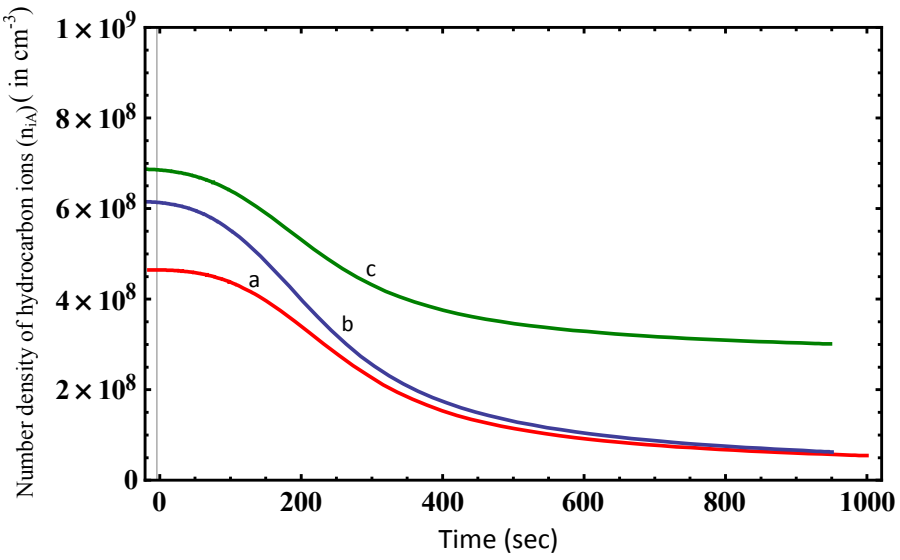

Fig. 3. Illustrates the time evolution of number density of hydrocarbon ions (in cm^{-3}) for different flow rate of nitrogen carrier gas (where a, b and c corresponds to J_{N2}= 10sccm, 20sccm and 30sccm,respectively).The other parameters are given in the text.

Figs. 2 and 3 illustrates the variation of the number density of hydrocarbon ions (in cm^{-3}) with time for different flow rates of ammonia (NH_3) carrier gas (i.e., J_{NH3}= 10sccm, 20sccm and 30sccm) and nitrogen (N_2) carrier gas (i.e., J_{N2}= 10sccm, 20sccm and 30sccm),respectively . The variation of the number density of hydrocarbon ions with flow rate of carrier gas and explanation for the process obtained in Figs. 2 and 3 are same as in Fig.1. When ammonia is taken as a carrier gas, the possible governing equation [36] for the above process is

NH_3^+ (Ammonia) + CH_4 (Methane) → NH_4 (Ammonia) + CH_3^+ (Methyl)

Now, when nitrogen is taken as a carrier gas, then possible governing equation is

N_2 (Nitrogen) + CH_4 (Methane) →no reaction

But for N, the possible reaction [37] is

N (Nitrogen) + CH_4 (Methane) → HCN^- (Hydrogen cyanide) + H_2 (Hydrogen) +H(Hydrogen)

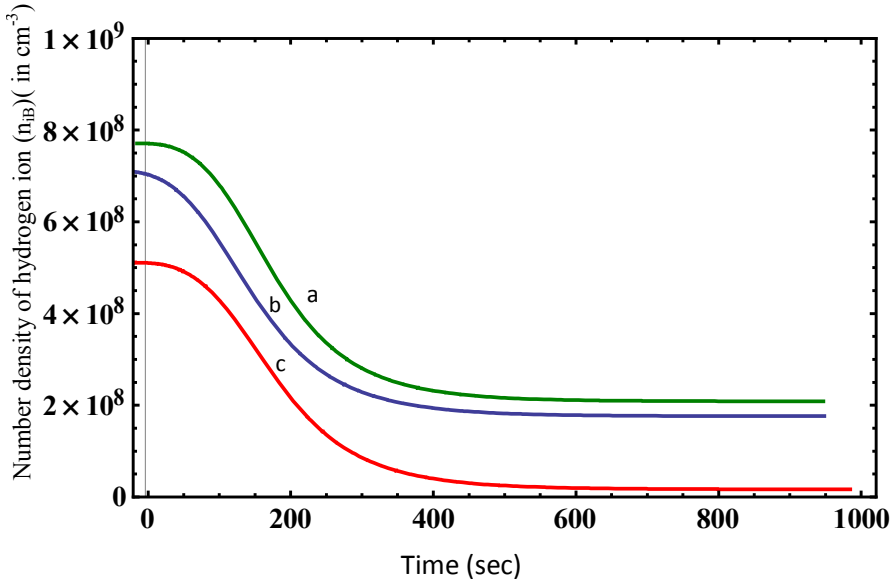

Fig.4. Illustrates the time evolution of number density of hydrogen ions (in cm^{-3}) for different flow rate of argon carrier gas (where a, b and c corresponds to J_{Ar}= 10sccm, 20sccm and 30sccm, respectively). The other parameters are given in the text.

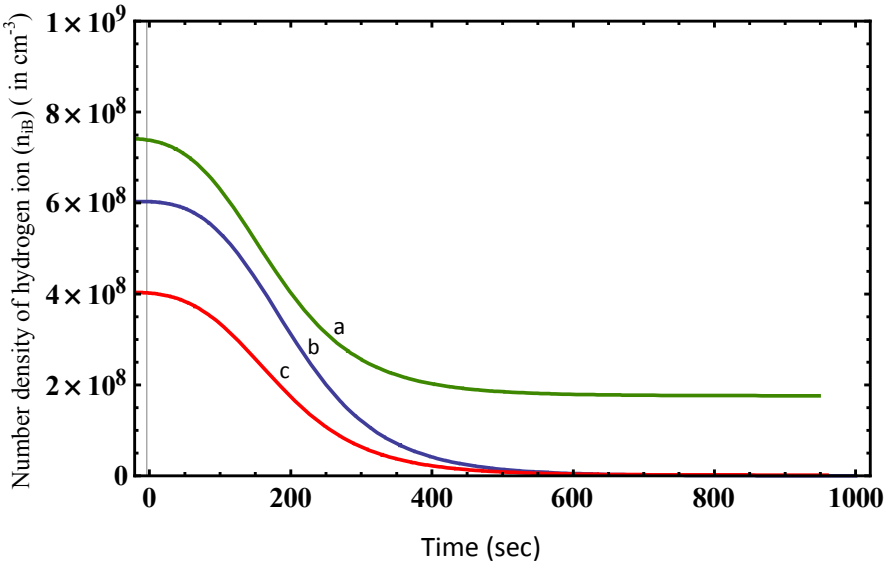

Fig. 5. Depicts the time evolution of number density of hydrogen ions (in cm^{-3}) for different flow rate of ammonia carrier gas (where a, b and c corresponds to J_{NH3}= 10sccm, 20sccm and 30sccm,respectively). The other parameters are given in the text.

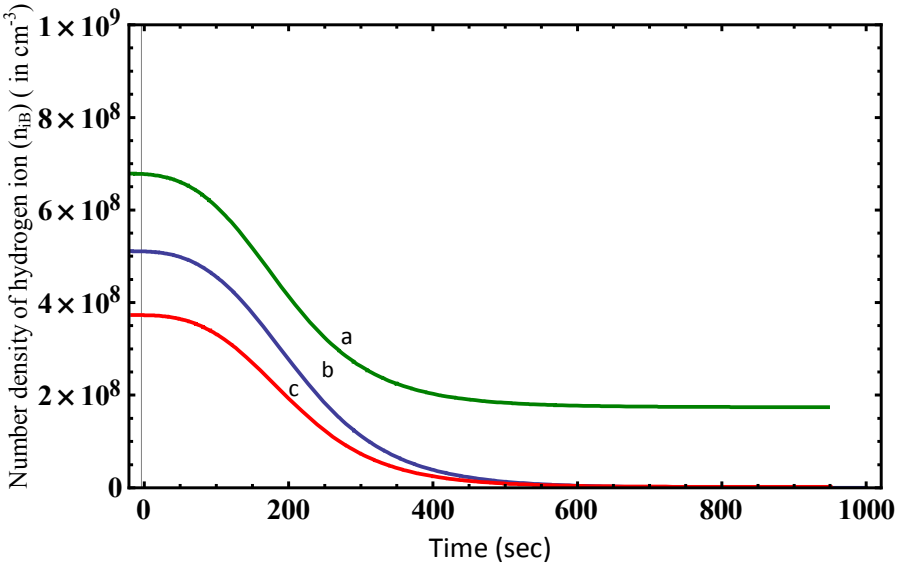

Fig. 6. Depicts the time evolution of number density of hydrogen ions (in cm^{-3})for different flow rate of nitrogen carrier gas (where a, b and c corresponds to J_{N2}= 10sccm, 20sccm and 30sccm,respectively). The other parameters are given in the text.

Figs. 4, 5 and 6 displays the variation of number density of hydrogen ions (in cm^{-3}) with time for different flow rates (in sccm) of argon (Ar), ammonia (NH_3) and nitrogen (N_2) carrier gases, respectively. It can be seen from Figs. 4, 5 and 6 that as the flow rate of carrier gas is increased the number density of hydrogen ions decreases. This may be ascribed to the fact that with increasing the carrier gas flow rate, the density of both hydrocarbon and hydrogen ions does increase, but hydrogen ions being more reactive than hydrocarbon ions further react with higher hydrocarbon ions in the plasma thereby increasing the density of hydrocarbon ions but decreasing their own numbers within the plasma. The possible governing equations are

$Ar^+ + H_2 \rightarrow Ar + H_2^+$

$H_2^+ + H_2 \rightarrow H_3^+ + H$

$$H_3^+ + C_x H_y \rightarrow \quad C_x H^+_{y+1} + H_2$$

From Figs.1 and 4, Figs. 2 and 5, and Figs. 3 and 6, we can compare the time evolution of densities of hydrocarbon and hydrogen ion with the carrier gas inflow. It can be inferred from Figs.1 and 4, Figs. 2 and 5, and Figs. 3 and 6 that for the same carrier gas inflow, the hydrogen ion decays faster than the hydrocarbon ion which validates the fact that hydrogen ions are more reactive than the hydrocarbon ions and hence induces the formation of higher hydrocarbons within the plasma.

The increase in the number density of hydrocarbon and decrease in the density of hydrogen with flow rate of carrier gas is in accordance with the results of Denysenko *et al.*[15].

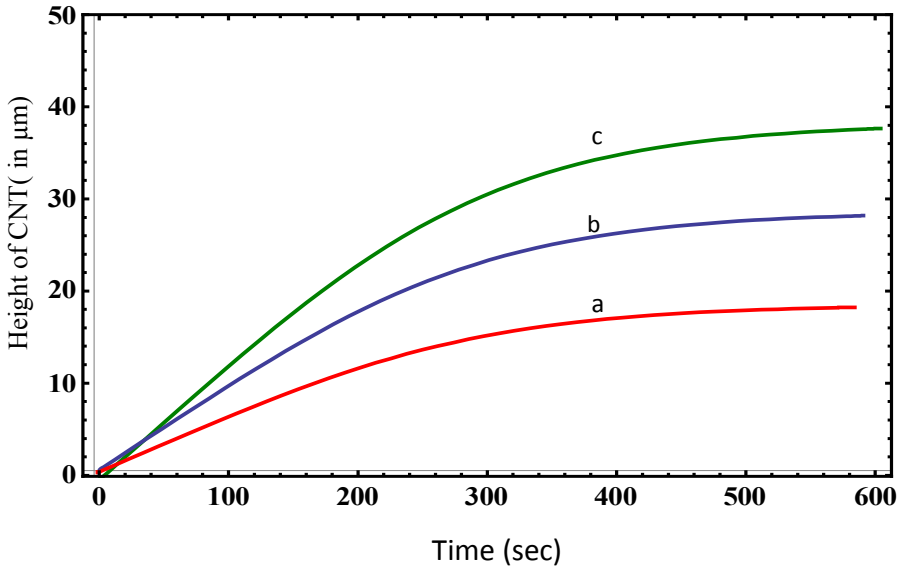

Fig. 7. Depicts the time evolution of height of CNT (in μm) for different flow rate of argon carrier gas (where a, b and c corresponds to J_{Ar}= 10sccm, 20sccm and 30sccm). The other parameters are given in the text.

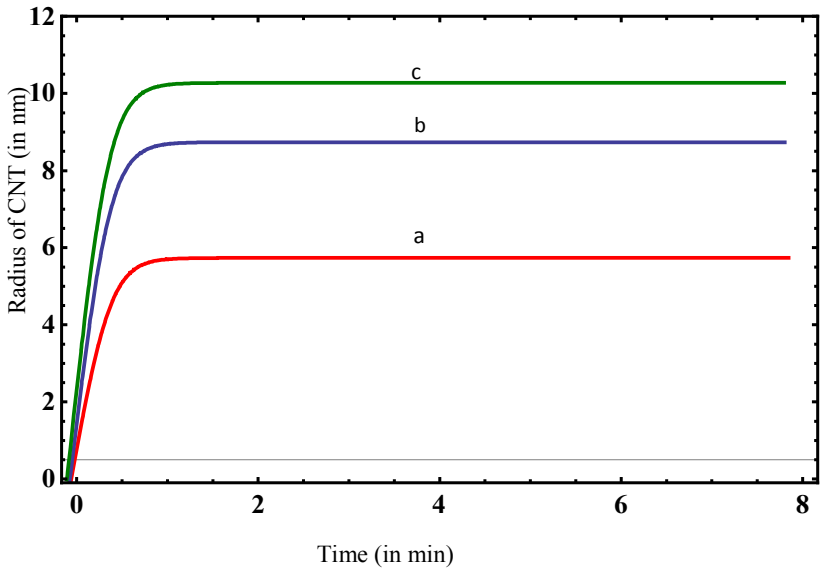

Fig. 8. Depicts the time evolution of radius of CNT (in nm) for different flow rate of argon carrier gas (where a, b and c corresponds to J_{Ar}= 10sccm, 20sccm and 30sccm,respectively). The other parameters are given in the text.

Figs. 7 and 8 illustrates the variation of height (in μm) and radius of CNT(in nm) with time as a function of argon carrier gas inflow rate (i.e., J_{Ar}= 10sccm, 20sccm and 30sccm), respectively. It can be seen from Figs. 7 and 8 that both the height and radius of CNT increases with carrier gas flow rate. This may be ascribed to the fact that as the density of hydrocarbon increases with the carrier gas flow rate, a larger number of hydrocarbon and carbon radicals become readily available for CNT growth, thereby increasing its height. Now, the increase of carrier gas inflow leads to lesser number density of hydrogen ions, thereby reducing the etching effects of hydrogen and hence giving larger radius of CNT tip.

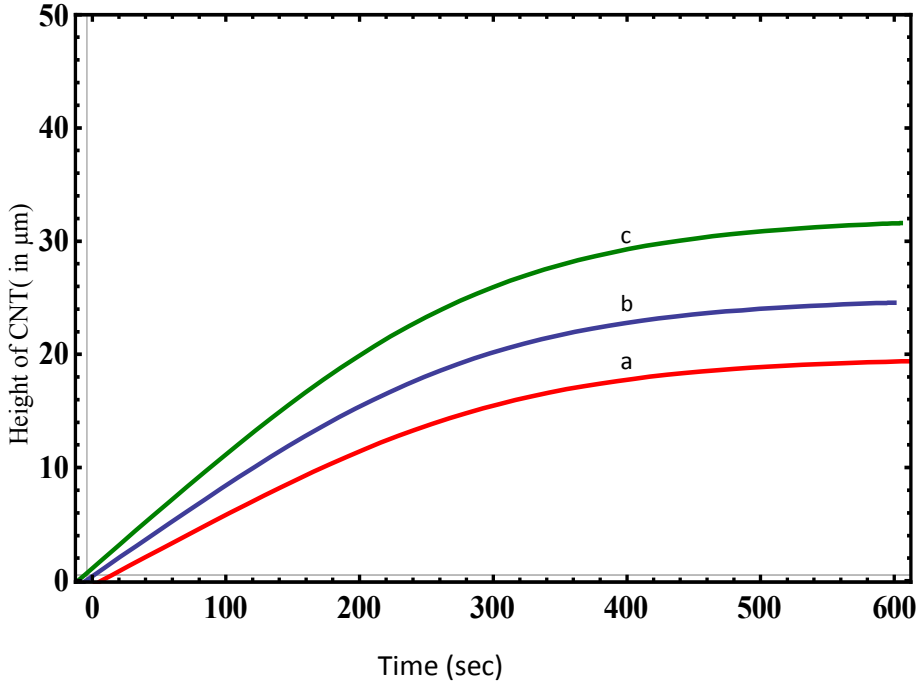

Fig. 9. Depicts the time evolution of height of CNT (in μm) for different flow rate of ammonia carrier gas (where a, b and c corresponds to J_{NH3}=10sccm,20sccm and 30sccm, respectively). The other parameters are given in the text

Fig. 9 illustrates variation of height of CNT (in μm) with time as a function of ammonia carrier gas inflow rate (i.e., J_{NH3}= 10sccm, 20sccm and 30sccm). The height of CNT increases with inflow rate of ammonia. This is because as the density of hydrocarbon increases with the ammonia carrier gas flow rate, a larger number of hydrocarbon and carbon radicals become readily available for CNT growth, thereby increasing its height.

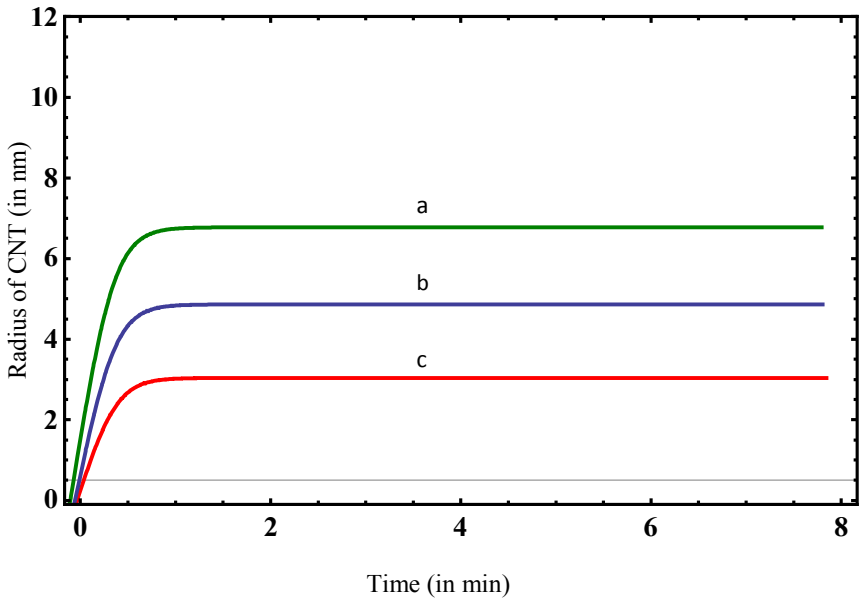

Fig. 10. Depicts the time evolution of radius of CNT (in nm) for different flow rate of ammonia carrier gas (where a, b and c corresponds to J_{NH3}=10sccm, 20sccm, and 30sccm, respectively). The other parameters are given in the text.

Fig. 10 illustrates the variation of radius of CNT (in nm) with time as a function of ammonia carrier gas inflow rate (i.e., J_{NH3}= 10sccm, 20sccm and 30sccm). The radius of CNT decreases with inflow rate of ammonia. With ammonia gas, the increase of carrier gas inflow leads to lesser number density of hydrogen ions. Now, in ammonia gas environment, there are nitrogen ions also along with hydrogen ions and although reduced hydrogen number density would decrease the etching of CNT by hydrogen ions. However, there would be some etching by nitrogen ions and hence the combined effect of etching by nitrogen and hydrogen would eventually result in reducing radius of CNT tip with gas inflow rate.

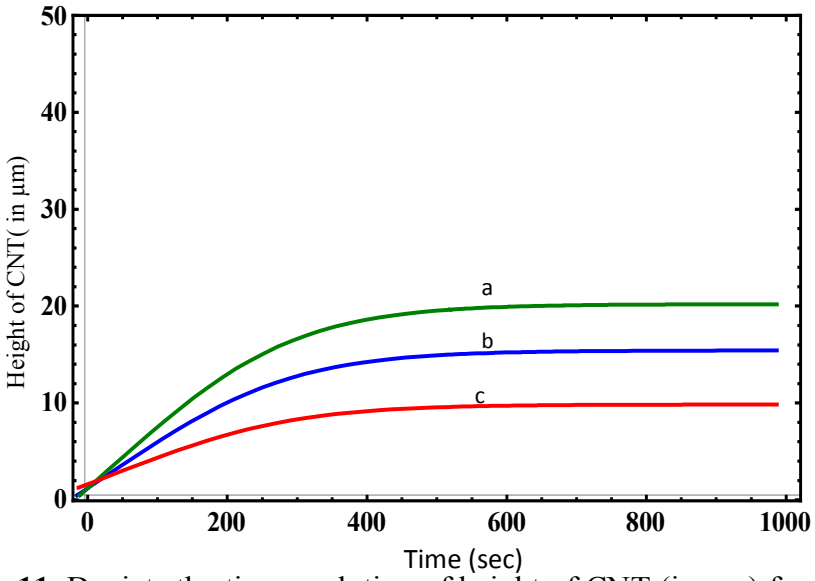

Fig. 11. Depicts the time evolution of height of CNT (in μm) for different flow rate of nitrogen carrier gas (where a, b and c corresponds to J_{N2}=10sccm, 20sccm and 30sccm, respectively). The other parameters are given in the text.

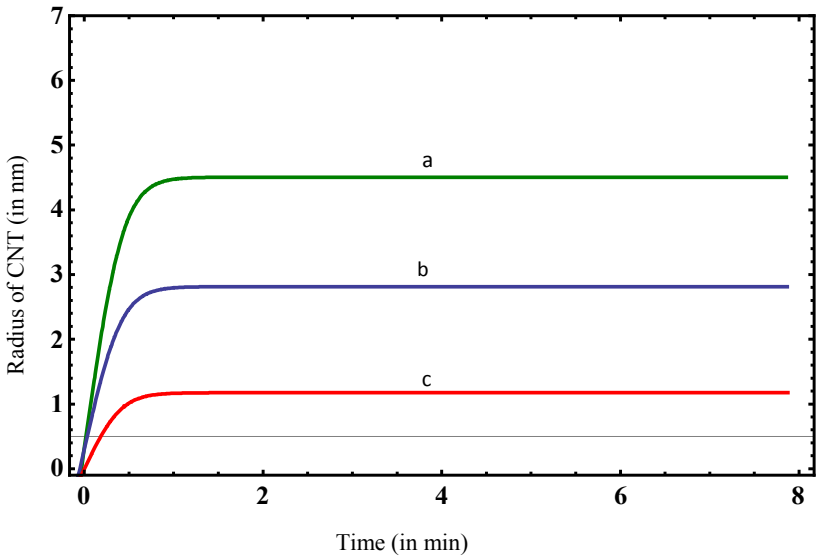

Fig. 12. Depicts the time evolution of radius of CNT (in nm) for different flow rate of nitrogen carrier gas (where a, b and c corresponds to J_{N2}= 10sccm, 20sccm, and 30sccm, respectively). The other parameters are given in the text.

Figs. 11and 12 illustrate the variation of height (in μm) and radius of CNT (in nm) with time as a function of nitrogen carrier gas inflow rate (i.e., J_{N2}= 10sccm, 20sccm and 30sccm). The height and radius of CNT

decreases with inflow rate of nitrogen. This may be ascribed to the fact that with the nitrogen carrier gas flow rate, a larger number of CN radicals formed in N_2 environment, which are volatile at room temperatures, and reduces the carbon flux to catalyst particle thereby producing lesser height and radius of CNTs[38].

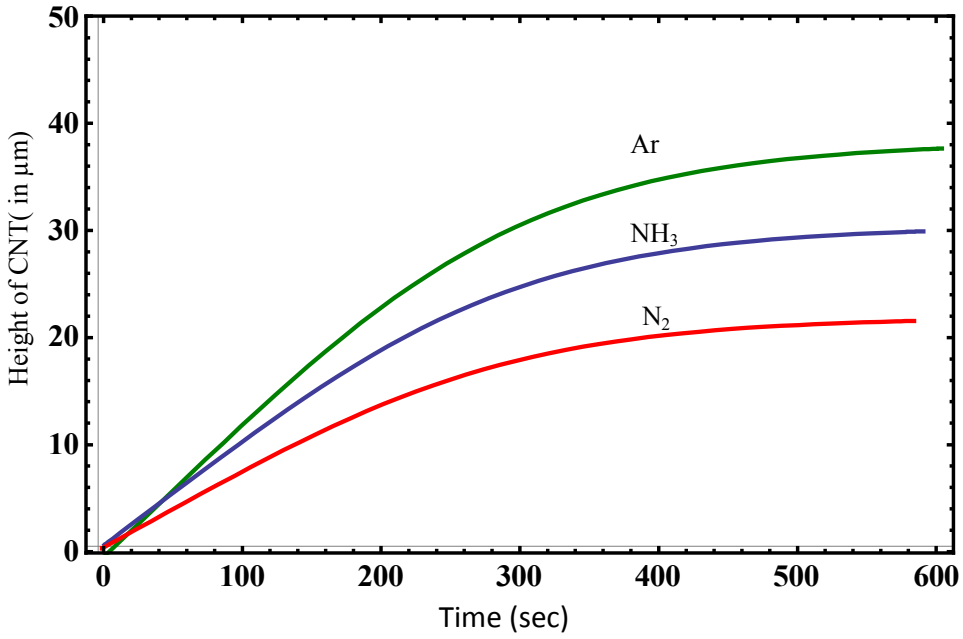

Fig. 13. Depicts the time evolution of height of CNT (in μm) for different carrier gases Ar, NH_3 and N_2 for a fixed flow rate of 10sccm for all the three carrier gases. The other parameters are given in the text.

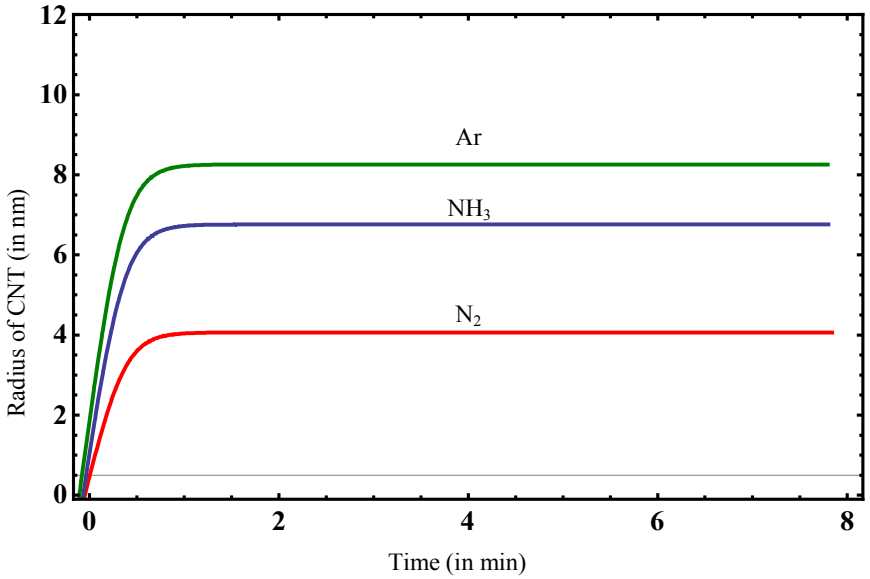

Fig. 14. Depicts the time evolution of radius of CNT (in nm) for different carrier gases Ar, NH_3 and N_2 for a fixed flow rate of 10sccm for all the three carrier gases. The other parameters are given in the text.

Figs. 13 and 14 depicts the time evolution of the height of CNT (in μm) and radius of CNT (in nm) for different carrier gases i.e., Ar, NH_3 and N_2 for a fixed flow rate of 10sccm for all the three carrier gases. Finally, from Figs.13 and 14, we can see that the height of CNT (in μm) and radius of CNT (in nm) is largest for argon followed by ammonia and then nitrogen. Thus, one can conclude that argon is the best carrier gas among those considered in the present problem followed by ammonia and then by nitrogen for better growth of CNTs in a reactive plasma medium. The results obtained in the present model comply with the experimental works of Kayastha *et al.* [6], Mi *et al.* [7], Jung *et al.*[8] , Mi and Jia [10] ,Qian *et al.* [11] and Malgas *et al.* [13].

9.5. CONCLUSION

A theoretical model is developed to investigate the effects of three different carrier gases and their flow rates on the growth of CNT by a PECVD process. The three different carrier gases e.g., argon (Ar), ammonia (NH_3) and nitrogen (N_2) are considered and their flow rates are varied to investigate their effects on height and radius of CNTs. The results hold good when, the flow rate of CH_4 (J_{CH4}) and H_2 (J_{H2}) is fixed and the substrate and catalyst temperatures are assumed to be the same. The initial ion number density and neutral atom density for hydrogen, hydrocarbon and carrier is assumed to be the same at 0.56×10^9 cm^{-3} and $1 \times 10^{14} cm^{-3}$, respectively. The ion and neutral temperature for hydrogen, hydrocarbon, and carrier is taken to be the same at 2200K and 2000K, respectively.

The main findings of the work can be summarized as follows:

(1) With Ar acting as a carrier gas, CNTs with better height and radius are obtained. This is due to the fact that number density of hydrocarbon increases and of hydrogen ions decreases with Ar carrier gas flow rate .The reaction mechanism is governed by Ar^+(Argon) + CH_4 (Methane) $\rightarrow$ CH_3^+ (Methyl) + H (Hydrogen)+ Ar(Argon). Since increase in hydrocarbon density, makes carbon radicals readily available for CNT growth thereby contributing to height of CNT. The decrease in hydrogen ion density reduces the etching effects of hydrogen and hence giving larger radius of CNT tip.

(2) With NH_3 as a carrier gas, CNTs with better height but smaller radius are obtained. This is because number density of hydrocarbon increases and of hydrogen ions decreases with NH_3 carrier gas

flow rate. The possible reaction equation is NH_3^+ (Ammonia) + CH_4 (Methane) → NH_4 (Ammonia) + CH_3^+ (Methyl). The increase in the height of CNT with ammonia flow rate is due to the larger availability of carbon radicals with hydrocarbon density. The reduction in radius of CNT is due to the combined etching effects of both hydrogen and nitrogen.

(3) When nitrogen is taken as a carrier gas, both the height and radius of CNT decreases. The possible reaction equation is N(Nitrogen) + CH_4 (Methane) → HCN^- (Hydrogen cyanide) + H_2 (Hydrogen) +H (Hydrogen). The reduction in both the height and radius of CNT with the nitrogen carrier gas flow rate is because in N_2 environment, a larger number of CN radicals formed which are volatile at room temperatures and reduces the carbon flux to catalyst particle thereby producing lesser height and radius of CNTs.

References

[1] V. I. Merkulov, A.V. Melechko , M.A. Guillorn, D. H. Lowndes and M. L. Simpson, Appl Phys. Lett. **79** ,2970(2001).

[2] M. S. Bell , K. B. K. Teo and W. I. Milne , J. Phys. D: Appl. Phys. **40**, 2285(2007).

[3] M. Su, B. Zheng, and J. Liu, Chem. Phys. Lett. **322**, 321 (2000).

[4] L. Delzeit, B. Chen, A. Cassell, R. Stevens, C. Nguyen, and M. Meyyappan, Chem. Phys. Lett. **348**, 368 (2001).

[5] L. Delzeit, I. McAninch, B. A. Cruden, D. Hash, B. Chen, J. Han, and M. Meyyappan, J. Appl. Phys. **91**, 6027 (2002).

[6] Vijaya Kayastha and Yoke Khin Yap, Svetana Dimovski and Yury Gogotsi, Appl. Phys. Lett. **85**, 3265(2004).

[7] Wanliang Mi, Jerry Yuesheng Lin, Qian Mao, Yongdan Li, Baoquan Zhang, J. Natural Gas Chem. **14** ,151(2005).

[8]Minjae Jung, Kwang Yong Eun, Jae-Kap Lee, Young-Joon Baik, Kwang-Ryeol Lee,Jong Wan Park, Diamond and Related Mat. **10**,1235(2001).

[9]Yoke Khin Yap , Vijaya Kayastha , Steve Hackney , Svetlana Dimovski and ury Gogotsi, Mat. Res. Soc. Symp. Proc. **818** (2004).

[10]Wanliang Mi, Dongmei Jia, J. Chil. Chem. Soc **55**, 153 (2010).

[11] Hai-sheng Qian, Feng-mei Han , Bing Zhang , Yan-chuan Guo , Jun Yue , Bi- xian Peng , Carbon **42** , 761 (2004).

[12]Setareh Monshi Toussi, Fakhru'l-razi, A. L. Chuah and A.R. Suraya, Sains Malaysiana **40**,197(2011).

[13]Gerald F. Malgas, Christopher J. Arendse, Nonhlanhla P. Cele, and Franscious R. Cummings, J. Mat. Sci. **43**,1020 (2008).

[14]Carolyn Reynolds, Binh Duong, and Supapan Seraphin, J.

Undergraduate Res. in Phys. August 27, (2010).

[15]I. B. Denysenko , S. Xu, J. D. Long, P.P. Rutkevych, N.A. Azarenkov and K. Ostrikov , J. Appl. Phys. **95,** 2713(2004).

[16]W.B. Choi, JU Chu, KS Jeong, EJ Bae, J-W Lee, J-J Kim, J-O Lee, Appl. Phys. Lett. **79,** 3696(2001).

[17]WA De Heer, A Chatelain, D. A Ugarte ,Science **270**,1179 (1995).

[18]W.B. Choi, D.S. Chung, J.H. Kang, HY Kim, Y.W. Jin, I.T. Han, Y .H. Lee,J.E. Jung, N. S. Lee,G. S. Park and J. M. Kim, Appl. Phys. Lett. **75**, 3129 (1999).

[19] W.I. Milne, K.B.K. Teo, G.A.J. Amaratunga, P. Legagneux, L. Gangloff, J-P Schnell,V. Semet, V. T. Binh and O. Groening ,J. Mater Chem. **14**,933(2004).

[20]W.I. Milne, K.B.K. Teo, M. Mann, I.Y.Y. Bu, G.A.J. Amaratunga, N. De Jonge, M. Allioux, J.T. Oostveen, P. Legagneux, E. Minoux, L. Gangloff, L. Hudanski, J.-P. Schnell, D. Dieumegard, F. Peauger, T. Wells, and M. El- Gomati, Phys. Stat. Sol. A **203**,1058(2006).

[21] H. Li ,J. Li J,C. Gu, Carbon **43**,849(2005).

[22] B. Gruner, M. Jag, A. Stibor, G. Visanescu, M. Haffner, D. Kern, A. Gunther, and J. Fortagh., Phys. Rev. A **80**,063422(2009).

[23] M. Sode, T. Schwarz- Selinger, and W. Jacob, J. Appl. Phys. **114**, 063302 (2013).

[24]H. Mehdipour, K. Ostrikov, and A. E. Rider, Nanotechnology **21**, 455605 (2010).

[25]M. A. Lieberman and A. J. Lichtenberg, *Principles of Plasma Discharges and Materials Processing* (Wiley Interscience Publication, USA, 1994).

[26]http://www.physics.usyd.edu.au/~mmmb/plasma/Chapter5.pdf.

[27]K. Ostrikov and S. Xu, *Plasma Aided Nanofabrication: From Plasma Sources to Nanoassembly* (Wiley-VCH, Weinheim, Germany, 2007).

[28]O. A. Louchev, C. Dussarrat, and Y. Sato, J. Appl. Phys. **86**, 1736 (1999).

[29]H. Chatham, D. Hils, R. Robertson, and A. C. Gallagher, J. Chem. Phys. **79**, 1301 (1983).

[30]R. L. Mills, P. C. Ray, B. Dhandapani, R. M. Mayo, and J. He, J. Appl. Phys. **92**, 7008 (2002).

[31]Sanjay K. Srivastava , A.K. Shukla , V.D. Vankar , V. Kumar, Thin Solid Films **492**,124(2005).

[32] I. Denysenko and N. A. Azarenkov, J. Phys. D: Appl. Phys. **44**, 17403(2011)

[33]M. S. Sodha , Shikha Misra, S. K. Mishra, Sweta Srivastava, J. Appl. Phys. **107**,103307(2010).

[34]I. Denysenko, K. Ostrikov, M. Y. Yu, and N. A. Azarenkov, J. Appl. Phys. **102**, 074308 (2007).

[35]G. Burmaka, I. B. Denysenko, K. Ostrikov, I. Levchenko, N. A. Azarenkov, Plasma Process. Polym. **11**, 798(2014).

[36]Michael A. Everest, John C. Poutsma, Jonathan E. Flad, and Richard N. Zare, J. Chem Phys. **111**, 2507(1999).

[37] P.A. Gartaganis and C.A. Winkler, Can J. Chem. **34**, 1457(1956).

[38] Y. K. Yap, S. Kida, T. Aoyama, Y. Mori, and T. Sasaki, Appl. Phys. Lett.**73**, 915 (1998).

CHAPTER 10

FUTURE SCOPE OF THE WORK

The work carried out in the thesis aims to study the growth of carbon nanotubes (CNTs) in a plasma medium with and without catalyst. The subsequent field emission from CNT is approximated based on the results obtained. The present thesis may help to provide a better insight into the growth of CNTs in a plasma environment and effects of plasma parameters (such as electron densities and temperatures, ion densities and temperatures) and process parameters (such as substrate bias, substrate temperature, flow rates of carrier gas etc.) on the growth profiles of CNT. The results may be extended to realize field emissions from CNT. The main findings of the work carried out in the present thesis can be summarized as:

1. The plasma parameters (i.e., electron densities and temperatures, ion densities and temperatures) contribute to the growth of CNT with smaller radius in plasma environment. The spherical CNT tip and cylindrical CNT surfaces grow with smaller radius when subjected to higher plasma densities and temperatures.
2. The presence of negative ions in a plasma environment is seen to enhance CNTs growth with smaller radii.
3. The growth of CNT in different plasma mediums such as carbon tetraflouride, methane, hydrogen, and argon is studied and it is found that CNT grows with larger radius in carbon tetraflouride, followed by argon, methane and hydrogen plasma.
4. The plasma composition affects the growth of CNTs and it is seen that if plasma is composed of heavy and light positive ions then the

growth of CNTs with smaller radii is enhanced as relative concentration of light to heavy ions is increased.

5. The growth of CNTs on a catalyst-substrate surface in a plasma environment can be controlled more efficiently and CNTs with desired growth profiles can be grown in such cases. The hydrocarbon density and substrate bias contributes to CNTs with larger heights and increase in hydrogen ion density gives CNTs with smaller radii owing to its etching effects.
6. The substrate temperature is set up to be an important parameter in the growth of CNT assisted by catalyst in a plasma ambiance. The height and radius of CNT increases with substrate temperature.
7. Different carrier gases influences CNTs growth differently. The carrier gas such as argon gives CNTs with larger height and radius, CNTs with larger height but smaller radius are seen to grow in ammonia carrier gas whereas nitrogen carrier gas impedes both the height and radius of CNT.
8. Based on all the above findings the field emission from the CNTs can be approximated. It may be seen that CNTs grown in higher plasma densities and temperatures, in presence of negative ions, in presence of heavy positive ions, in different plasma mediums such as hydrogen, with increased densities of hydrocarbon and hydrogen, and in different carrier gases with increasing flow rates, and at higher substrate temperatures would give better field emissions.

There is still a lot of work to be done and many questions that need to be answered before a complete picture of the growth of CNT in a plasma medium is painted. Some of the questions may be:

Q1. What is the exact role of radicals in the growth of CNT in a plasma medium? Are they detrimental to growth of CNT?

Q2. The role of atomic hydrogen in the growth of CNT is still an unanswered question.

Q3. There can be various combinations of substrates and catalysts for the growth of CNTs and different combinations yield different nanostructures ranging from nanofibres to nanotubes but the exact reasons behind different nanostructures growth in different substrates and catalysts needs to be looked into?

Q4. PECVD (plasma enhanced chemical vapor deposition) process is largely preferred over the conventional CVD (chemical vapor deposition) method for its low temperature growth and alignment effects. But what temperature during a PECVD process really qualifies to be called a low temperature ? Moreover, the electric field alignment of CNTs may be an important avenue of research.

Q5. Does the quest to achieve CNTs at low temperatures a deterrent to its yield?

All these questions among many others are yet to be answered before large quantities of CNTs at preferably low temperatures are obtained such that CNTs can be employed on larger scales for their more realistic applications.

LIST OF PUBLICATIONS

1. Included in thesis

A) In International refereed Journals

1. **Aarti Tewari** and Suresh C. Sharma , Effect of different carrier gases and their flow rates on the growth of carbon nanotubes, Phys. of Plasmas 22, 043501 (2015).
2. **Aarti Tewari** and Suresh C. Sharma ,Theoretical modeling of temperature dependent catalyst-assisted growth of conical carbon nanotube tip by plasma enhanced chemical vapor deposition process, Phys. of Plasmas **22**, 023505 (2015).
3. **Aarti Tewari** and Suresh C. Sharma , Modeling carbon nanotube growth on the catalyst-substrate surface subjected to reactive plasma, Phys. of Plasmas **21,** 063512 (2014).
4. **Aarti Tewari** and Suresh C. Sharma, Theoretical Investigations on the effect of different plasmas on Growth and Field Emission Properties of Spherical Carbon Nanotube (CNT) tip placed over Cylindrical Surfaces, Journal of Plasma Physics **79**, 939(2013).
5. **Aarti Tewari** , Ritu Walia, and Suresh C. Sharma, Role of negatively charged ions in plasma on the growth and field emission properties of spherical carbon nanotube tip, Phys. of Plasmas **19,** 013502 (2012).
6. Suresh C. Sharma and **Aarti Tewari**, Effect of plasma parameters on growth and field emission properties of electrons from cylindrical metallic carbon nanotube (CNT) surfaces, Phys. of Plasmas **18,** 083503 (2011).

7. Suresh C. Sharma and **Aarti Tewari** , Effect of plasma parameters on growth and field emission properties of spherical carbon nanotube (CNT) tip, Phys. of Plasmas **18**, 063503(June 2011).

B) Published Papers in Proceedings of International Conferences

8. **Aarti Tewari** and Suresh C. Sharma, Effect of plasma compositions on growth and field emission properties of spherical Carbon Nanotube (CNT) tip, Journal of Physics: Conference Series **548** , 012050(2014).

2. Not Included in thesis

C) In International refereed Journals

9. Isha Santolia, **Aarti Tewari**, Suresh C. Sharma, and Rinku Sharma ,Effect of doping on growth and field emission properties of spherical carbon nanotube tip placed over cylindrical surface, Phys. of Plasmas **21**, 063508 (2014).
10. Suresh C. Sharma **, Aarti Tewari** and Ravi Gupta ,Role of plasma and doping elements on the growth and field emission properties of metallic Carbon Nanotube(CNT),Journal of Atomic, Molecular, Condensate and Nanophysics **6**,195(2015)
11. Neha Gupta, **Aarti Tewari** and Suresh C. Sharma , "Role of plasma parameters on growth and field emission properties of 2D graphene sheet" Journal of Atomic, Molecular ,Condensate and Nanophysics **2**,215(2015).
12. Suresh C. Sharma and **Aarti Tewari**, Field emission of electrons from spherical conducting carbon nanotube (CNT) tip including the effect of image force, Canadian J. Physics **89**,875(2011).

(D) Published Papers in Proceedings of International Conferences

13. I. Santolia, **Aarti Tewari**, S C Sharma and R Sharma, Theoretical Investigations of the Effect of N- Doping on Growth and Field Emission Properties of Carbon Nanotubes (CNTs), Journal of Physics: Conference Series 548 ,012044,(2014).
14. **Aarti Tewari** and Suresh C. Sharma , Investigations on the role of negatively charged ions in a plasma on the growth and field emission properties of spherical tip placed over cylindrical carbon Nanotube(CNT) surfaces, 31st Intl. Conference on Phenomena in Ionized Gases held on14-19 July 2013 at Granada, Spain.
15. Suresh C. Sharma and **Aarti Tewari** , Theoretical investigations on the effect of plasma parameters on the growth and field emission properties of spherical tip placed over cylindrical carbon nanotube (CNT) surfaces, 31st Intl. Conference on Phenomena in Ionized Gases held on 14- 19 July 2013 at Granada, Spain.
16. **Aarti Tewari** and Suresh C. Sharma, Growth of cylindrical Carbon Nanotube (CNT) in a complex plasma and the effect of plasma parameters on the field enhancement factor, Proc. of 3rd Intl. Conf. on current developments in Atomic, Molecular, Optical & Nano Physics with Applications(CDAMOP 2011) held on December 14-16, 2011at Department of Physics and Astrophysics, University of Delhi, India, P. 206.
17. Suresh C. Sharma and **Aarti Tewari**, Growth of spherical carbon nanotube(CNT) in a complex plasma and the effect of plasma parameters on field enhancement factor, 30th Intl. Conference on Phenomena in Ionized Gases held from 28August-2September 2011at Queen's University Belfast, Northern Ireland, UK, P. C12-

132.

18. **Aarti Tewari** and Suresh C. Sharma, Field emission of electrons from metallic Carbon Nanotube CNTs), Indraprastha Intl. Conclave on Nano Science and Technology (IICNST-2010), held from 16- 17 Nov. 2010 at GGSIP University, New Delhi, India, P. 109.

(E) Communicated Papers in International Journals

19. **Aarti Tewari** and Suresh C. Sharma, Investigations on the role of plasma and process parameters on the catalyst–assisted growth of carbon nanotube. **J. Phys. D: Appl. Phys. (IOP Publishing).**